Mutational Identification of *cis*- and *trans*-acting Determinants of dMyc Protein Function

Dissertation
zur
Erlangung der naturwissenschaftlichen Doktorwürde
(Dr. sc. nat.)

vorgelegt der
Mathematisch-naturwissenschaftlichen Fakultät
der
Universität Zürich
von

Daniela Schwinkendorf

aus
Deutschland

Promotionskomitee

Dr. Peter Gallant (Leitung der Dissertation)
Prof. Dr. Alex Hajnal (Vorsitz)
Prof. Dr. Ernst Hafen
Prof. Dr. Wilhelm Krek
Dr. Christian Frei
Prof. Dr. Martin Eilers

Zürich, 2008

Table of content

Honour the springtide life ever adorning.
That all things has made!
Things smallest have some resurrectional morning.
The forms alone fade.
Life begets life,
Potencies higher surprise;
Kind begets kind,
Heedless of time as it flies;
Worlds pass away and arise.

Join in the joy of all life, every being,
Brief bloom of its spring;
Honor th`eternal, our human lot freeing
From fetters that cling;
Adding your mite,
With the eternal unite;
Though you decay,
Breathe as a moment you may,
Air of eternity`s day!

For my grandparents and Carmen

Abbreviations

>	FRT (abbreviation in genotype annotations, e.g. *ey>dm*^{P0})
aa	amino acid
AED	[time] after egg deposition
b-HLH-LZ	basic helix-loop-helix leucine zipper
DCMW	asparic acid(D)-cysteine(C)-methionine(M)-tryptophan(W)
DNA	deoxyribonuclein acid
dsRNA	double stranded RNA
FRT	flipase recombination target
GFP	green fluorescent protein
GM	*y w*/Y; (*GMR*-GAL4 UAS-dMyc^{132}; UAS-dMyc^{13} UAS-dMyc^{42})/(SM5^TM6B)
IgG	immunglobulin G
HAT	histone acetyltransferase
kb	kilo base pair
L1, L2, L3	first, second and third larval stage
MB1 (2,3)	Myc Box
OreR	OreR (wildtype strain)
ORF	open reading frame
PEST	proline(P)-glutamic acid(E)-serine(S)-threonine(T)
PCR	polymerase chain reaction
Pol	polymerase
qRT-PCR	qualitative real-time PCR
RNA	ribonucleic acid
RNAi	RNA interference
SAGA	Spt-Ada-Gcn5-acetyltransferase
UAS	upstream activating sequence
UTR	untranslated region

Zusammenfassung

Das Proto-Onkogen *myc* ist in menschlichen Krebsarten häufig fehlreguliert. Die Familie der *myc* Gene kontrolliert viele verschiedene zelluläre Prozesse wie zum Beispiel Zellwachstum und –proliferation, Metabolismus oder Apoptose. Die Faktoren, welche die Wirkung des Myc-Proteins von innen heraus bestimmen, beispielsweise welche Aufgabe die konservierten Bereiche innerhalb dieses Proteins in einem Organismus ausführen, sowie die Faktoren, die von ausserhalb auf Myc einwirken und dadurch Myc`s biologische Funktionen bestimmen sind noch immer unzureichend erforscht.

In dieser Arbeit haben wir die Rolle von dMyc, dem einzigen Homolog der Familie der Myc-Proteine in *Drosophila*, in Zellkultur und in einem voll entwickelten Organismus, der Fliege untersucht. dMyc kann teilweise tierisches c-Myc ersetzen. In einem ersten Projekt haben wir die konservierten Bereiche von dMyc (den N-Terminus, MB2, MB3) im Hinblick auf Zellwachstum, -proliferation und Apoptose genauer untersucht. Wildtypische und mutante dMyc-Proteine wurden in *Drosophila* S2 Zellen und in Fliegen exprimiert. Alle getesteten biologischen Funktionen von dMyc zeigten eine starke Abhängigkeit vom N-terminalen Bereich des Proteins. Erstaunlicherweise war MB2, welche in Vertebraten eine wichtige Rolle für die Rekrutierung von HAT-Komplexen zu Myc (TRRAP, RUBVL1) spielt, nur teilweise nötig für die Funktionen von dMyc. Eine dMyc-Mutante, welcher MB2 fehlt, konnte sogar ein dMyc Null-Allel bis zur Ausbildung einer voll entwickelten Fliege retten. Zudem konnten wir zeigen, dass MB3 die Stabilität von dMyc negativ beeinflusst. Darüber hinaus führte eine dMyc-Mutante, welche MB3 deletiert, zu einem erhöhten Wachstum sowie einer starken Zunahme von Zelltod. Die Fähigkeit, die Transkription der E-box abhängigen Zielgene oder der von RNA Polymerase III transkribierten Gene *in vivo* zu aktivieren, wurde jedoch nicht erhöht.

In einem zweiten Projekt haben wir einen loss-of-function Screen durchgeführt, um neue Kofaktoren von dMyc zu finden. Der Screen führte zu zwei Proteinen: Delta, einem Notch-Liganden, und Chinmo, welches die zeitliche Identität der Neuronen während der postembryonalen Entwicklung des Gehirns von *Drosophila* reguliert. Beide Proteine interagieren genetisch mit *dmyc* während der Augenentwicklung. Wir zeigen Beweise dafür, dass dMyc die Funktionen von Chinmo limitiert, da die schädlichen Effekte, die durch eine Überexpression von Chinmo entstehen, durch eine Reduktion der Proteinmenge von dMyc verringert werden können. Umgekehrt braucht dMyc Chinmo, um seine biologischen Funktionen in Flügelimaginalscheiben auszuführen. Darüber hinaus zeigen unsere Daten, dass Chinmo und dMyc physisch über die BTB/POZ Domäne von Chinmo interagieren und dass

Chinmo endogene Zielgene von Myc, welche im Zusammenhang mit der Proteinbiosynthese stehen, aktivieren kann. Chinmo transaktiviert zudem effizient Zielgene von dMyc und diese Aktivierung der Transkription is abhängig von dMyc.
Zusammenfassend deuten unsere Daten darauf hin, dass Chinmo ein wichtiger Koaktivator von dMyc ist und für die Ausführung einiger biologischer Funktionen von dMyc Bedeutung hat.

Summary

The Myc protein is a potent oncogene that is frequently misexpressed in human cancers. *myc* family genes control a wide variety of cellular processes such as cellular growth and proliferation, metabolism or apoptosis. However, the *cis*-acting determinants, for example the conserved protein domains, and the *trans*-acting determinants, e.g. the identity of the Myc-interacting proteins affecting Myc`s biological activity, are still incompletely understood.

In this study we investigated the role of dMyc, which is the only homologue of the Myc family members in *Drosophila* and can partially substitute for vertebrate c-Myc, in cell culture assays and *in vivo.* In a first project conserved motifs within the Myc protein (N-terminus, MB2, MB3) were analysed with regard to their role for cellular growth, proliferation and apoptosis. Wildtype and mutant forms of dMyc were expressed either in *Drosophila* S2 cells or in transgenic animals *in vivo*. We showed that the N-terminus of dMyc is necessary for all dMyc dependent functions. Amazingly, a deletion in the highly conserved MB2, which in vertebrate Myc proteins was shown to recruit proteins of HAT complexes to Myc (TRRAP, RUBVL1), only weakened dMyc activity, and a dMyc mutant lacking this domain was even able to rescue a dMyc null allele to adulthood. We further demonstrate that MB3 affects dMyc stability in a negative way. Moreover, a deletion of MB3 enhanced Myc`s ability to promote cell growth and apoptosis, but not its efficiency to activate transcription of E-box dependent target genes or RNA Pol III dependent endogenous targets *in vivo*.

In a second project we performed a loss-of-function screen in order to find new dMyc co-factors. The screen identified two proteins, Delta, a Notch ligand, and Chinmo, a protein that governs neuronal temporal identity during postembryonic development of the *Drosophila* brain. Both genetically interact with *dmyc* during eye development. We present evidence that dMyc is limiting for Chinmo since the deleterious effects of Chinmo overexpression are reduced by a reduction of dMyc levels. Conversely, dMyc depends on Chinmo to fulfil its biological activities in wing imaginal discs. Furthermore, our data show that Chinmo binds dMyc physically via its BTB/POZ domain and activates endogenous dMyc target genes associated with ribosome biosynthesis. Chinmo efficiently transactivates dMyc target genes, and this activation of transcription is fully dependent on dMyc. Taken together, our data suggest that Chinmo is a co-activator of dMyc that is necessary for some biological functions of dMyc.

General Introduction

The transcription factor Myc is a potent oncogene known to be involved in a wide variety of cancers. Originally, the *c-myc* gene was discovered as the cellular homologue of the avian myelocytomatosis retroviral *v-myc* oncogene in 1982 (Bishop, 1982). Myc family genes, *c-myc*, N-*myc*, and L-*myc* activate and repress a large number of target genes. Moreover, they were shown to have neoplastic potential (Marcu et al., 1992). Recent publications suggest, that c-Myc influences a wide variety of target genes involved in cellular processes like differentiation, angiogenesis, metabolism, cell growth, cell cycle progression and apoptosis during normal development (reviewed in Dang et al., 2006). Deregulation of Myc contributes to uncontrolled cell proliferation, genomic instability, escape from immune surveillance, immortalisation and independence of growth factors, which in turn leads to the formation of tumours. Therefore, Myc needs to be tightly regulated by external signals like growth factors.

Myc`s functional domains

The c-*myc* gene is located on human chromosome 8 and consists of three exons (Battey et al., 1983). The ORF starts at the second exon and codes for a protein of 439 amino acids (c-Myc 2). Translation initiation at a CUG in the first exon leads to a 454 amino acids long protein (c-Myc 1), and a third form arises from translational initiation at a conserved downstream AUG (c-Myc S), lacking most of the N-terminal part of the protein (Hann et al., 1988; Spotts et al., 1997).

b-HLH-LZ

Several years after the identification of *c-myc*, the Myc C-terminus was found to contain a helix-loop-helix motif (HLH) and a leucine zipper (LZ), motifs that had earlier been shown in other proteins to bind DNA (Landschulz et al., 1988). Myc family proteins appear to not homodimerise under physiological conditions but instead form heterodimers with the Max protein (Blackwood and Eisenman, 1991). So far, Myc was shown to depend on its binding partner Max, a small b-HLH-LZ protein. The heterodimer binds to so-called E-boxes (CACGTG) in order to bind DNA and activate target genes. Additionally, E-box related sites are bound by the heterodimer (Grandori et al., 1996).
However, we found out recently that dMyc, the homologue of c-Myc in *Drosophila*, is able to fulfil some functions independently of dMax. Thus, dMyc does not require dMax for induction of growth or endoreplication in polyploid larval tissues (Steiger et al., submitted).

In the rat PC12 pheochromocytoma cell line, a functional Max protein is not expressed (Hopewell and Ziff, 1995). Since overexpression of Myc in these cells leads to apoptosis, this suggests that Myc acts independently of Max in PC12 cells (Wert et al., 2001).

The N-terminus

The Myc N-terminus was found to function as a transactivation domain, spanning two conserved motifs, Myc Box 1 (MB1), located between amino acid 45-63 and Myc Box 2 (MB2), located between amino acid 128-144 (the numbering corresponds to human c-Myc).
Consistent with its role as transcriptional activation domain the Myc N-terminus was shown to recruit several co-factors like TRRAP (McMahon et al., 1998) or P-TEFb (Eberhardy and Farnham, 2002). Moreover, the evolutionary highly conserved MB2 is specifically implicated in the recruitment of the co-factors Tip48, Tip49 (Wood et al., 2000) to Myc.
In agreement with this observation, c-Myc S and an N-Myc truncation analogous to c-Myc S that lack the N-terminal region of Myc including MB1, but retain MB2, are unable to activate transcription (Cowling and Cole, 2008; Spotts et al., 1997). Surprisingly, c-Myc S retains the ability to regulate proliferation and apoptosis (Xiao et al., 1998), even in the absence of endogenous Myc.
These observations for MB1 contrast with other studies that suggest that MB1 is not necessary for transactivation (Oster et al., 2003). Moreover, a deletion of MB2 blocks all biological functions of Myc that were analysed in cell culture assays. Thus, Myc`s ability to induce proliferation in cell culture is inhibited when MB2 is deleted (Conzen et al., 2000; Hirst and Grandori, 2000). Myc is also unable to promote apoptosis and transformation when MB2 is missing (Conzen et al., 2000; Oster et al., 2003). Moreover, stable transfection of a MB2 mutant in 3T3-L1 preadiposite cells showed that such a mutation cannot block differentiation into adiposites anymore (Freytag et al., 1990).
However, Myc is not able to repress certain target genes, like *gas1* and *C/EBP*α, when MB2 is deleted indicating that this domain is normally involved in the repression of those genes (Lee et al., 1997; Li et al., 1994). Altogether, the ability to activate and repress target genes is dramatically reduced when MB2 is missing (Cowling and Cole, 2006; Li et al., 1994). Myc is also capable of autoregulation by repressing the c-*myc* locus itself. A c-Myc mutant lacking MB2 was not able to repress c-*myc* anymore but it was still able to repress *gadd45* (Oster et al., 2003). Thus, two different repression mechanisms by Myc must exist. Additionally, c-Myc S and a truncated form of N-Myc were shown to still repress c-Myc repressed targets,

but did not activate the c-Myc induced genes anymore (Cowling and Cole, 2008; Spotts et al., 1997).

Stabilization and degradation of Myc by the Ras pathway was also linked to the N-terminus, since Ras-induced phosphorylation of Ser62 leads to a stabilization of the Myc protein (Sears et al., 2000; Yeh et al., 2004). However, the role for MB1 and MB2 regarding their biological activities needs to be confirmed *in vivo*.

MB3 & MB4

The c-Myc protein contains two additional conserved domains (besides MB1, MB2 and the b-HLH-LZ), Myc Box 3 ($MB3^{188-199}$), located between amino acid 188-199 and Myc Box 4 (MB4), located between amino acid 317-334 (the numbering corresponds to human c-Myc (MB3) and human N-Myc (MB4)), which are situated in the central part of the protein. Deletion of $MB3^{188-199}$ potentiates Myc dependent induction of apoptosis and inhibits cell transformation (Herbst et al., 2005). A different nomenclature was used for a different region also called MB3, located between amino acid 259-270 (the numbering corresponds to human c-Myc), which we are going to use in the future, containing a highly conserved PEST-domain (Cowling and Cole, 2006). PEST regions (sequences rich in proline, glutamic acid, serine and threonine residues) are often associated with unstable proteins (Rogers et al., 1986). A deletion of 11 amino acids in the acidic region (MB3) of v-Myc reduced the efficiency to transform bone marrow cells (Heaney et al., 1986). Mutants containing deletions in the central acidic portion in the v-Myc protein moreover show differences in transformation of Japanese quail and chicken macrophages (Biegalke et al., 1987).

The MB4 motif was shown to be involved in apoptosis, transformation and G2 arrest (Cowling et al., 2006).

Biological functions of Myc

Regulation of the cell cycle by Myc

The cell cycle is defined by a series of events that lead to the duplication of a cell. It involves two major periods, the interphase in which cell growth takes place and the M-phase in which the cell divides. Defects in cell cycle regulation can result in cancerous growth and developmental abnormalities. To prevent such defects, the cell cycle needs to be tightly controlled. Early studies implicated c-Myc in the G0/G1 transition (Freytag, 1988). Some E-box containing genes that are involved in cell cycle regulation have been identified as direct Myc target genes. Among these genes are: *cyclinD1 & D2, cdk2, cyclinA, cdk4, cyclinB1, cdk1, cdc25A and E2F* (Bouchard et al., 2001; Hermeking et al., 2000; Menssen and Hermeking, 2002). A scheme of the cell cycle is shown in Figure I. Cyclin-dependent kinases (CDKs) are key regulatory proteins, which in connection with their positive regulators, cyclins, trigger the transition from one cell cycle phase to another.

Extracellular growth signals induce the expression of D-cyclins, the first cyclins to be synthesized in the cell cycle. *CyclinD2* was for example shown to be a direct target of Myc *in vivo* (Bouchard et al., 2001). Upon binding of Myc to the *cyclinD2* promoter, expression of *cyclinD2* is enhanced. The D-cyclins themselves activate *cdk4* (also a Myc target gene) and *cdk6*. After phosphorylation and inactivation of the Rb protein by cyclinD/cdk4 and cyclinD/cdk6, the transcription factor E2F is released, which itself activates *cyclinE*, *cyclinA* and other S-phase specific genes. It was demonstrated that constitutive expression of Myc leads to an increase in *cyclinE & A* (Jansen et al., 1993). Moreover, Myc and Ras accumulate active cyclinE/cdk2 and E2F (Leone et al., 1997). Finally, as a result of the above processes, the cyclinE/cdk2 complex drives the cell into S-phase.

Overexpression of Myc was shown to drive quiescent cells into the cell cycle, to promote S-phase entry and a shortening of G1-phase in cycling cells (Karn et al., 1989; Steiner et al., 1996). On the other hand, reduction of Myc levels prevents quiescent cells from entering the cell cycle in response to mitogenic signals (Roussel et al., 1991). Similar observations were made with a derivative of the rat1 fibroblast cell line, in which the endogenous c-*myc* gene had been knocked out. Those c-$myc^{-/-}$ cells had a prolonged G1 and G2 phase and three fold reduced proliferation rate. Thus, not only G1 is affected by Myc but also G2 (Mateyak et al., 1997).

Induction of growth promoting genes, but also suppression of growth inhibitory genes, leads to cell proliferation. The CDK inhibitors *p21* and *p15INK4B* were for example, shown to be

repressed by Myc (Staller et al., 2001; Wu et al., 2003). Myc was also shown to repress genes involved in growth arrest like *gas1* and *gadd45* (Lee et al., 1997; Marhin et al., 1997). The Cdc25 proteins are a family of phosphatases that remove inhibitory phosphates from Cdks. c-Myc was shown to induce cell proliferation by activation of genes like *cdc25A* (Galaktionov et al., 1996).

In summary, Myc directly controls genes involved in cell cycle regulation. This makes clear that misregulation of Myc directly affects the cell cycle.

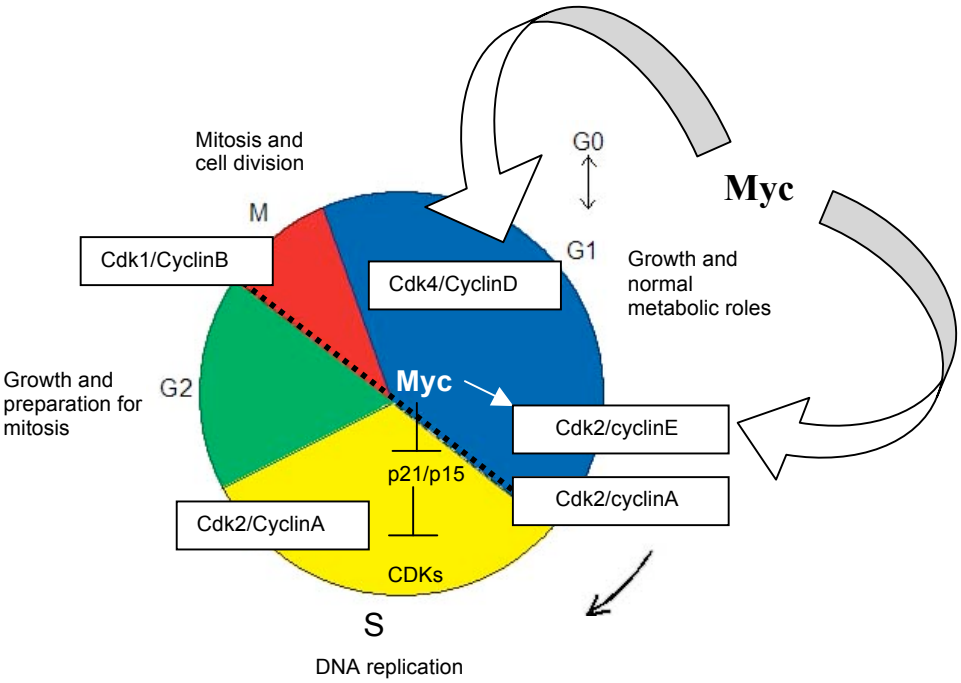

Figure I: The human cell cycle. Different CDKs and cyclins regulate different phases of the cell cycle. The dashed line indicates the two cell cycle checkpoints G1/S and G2/M. Damaged cells arrest in their progression through the cycle and, if the damage is irreparable, will be directed to undergo cell death. Myc directly regulates components of the cell cycle.

Regulation of cell growth by Myc

Regulation of cell growth is a major feature of Myc function. This has become even clearer as Myc was found to be involved not only in the activation of RNA Polymerase II-transcribed genes (reviewed in Dang 2006), but Myc was also found to activate the expression of RNA Polymerase I- & III-transcribed genes (Gomez-Roman et al., 2006; Gomez-Roman et al., 2003; Grewal et al., 2005). The protein synthetic machinery is regulated at two stages– ribosomal synthesis and translation initiation. Ribosomal biogenesis starts with rRNA transcription (Jacob, 1995), followed by RNA processing (Eichler and Craig, 1994) and is completed by transcription and translation of ribosomal proteins and assembly of the ribosomes. Translational initiation requires mRNAs and translation initiation factors (Hershey, 1991). Myc`s target genes include genes that encode rRNAs and proteins involved in ribosome biogenesis and protein synthesis and a number of those genes are direct targets of c-Myc, such as *5S RNA* and *tRNA* genes, which are transcribed by Polymerase III (Gomez-Roman et al. 2003). Thus, c-Myc promotes growth through enhancement of ribosomal biogenesis by regulation of all three RNA Polymerases.

This activity of Myc is demonstrated by Schuhmacher et al., 1999. These authors observed that Myc positively regulated protein synthesis in the B-cell line P493-6 that carries a conditional *myc* allele, and that Myc could induce a size increase in these cells. Additionally, liver cells and B-lymphocytes of mice overexpressing Myc were significantly larger (Iritani and Eisenman, 1999; Kim et al., 2000).

These data contrast with the observation that, after reduction of Myc levels, mice were smaller because of a reduction of cell number rather than cell size (Trumpp et al., 2001). However, the previous observation regarding Myc`s role in protein biosynthesis favours a role for Myc in the regulation of growth.

Regulation of cell death by Myc

There are two different pathways of apoptosis, the intrinsic pathway, which can be triggered by various intracellular cues such as DNA damage, hypoxia or oncogene activation. On the other hand there is the extrinsic pathway, which includes hormones, growth factors or cytokines. Myc was shown to affect both pathways. The first evidence that Myc is involved in the regulation of apoptosis was found in the early 1990s as a lot research on cell death was done (Askew et al., 1991; Evan et al., 1992). One of the earlier studies implicated that c-Myc-induced apoptosis can be inhibited by the proto-oncogene Bcl-2 in serum starved ovary cells or Rat1/MycER fibroblasts (Bissonnette et al., 1992; Fanidi et al., 1992). Later on, Myc was shown to enhance apoptosis by activating the ARF-Mdm2-p53 axis (reviewed in Meyer et al., 2006). In contrast, Myc proliferation-promoting activity is reduced when co-overexpressed with ARF, a tumour suppressor that stabilizes and thereby activates p53. The tumour suppressor p53 induces the cell cycle inhibitor p21, thus blocking cell cycle progression. Myc was demonstrated to inhibit p21 through interaction with Miz-1, thus the cell undergoes apoptosis rather than cell cycle arrest (reviewed in Meyer et al., 2006). In addition, p53 can directly repress c-*myc* by binding to the c-*myc* promoter (Ho et al., 2005). Thus, the levels of p53 and Myc determine the cell fate -cell cycle arrest or apoptosis. However, Myc-induced apoptosis seems to be influenced by various cues. The pro-apoptotic protein PUMA (P53-Up-regulated Modulator of Apoptosis) was shown to act downstream of Myc and p53. Loss of PUMA leads to a decrease of Myc-induced apoptosis (Jeffers et al., 2003). In 2007, the E3-ligase Cullin 7 (Cul7) was shown to directly bind to p53, leading to elevated p53 protein levels. Thus, Myc induced apoptosis is inhibited and Cul7 and Myc co-operate to transform Rat1 cells (Kim et al., 2007).

In summary, one can group a variety of pro-apoptotic proteins as “ambassadors of Myc-induced apoptosis” that act as tumour suppressors when Myc is deregulated and whose absence will favour Myc induced apoptosis and transformation, e.g. p53, ARF, BIM, 4EBP1 (reviewed in Meyer et al., 2006). Another group are the “abrogaters of Myc-induced apoptosis”, oncogenes that cooperate with deregulated Myc, block apoptosis and will trigger Myc to proliferation, e.g. Mdm2, Cul7, BCL-2, GSK3/FBW7, eIF4E (reviewed in Meyer et al., 2006).

Recently, a new aspect of Myc induced apoptosis was discovered in *Drosophila*. Wing imaginal discs containing clones that express lower levels of dMyc compared to their neighbouring cells were shown to be influenced by “cell competition”. Cells that express

higher levels of Myc (dm^{P0}/+) induced cell death in neighbouring cells that were homozygous mutant for the weak hypomorphic *myc* allele dm^{P0} (dm^{P0}/dm^{P0}) (Johnston et al. 1999). Conversely, cell clones that overexpress dMyc reduced the growth rate of their neighbouring wildtype cells and finally eliminated them (De La Cova et al., 2004; Moreno and Basler, 2004).

Myc, Max, Mxd: The network

The small Max protein was shown to be incapable of activating reporter genes (Kato et al., 1992), but to have very weak repressor activity when expressed at high levels (Kretzner et al., 1992). As described earlier, Myc forms heterodimers with its partner Max in order to activate target genes. Both proteins contain a b-HLH-Zip domain, which is necessary for dimerisation of the proteins and binding to DNA. In contrast to Myc, Max is able to form homodimers that can bind to E-box sequences *in vitro* (Berberich and Cole, 1992; Kato et al., 1992). The two complexes, Myc-Max and Max-Max, compete with each other for shared target genes (Sommer et al., 1998). Apart from Myc, Max interacts with other b-HLH-Zip proteins. Those proteins include Mnt (Hurlin et al., 1997), Mxd1-4 (Ayer et al., 1993; Hurlin et al., 1995; Zervos et al., 1993) and Mga (Hurlin et al., 1999). All of those proteins behave like Myc in the sense that they are unable to form homodimers, appear to be incapable to bind DNA alone and bind to E-box sequences together with Max. In contrast to Myc, they act as transcriptional repressors and (at least some of them) were shown to block Myc-dependent cell transformation in cell culture (Koskinen et al., 1995; Vastrik et al., 1995). As only one protein of the Mnt/Mxd/Mga transcription factors is present in *Drosophila*, dMnt, this introduction will predominantly focus on Mnt. To some extent the Mxd proteins are thought to have similar properties (with certain restrictions).

Since Max either binds to Myc or the Mnt/Mxd/Mga transcription factors, the question arose whether Max becomes rate limiting in some situations. Indeed, Max can become rate limiting in mouse embryo fibroblasts when c-Myc levels are elevated (Walker et al., 2005). A homozygous deletion of the Mnt protein led to different types of tumours in mice (Hurlin et al., 2003). The role of Mnt as a direct antagonist of Myc became even clearer by the fact that both regulate a similar set of target genes (Toyo-oka et al., 2006). Interestingly, elimination of Mnt partially rescues the slow growing phenotype of cells that contain reduced Myc levels and a loss of Mnt, like overexpression of Myc, sensitizes cells for apoptosis (Nilsson et al., 2004). Thus, the Max-Mnt complex is a direct antagonist of the Max-Myc complex.

Transcriptional activation by Myc

The Myc-Max complex is thought to recruit proteins of Histone Acetyl Transferase (HAT) complexes (TIP60, SAGA) and chromatin remodelling complexes (SWI/SNF), thereby creating a "histone code" which in turn loosens the chromatin structure and allows other factors to bind (Cowling and Cole, 2006; Wierstra and Alves, 2008). The above mentioned complexes are thought to facilitate transcription initiation and elongation. Consistent with this notion, Myc binds to DNA and activates transcription by recruiting TRRAP and increasing especially histone H4 acetylation on Myc target genes (Frank et al., 2001). Myc was also shown to bind to the DNA-helicase/ATPases Tip48 and Tip 49, which are components of the TIP60 HAT complex, like TRRAP (Wood et al., 2000).
On the other hand, the Max-Mnt heterodimer was shown to recruit the co-repressors Sin3A and Sin3B, which themselves interact with histone deacetylases (HDAC) (Hurlin et al., 1997; Popov et al., 2005), suggesting that these complexes promote a nucleosomal confirmation that is unfavourable for transcription by deacetylation of the chromatin (or by other actions).

TRRAP/ GCN5

One major co-factor of Myc is the huge **TR**ansactivation/ t**R**ansformation **A**ssociated **P**rotein (TRRAP) (McMahon et al., 1998). The N-terminus of Myc is required for the interaction since deletions of parts that inhibit transformation also inhibit interaction with TRRAP (McMahon et al., 1998). TRRAP is not only part of the TIP60 complex (Ikura et al., 2000), but also part of the SAGA complex (Grant et al., 1998). An internal domain (aa 1899-2026) of TRRAP was shown to be bound by Myc (Park et al., 2001). So far it is not clear whether the binding of Myc to TRRAP has a special effect on TRRAP activity or if it only recruits TRRAP (and the associated complexes).
The SAGA complex contains only one known catalytic subunit, GCN5 (Grant et al., 1997). GCN5 functions as a histone acetyltransferase and is recruited to Myc via TRRAP (McMahon et al., 2000). Myc was also demonstrated to be a substrate of GCN5 in mammals where it was shown that GCN5 acetylates Myc *in vivo* and thus increases Myc`s stability. As a consequence, the transcription of Myc target genes is increased (Patel et al., 2004).

Recently, TRRAP and GCN5 were implicated in the recruitment of RNA Polymerase III by Myc. The complex (c-Myc, TRRAP, GCN5) binds to the promoter of the RNA Poll III targets *5S RNA* and *tRNA* and histone H3 gets hyperacetylated, and in parallel TFIIIB binds to DNA. These two processes recruit RNA Pol III and lead to initiation of transcription (Kenneth et al., 2007).

RUVBL1&2

RUVBL1 (Tip49) and RUVBL2 (Tip48) are subunits of the TIP60 and SRCAP (**S**nf-2-**r**elated **C**REB-binding protein **a**ctivator **p**rotein) complex in animals (reviewed in Gallant, 2007). However they can also bind independently of TRRAP to Myc (Wood et al., 2000). Tip48 and Tip49 were not only implicated in binding to Myc but also to other transcription-associated proteins like β-catenin or E2F1 (only Tip49) (Bauer et al., 2000; Dugan et al., 2002). RUVBL1 & 2 are thought to be involved in chromatin remodelling in yeast, since RUVBL1 deletion disrupted the INO80 chromatin remodelling complex (Jonsson et al., 2004; Shen et al., 2000). A dominant-negative version of RUVBL1 enhanced Myc-induced apoptosis and inhibited transformation by Myc; proliferation was not affected by this mutant (Dugan et al., 2002).

HECTH9/SKP2

The activity of transcription factors is closely regulated by ubiquitination (Conaway et al., 2002). Also, ubiquitination of Myc was shown to enhance Myc`s potential to activate target genes and this went along with a reduced half-life (Salghetti et al., 1999). Ubiquitin ligases were found to interact with Myc, e.g. Skp2 (Kim et al., 2003; von der Lehr et al., 2003), HectH9 (Adhikary et al., 2005) and Fbw7 (see below).

Skp2 is an F-box protein and mediates ubiquitination by binding two regions in Myc (amino acids 129-147 [MB2] and 379-418). A Luciferase reporter assay revealed that Skp2 stimulated the activity of the α-*prothymosin* (a Myc target gene) promoter as efficiently as Myc alone and overexpression of both proteins increased the activity even further (von der Lehr et al., 2003). Skp2 was also able to activate endogenous Myc targets and this activation was Myc dependent. This suggests that activation of Myc target genes correlates with ubiquitination of Myc.

The E3 ubiquitin ligase HectH9 site-specifically ubiquitinates Myc *in vitro* and a mutation of six lysine residues in the centre of Myc reduced ubiquitination in transient assays. Moreover,

inhibition of HectH9 was shown to impair gene activation by Myc (Adhikary et al., 2005). Miz-1 was shown to antagonize the ubiquitination of Myc by HectH9.

Transcriptional repression by Myc

Myc is also capable of target gene repression by different mechanisms, one of which involves the transcriptional activator Miz-1. Myc causes trans-repression of Miz-1 target genes by direct interaction with Miz-1 (reviewed by Wanzel et al., 2003). The CDK inhibitor *p15* ^{INK4B} is upregulated upon binding of a Miz-1-p300 complex. The Myc-Max complex directly binds to Miz-1 and prevents activation of *p15*^{INK4B} by competing with p300 for the binding site in Miz-1 (Staller et al., 2001).

If DNA damage occurs p53 will be activated (by stabilization of the protein) and the affected cells will be stalled at the G1/S phase transition. P53 induces PUMA and other pro-apoptotic factors and *p21*^{Cip1}, resulting in apoptosis or cell cycle arrest. Myc repression of *p21*^{Cip1} was shown to influence DNA damage response by flipping the choice from cytostasis towards apoptosis by direct interaction with Miz-1 at the *p21*^{Cip1} promoter and thus preventing the inhibition of cell death by *p21*^{Cip1} (Seoane et al., 2002). *P21Cip1* and *p15*^{INK4B} do not contain a sequence specific E-box, consistent with the observation that repression by Myc influences a different set of target genes than activation (Seoane et al., 2002; Staller et al., 2001). Hence, Myc can activate and repress target gene expression by direct interaction with other co-factors.

Stabilization of Myc

GSK3/FBW7

Different serine/threonine-directed-kinases were shown to directly phosphorylate distinct sites in the c-Myc protein. Glykogen synthase kinase 3 (GSK3) phosphorylates T58 in the Myc N-terminus (reviewed in Hann, 2006). This phosphorylation requires a previous phosphorylation at S62 by RAS-activated pathways or by Cdk1 (Lutterbach and Hann, 1994; Sears et al., 2000). The ubiquitin ligase Fbw7 was shown to depend on phosphorylation of T58 to ubiquitinate c-Myc (Welcker et al., 2004). Fbw7 is mutated in many human epithelial cancers and this loss of Fbw7 is thought to increase tumourigenesis by stabilizing Myc. Thus, phosphorylation of Myc modulates Myc`s biological activity.

Myc in flies: The dMyc protein

In contrast to humans, flies carry only one Myc, Max and Mxd//Mnt homologue each, dMyc, dMax and dMnt (Gallant et al., 1996; Loo et al., 2005; *Steiger et al., 2008*). The first Myc mutant of any organism was found in the 1930s in *Drosophila* (Bridges, 1935). This mutation was called *diminutive* for its small body and bristle size and could be mapped in 1996 to the *dmyc* gene (Gallant et al., 1996; Lindsley and Zimm, 1992). The dMyc-dMax heterodimer binds canonical E-box sequences to activate the transcription of target genes and the dMax-dMnt complex antagonizes this function (Gallant et al., 1996; Loo et al., 2005).
In contrast to mammals, the N-terminus of dMyc in not very well conserved but it contains a well-conserved DCMW motif in MB2. Moreover, a centrally located PEST region and a b-HLH-LZ in the C-terminal part of the protein are conserved (reviewed in Gallant, 2006).
Importantly, the c-Myc and dMyc proteins are partially interchangeable. On the one hand, dMyc can rescue proliferation defects in mouse embryo fibroblasts that lack *c-myc* (Trumpp et al., 2001), transform rat fibroblasts when expressed along with human RasV12 (Schreiber-Agus et al., 1997) and substitute for c-Myc in transactivation assays in human cell culture (Gallant et al., 1996). On the other hand, c-Myc S and c-Myc 2 rescued a lethal *dmyc* allele to adulthood (Benassayag et al., 2005).
This shows that the Myc, Max and Mxd/Mnt proteins are functionally conserved from humans to flies, although the network is less complex, since only one homologue of each component exists in flies.
Two pathways controlling the expression of Myc in *Drosophila* have been identified so far: Wingless/Wnt and Decapentaplegic/BMP/TGF-β (reviewed by de la Cova and Johnston, 2006). Wingless was for example shown to repress dMyc in the zone of non-proliferating cells in the *Drosophila* wing imaginal disc (reviewed by de la Cova and Johnston, 2006).

Biological functions of dMyc

Weak hypomorphic *dmyc* alleles (dm^{P0}, dm^{1}) have a small body size, thin bristles and a prolonged development. In contrast to c-Myc mutants in vertebrates, those mutants only contain smaller, but not fewer, cells (Johnston et al., 1999; Trumpp et al., 2001). Among the dMyc target genes one can find ribosomal protein genes. Ribosomal gene mutations (so-called *Minute* mutations) lead to a smaller body size as a consequence of smaller cells, which is comparable to the phenotype of *dmyc* mutant alleles. Moreover, *Minute* mutants exhibit a thin bristle phenotype comparable to *dmyc* mutants. Conversely, nucleolar size is enhanced

upon overexpression of dMyc, indicating that ribosomal biogenesis is enhanced (Grewal et al., 2005). These observations suggest a link between dMyc activity, cell growth and ribosomal proteins.

Overexpression of dMyc in clones of wing imaginal discs resulted in an increase in cell size (by accelerating cellular growth) and in a shortened G1 phase of the cell cycle. Conversely, imaginal disc cells mutant for *dmyc* are reduced in size and have a prolonged G1 phase (Hulf et al., 2005; Johnston et al., 1999). Endoreplication, a process where DNA replication takes place in the absence of mitosis, resulting in enlarged nuclei, is occurring in the *Drosophila* fat body and salivary glands. This process is responsible for the massive growth of larvae during their development, since endoreplicating tissue makes up the major part of those larvae. Overexpression of dMyc in this tissue increases the size of endoreplicating cells (Pierce et al., 2004). This indicates that larval growth and endoreplication are controlled by dMyc.

Like *dmyc* mutants, *dmax* mutants are small, however the phenotypes are less severe (*Steiger et al., 2008*). This observation led to the question whether there are dMax-independent functions for dMyc. Indeed, not all biological functions of dMyc fully require dMax, like cell competition, endoreplication and the regulation of Pol III transcribed genes (*Steiger et al., 2008*).

The only member of the Mxd//Mnt family of Myc antagonists was called dMnt since it is most similar to Mnt regarding its size and structure. In contrast to an *mnt* knock-out in mice, a *dmnt* mutation in flies is viable; the mutant flies have larger cells and are bigger (Loo et al., 2005). DMnt was also shown to antagonize larval growth and endoreplication in the developing larvae (Pierce et al., 2004). Thus, dMyc, dMax and dMnt are required for proper regulation of cell and organismal size *in vivo.*

Transcriptional targets of dMyc

With the DamID technique, a protein of interest is tethered to *Escherichia coli* DNA adenine-methyltransferase (Dam). The Dam fusion will bind binding sites of the protein of interest *in vivo*, which in turn leads to local methylation. These sites can be mapped afterwards (van Steensel and Henikoff, 2000). This DamID technique was used to identify genomic binding sites of dMyc, dMnt and dMax in *Drosophila* KC cells. The methylated DNA fragments were analyzed by microarrays, which revealed that about 15% of the *Drosophila* coding regions was bound collectively by the 3 proteins. Those binding regions correlated with the presence of E-boxes, CG-repeats and DNA Replication Elements (DRE). Binding of dMyc to genomic

sites was significantly increased when dMax was expressed at high or low levels indicating that dMyc is very sensitive to dMax levels (Orian et al., 2003).

Microarray analysis revealed that upon downregulation of *dmyc* in *Drosophila* Schneider 2 cells by RNAi about 30 genes were significantly downregulated at 3 different time points after addition of dsRNA (Hulf et al., 2005). Those genes were predominantly involved in ribosome biogenesis, rRNA processing or RNA binding like *fibrillarin* or *CG1542*. A large number of those genes were also shown to be upregulated after dMyc overexpression. Moreover, those target genes contained specific Myc binding sites (E-boxes) that are located within the first 100 nucleotides after the transcription start site (Hulf et al., 2005). Those microarrays did not include RNA Polymerase I & III transcribed genes, which were later also shown to be target genes of Myc in mammals (Pol I & III) and *Drosophila* (Pol I) (reviewed by Gomez-Roman et al., 2006). During larval development dMyc controls ribosomal biogenesis and Pol I transcribed rRNA genes (Grewal et al., 2005).

Moreover, qRT-PCR experiments were performed on larvae overexpressing dMyc in the absence of *dmax*. The RNA polylmerase III transcribed gene *5S RNA* and $tRNA^{Leu}$ were strongly upregulated in those larvae (Steiger, 2007, PhD thesis). Thus, dMyc controls the expression of a wide variety of target genes, which account for Myc`s potential to induce growth.

Stability of dMyc

Moberg et al. (2004) found that Archipelago (Ago), an F-box component of SCF-ubiquitin ligase and the *Drosophila* ortholog of a human tumour suppressor (Fbw7), negatively regulates the levels and activity of dMyc protein *in vivo*. The interaction between c-Myc and Fbw7 is mediated by the WD repeat of Fbw7 and a conserved motif whose central feature is L-L-T-P-P in c-Myc. These authors also found 7 degenerated copies of this motif in dMyc and the copy with the best fit to the consensus was located within MB3. Therefore, there may be a connection between ubiquitination and degradation of dMyc and MB3.

Myc in tumours: Approaches for therapy

Myc controls cellular processes like cell growth and proliferation, apoptosis, cell cycle progression or differentiation. Thus, it is not surprising that Myc needs to be tightly regulated by external signals. Misregulation of Myc contributes to tumourigenesis, e.g. upon mutations in the pathways that control Myc (such as the Wg pathway). Such mutations lead to uncontrolled cell proliferation, apoptosis or independence of growth factors.

Myc`s involvement in human neoplasia was first shown by the observation that c-*myc* mRNA and protein is constitutively overexpressed in Burkitt`s lymphoma. This is caused by a chromosomal translocation that brings the immunoglobulin enhancer close to c-*myc* (reviewed in Vita and Henriksson, 2006). Since then Myc was found to be frequently deregulated in many types of human cancers. The chromosomal aberrations that lead to such tumours are not only translocations, but also gene amplification or point mutations (reviewed by Vita and Henriksson, 2006).

Since elevated Myc levels contribute to tumourigenesis, the question arose whether one could specifically inactivate Myc in the affected cancer cells. Myc inactivation in tumours results in proliferative arrest, differentiation and apoptosis, as shown by conditional transgenic mouse models (Arvanitis and Felsher, 2006). However, upon reactivation tumourigenesis is rapidly restored in some cases. Moreover, by additional genetic events tumours can become independent of Myc overexpression (Arvanitis and Felsher, 2006).

Although drugs that specifically target Myc could act on a wide variety of human cancers like haematological malignancies (e.g. Burkitt`s lymphoma, B-cell acute lymphocytic leukaemia) and solid tumours (e.g. breast cancer, melanoma, prostate caner), up to date there are no such drugs available. In part, this may be because Myc is a nuclear transcription factor lacking specific enzyme activity. Nevertheless, there are different strategies for targeting Myc in tissue culture cells. Antisense oligonucleotides and RNAi silence *myc* gene expression (Harel-Bellan et al., 1988; Wang et al., 2005) and small molecule inhibitors disrupt Myc/Max heterodimers, block interaction with co-factors, modulate the function of key target genes or affect Myc protein stability (Berg et al., 2002; Sundberg et al., 2006). We try to understand Myc functions *in vivo*, by using mutations to get a better understanding on how Myc controls cell proliferation, cell growth, apoptosis and differentiation. On the basis of this research an optimal drug might be established to control Myc induced cancers in humans.

Specific Aims of the project

Mutational analysis of dMyc protein *in vivo* (Chapter 1)

The aim of this project was to analyse the specific roles for the N-terminus as well as MB2 *in vivo* with regard to some biological aspects of Myc in tissue and in a living organism. Defining the function of the less understood MB3 was also of interest to this project.

For this purpose we used the model organism *Drosophila* to analyse effects of different dMyc mutants in a developing animal under controlled conditions. Conserved domains of Myc were either mutated (dMycMB2A) or deleted (dMycΔN, dMycΔMB2, dMycΔMB3) and the resulting proteins analysed with regard to their effects on cell size, cell number and apoptosis.

A deletion of the N-terminal domain in Myc completely abolished Myc`s biological activity. Surprisingly, mutation of MB2 only weakened, but did not fully inactivate dMyc function, such that an MB2-mutant form of dMyc could rescue the survival of a sizeable fraction of *dmyc*-null mutant flies. Transactivation, and the abilities to induce cell growth and apoptosis were only slightly affected by this deletion. Thus, the N-terminal part seems to be essential for all of dMycs biological functions and MB2 is important, but not essential, for all dMyc functions *in vivo*.

A special point was to analyse the functions of the highly conserved acidic domain (MB3), which is only poorly understood. We thought that such a highly conserved domain must have a specific function. We could show that a deletion of this acidic region stabilized the protein. Moreover, upon overexpression of dMycΔMB3 apoptosis was strongly enhanced. Interestingly, MB3 seems to be important for the activation of endogenous targets of dMyc like RNA Polymerase III transcribed genes. In summary, MB3 destabilizes dMyc and reduces some of Myc`s activities (apoptosis, growth) but not all (transactivation).

In vivo mutagenesis screen for dMyc co-factors (Chapter 2)

The aim of this project was to identify yet unknown dMyc co-factors *in vivo*.

Flies carrying the hypomorphic *myc* allele dm^{P0} are normally patterned and display only moderate growth defects: Very rarely they also show an aberrant eye morphology (<1 fly in 1000). Experiments with Pontin, a dMyc co-factor also known as RUVBL1 (Tip49) showed that the eye is particularly sensitive to a reduction in dMyc activity and that a transcriptional co-factor complex containing Pontin is critically required for dMyc function in the eye (Bellosta et al., 2005).

Encouraged by the results with Pontin, we carried out a large-scale loss-of-function mutagenesis screen to identify Pontin-like co-factors for dMyc. In parallel, the publicly available Exelixis and Drosdel collections of large genetically isogenic deletions were tested for interaction with dMyc. Since the breakpoints of those deletions are molecularly characterized, this facilitates the identification of genes of interest. So far we focused on one gene: c*hinmo* (*CG31666, rm, chnöpfli*), which was found in both screens. *Chinmo* not only interacted genetically with *dmyc* but the Chinmo protein also interacts physically with dMyc. Moreover, Myc was dependent on Chinmo to induce cell growth in clones of wing imaginal discs. Since transactivation of target genes was enhanced upon Chinmo and dMyc overexpression, we think that Chinmo acts as a co-activator of Myc.

Chapter I

Mutational analysis of dMyc protein *in vivo*

The conserved Myc Box 2 and Myc Box 3 regions are important, but not essential, for Myc function *in vivo*

D.Schwinkendorf & P.Gallant

Manuscript

The conserved Myc Box 2 and Myc Box 3 regions are important, but not essential, for Myc function *in vivo*

D.Schwinkendorf[2] & P.Gallant[1]

Zoologisches Institut,
Universität Zürich,
Winterthurerstrasse 190,
CH-8057 Zürich,
Switzerland

[1] author for correspondence:
gallant@zool.uzh.ch, +41446354812

[2]Molecular Life Sciences
University of Zurich
Winterthurerstrasse 190
CH-8057 Zurich
Switzerland

Abstract

Myc proto-oncoproteins are important regulators of growth and proliferation in development. Their functions have been evolutionarily conserved from insects to vertebrates, although the sequence conservation is limited to a few short domains. Here, we analyse the role of the most highly conserved domains, called Myc Boxes 2 and 3 (MB2 and MB3), and of the weakly conserved N-terminus for the biological activity of the single Myc protein in *Drosophila*, dMyc, in an animal *in vivo*. We find that a dMyc mutant lacking the N-terminus retains very little activity, even though this region does not affect dMyc protein levels. In contrast, deletion of MB3 stabilizes dMyc protein and increases its ability to promote growth and apoptosis, but at the same time also impairs Myc`s ability to activate RNA Polymerase III. Finally, mutation of the MB2 reduces transcriptional output and the biological activities of dMyc. Surprisingly though, dMyc without MB2 retains enough activity to partially rescue the lethality of a *dmyc* null mutation. Thus, although MB2 and MB3 are highly conserved in evolution, loss of either domain has comparatively mild consequences on Myc activity.

Keywords: growth, apoptosis, transcription, proteolysis

Introduction

Myc has been identified as a proto-oncogene that is frequently mutated and overexpressed in human and animal cancers (reviewed by Oster et al., 2002). During normal development and tissue homeostasis, Myc controls several cellular processes, most prominently growth, proliferation and apoptosis (de la Cova and Johnston, 2006; Pirity et al., 2006). These different activities of Myc have been attributed to its ability to stimulate or repress the transcription of many target genes (reviewed by Amati et al., 2001; Dang et al., 2006; Grandori et al., 2000). Myc is a rather atypical transcription factor, though, in that it controls a very large number of targets (up to 15% of all genes have been proposed to be modulated by Myc proteins; Fernandez et al., 2003; Orian et al., 2003), including genes transcribed by RNA Polymerases I & III. However, most of its targets are only moderately affected by Myc (reviewed by Dang et al., 2006). Experiments using chromatin immunoprecipitations followed by microarray analysis (ChIP-chip) even extrapolated that 25'000 genomic regions, many of which intergenic, are bound by c-Myc in human cells (Cawley et al., 2004; although these results were later disputed by Guccione et al., 2006). Some of these genomic targets may also reflect a transcription-independent role for Myc in the control of DNA replication that was recently described (Dominguez-Sola et al., 2007).

To molecularly understand how Myc controls its target genes and what might distinguish Myc from other transcription factors, several structure/function analyses of Myc have been carried out. Myc`s best understood domain, and the only one for which structural information is available (Nair and Burley, 2003), is the C-terminal basic-helix-loop-helix-leucine zipper region (bHLH-LZ) which serves as a dimerisation interface with a protein called Max (Blackwood and Eisenman, 1991) and also mediates the contact of Myc:Max heterodimers with DNA. In addition, several other proteins have been shown to contact this C-terminus, such as Miz-1 (see Cowling and Cole, 2006 for a recent review of Myc-interacting proteins; Peukert et al., 1997). This region is generally assumed to be essential for all of Myc`s activities, although recent reports suggest the existence of some C-terminus independent functions of Myc (Cowling and Cole, 2007; Steiger et al., 2008).

Myc`s N-terminal 143 amino acids contain a transcriptional regulatory domain (Kato et al., 1990) that interacts with different co-factors, such as TRRAP, a component of several histone acetyltransferase (HAT) complexes (McMahon et al., 1998), the STAGA HAT (Liu et al., 2003; Liu et al., 2008; McMahon et al., 2000), the DNA helicases Tip48 and Tip49 which also belong to different HAT and chromatin remodelling complexes (Wood et al., 2000), and the elongation factor P-TEFb (Eberhardy and Farnham, 2002). Accordingly, a version of c-

Myc that lacks the first 100 amino acids is inefficient in trans-activating its target genes (Hirst and Grandori, 2000; Spotts et al., 1997; Xiao et al., 1998), and it is unable to transform primary cells in culture (Xiao et al., 1998) or promote cell cycle re-entry of serum-starved fibroblasts (Hirst and Grandori, 2000). Surprisingly, though, such a truncated c-Myc protein retains substantial biological activity: it induces apoptosis in response to limitation of survival factors (Xiao et al., 1998), stimulates the rate of proliferation of exponentially growing fibroblasts (Hirst and Grandori, 2000), even in the complete absence of endogenous c-Myc (Xiao et al., 1998), and it can rescue a lethal mutation of the only *Drosophila myc* gene, *dmyc*, to viability (Benassayag et al., 2005).

These properties contrast with those of a short motif called Myc Box 2 (MB2) that is located between amino acids 128 and 143 in human c-Myc. The MB2 sequence is unique to Myc and evolutionarily highly conserved in all Myc proteins, down to invertebrates (reviewed in Gallant, 2006). Elimination of MB2 blocks or severely impairs all of Myc`s biological activities that have been tested in cultured cells: the ability to promote cellular proliferation (Conzen et al., 2000; Hirst and Grandori, 2000; Kenney et al., 2003; Lee et al., 1997), apoptosis (Conzen et al., 2000; Cowling et al., 2006; Dugan et al., 2002; Evan et al., 1992; Oster et al., 2003), transformation (Brough et al., 1995; Conzen et al., 2000; Cowling et al., 2006; Li et al., 1994; McMahon et al., 1998; McMahon et al., 2000; Nikiforov et al., 2002; Oster et al., 2003; Sarid et al., 1987; Stone et al., 1987), and block differentiation (Freytag et al., 1990a). Furthermore, an MB2-mutant Myc very inefficiently rescues the proliferation defect of rat fibroblasts lacking endogenous c-Myc (Bush et al., 1998; Nikiforov et al., 2002; Oster et al., 2003; Xiao et al., 1998). The MB2 motif is required for the efficient interaction with several co-factors such as TRRAP and associated HATs (Bouchard et al., 2001; Frank et al., 2001; McMahon et al., 1998; Nikiforov et al., 2002), the HAT complex component BAF53 (Park et al., 2002), TIP48 & TIP49 (Wood et al., 2000), Skp2 (Kim et al., 2003; von der Lehr et al., 2003), and for the stimulation of pre-mRNA capping (Cowling and Cole, 2007). Nevertheless, it has been shown that a Myc mutant lacking MB2 still efficiently activates the expression of some target genes and artificial reporters (Bello-Fernandez et al., 1993; Brough et al., 1995; Kato et al., 1990; Lee et al., 1997; Li et al., 1994; Nikiforov et al., 2002; Xiao et al., 1998), although many targets are only poorly activated by such a protein (Bouchard et al., 2001; Conzen et al., 2000; Cowling et al., 2006; Cowling and Cole, 2007; Hirst and Grandori, 2000; Kenney et al., 2003; Nikiforov et al., 2002). Such a MycΔMB2 mutant also fails to repress the genes that are normally down-regulated by wildtype Myc (Lee et al., 1997; Li et al., 1994), including the c-*myc* locus itself (Bush et al., 1998; Oster et al.,

2003; Penn et al., 1990). Importantly, the biological function of the MB2 cannot be replaced by the strong transactivation domain of the viral transcription factor VP16 (Brough et al., 1995), confirming that transcriptional activation is not the only job for this domain that is so important for the normal function of Myc.

Much less is known about the central 240 amino acids of Myc. This region is less conserved, with the exception of a motif called Myc Box 3 (MB3) that is found in all Myc proteins from insects to vertebrates (Cowling and Cole, 2006; note that the term "Myc Box 3" has been applied to a different region by Herbst et al., 2005). Although MB3 resembles a PEST domain, and hence might be expected to contribute to the degradation of Myc protein, its deletion does not affect Myc`s half-life (Herbst et al., 2004); this region also does not seem to contribute to transcriptional regulation by Myc (Kato et al., 1990). To date, MB3 has only been shown to be required for Myc`s ability to transform certain cell types (the rat fibroblast line Rat1a and primary chicken hematopoietic cells; Biegalke et al., 1987; Heaney et al., 1986; Stone et al., 1987). However, given its high evolutionary conservation, we consider it likely that MB3 fulfils some additional essential functions that may not be evident in cultured cells *in vitro* - and the same might possibly hold true for other conserved domains as well.

Therefore, we set out to address the importance of the conserved domains for Myc function *in vivo* in the context of intact tissues. We used *Drosophila melanogaster*, which contains a single Myc gene (*dmyc*) that is functionally interchangeable with its vertebrate counterparts (Benassayag et al., 2005; Gallant et al., 1996; Schreiber-Agus et al., 1997; Trumpp et al., 2001). Mutations in *dmyc* impair growth, such that flies carrying hypomorphic *dmyc* alleles (e.g. dm^{P0}) are delayed in their development and eclose as small adults (Johnston et al., 1999), whereas dm^{4} mutant flies (null for *dmyc*) fail to grow as larvae and die within a few days of hatching (Pierce et al., 2008b; Pierce et al., 2004; Steiger et al., 2008). Conversely, overexpression of dMyc promotes cellular growth (Johnston et al., 1999), endoreplication (Maines et al., 2004; Pierce et al., 2004), and apoptosis (De La Cova et al., 2004; Montero et al., 2008b). In the present study, we expressed wildtype and mutant forms of dMyc (carrying mutations in MB2, MB3, or the N-terminus) in *Drosophila* S2 cells or *in vivo*. These experiments revealed a strong requirement for the N-terminus for all dMyc-dependent activities. Surprisingly, mutation of MB2 only weakened, but did not fully inactivate dMyc function, such that an MB2-mutant form of dMyc could rescue the survival of a sizable fraction of *dmyc*-null mutant flies. Finally, deletion of MB3 stabilized dMyc protein, and increased several of dMyc`s activities, but not its efficiency of transactivation.

Results

MB3 contributes to transactivation and to dMyc degradation

To investigate the *in vivo* roles of the most highly conserved domains of dMyc, we mutated or deleted MB2, MB3 and the entire N-terminus (Fig. 1A). The different mutants, as well as wildtype dMyc were tagged with a triple HA-epitope at their N-termini and cloned under the control of GAL4-activatable UAS-elements. For transient expression in *Drosophila* S2 cells, these constructs were then co-transfected with a GAL4-expression plasmid, yielding comparable levels of proteins of the expected sizes (Fig. 1B). Upon transient co-transfection with a GAL4-expression plasmid in *Drosophila* S2 cells, all constructs produced comparable levels of proteins of the expected sizes (Fig. 1B).

The same UAS-plasmids were also used to generate transgenic flies. The transgenes that were used in this and all following experiments were generated with the help of the ΦC31 system for targeted transgenesis (Bischof et al., 2007; Groth et al., 2004; Venken et al., 2006). With this method, all constructs are integrated at the same, molecularly defined, genomic region, thus equalizing mRNA expression levels for all mutants and eliminating potentially confounding integration site effects. Indeed, all dMyc proteins accumulate to similar levels (Fig. 1C), with the exception of the more stable dMycΔMB3 protein.

Although dMycΔMB3 accumulated to somewhat higher levels (Fig. 1B); this difference was more pronounced upon stable expression of the different dMyc proteins in transgenic flies (Fig. 1C). These increased levels of dMycΔMB3 are due to a higher stability of the mutant protein, as shown in Fig. 1D. When protein synthesis was blocked in S2 cells that ectopically expressed different dMyc versions, the wildtype protein disappeared with a half-life of 23±1 min (Fig. 1D), which is similar to the stability of vertebrate c-Myc (Oster et al., 2002). The ΔMB3 mutant had a significantly longer half-life of 49±8 min (average of 3 independent experiments; p=0.02), suggesting that MB3 normally contributes to the destabilization and proteolytic degradation of dMyc. Although no such role has been described for the vertebrate MB3, it should be noted that c-Myc MB3 has only been analysed in one cell line (U2OS cells), and that c-Myc domains have been shown to contribute differentially to its degradation in different cell types (Herbst et al., 2004). From the data shown in Figs. 1B and C, we deduce that MB3 plays a role in dMyc degradation in S2 cells and *in vivo*.

To confirm that the conserved domains also have a role in trans-activation in *Drosophila* (as has been extensively shown for Myc`s N-terminus and MB2 in vertebrates – see

Introduction), we transfected the different dMyc mutants in S2 cells, together with a plasmid coding for *Renilla* luciferase under the control of the promoter of the dMyc target *CG5033* (Hulf et al., 2005), and with a second plasmid in which firefly luciferase is controlled by a mutant derivative of the same promoter that lacks the sole dMyc binding site. Thus, the ratio of *Renilla* to firefly luciferase faithfully reflects dMyc activity, such that RNAi-mediated down-regulation of *dmyc* decreases this ratio by up to 4-fold (Furrer et al., in preparation), whereas overexpression of dMycWT increases the ratio by more than 2-fold (Fig. 2A). Consistent with published observations for c-Myc MB2, mutation of MB2 reduces the ability of dMyc to transactivate this reporter, but does not completely abolish it, whereas the deletion of the N-terminus eliminates dMyc`s transactivation potential. Surprisingly, dMycΔMB3 transactivates the reporter with a similarly reduced efficiency as dMycΔMB2, suggesting that MB3 is also required for full transcriptional activation of a dMyc reporter.

This observation prompted us to investigate the ability of dMycΔMB3 to activate different endogenous targets of dMyc. Specifically, we wanted to determine how efficiently the mutant protein controls its target genes *in vivo*, in the absence of endogenous dMyc. The transgenes, that were used in this and all following experiments, were generated with the help of the ΦC31 system for targeted transgenesis (Bischof et al., 2007; Groth et al., 2004; Venken et al., 2006). With this method, all constructs are integrated at the same, molecularly defined, genomic region, thus equalizing mRNA expression levels for all mutants and eliminating potentially confounding integration site effects. Indeed, all dMyc proteins accumulate to similar levels (Fig. 1C), with the exception of dMycΔMB3, which is more stable than dMycWT (Fig. 1D). To assay their effects on target gene expression, the dMycWT and dMycΔMB3 transgenes were first combined with a chromosome carrying the *dmyc* null allele dm^4, a "*tub*-FRT-dMyc-FRT-GAL4" transgene (which drives ubiquitous expression of a dMycWT cDNA and thereby fully rescues the lethality of the *dmyc* mutant; Bellosta et al., 2005) and a hs-FLP construct. Following a massive heat-shock of 2 hours at 37°, virtually all cells have eliminated the rescuing dMyc cDNA and express GAL4 instead (Hulf et al., 2005), which in turn drives the expression of the UAS-controlled dMycWT or dMycΔMB3 transgenes. Eight hours later (before any overt signs of apoptosis – see below), total RNA was isolated and analysed for the abundance of *dmyc* and some of its targets. As shown in Fig. 2B, by this time the level of endogenous *dmyc* mRNA has dropped by 4-fold (and the same is presumably also true for dMyc protein, given its short half-life). As a consequence, the dMyc targets *CG5033*, *nnp1* (both controlled by single dMyc-dependent E-boxes and transcribed by RNA Pol II; Hulf et al., 2005) and $tRNA^{Leu}$ (activated via a dMax-independent pathway and

transcribed by RNA Pol III; Steiger et al., 2008) are all clearly reduced in abundance (compare "control" samples, that have not been subjected to a heat-shock, with "-" samples, that do not express any dMyc transgene). Both dMycWT and dMycΔMB3 flies overexpress the transgenic *dmyc* mRNA to the same level, but the latter flies contain significantly lower amounts of the dMyc target *nnp1* ($p<0.01$) and comparable amounts of *CG5033* – even though the mutant dMyc protein is likely to be present at higher concentrations. dMycΔMB3 is even more impaired in activating the Pol III targets $tRNA^{Leu}$ and *snoRNA U3*. These results are consistent with a role for MB3 in controlling transactivation, and they suggest that this domain is particularly important for the activation of Pol III. The molecular basis for this effect is currently unclear; the only Myc-interacting protein that is currently known to be specifically involved in Pol III-dependent transcription, Brf (Gomez-Roman et al., 2003; Steiger et al., 2008), binds with similar efficiency to both dMycΔMB3 and dMycWT (data not shown).

Overexpression of dMyc mutants *in vivo*

Myc proteins are important both for normal development and tissue homeostasis, when they are expressed at physiological levels, and in the etiology of tumours, where they are frequently overexpressed. While Myc`s physiological activities can account for much of its potency as an oncoprotein, it is conceivable that Myc takes on additional, qualitatively different, functions when expressed at supra-physiological levels. For these reasons, we wanted to investigate the activities of our dMyc mutants first in mere overexpression situations, and second in the presence of hypomorphic or amorphic *dmyc* alleles, where the ability of the mutant proteins to substitute for endogenous dMyc could be probed.

As a first step, we analysed the ability of the different dMyc mutants to promote growth upon overexpression. It has previously been shown that overexpression of dMycWT under the control of *GMR*-GAL4 strongly increases the size of adult ommatidia (Montero et al., 2008b; Secombe et al., 2007; Steiger et al., 2008); since this driver expresses GAL4 in the eye imaginal discs from the late 3rd larval instar on, it mainly influences the final growth and differentiation phase of the eye cells, but not the proliferation of their precursors and the final number of ommatidia. Consistent with their effect on the dMyc reporter in S2 cells, the MB2 mutants are still able to promote growth, albeit to a lesser extent than dMycWT, and dMycΔN is inactive in this assay (Figs. 3A, B). Surprisingly, dMycΔMB3 increases ommatidial size more than dMycWT and additionally induces considerable roughness of the eye. Such a morphology (caused by a combination of excessive growth and apoptosis) is also observed

when dMycWT is expressed at higher levels (Steiger et al., 2008), indicating that dMycΔMB3 is more active than dMycWT in this assay (which contrasts with the situation in S2 cells). Most likely, this increased activity is due to the higher levels to which dMycΔMB3 accumulates. When dMyc degradation is reduced, by heterozygosity for the F-box protein Archipelago/Fbw7, which has been shown to control dMyc proteolysis (Moberg et al., 2004), dMycWT increases ommatidial size much more efficiently, virtually to the same extent as dMycΔMB3 (in an *ago*/+ background, the difference between these two proteins is not statistically significant; Fig. 3C). Since the effect of dMycΔMB3 is only marginally enhanced by the *ago* mutation, this further suggests that this mutant is not further stabilized, and hence that the Ago-dependent dMyc-ubiquitination and -degradation requires MB3.

The different dMyc mutants show similar growth-promoting abilities when over-expressed under the control of *ap*-GAL4 in the dorsal compartment of wing imaginal discs. The resulting size difference between the dorsal and the ventral compartments results in a moderate (ΔMB2, MB2A; Fig. 3D3, 4) or strong (WT, Fig. 3D5) bending down of the adult wings. dMycΔN again shows no activity (Fig. 3D2), even though this bending provides a very sensitive read-out for growth inducers (see Montagne et al., 1999). dMycΔMB3 reveals other phenotypes (Fig. 3D6) that can also be observed upon overexpression of a different, stronger dMycWT transgene (e.g. dissociation of the dorsal and ventral wing surface, necrotic patches; data not shown), and that suggest that the dMyc-induced excessive apoptosis overwhelms its growth-promoting ability. Indeed, TUNEL staining of 3rd instar larval wing discs (Fig. 4) reveals that all dMyc proteins (except for dMycΔN) induce apoptosis (as previously reported for dMycWT; Montero et al., 2008b), but that dMycΔMB3 clearly has the highest activity. Thus, like in the eye, dMycΔMB3 is more active than dMycWT.

The experiments described so far document the effects of the different dMyc mutants on final adult tissue size. To demonstrate directly to which extent dMyc proteins promote the *rate* of cellular growth, we expressed the different proteins in clones of cells in wing imaginal discs carrying an "*act*-FRT-stop-FRT-GAL4" cassette, an hs-FLP transgene and a UAS-GFP marker. Overexpression clones were induced by a 10' heat-shock at 37°, which drives the expression of FLP recombinase leading to the activation of GAL4 in a few (random) cells of the disc, and analysed 73 hours later (after 6 to 7 cell doublings). The co-expressed GFP allowed for the identification of the clones; since larval wing discs consist essentially of a monolayer of undifferentiated cells, the areas of such clones provide a good measure for their volume increase, i.e. their rate of growth. Consistent with published observations (Johnston et al., 1999), dMycWT overexpression strongly promotes clonal growth (Figs. 5A, B), and so

does dMycMB2A. As expected, dMycΔN does not affect the growth rate of these clones. However, dMycΔMB3 significantly reduces clonal area, suggesting that its powerful pro-apoptotic ability (see Fig. 4) overcomes the proliferative capacity of these clones.
Taken together, the overexpression studies demonstrate that the N-terminus is essential for dMyc`s ability to promote growth, whereas a mutation of MB2 only moderately impairs dMyc activity; loss of MB3 increases dMyc protein levels and concomitantly also the biological activity of dMyc.

Rescue of *dmyc* mutant eyes by dMyc protein mutants

Normal eye development requires dMyc, and strong hypomorphic or null alleles of *dmyc* result in smaller eyes, composed of fewer and smaller ommatidia (Bellosta et al., 2005; Steiger et al., 2008; see also Fig. 6, below). Therefore the eye constitutes a good organ for analysing the normal biological activities of dMyc proteins. To reveal the phenotype of such *dmyc* mutant eyes without lowering dMyc activity in the rest of the body (which would interfere with organismal viability), we combined the rescuing transgene "*tub*-FRT-dMyc-FRT-GAL4" (described above) with a transgene expressing FLP recombinase under the control of the *eyeless* regulatory region (*ey*-FLP), such that the dMyc cDNA is "flipped-out" in eye precursor cells specifically, starting early in development, and GAL4 is expressed instead. The FLP-mediated replacement of dMyc with GAL4 is highly efficient, as shown in Fig. 6A, where the flies described above also carried a *mini-white* gene (conferring red eye colour), flanked by two FRT-sites (Brogiolo et al., 2001): only a small patch of ommatidia retains the *mini-white* gene and hence has not expressed sufficient amounts of FLP recombinase. This picture also reveals the eye size reduction caused by the loss of *dmyc*. We used this system to express the different dMyc variants in eyes that were wildtype for dMyc, or carried the hypomorphic allele dm^{P0}, or the null allele dm^{4}. Importantly, transgene expression in this assay is maintained from earliest eye specification to the terminal differentiation phase, and therefore affects both the final number and size of the resulting ommatidia.
All dMyc mutants significantly increase ommatidial size as compared to control, with the effects being largest in the dm^{4} background that lack endogenous *dmyc* altogether, as might be expected (Figs 6B, C). Even dMycΔN, which was inactive in all other assays, increases ommatidial size by 10% in a dm^{+} background; the difference to the *GMR*-driven overexpression experiment shown above is presumably due to the different expression dynamics of the two GAL4 drivers [*GMR* is not expressed in all cell types of the

differentiating eye (Ellis et al., 1993), but *tub* should be ubiquitously expressed, and furthermore level and duration of GAL4 expression are likely to differ between the two systems]. The ΔN mutant also stimulates proliferation and significantly increases the number of ommatidia in dm^4 mutant eyes (Fig. 6D, compare "-" and "ΔN"), thus demonstrating its activity both during the earlier proliferative and the later differentiation phase. Note that we would not expect any dMyc mutant to increase the number of ommatidia in dm^+ and dm^{P0} eyes, since these genotypes have a wildtype number of ommatidia to start with (Fig. 6D; Bellosta et al., 2005) and dMyc overexpression does not increase cell division rates in wildtype cells (Johnston et al., 1999). Instead, expression of the other dMyc forms slightly or significantly reduces the number of ommatidia in this assay, reflecting the pro-apoptotic activity of these proteins (Bellosta et al., 2005). As before, this effect is strongest for dMycΔMB3, as can also been seen by the obvious roughness of the eyes expressing this mutant (Fig. 6B). Taken together, this experiment confirms the growth- and apoptosis-promoting capabilities of the different dMyc mutants, and it shows that the dMycΔN form also retains some activity.

Organismal rescue of *dmyc* mutants

As a final, most stringent functional assay we wanted to determine to which extent the different dMyc mutants could drive the entire development in the absence of endogenous dMyc. For this purpose, we first expressed the transgenes under the control of different ubiquitous GAL4 drivers (Table 1). The weak line *arm*-GAL4 produced no detectable effect (lethality or rescue) in any cross, whereas the other GAL4 drivers resulted in excessive expression of the dMyc transgenes that killed wildtype (dm^+) animals, and they did not rescue different lethal *dmyc* alleles (dm^{PL35}, dm^{PG45} and dm^2 are hypomorphic, and dm^4 is a null). Partial rescue of lethality was only observed in three combinations: when expressed under the control of *da*-GAL4, dMycΔN rescued dm^{PL35}, and the enhancer trap allele dm^{PG45} (which is both mutant for dmyc and expresses GAL4 in a dmyc-like pattern; Benassayag et al., 2005) was rescued by both dMycΔN and dMycMB2A. This is the second observation to demonstrate that the ΔN mutant retains some biological function *in vivo*. Note that expression of dMycWT under the control of dm^{PG45} has been reported to cause dominant lethality (i.e. in a dm^{PG45}/dm^+ background; Benassayag et al., 2005), presumably because the GAL4/UAS system amplifies the transcriptional output of the *dmyc* locus to lead to excessive expression of the UAS-transgene. An analogous amplification explains the lethality of a dMycWT transgene when expressed under the control of a *tub*-GAL4 driver, whereas a transgene

expressing dMycWT directly under *tubulin* control causes no harm in flies and even rescues a *dmyc* null mutant (see above). Such considerations prompted us to generate a second series of transgenes, in which the expression of the different dMyc mutants is controlled directly by the *tubulin* regulatory sequences; these transgenes were integrated in the same chromosmal location as before using the ΦC31 system. All transgenes could be established, although *tub*-dMycΔMB3 showed some dominant lethality in a dm^+ background and could not be maintained as a homozygous line. Both dMycWT and dMycΔMB3 rescued the lethality of dm^4 mutant flies (Fig. 7A, B), although the resulting adults were smaller than control (Fig. 7B, C). Expression of dMycΔN did not lead to any escapers, but much to our surprise, a substantial fraction of dMycΔMB2 expressing dm^4 flies (15% of the expected number) survived development when 2 copies of the transgene were present and enclosed as normally patterned adults (Fig. 7). This fraction even increases to around 39% when the dMyc antagonist dMnt is simultaneously mutated, i.e. in a dm^4 $dmnt^1$ background, where dMyc targets have been shown to be partially derepressed (Pierce et al., 2008b). Thus, in the absence of any endogenous dMyc MB2 is not absolutely required to promote the full development from egg to adult.

Discussion

Myc proteins show a comparatively low overall sequence conservation between the most distant known family members from insects and vertebrates, but they all contain a short, highly conserved sequence motif, the Myc Box 2 (MB2). The very fact that this domain is conserved suggests an indispensable function, and MB2 has indeed been shown to play an essential role in different tissue culture based assays. However, the variety of cell types that have been tested in tissue culture (most frequently fibroblasts), as well as the types of biological read-outs that have been used (typically proliferation, apoptosis or transformation), are both limited. As Myc interacts with many different transcriptional co-factors, we speculated that the proteins contacting MB2 might be important for the expression of only a subset of Myc`s targets, or essential only in certain cell types, or required for only certain biological processes. By expressing MB2-mutant forms of Myc *in vivo*, we exposed the proteins to a variety of different contexts. We expected that the mutants would be inactive in most situations, but possibly retain some activity in a particular assay. Unexpectedly however, MB2 mutants showed an intermediate activity in all our assays (often close to that of dMycWT). Most strikingly, dMycΔMB2 was able to rescue mutant animals lacking all endogenous dMyc, which would otherwise all have died during development. This finding suggests that MB2 does not contribute a qualitatively unique and essential function to Myc, but instead may act to enhance Myc`s transcriptional output or modulate it in response to external signals. It further implies that no essential co-factor relies on MB2 for its interaction with Myc, either because no MB2-interacting protein is essential for Myc function, or because all MB2-interacting essential co-factors also contact Myc via additional redundant domains. At present we cannot address these possibilities experimentally, since no protein has been found to contact MB2 in *Drosophila*; two candidates we investigated (dGCN5 and Tip49/Pontin) bound dMyc independently of the presence of MB2 (data not shown). Thus, we can only speculate about reasons for the partial dispensability of MB2; for example, the activation of a Myc target that normally relies on an MB2-dependent HAT might be partially taken over by an MB2-independent HAT, or such a Myc target gene might instead be activated by a histone acetylation-independent process (such as nucleosomal remodelling), or other targets might supplant the function of such genes. In either case, our observations provide an example of unexpected biological plasticity, in light of the exceptional evolutionary conservation of this MB2.

By comparison, the elimination of the entire N-terminus has substantially more severe effects. Nevertheless, the dMycΔN protein (which corresponds to the naturally occurring c-Myc S variant in vertebrates) clearly retains some activity. Similar to human c-Myc S (Benassayag et al., 2005), dMycΔN can rescue the lethality of the dm^{PG45} allele; as dm^{PG45} is a hypomorphic (albeit strong) *dmyc* allele, some dMyc activity must still be present in these flies and might cooperate with dMycΔN in this rescue. However, dMycΔN also significantly enhances the size and number of ommatidia that lack *dmyc* altogether (Fig. 6), demonstrating that this mutant has the ability to stimulate cellular growth and proliferation on its own (although, like c-Myc S, it cannot induce apoptosis – Fig. 4). This growth effect is comparatively weak and not seen in other overexpression experiments, though, essentially confirming studies of vertebrate Myc that have assigned an important biological role to this part of the protein.

A primary goal of our work was to investigate the second highly conserved domain in dMyc, MB3. MB3 resembles PEST motifs that control protein degradation, and indeed deletion of MB3 stabilizes dMyc; consistent with the increased abundance, expression of dMycΔMB3 leads to more growth and apoptosis than expression of dMycWT. However, PEST motifs are normally similar in their amino acid composition rather than in their exact amino acid sequence, suggesting that additional evolutionary constraints are imposed on MB3. One such constraint may be found in *myc`s* genomic structure: in all *myc* genes MB3 straddles the boundary between exons 2 and 3 (Gallant, 2006), and the codons adjacent to the splice site may be under selective pressure that has nothing to do with the amino acids they are coding for. We favour the converse explanation, though, that the position of the splice sites may have been conserved as a consequence of the conservation of the adjacent exonic sequences. In the context of our overexpression cDNA`s (that obviously lack the large *myc* intron 2, and where splicing does not occur) the dMycΔMB3 mutant also shows an impairment in transcriptional activation towards an E-box dependent reporter in tissue culture cells, and towards RNA Pol III dependent endogenous targets *in vivo*. In many transcription factors, including c-Myc (Kim et al., 2003; von der Lehr et al., 2003), protein domains controlling degradation and transcriptional activation overlap, and these two processes are functionally coupled, possibly to ensure a short half-life of the transcriptionally active protein (Muratani and Tansey, 2003b). Thus, MB3 might link Myc degradation and its activity, in particular towards certain targets. However, at present we cannot exclude the possibility that the control of transcription and degradation are two uncoupled activities of MB3, and future experiments will be required to address this issue.

Figure legends

Figure 1. Description of dMyc mutants.
A, schematic representation of the dMyc mutants used in this work. All constructs contain an N-terminal triple HA-tag, with the coordinates referring to the untagged dMyc. The MB2 and MB3 sequences shown on the top are derived from human c-Myc (upper line) and dMyc (lower line); the dots in c-Myc represent a 6 residue acidic stretch lacking in dMyc, and the vertical line shows the junction between exons 2 and 3 that is conserved in *myc* genes. B, average ommatidial area (± standard deviation) for the indicated genotypes (corresponding to the eyes in panel A), calculated from 20 centrally located ommatidia from at least 5 independent eyes per genotype. All areas are significantly larger than the corresponding "-" control with $p<0.01$ (Students t-test), except for "dm^+; ΔN" where $p=0.03$. ***B***, Western blot of *Drosophila* S2 cells transiently transfected with UAS-plasmids coding for the indicated HAdMyc variants together with a *tub*-GAL4 plasmid. The cells were lysed at 48 hours after transfection. The same blot was probed with anti-HA antibodies (top panel) to reveal HAdMyc and with anti-α-Tubulin antibodies (bottom panel) as a loading control. ***C***, expression level of the HAdMyc variants in transgenic flies. Third instar larvae of the genotype "*y w/Y; tub*-HAdMyc" were collected at 5 days of age and processed for Western blot. In each lane, the equivalent of 2.2 larvae was loaded. The same blot was probed with anti-HA antibodies (top panel) to reveal HAdMyc and with anti-α-Tubulin antibodies (bottom panel) as a loading control. The anti-α-Tubulin blot serves as a loading control. ***D***, HAdMycWT and HAdMycΔMB3 were expressed in S2 cells as described above. At 48 hours after transfection, cycloheximide was added to the cells to a final concentration of 100 µg/ml and at the indicated times thereafter cell lysates were prepared and analysed by SDS-PAGE and Western blotting using an anti-HA antibody.

Figure 2: Effect of dMyc mutants on target gene expression.
A, endogenous dMyc was down-regulated with RNAi in S2 cells and the indicated dMyc mutants were expressed instead. The graph shows the relative activity of the co-transfected luciferase reporter (wildtype reporter divided by mutant reporter), with the relative activity of dMycWT set to 100%; shown are the averages (± standard deviations) of 2 independent transfections from a representative experiment. ***B***, expression of endogenous dMyc targets in dmyc-mutant larvae in response to the indicated transgenes. The *dmyc*-null mutation was exposed, and the transgene expression triggered, by a heat-shock; "control" samples did not receive any heat-shock and "-" did not express any transgene. Shown are the averages (± standard deviations) of two biologically independent samples.

Figure 3: Effect of dMyc overexpression on ommatidial size and wing shape.
A, scanning electron micrographs of representative eyes expressing single UAS-transgenes with the indicated dMyc mutants under the control of *GMR*-GAL4; "-" eyes express a UAS-transgene lacking any cDNA. ***B***, average ommatidial area (± standard deviation) for the indicated genotypes (corresponding to the eyes in panel A), calculated from 20 centrally located ommatidia from 5 independent eyes per genotype. "**" indicates genotypes whose ommatidia are significantly larger than "-" ommatidia with $p<0.01$. ***C***, analogous experiment in flies that are heterozygous for the *archipelago* alleles ago^1 or ago^3; the first three values for wildtype eyes (labelled +/+) are identical to the corresponding genotypes in panel B. ***D***, representative frontal views of adult wings of flies carrying one copy of *ap*-GAL4 (driving GAL4 expression in the dorsal wing compartment) and one UAS-transgene coding for the indicated dMyc version, or no cDNA at all ("-").

Figure 4: Induction of apoptosis by overexpressed dMyc.
TUNEL-staining of third instar larval wing imaginal discs carrying one copy of *ap*-GAL4 and one UAS-transgene coding for the indicated dMyc version, or containing no cDNA at all ("-"). The TUNEL-positive region in the panel showing a ΔMB3 wing disc provides a good reflection of the GAL4 expressing domain.

Figure 5: Stimulation of clonal growth by overexpressed dMyc.
A, third instar larval wing imaginal discs with typical 73 hour old clones (marked in green) expressing GFP and the indicated dMyc variant. Blue colour shows the nuclei stained with Hoechst 33342 dye. ***B***, average clonal area from discs corresponding to the genotypes shown in panel A. Number of analysed clones (in parentheses the corresponding genotype): 50 (-), 45 (WT), 42 (ΔN), 53 (MB2A), 40 (ΔMB3).

Figure 6: Effects of continuous dMyc expression on ommatidial size and number.
A, efficiency of the *ey*-FLP system. Red ommatidia in either panel retain the "FRT-w^+ *stop*-FRT" cassette and express the rescuing dMyc cDNA, whereas the white ommatidia lack this cassette and the dMyc cDNA, and hence expose the dm^4 mutant. Genotypes: 1, "*w* dm^4 *tub*-FRT-dMyc *stop*-FRT-GAL4 *ey*-FLP/Y; *GMR*-FRT-w^+ *stop*-FRT-GAL4/+"; 2, "*w* dm^4 *tub*-FRT-dMyc y^+ *stop*-FRT-GAL4 hs-FLP/Y; *GMR*-FRT-w^+ *stop*-FRT-GAL4/+". ***B***, scanning electron micrographs of representative eyes of the indicated genotype. Sex chromosomes are "*y w tub*-FRT-dMyc *stop*-FRT-GAL4 *ey*-FLP/Y" (labelled "dm^+"), "*w* dm^{P0} *tub*-FRT-dMyc *stop*-FRT-GAL4 *ey*-FLP/Y" (labelled "dm^{P0}"), "*w* dm^4 *tub*-FRT-dMyc *stop*-FRT-GAL4 *ey*-FLP/Y" (labelled "dm^4"); in addition, these flies carry one UAS-transgene coding for the dMyc variant indicated in the picture; "-" corresponds to a UAS-transgene lacking any cDNA. ***C***, average ommatidial area (± standard deviation) for the indicated genotypes (corresponding to the eyes in panel B), calculated from 20 centrally located ommatidia from 5 independent eyes per genotype. All areas are significantly larger than the corresponding "-" control with $p<0.01$ (Students t-test), except for "dm^+; ΔN" where $p=0.03$. ***D***, average ommatidial number (± standard deviation) for the indicated genotypes (corresponding to the eyes in panel B). Asterisks indicate significance of difference to the corresponding "-" genotype, with $p<0.05$ (*) and $p<0.01$ (**).

Figure 7: Rescue of a *dmyc*-null mutation by the expression of dMyc protein mutants under the direct control of the *tubulin*-promoter.
A, dissecting microscope pictures of rescued *dmyc*-null mutant adult males expressing two copies of the indicated transgenes. ***B***, relative survival rate for the indicated genotypes (the expected number of "*w* dm^4/*Y*" or "*w* dm^4 $dmnt^1$/Y" males carrying one or two copies of the indicated "*tub-HAMyc*^{mut}" transgenes was calculated from the number of recovered dm^4/dm^+ heterozygous females from the same cross, and set to 100%). For each genotype 300-800 flies in total were scored (except for *w* dm^4/Y; *tub-HAMycΔMB3/+:* 91 flies, *w* dm^4 $dmnt^1$/Y; *tub-HAMycΔN*: 64 flies, *w* dm^4 $dmnt^1$/Y; *tub-HAMycWT*: 229 flies), of which rescued *Myc*-mutant made up one quarter (one eight for the *tub-HAMycΔMB3* transgenes). ***C***, average weight of at least 13 male flies per genotype (except dm^4/Y; *tub-HAMycΔMB3/+*: 8 flies); the error bars indicate standard deviation. The control genotype is "*y w*".

Table 1: Ability of dMyc mutants to rescue the lethality of *dmyc* alleles.
"yes" indicates that some adult males carrying the *dmyc* allele indicated in the first column plus a single copy of the GAL4 driver shown in the second column and of the UAS-transgene listed above the table survived to adulthood; "-" indicates that no such flies were ever observed, and an empty field indicates that the corresponding cross was not done.

Materials and Methods

Cloning and expression of dMyc proteins

A cDNA for wildtype dMyc with a triple HA-epitope at its N-terminus (Bellosta et al., 2005) was cloned into a pBS-vector carrying a single ΦC31 *att*B site, 5 UAS repeats, a *hsp70* basal promoter, the SV40 polyA signal, and *mini-white* as a marker (Bischof et al., 2007). By site-directed mutagenesis the following mutant derivatives were created (numbering relative to untagged dMyc): dMycΔN: lacking amino acids 1 – 65; dMycMB2A: containing "AAAA" instead of "DCMW"; dMycΔMB2: "GP" substituted for residues 68-84; dMycΔMB3: "F" substituted for residues 405-422. The same cDNAs were also cloned directly under the control of the β-*tubulin* promoter (see Bellosta et al., 2005) into an analogous pBS-vector lacking UAS- and hsp70-sequences. Full sequences are available upon request.

Tissue culture: transfections & biochemistry

Drosophila S2 cells were cultured at 24°C in 1x Schneider`s *Drosophila* medium (Gibco/BRL), supplemented with 10% fetal bovine serum, 1% Penicillin/Streptomycin. To assess dMyc stability, $5x10^6$ cells were seeded per well of a 6-well culture plate and transfected in 1ml of serum-free medium containing 10µl cellfectin (Invitrogen) and 10µg plasmid DNA made up of 5µg *tub*-GAL4 and 5µg UAS-plasmids; 15-16h later, complete medium was added for 48h, before cells were either directly processed for SDS-PAGE or cycloheximide (Sigma) was added to 100µg/ml. Cells were harvested at the indicated time points and washed with 1xPBS, lysed in Laemmli sample buffer and analysed by SDS-PAGE and immunoblotting. Western blots were then either exposed on X-ray films (using multiple exposures for each experiment) or scanned with a CCD camera (Fuji LAS-3000). Band intensities were determined using ImageJ software, and half-lives calculated by linear regression of log-transformed data. To document transgene expression *in vivo*, uncrowded wandering larvae were homogenized directly in sample buffer and analyzed as described.
Primary antibodies for Western blotting were: mouse anti-HA epitope (BAbCO), rabbit anti-HA epitope (Dunn Labortechnik GmbH), mouse anti-α-Tubulin (Sigma). Secondary antibodies were HRP-coupled anti-rabbit or anti-mouse (GE Healthcare) and for detection the enhanced chemiluminescence kit (Amersham) was used.

Luciferase reporter experiments

Reporter assays were carried out as previously described (Hulf et al., 2005). Briefly, $1.3x10^6$ cells/well of a 24-well cell culture plate were transfected with 0.65ml serum-free medium containing 4.2µl cellfectin (Invitrogen) and 2.6µg plasmid DNA (consisting of a 1:1 mix of "*CG5033*^{wt}-Renilla luciferase" and "*CG5033*$^{\Delta Ebox}$-firefly luciferase" reporters, *tub*-GAL4 and UAS-plasmids). After 15-16h, 0.65ml complete media was added; 24h later, cells were washed in 1xPBS, lysed in 1x Passive Lysis Buffer (Dual-Luciferase kit, Promega), and relative reporter expression determined on a Wallac luminometer.

***Drosophila* lines**

Transgenic flies were established by integrating the different *att*B plasmids into the *att*P landing site ZH-86Fb (Bischof et al., 2007; http://www.frontiers-in-genetics.org/), and confirmed by PCR. Source of additional flies: GAL4 drivers (*Drosophila* stock centre at Bloomington), *act*-FRT-CD2-FRT-GAL4 (Neufeld et al., 1998), *GMR*-FRT-w^+-FRT-GAL4 (Brogiolo et al., 2001), *tub*-FRT-dMyc-FRT-GAL4 (De La Cova et al., 2004), *ago*^{1} & *ago*^{3} (Moberg et al., 2001), *dm*^{P0} (Johnston et al., 1999), *dm*^{2} (Maines et al., 2004), *dm*^{4} (Pierce et al., 2004), *dmnt*^{1} *dm*^{4} (Pierce et al., in press), *dm*^{PL35} & *dm*^{PG45} (Benassayag et al., 2005).

Immunocytochemistry

For TUNEL staining of wing imaginal discs, wandering third instar larvae were fixed in 4% paraformaldehyde for 20', washed with 1x PBT (0.1% Tween-20 in PBS [130mM NaCl, 7mM Na_2HPO_4, 3mM NaH_2PO_4]) for 20', post-fixed in ethanol/PBS (2:1) for 5' at –20° C, washed with 3 changes of 0.1% Tween-20/PBS over 15', pre-treated with 10mM sodium citrate (pH 6) for 30' at 70°C, equilibrated in Equilibration Buffer (ApopTag Red In Situ Apoptosis Detection Kit, Chemicon) for 10', then incubated with TdT enzyme (Chemicon kit) for 1h at 37°C, Stop/Wash Solution (Chemicon kit) for 10', Rhodamine-coupled anti-DIG antibodies (Chemicon kit) for 30', and 3 changes of 0.1% Tween-20/PBS (containing 0.5 µg/ml Hoechst 33342 for the first step).

For anti-cleaved caspase 3 stainings, wandering third instar larvae were fixed in 4% paraformaldehyde/PBS for 20' at room temperature and washed with 1x PBT. Rabbit anti-cleaved caspase 3 (Cell Signalling Technology) was added over night at 4°C. Samples were washed with PBT, incubated with Texas Red-coupled anti-rabbit antibodies (Jackson Immuno

Research Lab) and 0.5µg/ml Hoechst 33342 for 2h at room temperature, and washed again with PBT.

For clonal area measurements, larvae carrying the "*act*-FRT-CD2-FRT-GAL4" construct, UAS-GFP and the appropriate UAS-dMyc transgene, were heat-shocked for 10' at 37° C in a water bath, dissected 73h later, fixed in 4% paraformaldehyde for 20', and washed with 3 changes of PBT (containing 0.5µg/ml Hoechst 33342 for the first step) over 60'.

Wing discs were dissected and mounted in Vectashield Mounting Medium (Vectashield), and analysed on a Leica DMRA compound microscope at a 10x ocular magnification. Clonal area was determined from at least 40 clones per construct using Adobe Photoshop.

QRT-PCR

Larvae were grown under uncrowded conditions, heat-shocked at wandering stage for 2h at 37°C in a water bath, collected 8h later into liquid nitrogen, and stored at -80°C. To extract RNA, 10 whole larvae were homogenized in 1ml TRIZOL (Invitrogen) with a Polytron tissue homogenizer, following the manufacturers instructions. Upon precipitation, RNA was redissolved in 20µl RNAse-free water and analysed for its integrity on a Bioanalyzer (Agilent). Genomic DNA was eliminated using the Turbo DNAse free kit (Ambion) and cDNAs were synthesized from 1µg of template RNA using the Omniscript kit (Qiagen). Parallel control reactions containing only RNA provided templates for "-RT" samples. Quantitative real-time PCR (qRT-PCR) reactions were performed in triplicates on an ABI7900 Real Time PCR Instrument (Applied Biosystems), using the SYBR Green PCR Master Mix (Applied Biosystems). Data were analysed with SDS 2.0 software (Applied Biosystems) and Microsoft Excel, using the ΔΔCt method and the average of the expression levels of *actin5C*, *Rab6* and *Sec24* as internal reference for each biological sample.

Primer sequences: Rab6: 5'-TGCACGTGGCCAAGTCCTA & 5'-CAGCGAACGCGACTGCTA; Sec24 5'-CCACTCCCCTGCCATCCT & 5'-ACCCCAAACCCAGCAACA; CG5033: 5'-TAACCGCTCGGCTTTAATTCA & 5' CCCTTGCTCTTGGAGAATGG. The remaining primers and the PCR conditions have been described (Steiger et al., 2008).

Analysis of adult flies

Flies were kept on standard *Drosophila* medium and test crosses performed in climate-controlled chamber at 25°.

Scanning electron microscope pictures were taken with a JEOL JSM-6360 LV microscope and a magnification of 180x. Flies were frozen at –20°C for at least one day, slowly defrosted at 0°C and directly used for electron microscopy. For determination of ommatidial size, the area of 20 centrally located ommatidia was determined from 5 fly eyes of the same genotype using Adobe Photoshop. The same photomicrographs were also used to determine the total number of ommatidia per eye. Obvious fusions of two ommatidia were counted as two individual ommatidia.

To determine adult weights, 1-2 day adult flies were frozen at –20°C for at least one day, defrosted at room temperature and weighed on a Mettler Toledo MX5 micro balance.

Acknowledgements

We thank D.Steiger for comments on the manuscript, Regina Perez for technical assistance, and J.Bischof, K.Basler, H.Stocker, E.Hafen for flies. This research was supported by a grant from the SNF.

References

Amati, B., Frank, S. R., Donjerkovic, D., and Taubert, S. (2001). Function of the c-Myc oncoprotein in chromatin remodeling and transcription. Biochim Biophys Acta *1471*, M135-145.

Bello-Fernandez, C., Packham, G., and Cleveland, J. L. (1993). The Ornithine Decarboxylase Gene is a Transcriptional Target of c-Myc. Proceedings of the National Academy of Sciences *90*, 7804-7808.

Bellosta, P., Hulf, T., Diop, S. B., Usseglio, F., Pradel, J., Aragnol, D., and Gallant, P. (2005). Myc interacts genetically with Tip48/Reptin and Tip49/Pontin to control growth and proliferation during Drosophila development. Proc Natl Acad Sci USA *102*, 11799-11804.

Benassayag, C., Montero, L., Colombie, N., Gallant, P., Cribbs, D., and Morello, D. (2005). Human c-Myc isoforms differentially regulate cell growth and apoptosis in Drosophila melanogaster. Mol Cell Biol *25*, 9897-9909.

Biegalke, B. J., Heaney, M. L., Bouton, A., Parsons, J. T., and Linial, M. (1987). MC29 deletion mutants which fail to transform chicken macrophages are competent for transformation of quail macrophages. J Virol *61*, 2138-2142.

Bischof, J., Maeda, R. K., Hediger, M., Karch, F., and Basler, K. (2007). An optimized transgenesis system for Drosophila using germ-line-specific phiC31 integrases. Proc Natl Acad Sci USA *104*, 3312-3317.

Blackwood, E. M., and Eisenman, R. N. (1991). Max: a helix-loop-helix zipper protein that forms a sequence-specific DNA-binding complex with Myc. Science *251*, 1211-1217.

Bouchard, C., Dittrich, O., Kiermaier, A., Dohmann, K., Menkel, A., Eilers, M., and Luscher, B. (2001). Regulation of cyclin D2 gene expression by the Myc/Max/Mad network: Myc-dependent TRRAP recruitment and histone acetylation at the cyclin D2 promoter. Genes Dev *15*, 2042-2047.

Brogiolo, W., Stocker, H., Ikeya, T., Rintelen, F., Fernandez, R., and Hafen, E. (2001). An evolutionarily conserved function of the Drosophila insulin receptor and insulin-like peptides in growth control. Current Biology *11*, 213-221.

Brough, D. E., Hofmann, T. J., Ellwood, K. B., Townley, R. A., and Cole, M. D. (1995). An essential domain of the c-myc protein interacts with a nuclear factor that is also required for E1A-mediated transformation. Molecular & Cellular Biology *15*, 1536-1544.

Bush, A., Mateyak, M., Dugan, K., Obaya, A., Adachi, S., Sedivy, J., and Cole, M. (1998). c-myc null cells misregulate cad and gadd45 but not other proposed c-Myc targets. Genes Dev *12*, 3797-3802.

Cawley, S., Bekiranov, S., Ng, H. H., Kapranov, P., Sekinger, E. A., Kampa, D., Piccolboni, A., Sementchenko, V., Cheng, J., Williams, A. J.*, et al.* (2004). Unbiased mapping of transcription factor binding sites along human chromosomes 21 and 22 points to widespread regulation of noncoding RNAs. Cell *116*, 499-509.

Conzen, S. D., Gottlob, K., Kandel, E. S., Khanduri, P., Wagner, A. J., O'Leary, M., and Hay, N. (2000). Induction of cell cycle progression and acceleration of apoptosis are two separable functions of c-Myc: transrepression correlates with acceleration of apoptosis. Mol Cell Biol *20*, 6008-6018.

Cowling, V. H., Chandriani, S., Whitfield, M. L., and Cole, M. D. (2006). A conserved Myc protein domain, MBIV, regulates DNA binding, apoptosis, transformation, and G2 arrest. Mol Cell Biol *26*, 4226-4239.

Cowling, V. H., and Cole, M. D. (2006). Mechanism of transcriptional activation by the Myc oncoproteins. Seminars in Cancer Biology *16*, 242.

Cowling, V. H., and Cole, M. D. (2007). The Myc Transactivation Domain Promotes Global Phosphorylation of the RNA Polymerase II Carboxy-Terminal Domain Independently of Direct DNA Binding. Mol Cell Biol *27*, 2059-2073.

Dang, C. V., O'Donnell, K. A., Zeller, K. I., Nguyen, T., Osthus, R. C., and Li, F. (2006). The c-Myc target gene network. Seminars in Cancer Biology *16*, 253.

De La Cova, C., Abril, M., Bellosta, P., Gallant, P., and Johnston, L. A. (2004). Drosophila myc regulates organ size by inducing cell competition. Cell *117*, 107-116.

de la Cova, C., and Johnston, L. A. (2006). Myc in model organisms: A view from the flyroom. Seminars in Cancer Biology *16*, 303.

Dominguez-Sola, D., Ying, C. Y., Grandori, C., Ruggiero, L., Chen, B., Li, M., Galloway, D. A., Gu, W., Gautier, J., and Dalla-Favera, R. (2007). Non-transcriptional control of DNA replication by c-Myc. Nature *448*, 445-451.

Dugan, K. A., Wood, M. A., and Cole, M. D. (2002). TIP49, but not TRRAP, modulates c-Myc and E2F1 dependent apoptosis. Oncogene *21*, 5835-5843.

Eberhardy, S. R., and Farnham, P. J. (2002). Myc recruits P-TEFb to mediate the final step in the transcriptional activation of the cad promoter. J Biol Chem *277*, 40156-40162.

Ellis, M. C., O'Neill, E. M., and Rubin, G. M. (1993). Expression of Drosophila glass protein and evidence for negative regulation of its activity in non-neuronal cells by another DNA-binding protein. Development *119*, 855-865.

Evan, G. I., Wyllie, A. H., Gilbert, C. S., Littlewood, T. D., Land, H., Brooks, M., Waters, C. M., Penn, L. Z., and Hancock, D. C. (1992). Induction of apoptosis in fibroblasts by c-myc protein. Cell *69*, 119-128.

Fernandez, P. C., Frank, S. R., Wang, L., Schroeder, M., Liu, S., Greene, J., Cocito, A., and Amati, B. (2003). Genomic targets of the human c-Myc protein. Genes Dev *17*, 1115-1129.

Frank, S. R., Schroeder, M., Fernandez, P., Taubert, S., and Amati, B. (2001). Binding of c-Myc to chromatin mediates mitogen-induced acetylation of histone H4 and gene activation. Genes Dev *15*, 2069-2082.

Freytag, S. O., Dang, C. V., and Lee, W. M. (1990). Definition of the activities and properties of c-myc required to inhibit cell differentiation. Cell Growth Differ *1*, 339-343.

Gallant, P. (2006). Myc / Max / Mad in invertebrates - the evolution of the Max network. CTMI *302*, 237-254.

Gallant, P., Shiio, Y., Cheng, P. F., Parkhurst, S. M., and Eisenman, R. N. (1996). Myc and Max homologs in Drosophila. Science *274*, 1523-1527.

Gomez-Roman, N., Grandori, C., Eisenman, R. N., and White, R. J. (2003). Direct activation of RNA polymerase III transcription by c-Myc. Nature *421*, 290-294.

Grandori, C., Cowley, S. M., James, L. P., and Eisenman, R. N. (2000). The Myc/Max/Mad network and the transcriptional control of cell behavior. Annu Rev Cell Dev Biol *16*, 653-699.

Groth, A. C., Fish, M., Nusse, R., and Calos, M. P. (2004). Construction of transgenic Drosophila by using the site-specific integrase from phage phiC31. Genetics *166*, 1775-1782.

Guccione, E., Martinato, F., Finocchiaro, G., Luzi, L., Tizzoni, L., Dall' Olio, V., Zardo, G., Nervi, C., Bernard, L., and Amati, B. (2006). Myc-binding-site recognition in the human genome is determined by chromatin context. Nat Cell Biol *8*, 764-770.

Heaney, M. L., Pierce, J., and Parsons, J. T. (1986). Site-directed mutagenesis of the gag-myc gene of avian myelocytomatosis virus 29: biological activity and intracellular localization of structurally altered proteins. Journal of Virology *60*, 167-176.

Herbst, A., Hemann, M. T., Tworkowski, K. A., Salghetti, S. E., Lowe, S. W., and Tansey, W. P. (2005). A conserved element in Myc that negatively regulates its proapoptotic activity. EMBO Rep *6*, 177-183.

Herbst, A., Salghetti, S. E., Kim, S. Y., and Tansey, W. P. (2004). Multiple cell-type-specific elements regulate Myc protein stability. Oncogene *23*, 3863-3871.

Hirst, S. K., and Grandori, C. (2000). Differential activity of conditional MYC and its variant MYC-S in human mortal fibroblasts. Oncogene *19*, 5189-5197.

Hulf, T., Bellosta, P., Furrer, M., Steiger, D., Svensson, D., Barbour, A., and Gallant, P. (2005). Whole-genome analysis reveals a strong positional bias of conserved dMyc-dependent E-boxes. Mol Cell Biol *25*, 3401-3410.

Johnston, L. A., Prober, D. A., Edgar, B. A., Eisenman, R. N., and Gallant, P. (1999). Drosophila myc regulates cellular growth during development. Cell *98*, 779-790.

Kato, G. J., Barrett, J., Villa, G. M., and Dang, C. V. (1990). An amino-terminal c-myc domain required for neoplastic transformation activates transcription. Molecular & Cellular Biology *10*, 5914-5920.

Kenney, A. M., Cole, M. D., and Rowitch, D. H. (2003). Nmyc upregulation by sonic hedgehog signaling promotes proliferation in developing cerebellar granule neuron precursors. Development *130*, 15-28.

Kim, S. Y., Herbst, A., Tworkowski, K. A., Salghetti, S. E., and Tansey, W. P. (2003). Skp2 regulates Myc protein stability and activity. Mol Cell *11*, 1177-1188.

Lee, T. C., Li, L. H., Philipson, L., and Ziff, E. B. (1997). Myc represses transcription of the growth arrest gene gas1. Proceedings of the National Academy of Sciences of the United States of America *94*, 12886-12891.

Li, L. H., Nerlov, C., Prendergast, G., MacGregor, D., and Ziff, E. B. (1994). c-Myc represses transcription in vivo by a novel mechanism dependent on the initiator element and Myc box II. Embo Journal *13*, 4070-4079.

Liu, X., Tesfai, J., Evrard, Y. A., Dent, S. Y., and Martinez, E. (2003). c-Myc transformation domain recruits the human STAGA complex and requires TRRAP and GCN5 acetylase activity for transcription activation. J Biol Chem *278*, 20405-20412.

Liu, X., Vorontchikhina, M., Wang, Y.-L., Faiola, F., and Martinez, E. (2008). STAGA Recruits Mediator to the MYC Oncoprotein To Stimulate Transcription and Cell Proliferation. Mol Cell Biol *28*, 108-121.

Maines, J. Z., Stevens, L. M., Tong, X., and Stein, D. (2004). Drosophila dMyc is required for ovary cell growth and endoreplication. Development *131*, 775-786.

McMahon, S. B., Van, B. H., Dugan, K. A., Copeland, T. D., and Cole, M. D. (1998). The novel ATM-related protein TRRAP is an essential cofactor for the c-Myc and E2F oncoproteins. Cell *94*, 363-374.

McMahon, S. B., Wood, M. A., and Cole, M. D. (2000). The essential cofactor TRRAP recruits the histone acetyltransferase hGCN5 to c-Myc. Molecular & Cellular Biology *20*, 556-562.

Moberg, K. H., Bell, D. W., Wahrer, D. C., Haber, D. A., and Hariharan, I. K. (2001). Archipelago regulates Cyclin E levels in Drosophila and is mutated in human cancer cell lines. Nature *413*, 311-316.

Moberg, K. H., Mukherjee, A., Veraksa, A., Artavanis-Tsakonas, S., and Hariharan, I. K. (2004). The Drosophila F box protein archipelago regulates dMyc protein levels in vivo. Curr Biol *14*, 965-974.

Montagne, J., Stewart, M. J., Stocker, H., Hafen, E., Kozma, S. C., and Thomas, G. (1999). Drosophila S6 kinase: A regulator of cell size. Science *285*, 2126-2129.

Montero, L., Müller, N., and Gallant, P. (2008). Induction of apoptosis by *Drosophila* Myc. Genesis *46*, 104-111.

Muratani, M., and Tansey, W. P. (2003). How the ubiquitin-proteasome system controls transcription. Nat Rev Mol Cell Biol *4*, 192.

Nair, S. K., and Burley, S. K. (2003). X-ray structures of Myc-Max and Mad-Max recognizing DNA. Molecular bases of regulation by proto-oncogenic transcription factors. Cell *112*, 193-205.

Neufeld, T. P., de la Cruz, A. F., Johnston, L. A., and Edgar, B. A. (1998). Coordination of growth and cell division in the Drosophila wing. Cell *93*, 1183-1193.

Nikiforov, M. A., Chandriani, S., Park, J., Kotenko, I., Matheos, D., Johnsson, A., McMahon, S. B., and Cole, M. D. (2002). TRRAP-dependent and TRRAP-independent transcriptional activation by Myc family oncoproteins. Mol Cell Biol *22*, 5054-5063.

Orian, A., Van Steensel, B., Delrow, J., Bussemaker, H. J., Li, L., Sawado, T., Williams, E., Loo, L. W., Cowley, S. M., Yost, C*., et al.* (2003). Genomic binding by the Drosophila Myc, Max, Mad/Mnt transcription factor network. Genes Dev *17*, 1101-1114.

Oster, S. K., Ho, C. S., Soucie, E. L., and Penn, L. Z. (2002). The myc oncogene: MarvelouslY Complex. Adv Cancer Res *84*, 81-154.

Oster, S. K., Mao, D. Y., Kennedy, J., and Penn, L. Z. (2003). Functional analysis of the N-terminal domain of the Myc oncoprotein. Oncogene *22*, 1998-2010.

Park, J., Wood, M. A., and Cole, M. D. (2002). BAF53 forms distinct nuclear complexes and functions as a critical c-Myc-interacting nuclear cofactor for oncogenic transformation. Mol Cell Biol *22*, 1307-1316.

Penn, L. J., Brooks, M. W., Laufer, E. M., Littlewood, T. D., Morgenstern, J. P., Evan, G. I., Lee, W. M., and Land, H. (1990). Domains of human c-myc protein required for autosuppression and cooperation with ras oncogenes are overlapping. Mol Cell Biol *10*, 4961-4966.

Peukert, K., Staller, P., Schneider, A., Carmichael, G., Hanel, F., and Eilers, M. (1997). An alternative pathway for gene regulation by myc. Embo Journal *16*, 5672-5686.

Pierce, S., Yost, C., Delrow, J., McMacken, S., Flynn, E. M., and Eisenman, R. (in press). Drosophila Growth and Development in the Absence of dMyc and dMnt. Dev Biol.

Pierce, S. B., Yost, C., Anderson, S. A. R., Flynn, E. M., Delrow, J., and Eisenman, R. N. (2008). Drosophila growth and development in the absence of dMyc and dMnt. Developmental Biology *315*, 303.

Pierce, S. B., Yost, C., Britton, J. S., Loo, L. W., Flynn, E. M., Edgar, B. A., and Eisenman, R. N. (2004). dMyc is required for larval growth and endoreplication in Drosophila. Development *131*, 2317-2327.

Pirity, M., Blanck, J. K., and Schreiber-Agus, N. (2006). Lessons learned from Myc/Max/Mad knockout mice. Curr Top Microbiol Immunol *302*, 205-234.

Sarid, J., Halazonetis, T. D., Murphy, W., and Leder, P. (1987). Evolutionarily conserved regions of the human c-myc protein can be uncoupled from transforming activity. Proceedings of the National Academy of Sciences of the United States of America *84*, 170-173.

Schreiber-Agus, N., Stein, D., Chen, K., Goltz, J. S., Stevens, L., and DePinho, R. A. (1997). Drosophila Myc is oncogenic in mammalian cells and plays a role in the diminutive phenotype. Proc Natl Acad Sci USA *94*, 1235-1240.

Secombe, J., Li, L., Carlos, L., and Eisenman, R. N. (2007). The Trithorax group protein Lid is a trimethyl histone H3K4 demethylase required for dMyc-induced cell growth. Genes Dev *21*, 537-551.

Spotts, G. D., Patel, S. V., Xiao, Q. R., and Hann, S. R. (1997). Identification of downstream-initiated c-myc proteins which are dominant-negative inhibitors of transactivation by full-length c-myc proteins. Molecular & Cellular Biology *17*, 1459-1468.

Steiger, D., Furrer, M., Schwinkendorf, D., and Gallant, P. (submitted). Max-independent functions of Myc in *Drosophila*.

Stone, J., de, L. T., Ramsay, G., Jakobovits, E., Bishop, J. M., Varmus, H., and Lee, W. (1987). Definition of regions in human c-myc that are involved in transformation and nuclear localization. Molecular & Cellular Biology *7*, 1697-1709.

Trumpp, A., Refaeli, Y., Oskarsson, T., Gasser, S., Murphy, M., Martin, G. R., and Bishop, J. M. (2001). c-Myc regulates mammalian body size by controlling cell number but not cell size. Nature *414*, 768-773.

Venken, K. J. T., He, Y., Hoskins, R. A., and Bellen, H. J. (2006). P[acman]: A BAC Transgenic Platform for Targeted Insertion of Large DNA Fragments in D. melanogaster. Science %R 101126/science1134426 *314*, 1747-1751.

von der Lehr, N., Johansson, S., Wu, S., Bahram, F., Castell, A., Cetinkaya, C., Hydbring, P., Weidung, I., Nakayama, K., Nakayama, K. I*., et al.* (2003). The F-box protein Skp2 participates in c-Myc proteosomal degradation and acts as a cofactor for c-Myc-regulated transcription. Mol Cell *11*, 1189-1200.

Wood, M. A., McMahon, S. B., and Cole, M. D. (2000). An ATPase/helicase complex is an essential cofactor for oncogenic transformation by c-Myc. Mol Cell *5*, 321-330.

Xiao, Q., Claassen, G., Shi, J., Adachi, S., Sedivy, J., and Hann, S. R. (1998). Transactivation-defective c-MycS retains the ability to regulate proliferation and apoptosis. Genes Dev *12*, 3803-3808.

Figures

Figure 1

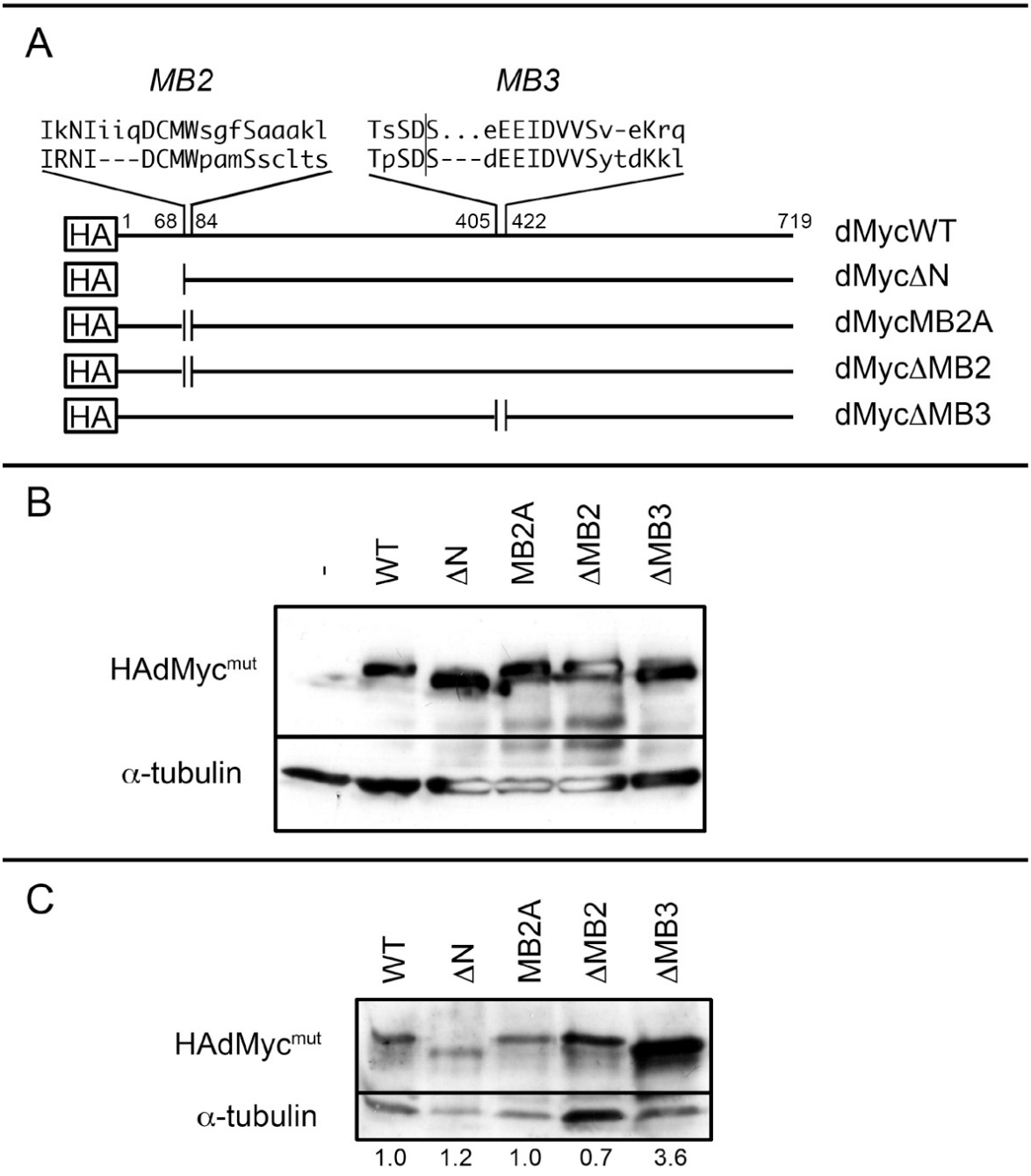

Figure 1a

Figure 1

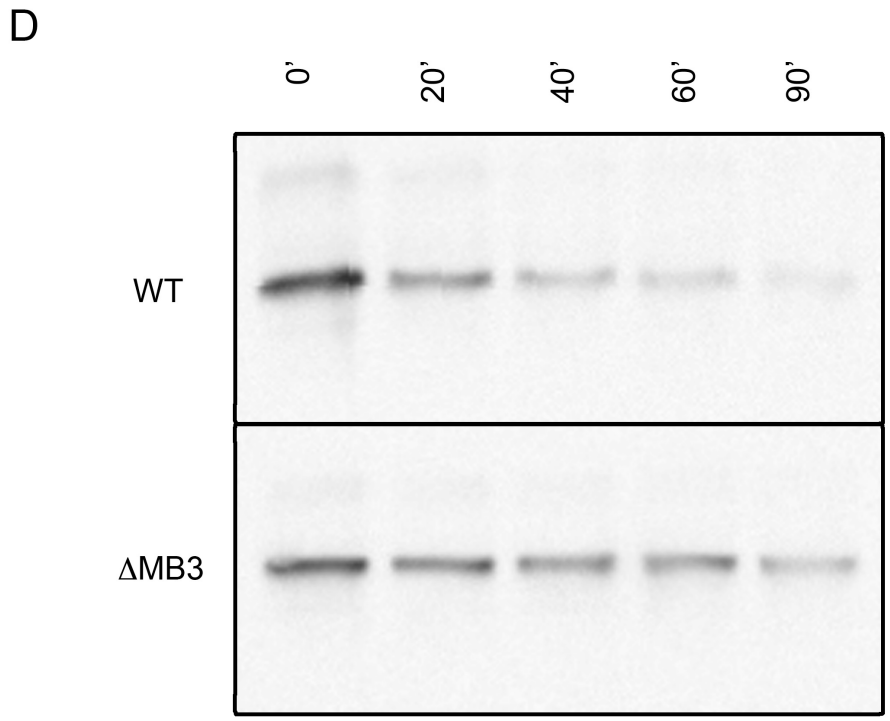

Figure 1b

Figure 2

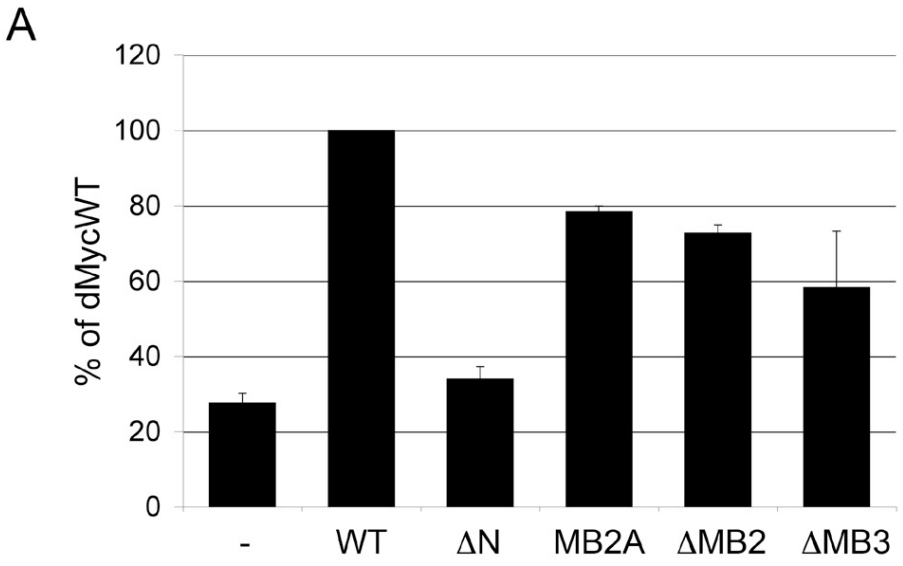

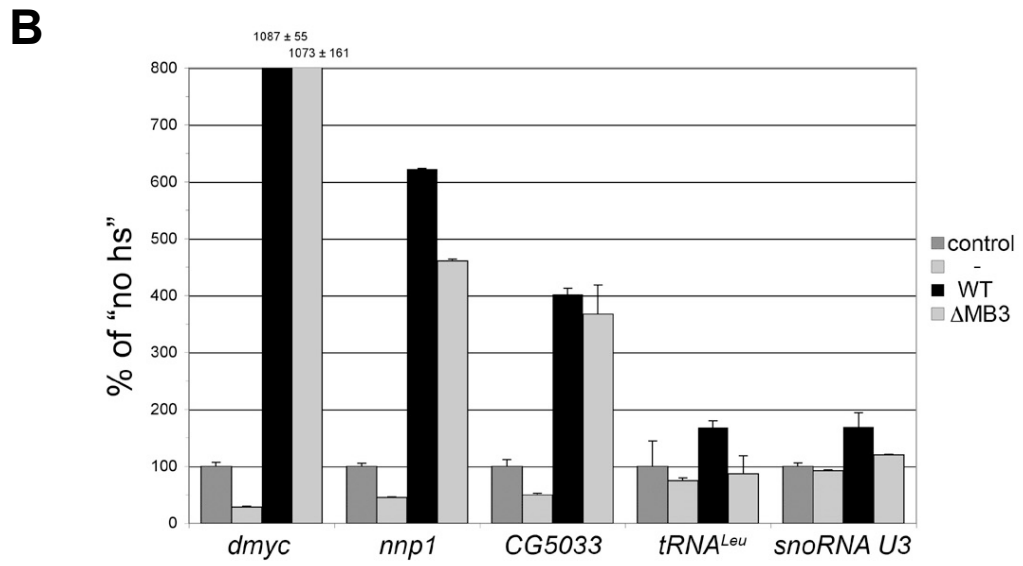

Figure 2

Figure 3

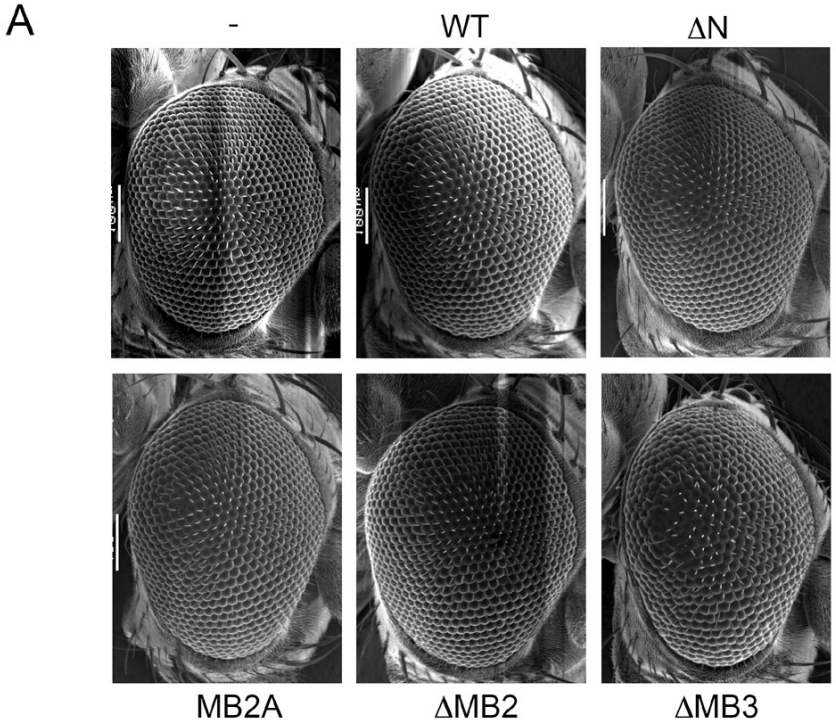

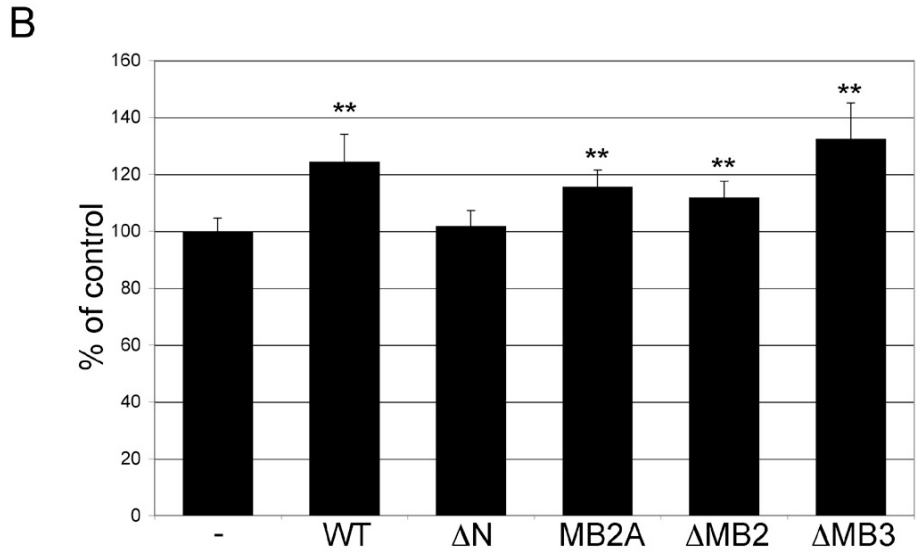

Figure 3a

Figure 3

C

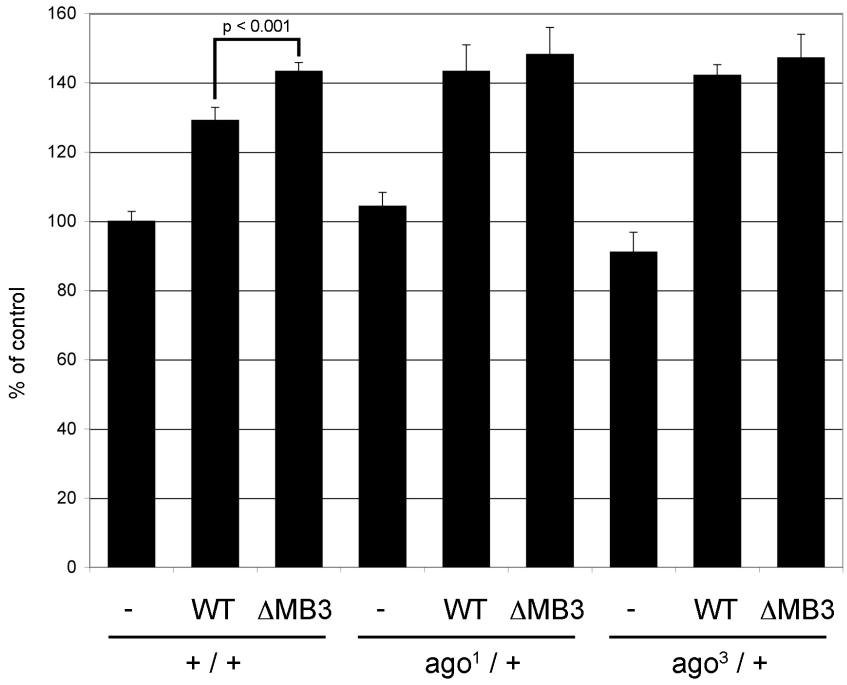

D

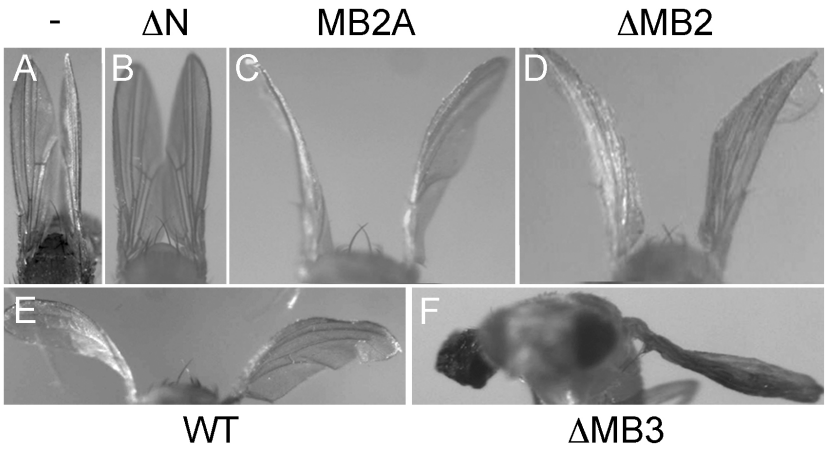

Figure 3b

Figure 4

A

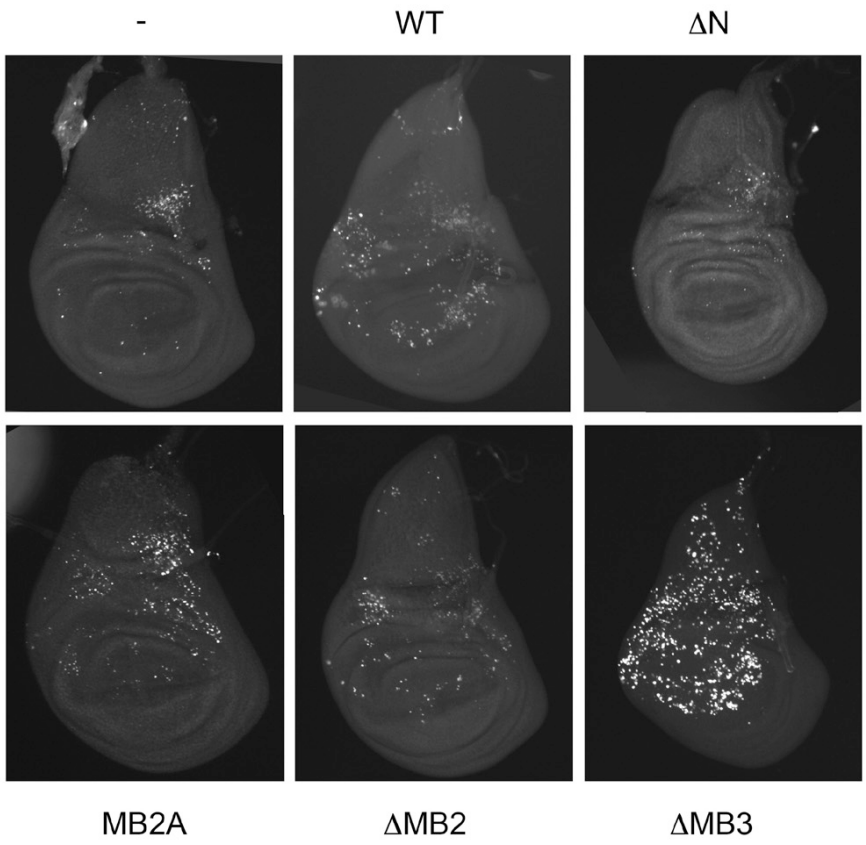

Figure 4

Figure 5

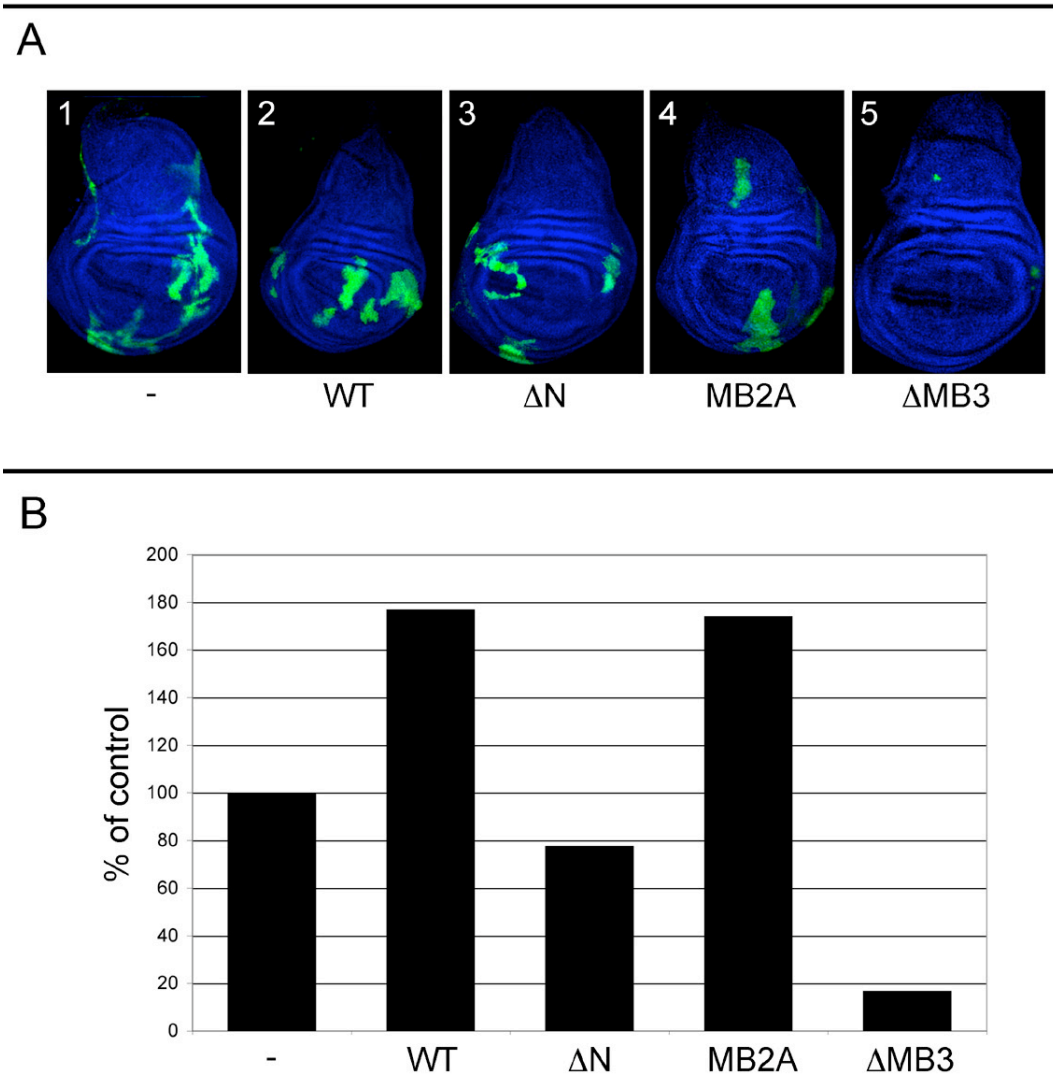

Figure 5

Figure 6

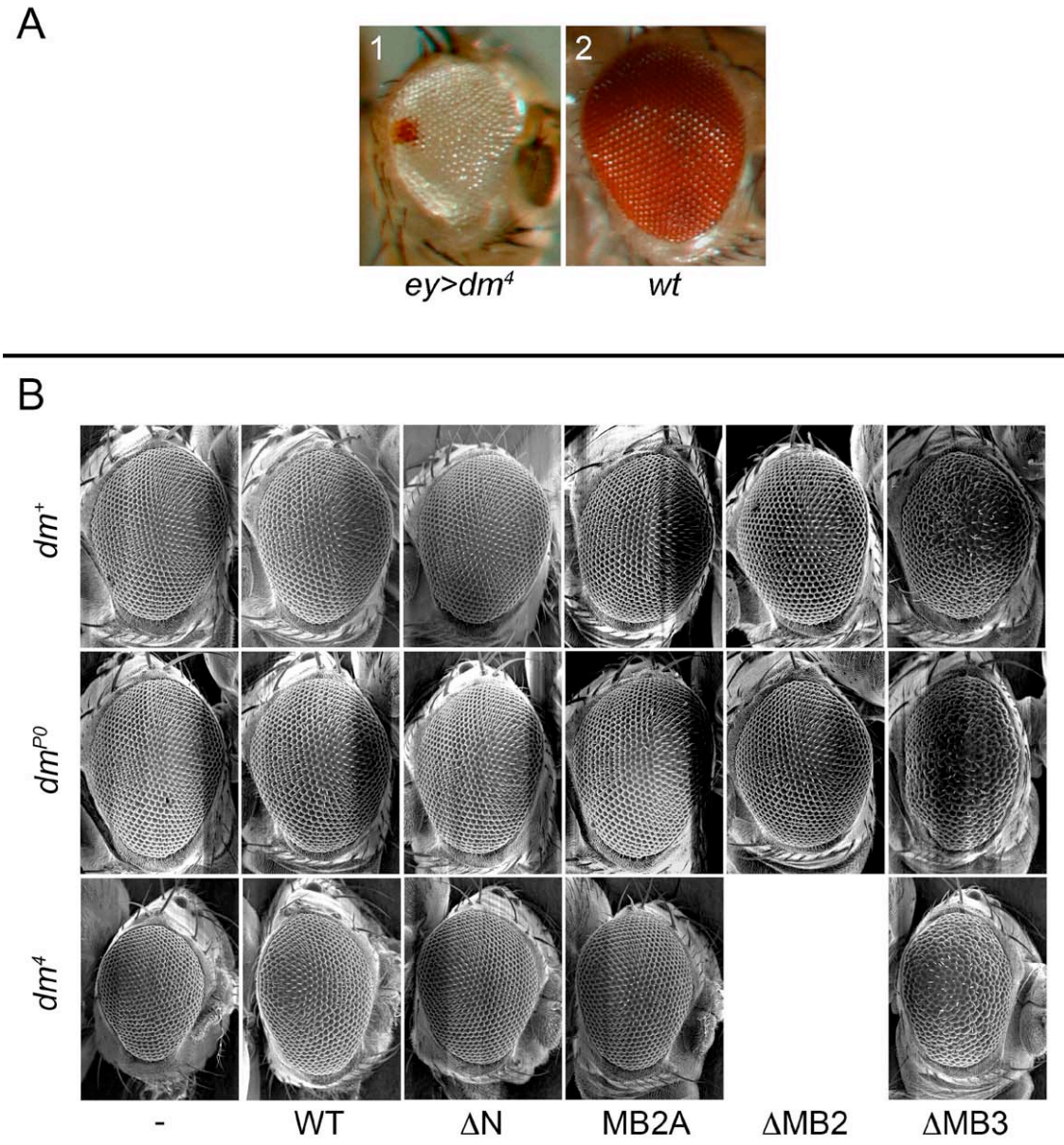

Figure 6a

Figure 6

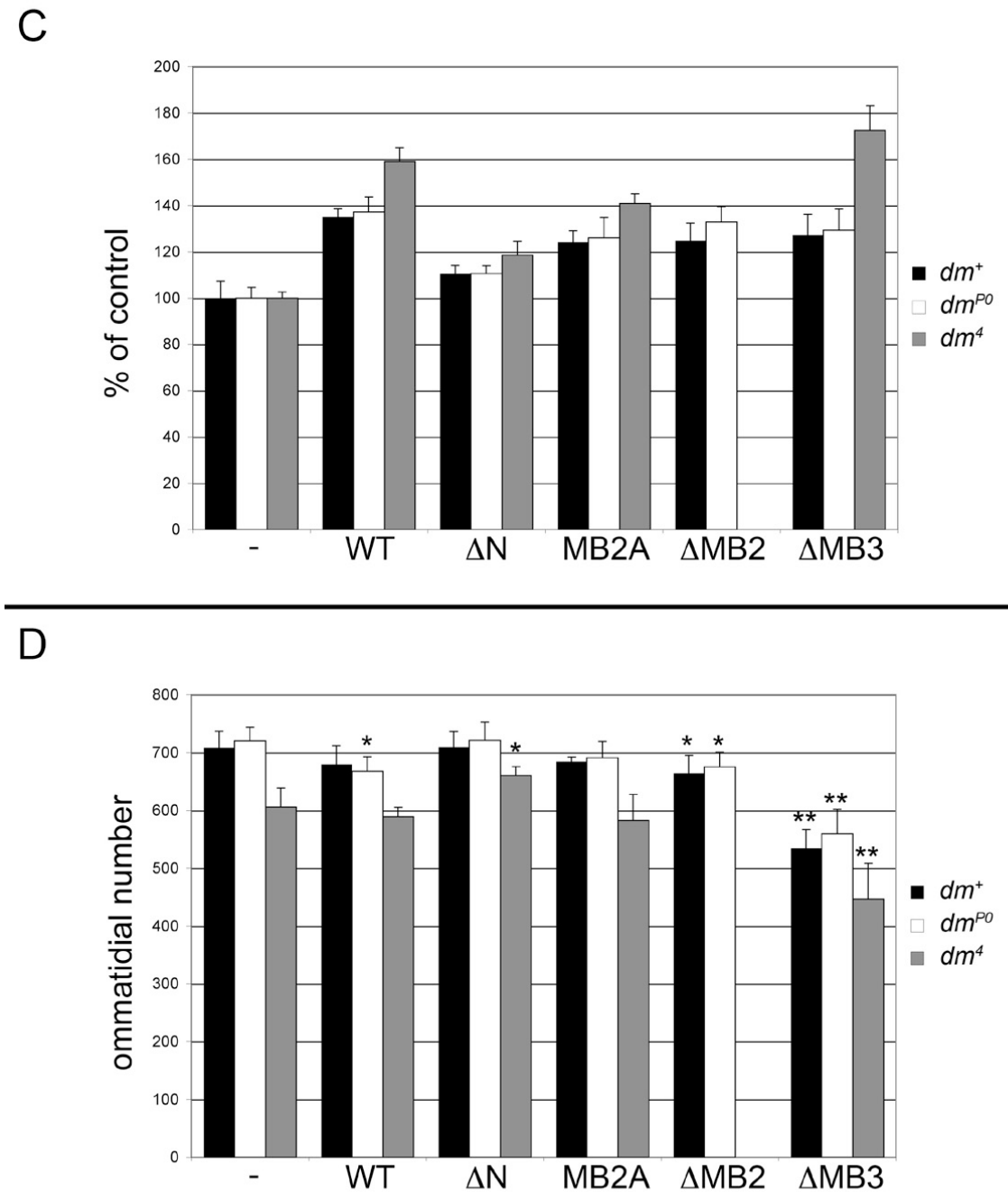

Figure 6b

Figure 7

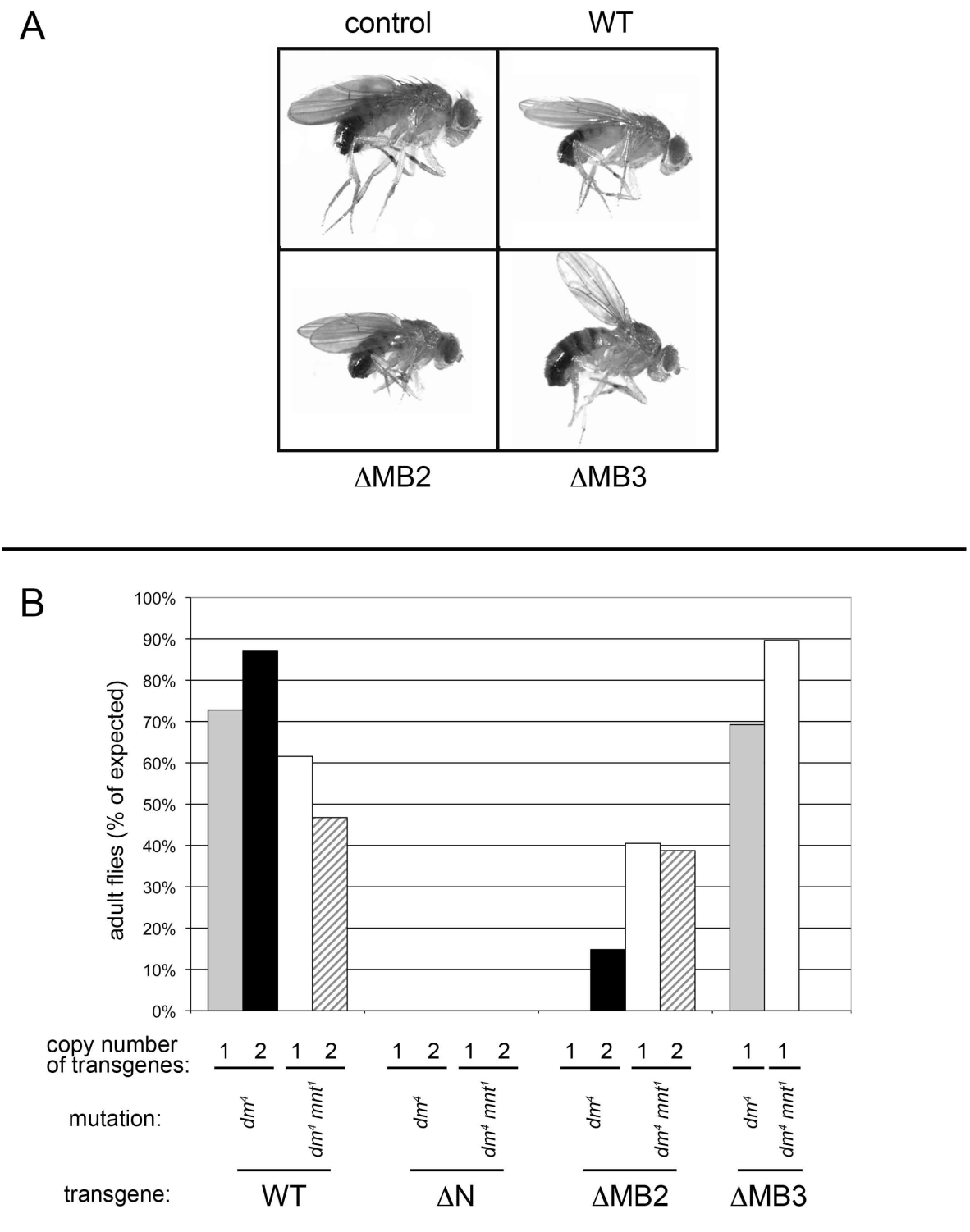

Figure 7a

Figure 7

C

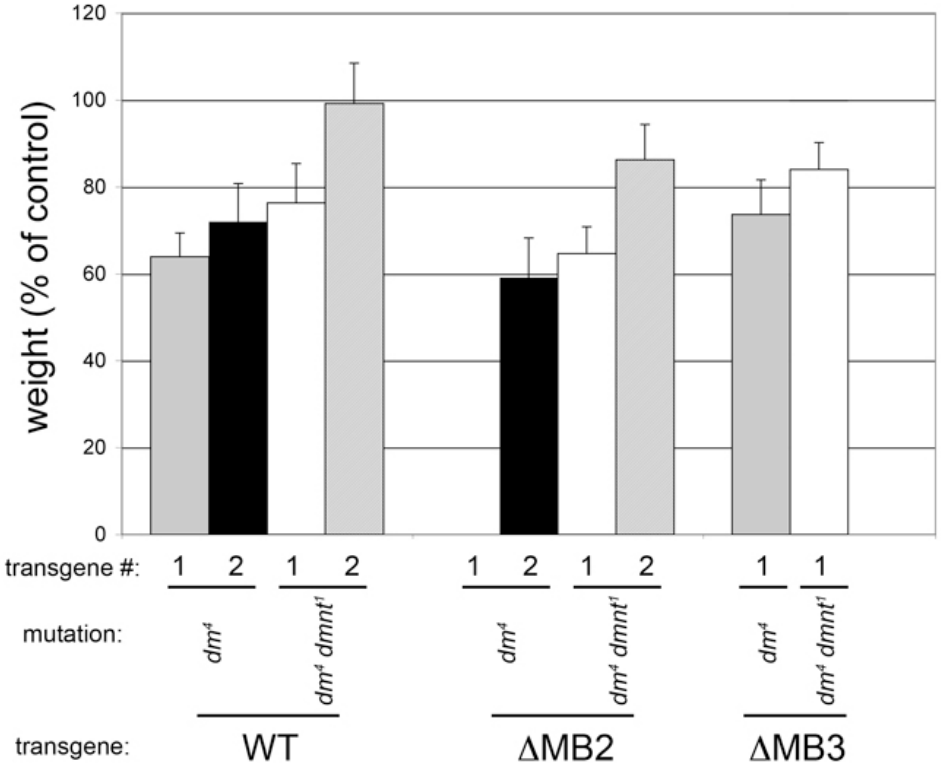

Figure 7b

Table 1

		transgene					
dmyc	*GAL4 driver*	**-**	**WT**	**ΔN**	**MB2A**	**ΔMB2**	**ΔMB3**
+	**arm**	yes	yes	yes	yes		yes
+	**act**	yes	-	yes	-		-
+	**da**	yes	-	yes	-		-
+	**tub**	yes	-	yes	-		-
PL35	**arm**	-	-	-	-		-
PL35	**da**	-	-	yes	-	-	-
PL35	**tub**	-	-	-	-	-	-
PG45	**(dmyc)**	-	-	yes	yes		-
2	**arm**	-	-	-	-		-
2	**da**	-	-	-	-	-	-
2	**tub**	-	-	-	-	-	-
4	**arm**	-	-	-	-		-
4	**da**	-	-	-	-	-	-
4	**tub**	-	-	-	-	-	-

Table 1

Additional experiments not shown in the manuscript

1. Integration site determination

The site-directed phage ϕC31 integration system was used for transgenesis to integrate all constructs in the same locus and eliminate differences in expression levels or pattern caused by differences in genomic environment. All UAS-dMyc (mutant) constructs were generated by integration into the line ZH-86Fb (Bischof et al., 2007). In order to confirm that the different UAS-constructs of our dMyc mutations were integrated into the correct position in the fly genome, PCR assays were performed on genomic DNA of the different UAS-dMyc transgenic flies.

The first primer iPCRSV40F1 was selected to bind directly after the open reading frame in the SV40 polyA site of the pUASTB plasmid, the second primer ZH*att*P14R was selected to bind in the *att*P landing site of the fly genome. A product length of 950 base pairs was expected in the case of correct integration. All transgenics show a band with the expected length (shown in Figure 1). As a control, genomic DNA of *y w* animals was taken. As expected no band could be observed for the control. Therefore, all constructs are integrated at the expected location.

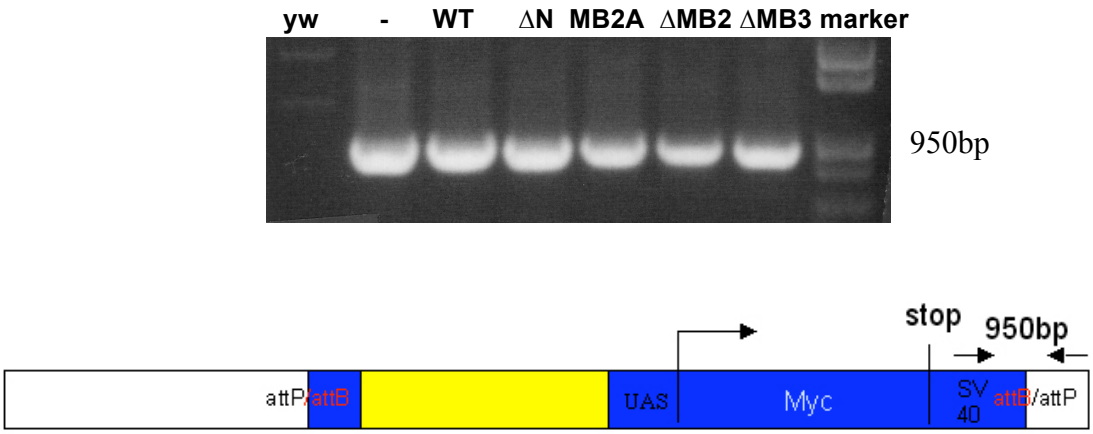

Figure 1: Electrophoretic separation of the PCR products for confirmation of the correct integration site of the different dMyc mutant constructs in the fly genome. The expected band of 950bp was observed in two independent experiments for all strains except *y w* genomic DNA.

Label:	Genotype:
yw	*y w*
-	*y w*; M{3xP3-RFP.*att*P'}ZH-86Fb
WT	*y w*; M{3xP3-RFP.*att*P/B UAS-dMycWT}ZH-86Fb
ΔN	*y w*; M{3xP3-RFP.*att*P/B UAS-dMycΔN}ZH-86Fb
MB2A	*y w*; M{3xP3-RFP.*att*P/B UAS-dMycMB2A}ZH-86Fb
ΔMB2	*y w*; M{3xP3-RFP.*att*P/B UAS-dMycΔMB2}ZH-86Fb
ΔMB3	*y w*; M{3xP3-RFP.*att*P/B UAS-dMycΔMB3}ZH-86Fb

2. Luciferase assay (nnp1)

Previously, we analysed how the different dMyc mutants activate a dMyc-dependent luciferase reporter construct derived from the dMyc target gene *CG5033*. To demonstrate that the effects on transactivation that we saw for the different dMyc domain mutants show the same activities towards a second reporter system, we repeated the Luciferase assay and used the promoter of another dMyc target gene *nnp1*, instead.

For this reason, S2 cells were transfected with the different dMyc mutants, together with a *Renilla* luciferase reporter construct under the control of the promoter of the dMyc target gene *nnp1* (Hulf et al., 2005) and a second construct, where the E-Box, which is the binding site for Myc, was mutated into an EcoRI site. This mutation abolishes dMyc-binding and thus renders the reporter construct dMyc-unresponsive. This mutant promoter was used to drive firefly luciferase. Hence, the ratio of *Renilla* to firefly luciferase directly reflects dMyc activity.

A deletion of the N-terminus strongly reduces dMyc`s transactivation ability not only when *CG5033* was used as a promoter but also in case of *nnp1* (as shown in Figure 2). A deletion (dMycΔMB2) or mutation (dMycMB2A) of the highly conserved Myc Box 2, as well as a deletion of the highly conserved Myc Box 3 (dMycΔMB3) reduces the potential of dMyc transactivation, however some function still remains. In the manuscript we showed that all proteins are expressed at comparable levels and that (if anything) dMycΔMB3 is more abundant than dMycWT. This confirms that MB2 and MB3 are both necessary for full transactivation of dMyc target genes. Moreover, this demonstrates that the effects of the different dMyc mutants with respect to their transactivation ability are not restricted to one dMyc target gene, since another target gene, *nnp1* shows the same response to the dMyc mutants.

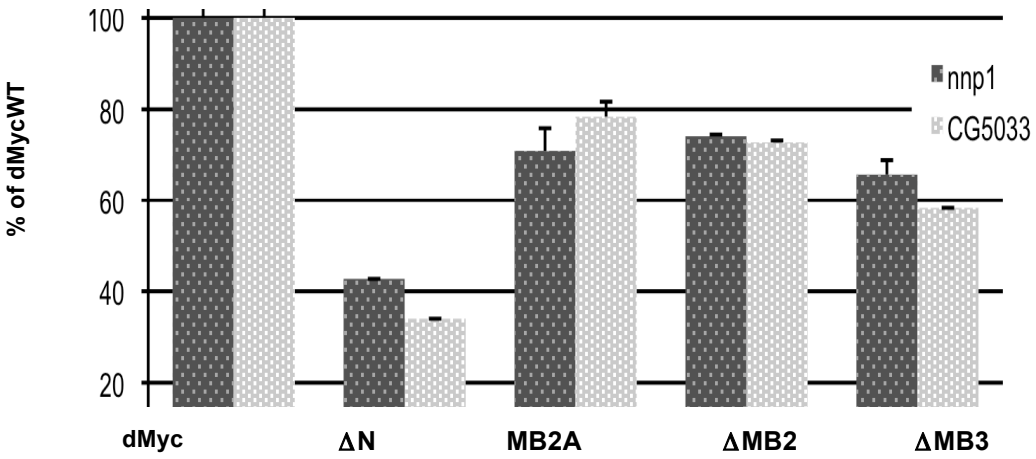

Figure 2: Transactivation ability of the different dMyc mutants relative to dMycWT for Myc target genes *nnp1* and *CG5033*. Plotted is the mean of 2 repeats, error bars indicate the standard error of the mean.

3. Expression levels of dMyc target genes not shown in the manuscript

In the manuscript we pointed out that dMycΔMB3 differentially activates different endogenous target genes of dMyc *in vivo*. For example, the ability of dMycΔMB3 to activate the Pol III genes $tRNA^{Leu}$ and *snoRNA U3* was clearly reduced as compared to dMycWT. However, both proteins activated other dMyc target genes equally efficiently.

For this experiment we used flies that are null for *dmyc* and carried a ubiquitously expressed dMycWT cDNA "*tub*-FRT-dMyc-FRT-GAL4" and an hs-FLP construct, to rescue the null mutant phenotype. A massive heat shock (2 hours at 37°C) was given 5 days after egg deposition (AED) in order to uncover the null mutant phenotype. At the same time, GAL4 was expressed in these flies and drove the expression of the UAS-controlled dMycWT or dMycΔMB3 transgenes, allowing us to analyse the effect of the different constructs in the absence of endogenous dMyc. By TUNEL staining we observed increased numbers of apoptotic cells in wing imaginal discs of flies with the genotype "*w* dm^4 *tub*-FRT-dMyc-FRT-GAL4 hs-FLP; UAS-dMycΔMB3" compared to control flies carrying the empty transgene pUASTB 12 hours after the heat shock; however, 8 hours after the heat shock no cell death was observed. Therefore, we decided to analyse the dMyc target levels 8 hours after the heat shock, because this furthermore increases the chance for observing direct dMyc effects.

To examine leakiness of the GAL4-system described above, a probe for the HA-tag was included that only detects the UAS-HAdMyc transgenes. Since control flies do not get a heat-shock they should not express the HA-tag. To analyse, if this holds true, responsiveness of the different cDNAs on HA-tag primers was examined. We could show that HA-tag levels are upregulated by about 20x upon heat-shock (compare control and WT). However, the UAS-HAdMyc transgene seems to be a bit leaky since HA-tag levels are 10x higher compared to a second control, lacking an HA-tag (*w* dm^4 *tub*>dMyc>GAL4 hs-FLP/Y; pUASTB/+). In the manuscript we showed, that *dmyc* mRNA levels were 10x higher after induction (compare control and WT). Thus, the total amount of dMyc before the heat-shock (*tub*>dMyc and leakiness of UAS-HAdMyc) equates to 10% of UAS-HAdMyc after the heat-shock. In this experiment we could show, that the amount of UAS-HAdMyc before the heat-shock equates to 5% of UAS-HAdMyc after the heat-shock. Thus, the *tub*>dMyc transgene contributes another 5% (as compared to the sample "WT + heat-shock") of the expression before heat-shock.

The microarray analysis of dMyc targets (Hulf et al., 2005) included all RNA Polymerase II protein-coding genes known at that time, but RNA Polymerase I & III transcribed genes were not analysed. Several dMyc targets, that were consistently responsive to changes in dMyc levels (i.e. in several different microarray experiments) and that contained (or not) a downstream E-box (i.e. potentially belong to different classes of dMyc targets) were selected as examples for RNA Pol II transcribed genes, to identify genes that are differentially regulated by dMycΔMB3 and dMycWT. One of these genes is *CG18610*, which is assumed to be involved in transcription elongation (based on sequence annotation). As illustrated in Figure 3, *CG18610* is induced to about 150% by expression of dMycWT, but no difference could be observed between the expression levels of *CG18610* in dMycWT or dMycΔMB3 larvae.

We also included genes transcribed by RNA Pol III for our analysis since it had been shown previously that Myc also controls the transcription of those genes (Gomez-Roman et al., 2003; Grewal et al., 2005; Steiger et al., 2008). In the manuscript we show that dMyc ΔMB3 is impaired in activating the Pol III targets $tRNA^{Leu}$ and *snoRNA U3*. The mRNA level of a third Pol III target, *5S RNA*, was not affected by overexpression of dMyc (shown in Figure 3).

As a last group of candidates we analysed genes of the apoptotic pathway since we have shown that apoptosis is strongly enhanced after overexpression of dMycΔMB3 in the wing imaginal disc. Since a deletion of MB3 enhanced not only stability of the dMyc protein but also its ability to induce apoptosis, we thought that direct dMyc target genes might also be affected by this deletion in a positive manner. Montero et al. 2008, showed that the pro-apoptotic genes *reaper* and *sickle* are potential targets of dMyc. Thus, we analysed *sickle* and *reaper* by qRT-PCR. Overexpression of dMycΔMB3 did not affect the expression of *sickle* and *reaper* (as demonstrated in Figure 3).

Taken together, these data show that there is a role for MB3 in controlling transactivation at least of RNA Pol III genes since the RNA Pol III genes $tRNA^{Leu}$ and *snoRNA U3* showed a clear upregulation upon overexpression of dMyc but not upon overexpression of dMycΔMB3 in this assay. However, no upregulation of other E-box dependent genes or genes of the apoptotic pathway were observed, which suggests that MB3 plays a specific role in the activation of Pol III genes.

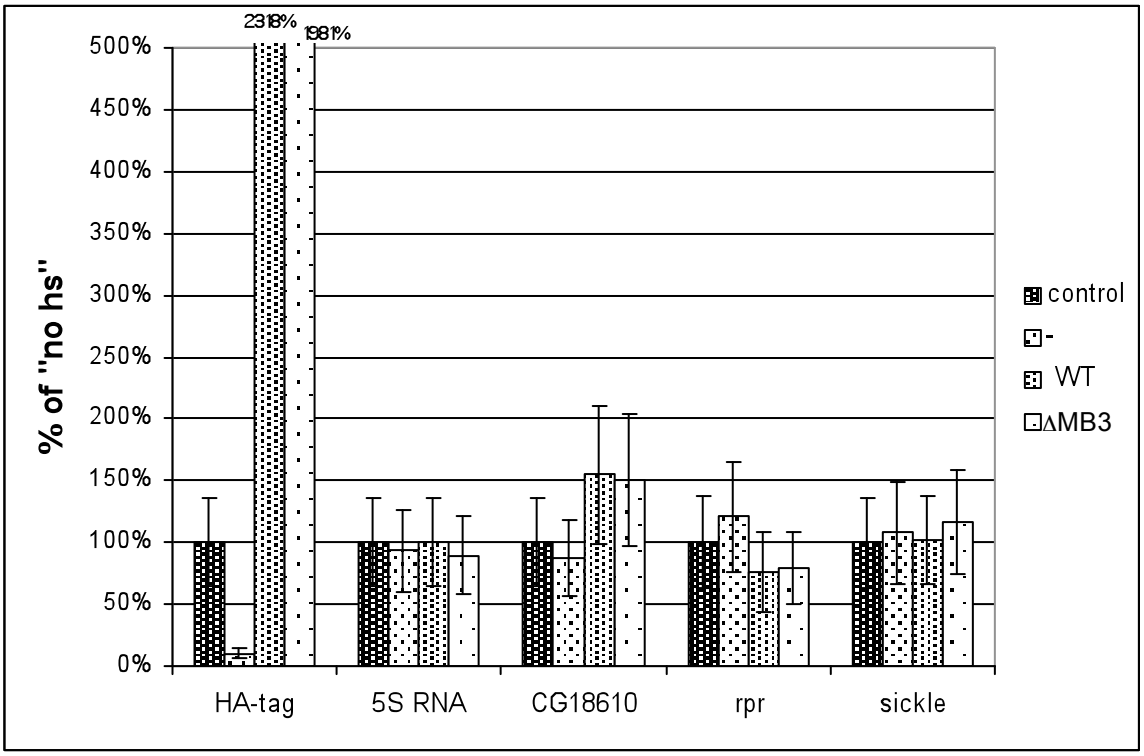

Figure 3: Transcript levels of different dMyc target genes as determined by qRT-PCR of larvae overexpressing dMycWT, dMycΔMB3 or no dMyc protein (-) compared to control larvae (dMycWT without hs). Samples were taken 8h after the hs (for details see Materials and Methods). Error bars indicate standard deviation of the mean of two independent biological replicates.

Label:	Genotype:
control (no hs)	*w dm*^{4} *tub*>dMyc>GAL4 hs-FLP/Y; UAS-dMycWT/UAS-dMycWT
-	*w dm*^{4} *tub*>dMyc>GAL4 hs-FLP/Y; pUASTB/pUASTB
WT	*w dm*^{4} *tub*>dMyc>GAL4 hs-FLP/Y; UAS-dMycWT/UAS-dMycWT
ΔMB3	*w dm*^{4} *tub*>dMyc>GAL4 hs-FLP/Y; UAS-dMycΔMB3/UAS-dMycΔMB3

4. Inhibition of apoptosis by co-overexpression of p35

To find out if the apoptosis we saw after overexpression of the different dMyc mutants in the dorsal compartment of the wing disc (see Figure 4, manuscript) carries all the hallmarks of classical apoptosis, i.e. can also be inhibited by the pan-caspase inhibitor p35, we co-overexpressed p35 together with the dMyc mutants. An additional motivation for this experiment was to see what happens when the death-promoting activity of dMycΔMB3 is blocked - do we then see a massive overgrowth, because dMycΔMB3 is much more active than dMycWT?

Apoptotic cells were marked with anti-cleaved caspase 3 antibody and visualized by a red fluorescent antibody. P35 fully inhibits apoptosis in all cases, also for a deletion of the acidic domain, which otherwise showed the strongest apoptotic effects (Figure 4, panel G). Thus, the observed apoptosis is a result of caspase activation. However, we could not observe an overgrowth of the dorsal compartment of the wing discs using this assay.

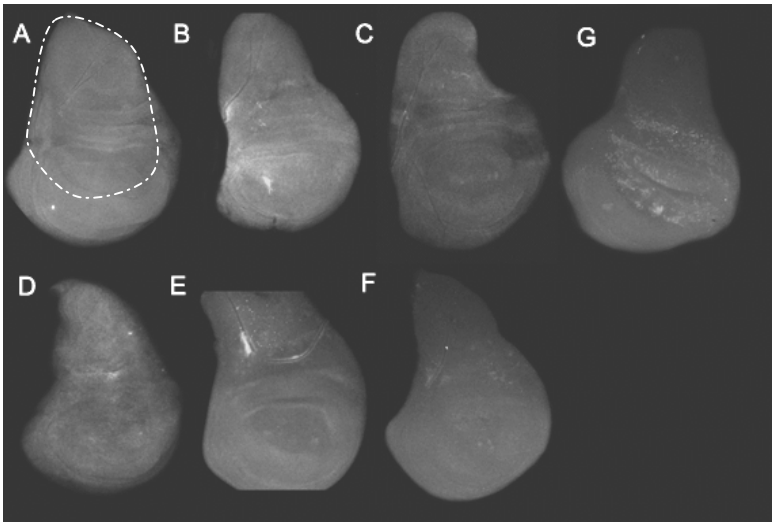

Figure 4: Overexpression of dMycΔMB3 causes apoptosis (G); co-overexpression of UAS-p35 completely inhibits apoptosis for all genotypes (A-F). Transgenes are expressed in the dorsal compartment of the wing disc. The white line marks area of expression. Top=dorsal, bottom=ventral. The phenotype was observed in the majority of the wing discs of one biological replicate. White dots seen in panel G are apoptotic cells that are marked with an anti-cleaved caspase 3 antibody.

Label:	Genotype:
A	*y w*; *ap*-GAL4/+; UAS-p35/pUASTB
B	*y w*; *ap*-GAL4/+; UAS-p35/UAS-dMycWT
C	*y w*; *ap*-GAL4/+; UAS-p35/UAS-dMycΔN
D	*y w*; *ap*-GAL4/+; UAS-p35/UAS-dMycMB2A
E	*y w*; *ap*-GAL4/+; UAS-p35/UAS-dMycΔMB2
F	*y w*; *ap*-GAL4/+; UAS-p35/UAS-dMycΔMB3
G	*y w*; *ap*-GAL4/+; +/UAS-dMycΔMB3

5. Inhibition of apoptosis leads to overgrowth in the eye

Co-overexpression of p35 in the wing imaginal discs (see results section, 4.) inhibited apoptosis caused by overexpression of dMyc. Moreover, ommatidial size is reduced after additional overexpression of dMyc mutants in eyes that already highly overexpress dMycWT (Steiger et al., 2008; Montero et al., 2008) presumably because, at high levels of expression, dMyc-induced apoptosis overcomes dMyc-induced growth, resulting in a net decrease of ommatidial and tissue size. As we have previously shown that ommatidial size of eyes highly overexpressing dMycWT can be increased by blockage of apoptosis (Montero et al., 2008; Steiger et al., 2008), we were interested if the size of ommatidia expressing mutant dMyc proteins can be enhanced after inhibition of apoptosis.

For this purpose we overexpressed the dMyc mutants with *GMR*-GAL4, either alone or in combination with the pancaspase-inhibitor p35. Overexpression of the different dMyc mutants does not affect roughness of the eye (except for dMycΔMB3), suggesting that only growth and not apoptosis are affected by such mutants (see manuscript, Figure 3). This goes along with the observation that strong overexpression of dMyc is necessary to induce apoptosis (Steiger et al, submitted). Moreover, overexpression of one copy of dMyc in third instar eye imaginal discs does not induce apoptosis (P.Gallant, unpublished observation). Thus, only overexpression of dMycΔMB3 induces apoptosis. After co-overexpression of p35 and dMycWT or dMycΔMB3 the ommatidial pattern gets distorted, all other eyes look normal (Figure 5). The size of 20 centrally located ommatidia of 5 individual eyes per genotype was analysed and plotted in Figure 6. We observed an increase in ommatidial size for all dMyc expressing lines. However, the strongest increase was monitored with dMycΔMB3. Ommatidial size is enhanced by 35% when p35 is co-expressed (Figure 6).

This supports that the rough eye phenotype we observed (Figure 5, panel F) is caused by a combination of excessive growth and apoptosis, since ommatidia blocked from undergoing apoptosis, which overexpressed dMyc showed a strong increase in ommatidial size.

The p-values for "*GMR*-GAL4; UAS-p35/+" vs. "*GMR*-GAL4; UAS-p35/UAS-dMycΔN" were not significant ($p \geq 0.5$) indicating that this mutant is biologically inactive as described earlier. However, the observation that all other dMyc mutants were capable of inducing apoptosis (since all of them showed a significant increase in ommatidial size after co-overexpression with UAS-p35) suggests that not only dMycΔMB3 induces apoptosis after overexpression in the eye. There are three possible explanations for this observation. First, p35 also blocks normal occurring apoptosis, since even the control genoptype is affected by

inhibition of apoptosis (compare "-" black and grey bars), although not significantly. Second, the different dMyc mutants induce apoptosis, which is not quite obvious and was not described before. Third, a big amount of dMyc-induced apoptosis in the eye might take place during pupariation, which we never analysed by TUNEL staining. However, due to the observed phenotypes the apoptosis must be limited. This experiment demonstrates clearly, the strength of dMycΔMB3 in induction of growth, when the "negative" pro-apoptotic effects are turned off.

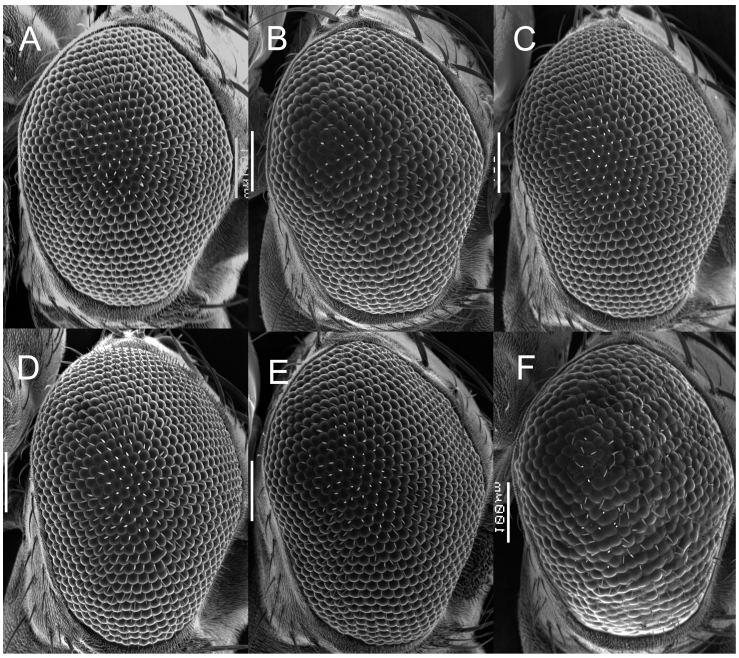

Figure 5: Section electron microscope pictures (SEM) of eyes overexpressing p35 and dMyc mutants. Panel F resembles the "GM" phenotype, which we observed after strong overexpression of dMyc (Steiger et al., 2008). The phenotype was observed for the majority of the flies with the corresponding phenotype.

Label:	Genotype:
A	*y w*; *GMR*-GAL4/+; UAS-p35/pUASTB
B	*y w*; *GMR*-GAL4/+; UAS-p35/UAS-dMycWT
C	*y w*; *GMR*-GAL4/+; UAS-p35/UAS-dMycΔN
D	*y w*; *GMR*-GAL4/+; UAS-p35/UAS-dMycMB2A
E	*y w*; *GMR*-GAL4/+; UAS-p35/UAS-dMycΔMB2
F	*y w*; *GMR*-GAL4/+; UAS-p35/UAS-dMycΔMB3

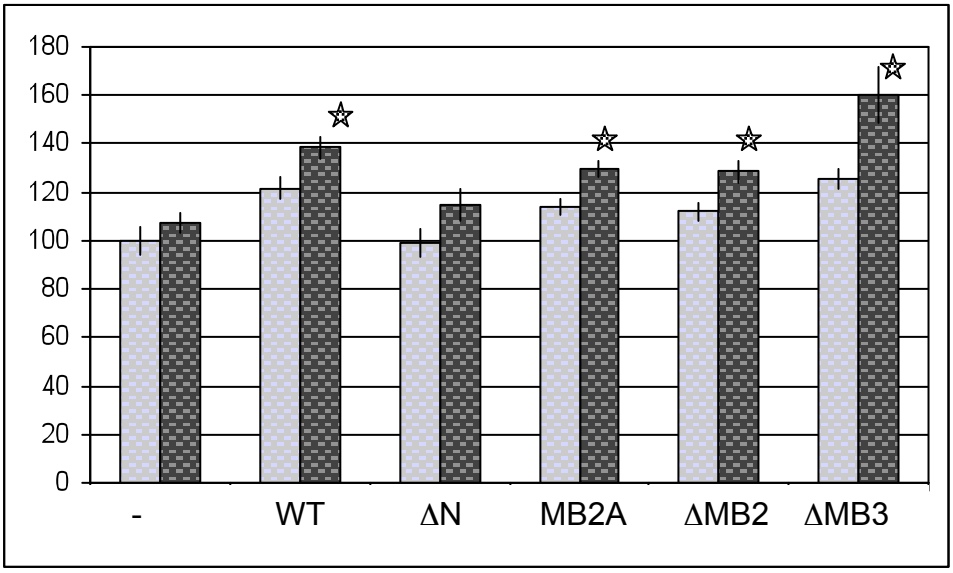

Figure 6: Ommatidial size determined from 5 independent eyes per genotype, measured after overexpression of dMyc with *GMR*-GAL4, either alone (grey bar) or in combination with p35 (black bar). Co-overexpression of p35 enhances ommatidial size. Error bars indicate standard deviation of the means of the counted eyes. *GMR*-GAL4 crossed to control was set to 100% and all other ommatidial sizes were calculated to this reference. Stars indicate significant difference between the genotypes "*GMR*-GAL4; UAS-p35/+" vs. "*GMR*-GAL4; UAS-p35/UAS-dMyc(mutant)" ($p \leq 0.05$).

Label:	column:	Genotype:
-	grey	*y w*; *GMR*-GAL4/+; pUASTB/+
	black	*y w*; *GMR*-GAL4/+; UAS-p35/pUASTB
WT	grey	*y w*; *GMR* -GAL4/+; UAS-dMycWT/+
	black	*y w*; *GMR*-GAL4/+; UAS-p35/UAS-dMycWT
ΔN	grey	*y w*; *GMR*-GAL4/+; UAS-dMycΔN/+
	black	*y w*; *GMR*-GAL4/+; UAS-p35/UAS-dMycΔN
MB2A	grey	*y w*; *GMR*-GAL4/+; UAS-dMycMB2A/+
	black	*y w*; *GMR*-GAL4/+; UAS-p35/UAS-dMycMB2A
ΔMB2	grey	*y w*; *GMR*-GAL4/+; UAS-dMycΔMB2/+
	black	*y w*; *GMR*-GAL4/+; UAS-p35/UAS-dMycΔMB2
ΔMB3	grey	*y w*; *GMR*-GAL4/+; UAS-dMycΔMB3/+
	black	*y w*; *GMR* -GAL4/+; UAS-p35/UAS-dMycΔMB3

6. Interaction with dMyc co-factors

In order to determine which factor is responsible for the biological defects we observed *in vivo* with the different dMyc mutants, two known dMyc co-factors, Pontin and GCN5, were analysed for their binding ability to the different dMyc mutants.

6.1 Interaction with Pontin

Pontin, also called Tip49 in humans, is an essential partner for Myc during normal development and it plays an important role in the control of Myc-dependent transcription, growth and proliferation. Flies carrying the hypomorphic allele dm^{P0} are normally patterned and display only moderate growth defects. Heterozygosity for the dMyc-co-factor Pontin showed no effect in a wildtype background, but it dramatically enhanced the defects of hypomorphic *dmyc* mutations. Up to 100% of "dm^{P0}/Y; $pontin^{5.2}$/+" flies had a strong eye defect (Bellosta et al., 2005). Not only the eye is affected by this phenotype but also the survival rates are reduced, the duration of development is prolonged and the overall size of the animals is decreased, indicating that growth and/or proliferation is generally impaired.
Pontin is also required on its own for tissue growth *in vivo*, since homozygous mutant $pont^{-/-}$ larvae grow poorly although they hatch normally, as was shown for $dmyc^{-/-}$ mutant larvae. Moreover, mitotic clones mutant for either *dmyc* or *pont* suffered from cell competition, consistent with the idea that dMyc and Pontin control the same processes (Bellosta et al., 2005).
The interaction with Tip49 requires Myc Box 2 in c-Myc (Wood et al., 2000), since immunoprecipitations from human 293 cells expressing FLAG-c-Myc (mutants) showed that a deletion of Myc Box 1 was still able to bind Tip49 to the same extent as full-length c-Myc, but a larger deletion of Myc Box 2 was substantially reduced in binding to Tip49. Indeed, Bellosta et al., 2005 showed by GST-pull downs that Pont binds physically to dMyc *in vitro.* However, studies to distinguish the direct binding site for Tip49 in Myc are still missing. To analyse if Pontin still binds to the mutant dMyc proteins, especially to MB2, we performed co-immunoprecipitations of Pont and different dMyc mutants in S2 cells.
Co-immunoprecipitations were performed upon transfection of UAS-Myc-Pontin together with different UAS-HA-dMyc (mutant) plasmids and *tub*-GAL4. Forty-eight hours after transfection, cells were lysed and co-immunoprecipitations were performed as described in Materials and Methods. The first Western blot in Figure 7 shows that all tested dMyc mutants still physically bind to Pont whereas in control IPs, where dMyc or Pontin were transfected

alone, no interaction could be observed (Figure 7, panel A). Supernatants taken before the first washing step of the beads (Figure 7, panel B) show that dMyc was present in the control IP (when dMyc was transfected alone). Furthermore, all dMyc mutants were equally capable of binding to Pont. This indicates that all our dMyc mutants still contain the binding site for Pontin. Thus, Pontin is not responsible for the defects we observed and described earlier for the different dMyc mutations.

We were interested, if a dMyc mutation that lacks the ability to bind to Pontin would behave similarly as the mutants we already analysed with regard to its biological functions. Therefore, we tried to map the correct binding site for Pontin with additional mutations of dMyc (see Figure 8) and tested them by co-IP.

Smaller dMyc mutants, who still contained the N-terminus of dMyc, strongly bound Pontin (Δ294C, Δ403C, Δ523C), as demonstrated in Figure 9. Surprisingly, ΔN294, which lacks the first 294 amino acids of dMyc, was also still capable of binding to Pontin. However, bigger deletions in the N-terminus reduced or completely abolished binding (ΔN403, ΔN523). No conclusion can be drawn from ΔN626, since much lower amounts of this protein were detected in the transfected S2 cells than of the other dMyc mutants.

These data suggest that either two binding sites for Pont exist in dMyc, or that there is one long interaction site, of which MB2 is an important but not essential part, since complementary constructs (Δ294C and ΔN294, that do not overlap each other) showed a strong interaction with Pontin. Similarly, Wood et al. 2000 were not able to fully abolish binding between their big Myc Box 2 deletions in c-Myc (Δ118-152) and Tip49, which is consistent with our data. As a next step, the binding site for Pontin needs to be mapped more precisely before any *in vivo* assays can be done with such a mutation.

In a second assay we wanted to rescue the eye phenotype of "dm^{P0}/Y; $pontin^{5.2}$/+" flies by overexpression of dMycWT and different dMyc mutants. If one of the mutants would lack the binding domain for Pontin in dMyc, it should not rescue the strong eye defect.

For the rescue experiment, flies carrying the hypomorphic allele dm^{P0} were provided with a ubiquitously expressed *dmyc* cDNA under the control of the *tubulin*-promoter. The cDNA was flanked by FRT-sites, which will recombine with each other when FLP-recombinase is expressed. Since the *eyeless* promoter was used to express this FLP-recombinase, the *dmyc* cDNA will be eliminated only in the eye and head capsule, thus revealing the hypomorphic phenotype in this tissue. The rest of the fly remains unaffected. This line was called *ey>*dm^{P0} for simplification, which stands for the genotype: "*w* dm^{P0} *tub*-FRT-dMyc-FRT-GAL4 *ey*-FLP".

As mentioned above, heterozygosity for Pontin in *ey>dm*^{P0} flies leads to a strong eye defect. By overexpressing dMyc (mutants) in this background, we were able to rescue the eye defects (see Figure 10) - not only the reduction in ommatidial number that is very typical for "*ey>dm*^{P0}; *pont*$^{5.2}$/+" eyes, but also the roughness of the eye. The roughness that is observed after expression of dMycΔMB3 presumably reflects a dMyc overexpression phenotype of the strong dMycΔMB3 mutant. A similar roughness is also observed when dMycΔMB3 is expressed in a *dm*$^{+}$ background (see manuscript, Figure 3).

Consistent with the interaction studies shown above, also dMycΔN fully rescued the eye phenotype, although it was biologically inactive in most of our assays (see manuscript). Thus, additional important dMyc co-factors besides Pontin might bind to its N-terminus to control Myc`s biological activity.

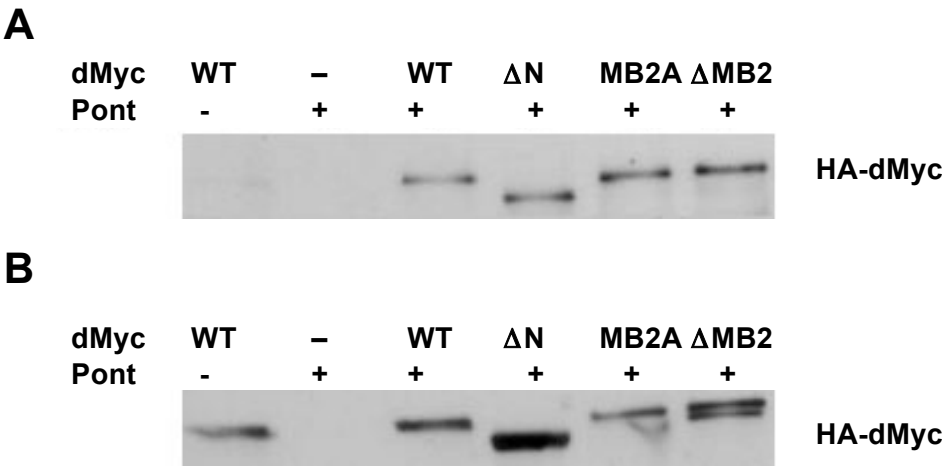

Figure 7: Binding of Pontin to different dMyc mutants. Shown are S2 cell lysates after co-transfection of Pont and dMyc (mutants), immunoprecipitation with Protein-G beads and mouse anti-dMyc antibodies. Precipitated proteins were resolved by SDS/PAGE and Western blotted for HAdMyc with anti-HA antibodies. The text above the picture indicates the expressed proteins. All constructs were still able to bind Pont. Panel A: IP, Panel B: supernatants of cell lysates after incubation with antibodies and beads. The experiment was performed in two independent biological replicates with similar results.

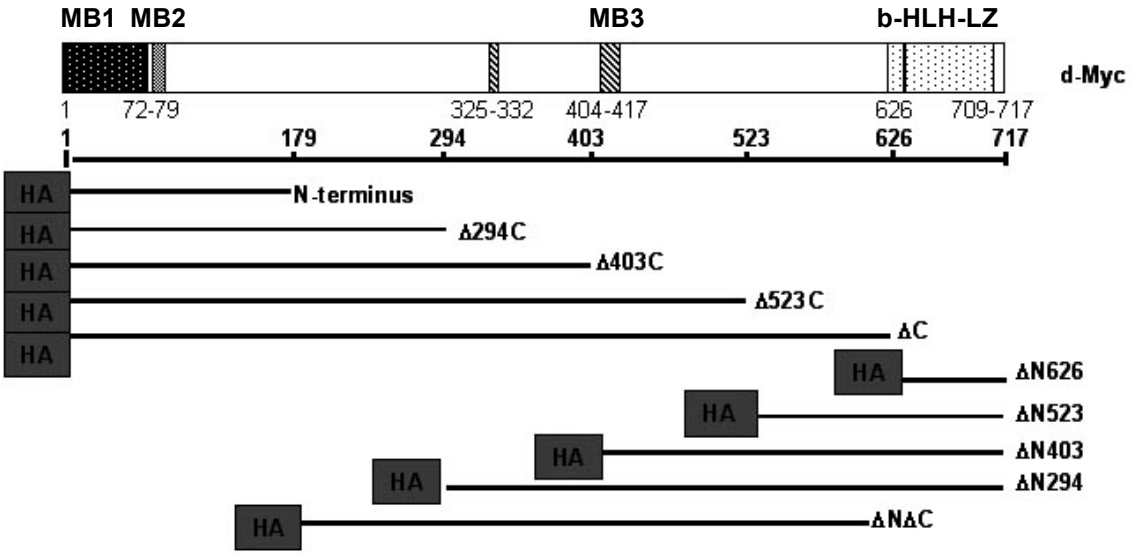

Figure 8: Additional dMyc mutant constructs (small dMyc mutations), which were used for co-immunoprecipitation assays. All constructs carry an HA-tag at their N-terminus and were cloned into pUASTB.

A

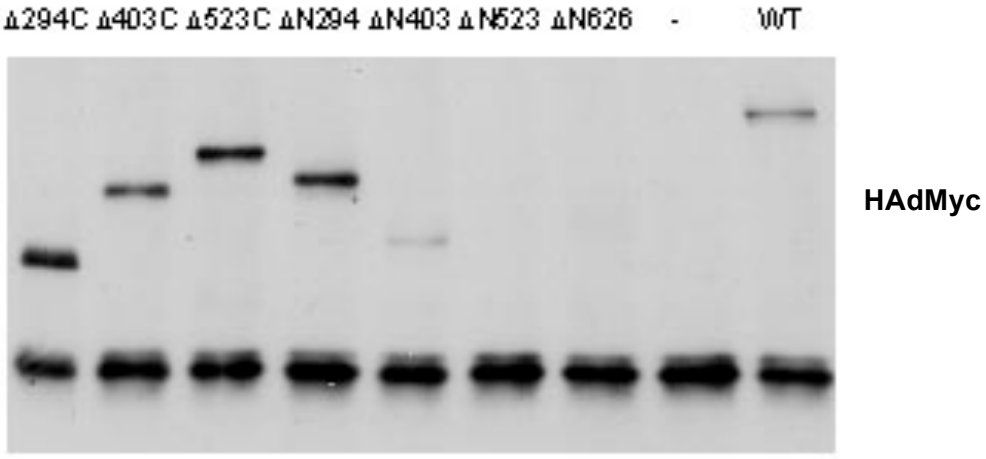

B

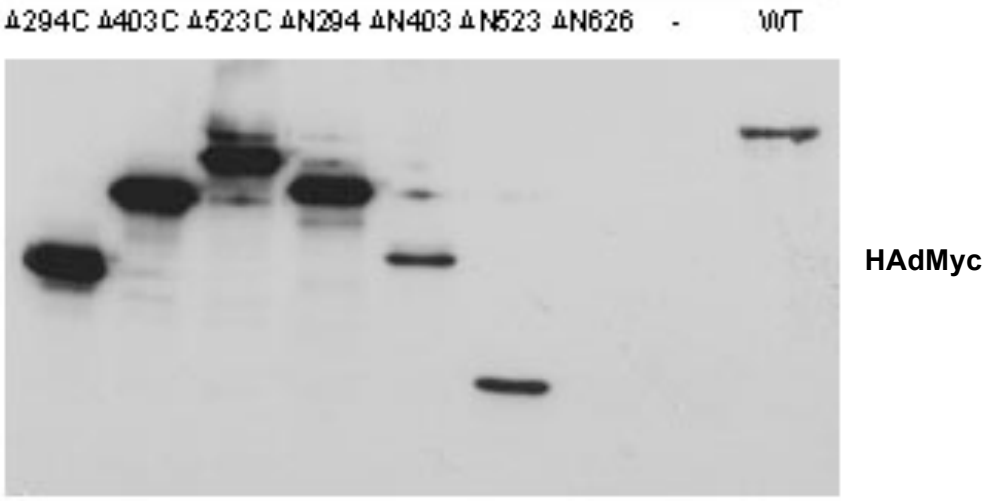

Figure 9: Binding of Pontin to different dMyc mutants. Shown are S2 cell lysates after co-transfection of Pont and dMyc (mutants), immunoprecipitation with Protein-G beads and mouse anti-HA antibody. Precipitated proteins were resolved by SDS/PAGE and Western blotted for dMyc with anti-HA antibody. The text above the picture indicates the expressed proteins. All C-terminal deletions still allow full binding to Pont. Big N-terminal deletions reduce or abolish binding to Pont. Panel A: IP, Panel B: supernatants of cell lysates after incubation with antibodies and beads. The experiment was performed in two independent biological replicates with similar results.

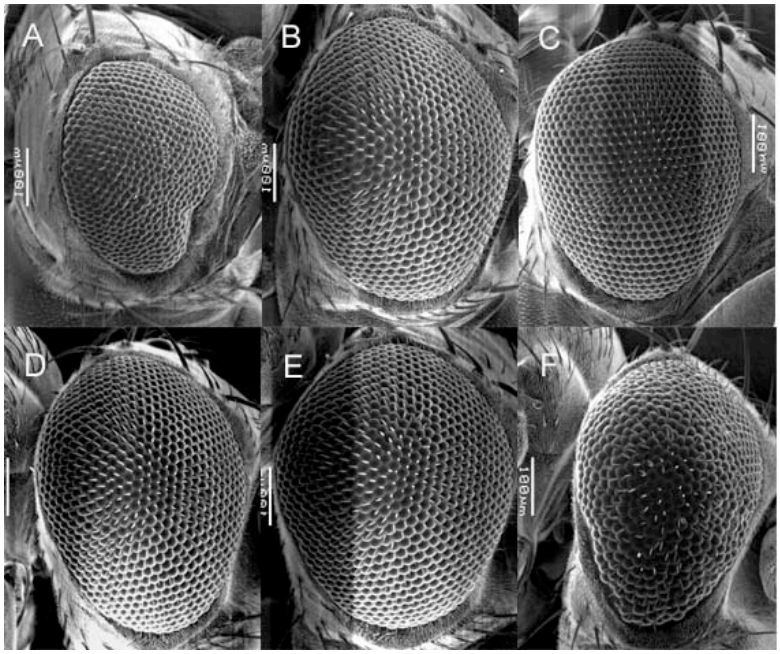

Figure 10: Scanning electron microscope pictures (SEM) of flies hypomorphic for *dmyc*, heterozygous for *pont*$^{5.2}$ and overexpressing different dMyc constructs. The strong eye phenotype of control flies (panel A) could be rescued with all constructs. The experiment was performed in two independent biological replicates.

Label:	Genotype:
A	*w dm*^{P0} *tub*>dMyc>GAL4 *ey*-FLP/Y; *pont*$^{5.2}$/pUASTB
B	*w dm*^{P0} *tub*>dMyc>GAL4 *ey*-FLP/Y; *pont*$^{5.2}$/UAS-dMycWT
C	*w dm*^{P0} *tub*>dMyc>GAL4 *ey*-FLP/Y; *pont*$^{5.2}$/UAS-dMycΔN
D	*w dm*^{P0} *tub*>dMyc>GAL4 *ey*-FLP/Y; *pont*$^{5.2}$/UAS-dMycMB2A
E	*w dm*^{P0} *tub*>dMyc>GAL4 *ey*-FLP/Y; *pont*$^{5.2}$/UAS-dMycΔMB2
F	*w dm*^{P0} *tub*>dMyc>GAL4 *ey*-FLP/Y; *pont*$^{5.2}$/UAS-dMycΔMB3

6.2 Interaction with GCN5

GCN5, a histone acetyltransferase, was found as a component of the SAGA complex, which also includes, amongst others, ADA1-3 and TRRAP. The N-terminal domain of c-Myc has been reported to interact with GCN5, and deletion of Myc Box 2 causes loss of both interaction with TRRAP and GCN5 (McMahon et al., 2000). Recently, it was shown that GCN5 is also involved in RNA Pol III-dependent transcriptional activation, since c-Myc recruited the co-factors TRRAP and GCN5 to *tRNA* and *5S RNA* genes and stimulated acetylation of histone H3 at these loci (Kenneth et al., 2007).

Therefore, we were interested if a Myc Box 2 deletion abolishes binding to GCN5. Different dMyc mutants were expressed in S2 cells to address this question and cell lysates were prepared for immunoprecipitation against endogenous GCN5; the associated HAdMyc was revealed by Western blotting with an anti-HA antibody. Indeed, dMycWT interacted with GCN5 (Figure 11) and a deletion of the N-terminus of dMyc did not abrogate this interaction. Furthermore, other tested proteins carrying deletions of Myc Box 2, or of the first 294 amino acids of dMyc were still capable of binding to GCN5 (data not shown). Thus, at least part of the binding site for GCN5 lies between amino acid 295 and the C-terminus.

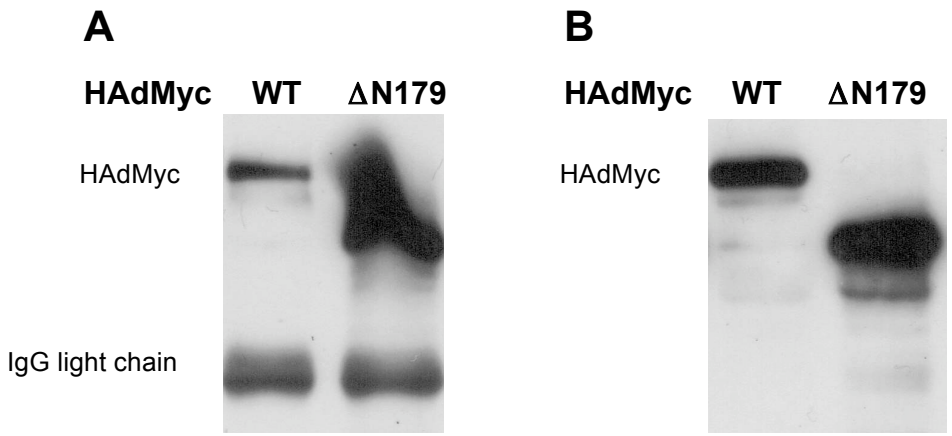

Figure 11: Western blot showing physical interaction between HAdMyc and GCN5. S2 cells were transiently transfected with plasmids coding for the indicated forms of HA-tagged dMyc. After 48h, protein complexes were immunoprecipitated with an antibody directed against endogenous GCN5. Precipitated proteins were resolved by SDS/PAGE and Western blotted for dMyc with anti-HA antibody. The text above the picture shows the expressed proteins. dMycWT (HAdMycWT) and a deletion of the first 179 amino acids of dMyc (HAdMycΔN179) are still able to bind to GCN5. Panel A: IP, Panel B: supernatant taken before the first washing step of the beads. HAdMyc alone does not bind to protein G beads (data not shown). "IgG" marks the light chain of the antibody.

7. Interaction of dMyc mutants with *dmax* dsRNA

Expression of *dmax* dsRNA with the eye-specific GMR-GAL4 driver did not alter ommatidial size and overall eye morphology in a wildtype background (Steiger et al., 2008). However, when dMyc was strongly overexpressed, *dmax* dsRNA reduced ommatidial size and strongly increased the roughness of the eye. This observation was a first indication that dMyc has functions that do not require dMax (Steiger et al., 2008). Specifically, dMyc can induce apoptosis in a dMax-independent manner when dMyc is expressed at very high levels, but most probably not all dMyc-dependent apoptosis is independent of dMax. In the manuscript we showed that dMycΔMB3 is a very potent inducer of apoptosis. Therefore, it appears quite possible that this dMycΔMB3-dependent activity is dMax-independent. If this were true, a reduction of dMax-levels (by dsRNA) in a dMycΔMB3-overexpression background would change the eye phenotype to a lesser extent than when dMax-levels are reduced in the presence of overexpressed dMycWT.

Thus, we crossed flies, which were homozygous for *GMR*-GAL4 and contained UAS-dMyc (mutants) to flies containing 2 different *dmax* inverted repeats (*dmax*-IR$^{6\text{-}1}$, *dmax*-IR$^{5\text{-}2}$).

Overexpression of either control transgenes (A), dMycWT (B), dMycΔMB2 (C) and of dMycΔMB3 (D) in the eye are depicted in Figure 12. Compared to the pictures of the lower panel, which included *dmax* dsRNA, no enhancement of the roughness was observed except for panel H, were dMycΔMB3 is expressed. However, dMycΔMB3 also causes a more severe eye defect than dMycWT, so it is not so easy to compare modification of the dMycΔMB3- and of the dMycWT-phenotype. This observation confirmed that when dMyc is expressed at high levels, as it is the case for dMycΔMB3, a reduction of dMax levels enhances the roughness of the eye. However, no conclusion can be drawn if the ommatidial size is reduced in those eyes (as observed by Steiger et al., 2008), since this has not yet been analysed. It is also not clear if the dMycΔMB3-dependent activity is dMax-independent.

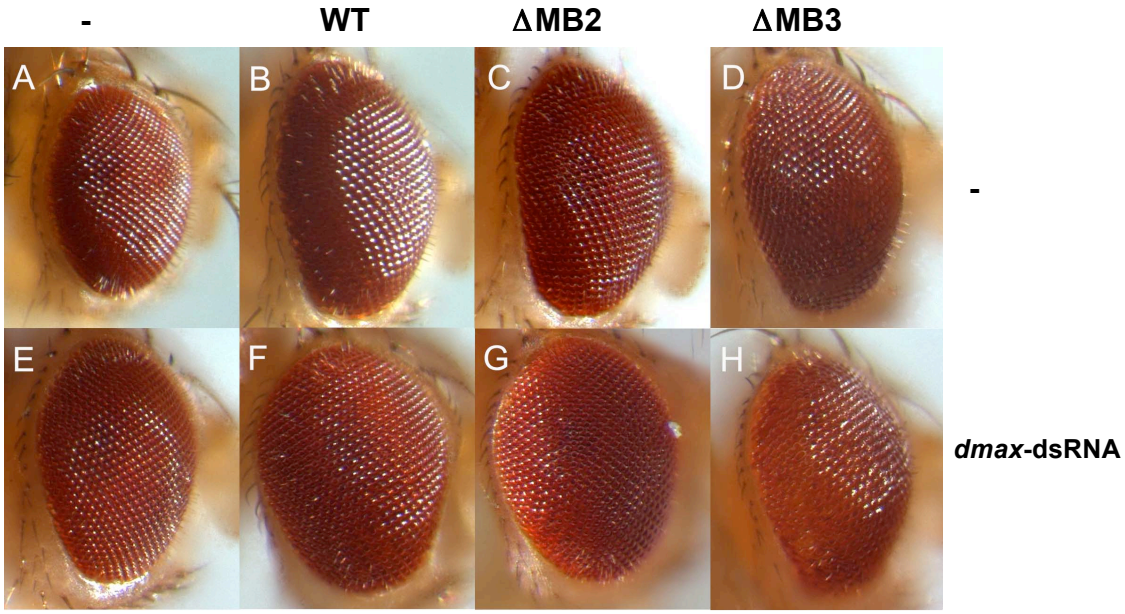

Figure 12: Dissection microscope pictures of eyes overexpressing dMyc (mutants) in the absence (upper panel) or presence of *dmax* dsRNA. The ommatidia in panel H look rougher than those in panel D, all other eyes seemed unaffected by a loss of *dmax*. The phenotype was observed for the majority of the corresponding genotypes (>80%).

Label:	Genotype:
A	*y w*; *GMR*-GAL4/+; pUASTB/+
B	*y w*; *GMR*-GAL4/+; UAS-dMycWT/+
C	*y w*; *GMR*-GAL4/+; UAS-dMycΔMB2/+
D	*y w*; *GMR*-GAL4/+; UAS-dMycΔMB3/+
E	*y w*; *GMR*-GAL4/+; pUASTB/UAS-*dmax*-IR(5-2) UAS-*dmax*-IR(6-1)
F	*y w*; *GMR*-GAL4/+; UAS-dMycWT/UAS-*dmax*-IR(5-2) UAS-*dmax*-IR(6-1)
G	*y w*; *GMR*-GAL4/+; UAS-dMycΔMB2/UAS-*dmax*-IR(5-2) UAS-*dmax*-IR(6-1)
H	*y w*; *GMR*-GAL4/+; UAS-dMycΔMB3/UAS-*dmax*-IR(5-2) UAS-*dmax*-IR(6-1)

Discussion of additional experiments

Myc`s role on *cis*-acting determinants *in vivo* was investigated in this study. Except for the N-terminus there are regions in the Myc protein that are fairly conserved from humans to flies (MB2, MB3, b-HLH-LZ). The N-terminus of dMyc is required for most dMyc-dependent activities, although dMycΔN retains some ability to promote eye development and to rescue a lethal *dmyc*-mutation. In contrast, deletion of the best-conserved motif MB2 had rather mild effects and a dMyc mutant derivative lacking this MB2 was even capable of rescuing a *dmyc* null allele to adulthood. Interestingly, a deletion of the acidic MB3 domain not only stabilized the protein but also enhanced its ability to induce apoptosis, but not its efficiency to induce distinct dMyc target genes (discussed in the manuscript).

MB1

A deletion of the N-terminus of dMyc dramatically reduced all biological functions of dMyc. However, dMycΔN could rescue not only ommatidial size of a dMyc null allele (although weakly), but it also significantly rescued the reduced ommatidial number in such flies. In the additional experiments we could show that such a mutant was moreover capable of binding the Myc co-factors Tip49 and GCN5. This interaction might be the reason why dMycΔN retains some activity. Together with the previous observations, our results suggest that apoptosis and transactivation, as well as the induction of cell growth and proliferation, mostly depend on the dMyc N-terminus. This is consistent with the observation for c-Myc S (which resembles dMycΔN) in that the human c-Myc S isoform led to viability when expressed in a lethal *dmyc* mutant background. Apoptosis was not induced in those flies (Benassayag et al., 2005). However, our observations suggest that some co-factors, that might be necessary for the induction of cell-autonomous apoptosis or cell growth by Myc, do not bind dMycΔN anymore (or have a significantly reduced binding capability), and that dMyc target genes involved in those processes are not (or less) activated by dMycΔN. These co-factors need to be determined in future experiments.

MB2

The highly conserved MB2 was shown to recruit several co-factors to c-Myc. Among them were TRRAP and GCN5, which are involved in the acetylation of histones (McMahon et al., 1998; McMahon et al., 2000) or Tip48 and Tip49, which function as ATPase/helicases (Wood

et al., 2000). MB2 was also shown to be necessary for the induction of apoptosis, transformation (Conzen et al., 2000; Oster et al., 2003) and for the blockage of differentiation (Freytag et al., 1990). Additionally, the ability to activate and repress target genes was dramatically reduced by deletion of MB2 (Cowling and Cole, 2006; Li et al., 1994). However, some Myc target genes were still repressed upon deletion of MB2 (Lee et al., 1997; Li et al., 1994). Myc is also capable of autoregulation by repressing the c-*myc* locus itself, and this was shown to be dependent on MB2 (Oster et al., 2003).

In contradiction to published observations, a dMycΔMB2 mutant retains substantial activity *in vivo*. Thus, cell growth, cell proliferation and apoptosis were comparable to dMycWT or only weakly reduced. The MB2 mutants were even capable to partially rescue a dMyc null allele to adulthood (albeit the resulting flies were small). Consistent with this observation, the dMyc co-factors Tip49 and GCN5, which were shown to be essential for Myc activity, are still capable of binding to dMycΔMB2 (6.1, 6.2). Indeed, Wood et al. 2000 still observed residual binding between their big Myc Box 2 deletion (c-MycΔ118-152) and Tip49, which is consistent with our data, indicating that a second binding site is partially sufficient for the interaction with Pontin. This might also account for the interaction with GCN5 (which is recruited to Myc by TRRAP and thus binds the same sites in c-Myc as TRRAP). A deletion in N-Myc (Δ110-116=MB2) completely abolished binding to GCN5 (McMahon et al., 2000), however, binding of TRRAP to c-Myc required aa 1-110 (N-terminus) and aa 129-145 (MB2) (McMahon et al., 1998). Thus, both the N-terminus and MB2 might be important in flies and one of those sites is sufficient for binding of GCN5 to dMyc via TRRAP.

However, this raises the question why dMycΔMB2 had a clearly reduced potential to activate target genes compared to dMycWT, since both tested co-factors bind with the same efficiency. This might be due to the fact that we have not tested all proteins that have been proposed to bind MB2 –like Tip48. On the other hand deletion of MB2 might disrupt the binding to a yet unidentified partner for MB2. The MB2 domain might also be required for intra-molecular binding, which would normally stabilize the 3D protein structure of Myc.

A completely different hypothesis is that MB2 might be important for the activation of a distinct set of target genes e.g. RNA Pol II & III targets. The c-Myc N-terminus (both aa 1-110 and aa 106-143) was shown to be necessary for activation of RNA Pol III target genes. The mechanism of this interaction is yet unknown but might be dependent on the basal Pol III co-factor TFIIIB (Cowling and Cole, 2006). Moreover, we show evidence that transactivation by dMycΔMB2 is reduced by using the promoter regions of the RNA Pol II transcribed genes *CG5033* and *nnp1* (see manuscript, results section 2.). If only endogenous dMyc target genes

transcribed by RNA Pol II & III are directly affected by a loss of MB2 needs to be investigated in future times.

It was also shown that a deletion in MB2 directly affects transcription, which might explain the growth deficits between dMycWT and dMycΔMB2. Myc directly activates CDK7 (the kinase subunit of the transcription factor TFIIH), which in turn phosphorylates serine amino acids on the C-terminal domain of RNA Polymerase II, necessary for initiation of transcription. The MB2 motif was shown to directly interact with CDK7, thus recruiting TFIIH to the binding sites of different target genes (Cowling and Cole, 2007). By binding of the "Myc-TFIIH"-complex to transcription initiation sites of their target genes, mRNA cap methylation is increased and hence translation. Thus, a deletion of MB2 affects transcription of target genes and mRNA metabolism. Altogether it is quiet surprising that such a highly conserved domain like MB2 is not absolutely essential, but plays only a quantitative role in the way that it only reduces/weakens dMyc`s biological functions (e.g. growth, apoptosis, transactivation).

MB3

To investigate the role of the less studied but highly conserved MB3 in Myc was one of the goals of this study. A PEST domain is located inside this region and such a domain is often linked with unstable protein (Rogers et al., 1986). Indeed, compared to dMycWT, dMycΔMB3 was more stable in S2 cells. A deletion of MB3 moreover enhanced cell growth and apoptosis compared to dMycWT and a dMycΔMB3 mutant could fully rescue a *dmyc* null allele to the same extent as dMycWT. On the other hand dMycΔMB3 had a reduced potential to activate transcription in cell culture assays and was impaired to activate RNA Polymerase III target genes *in vivo*.

Our data provide strong evidence that first, co-expression of p35, a caspase inhibitor, blocked dMycΔMB3 induced apoptosis, indicating that this process involves caspases (results section, 4.). Second, growth could be increased after co-expression of p35 (results section, 5.). Third, the expression levels of the pro-apoptotic genes *reaper (rpr)* and *sickle (skl)* were not affected by overexpression of dMycΔMB3, as assayed by qRT-PCR, suggesting that apoptosis is triggered by a different mechanism than by the induction of *rpr* or *skl* (results section, 3).

The fact that dMycΔMB3 is more stable might account for the effects on cell growth and proliferation, however it cannot explain the reduced transactivation of target genes by dMycΔMB3.

We showed that dMycΔMB3 behaves qualitatively differently than dMycWT at the level of transcription. This suggests that ubiquitination of dMyc and transcriptional activation of distinct target genes is controlled by MB3. It was shown earlier that degradation and transcriptional activation are connected and that transcriptional activation domains are often linked to ubiquitination sites, so-called degrons (reviewed in Muratani and Tansey, 2003). One the one hand, our data are consistent with the possibility that MB3 is the binding site for the F-box protein Ago, since a mutation in *ago* does not further enhance (or reduce) ommatidial size after overexpression of dMycΔMB3 compared to dMycWT in the eye, which one would expect as reducing the gene dose of *ago* was demonstrated to enhance dMyc stability. The finding that the degron for Ago binding in c-Myc is most similar to dMycMB3 supports this idea (Moberg et al., 2004). On the other hand, dMycΔMB3 was impaired in the activation of $tRNA^{Leu}$ and *snoRNA U3*. Thus, there might be a link between activation of RNA Pol III target genes and degradation of dMyc.

It stands to reason that dMycΔMB3 induced apoptosis is not only a result of increased dMyc stability but also of binding to other co-factors or repression/activation of target genes of dMyc, involved in the apoptotic pathway. Recently, it was shown that overexpression of dMyc or reducing the gene dose of *ago* leads to apoptosis in "GM" flies (which already overexpress three copies of dMyc) (Steiger et al., 2008{Secombe, 2007 #2546). Thus, the induced apoptosis observed upon overexpression of dMycΔMB3 might be a direct consequence of Myc induced cell autonomous apoptosis and the loss of binding to Ago. Which suggests that the apoptosis induced by dMycΔMB3 is based on increased stability of the protein. Moreover, the observation that inhibition of apoptosis by p35 increased ommatidial size better than dMycWT rather suggests that dMycΔMB3 induced apoptosis is increased due to enhanced stability of the protein. However, we cannot rule out that MB3 suppresses apoptosis by a different mechanism. The qualitative different effects of dMycWT and dMycΔMB3 on transcription (see manuscript) further support this idea. However, further experiments are necessary to determine the mechanism on how dMycΔMB3 induces apoptosis.

Chapter 2

In vivo mutagenesis screen for dMyc co-factors

Summary

Flies carrying the hypomorphic *myc* allele dm^{P0} are normally patterned and display only moderate growth defects. Experiments with the dMyc-cofactor Pontin/Tip49, an ATPase/helicase protein that is also part of the Tip60 complex, have shown that the eye is particularly sensitive to a reduction in dMyc activity and that a transcriptional co-factor complex containing Pontin is critically required for Myc function in the eye. Encouraged by the results with Pontin, we carried out a large-scale loss-of-function mutagenesis screen to identify Pontin-like co-factors for Myc. In parallel, the publicly available Exelixis and DrosDel collections of large isogenic deletions have been tested for interaction with dMyc. The breakpoints of those deletions are molecularly characterized, which facilitated the identification of selected genes of interest. In this project we identified two genes that have previously been unknown to interact with dMyc: *Delta* and *chinmo*.

Delta (a Notch ligand) interacts genetically with different *dmyc* mutations, however, other components of the Notch signalling pathway did not affect the eye morphology in a *dmyc* mutant background.

Chinmo was initially found in a screen for factors that specify distinct birth order-dependent cell fates in an extended neuronal lineage. Our screen, as well as another screen for factors involved in growth control, attributes an additional biological function to Chinmo. We provide evidence that Chinmo interacts not only genetically, but also physically with dMyc. On the one hand, dMyc is limiting for Chinmo function, since the deleterious defects of Chinmo overexpression are reduced by a reduction of dMyc levels; on the other hand, Chinmo is necessary for dMyc function *in vivo,* since homozygous *chinmo* mutant clones fail to overgrow after overexpression of dMyc. A Luciferase assay in S2 cells showed that Chinmo can transactivate Myc dependent reporter genes. Moreover, this induction is enhanced by the co-overexpression of Myc. Importantly, levels of overexpressed Myc are not affected by co-expressed Chinmo in S2 cells suggesting that Chinmo does not enhance dMyc stability. Furthermore, co-IP experiments showed a direct interaction between the two proteins. Two derivatives of Chinmo have been established that lack either one of the two functional domains, an N-terminal BTB/POZ domain or a C-terminal Zn-finger (ZnF) domain. Deletion of the BTB domain completely abolished binding to dMyc, whereas a deletion of the ZnF did not. Finally, Chinmo activates endogenous dMyc targets involved in ribosome biosynthesis. Thus, Chinmo seems to affect the transactivation activity of dMyc. The mechanism behind this action and the connection between the functions of dMyc

published so far (e.g. in growth control and cell competition) and the role of Chinmo (e.g. in neurogenesis) still needs to be investigated.

Introduction

Identification of Chinmo

In order to find new co-factors of dMyc, a loss-of-function screen was performed in our laboratory. This screen was based on the hypomorphic allele dm^{P0} that carries an P-element insertion 99 nucleotides upstream of the longest isolated *dmyc* cDNA (Johnston et al., 1999). Homozygous dm^{P0} females are sterile and males are characterised by a slightly delayed development, thin bristles and a weak reduction in body size and viability (reduced to 54%). Very rarely, mutant flies exhibit a weak eye defect with small, irregularly shaped, slightly rough eyes. Moreover, ommatidial size is significantly reduced (Bellosta et al., 2005). Heterozygosity for the dMyc co-factor Pontin shows no phenotypic defects in a wildtype background, but it dramatically enhances the defects of the dm^{P0} mutation. In particular, up to 100% of males with the genotype "dm^{P0}/Y; $pontin^{+/-}$" exhibit an easily discernable eye phenotype. Thus, a transcriptional co-factor complex containing Pontin is critically required for dMyc function in the eye.

Stimulated by this result, we initiated an EMS-screen in order to find other postulated co-factors of the Pontin-containing complex. This screen might also lead to the identification of other factors functioning in complexes with similar activities, factors that downregulate the abundance of *dmyc* transcripts or genes that affect dMyc stability. This screen led to the identification of a new dMyc interacting gene: *chinmo*.

The insect brain

The mushroom bodies (MB) or *corpora pedunculata* are a pair of structures in the brain of insects and other arthropods (Figure A, blue). They are usually described as lobed neuropils (dense networks of neurons and glia). They get their name from their roughly hemispherical *calyx*, a protuberance that is joining to the rest of the brain by a central nerve tract or *peduncle* that extend through the midbrain. Mushroom bodies are involved in olfactory learning and memory (Zars, 2000). Genes expressed early in their development share homology with genes involved in the early development of comparable regions in mammalian forebrain (Kurusu et al., 2000). The matrix of the mushroom bodies consists of ensembles of intrinsic neurons, which make synapses only within the structure where their soma is located, the so-called Kenyon cells. These are derived from globuli cells situated above the calyx. Globuli cells are the smallest neurons of the mid-brain. A fruitfly mushroom body comprises about 3,000 Kenyon cells.

Systematic clonal analysis demonstrates that a single mushroom body neuroblast sequentially generates at least 3 types of morphologically distinct neurons. Neurons projecting into the γ lobe of the adult MB are born first, prior to the mid-3rd instar larval stage. Neurons projecting into the α' and β' lobes are born between the mid-3rd instar larval stage and puparium formation. Finally, neurons projecting into the α and β lobes are born after puparium formation (Crittenden et al., 1998; Lee et al., 1999).
The best known input neurons in the *Drosophila* olfactory system are projection neurons (PNs) which connect single glomeruli of the antennal lobe, based upon lineage and birth order, to the lateral horn and send side branches into the posterior part of the mushroom body, the calyx (Heisenberg, 1998).

Chinmo`s role in the development of the brain

So far, a mechanism identifying temporal identity in the neuroblast lineage was not known. In 2006, Zhu et al., published an EMS screen to find genes involved in specification of temporal identity in mushroom bodies in mosaic organisms (Zhu et al., 2006). They found one mutant in ~3500 screened chromosome arms, which they called *chinmo* due to the observed phenotype (*chinmo*= **ch**ronologically **in**appropriate **mo**rphogenesis). *Chinmo* mosaic flies had fewer γ and α`β` neurons and more late-born pαβ and αβ neurons. The affected gene was identified and shown to code for a protein containing a BTB/POZ domain and two C_2H_2 zinc fingers. Chinmo is expressed in early-born γ neurons, to a lower extent in the next born α`β` neurons and absent from the latest born pαβ and αβ neurons and neuroblasts (Figure B). The group could show that the 5`UTR is essential for establishing a temporal gradient of the Chinmo protein.
In mushroom bodies and projection neurons a loss of *chinmo* autonomously caused early-born neurons to adopt the cell fate of late-born neurons. Conversely, overexpression of Chinmo in the neuroblast lineage caused late-born neurons to adopt the cell fate of early born neurons. Thus, Chinmo specifies at least three different cell fates in the neuroblast lineage (high protein= γ neurons, low protein= α`β`neurons, no protein= pαβ neurons).

Myc`s role in neurogenesis

Betschinger et al., 2006 demonstrated that dMyc is expressed in larval neuroblasts, but not in their differentiating daughter cells. However, in clones mutant for the growth inhibitor *brat*, dMyc was expressed in all cells and the nucleoli were enlarged. Both daughter cells started to grow and behaved like neuroblasts leading to brain tumours in those larvae. Thus, Brat posttranscriptionally inhibits dMyc in the differentiating daughter cells. Therefore, the effect of the *brat* mutant might be the result of overexpression of dMyc. Orian et al., 2007 could show that dMyc and the Notch co-repressor Groucho act together to regulate their common target genes *vnd* and *int* (downstream targets of EGF signalling) during neuronal development in the embryo. Moreover they showed that dMyc promotes neurogenesis in the embryonic PNS and the CNS (and possibly the larval PNS). Thus, Myc is expressed in the nervous system in flies, where it is required for precursor cell proliferation and possibly cell fate determination of neuroblasts. This raises the possibility that dMyc and Chinmo might work together to regulate neuronal differentiation.

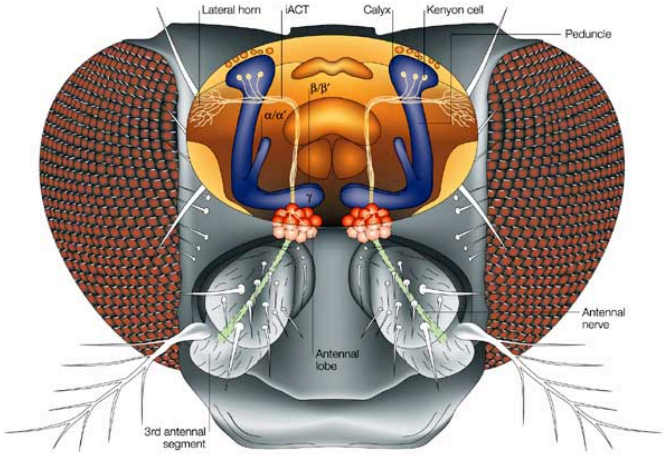

Figure A: Odour information is carried from the third antennal segments and maxillary palps (not shown) to the antennal lobes, where receptor fibres are sorted according to their chemospecificities in about 40 glomeruli. These represent the primary odour qualities, which are reported to two major target areas in the brain, the dorsolateral protocerebrum (lateral horn) and the calyx of the mushroom body. The inner antennocerebral tract (iACT) connects individual glomeruli to both areas. α/α', β/β' and γ mark the three mushroom body subsystems (taken from M.Heisenberg, Nature Reviews Neuroscience 4, 266-275, April 2003).

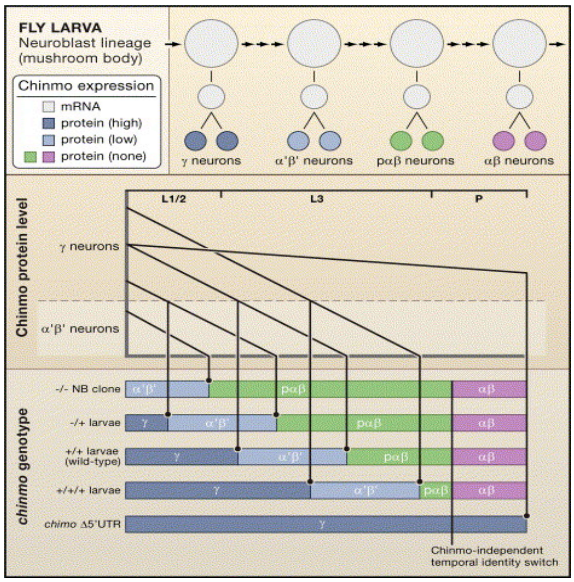

Figure B: *Chinmo* mRNA (light-grey) is homogenously expressed during neuroblast development. Protein levels (blue) are reduced with further development in the neuroblast lineage of the mushroom body in the larval fly brain (upper panel). Chinmo specifies temporal identity of neural progeny in a dose-dependent manner. Five different genotypes are represented. The diagonal lines depict the gradient of Chinmo protein expression over time in each genotype, with the vertical lines being connected to the corresponding neural identities: γ, α′β′, pαβ, and αβ neurons (lower panel) (taken from Chris Q. Doe, Cell 127, 2: 254-256).

Results

1. *In vivo* mutagenesis screen

Males "*y w*/Y; P{w^+}CG31666; P{w^+}CG32111" ("OG") were mutagenised with EMS, a chemical agent that induces primarily point mutations randomly in the whole genome. Those males were crossed to flies with the genotype "*w* dm^{P0} *tub*-FRT-dMyc-FRT-GAL4 *ey*-FLP" (*ey>*dm^{P0}, described in Chapter I, results section 6.). F1 flies with the genotype "*w* dm^{P0} *tub*-FRT-dMyc-FRT-GAL4 *ey*-FLP/Y; P{w^+}CG31666*/+; P{w^+}CG32111*/+" were screened for eye defects (* =mutagenised). Flies with an obvious eye defect were kept, retested and balanced to obtain a stock. In total, 53950 flies were screened and 236 lines were established (Scioscia Hsiko Ait, 2004, diploma thesis). Among these lines, 5 complementation groups were found, which consisted of only 2 alleles each. This indicates that the screen was not saturated.

In parallel to the EMS-screen, we crossed all available DrosDel and Exelixis deficiencies to our tester line (*ey>*dm^{P0}). DrosDel deficiencies were generated by Ryder et al., 2007 and the Exelixis lines by Parks et al., 2004. Those deficiencies consist of large chromosomal deletions with characterised breakpoints and have a genetically isogenic background. Together they uncover more than 79,5% of the *Drosophila* genome. Deficiencies on the X-chromosome could not be analysed since *dmyc* is located on this chromosome, and only hemizygous dm^{P0} and *ey>*dm^{P0} flies show a phenotype.

A total of 605 deficiency lines were individually crossed to *ey>*dm^{P0} virgins and the "*ey>*dm^{P0}/Y" sons heterozygous for the deficiency were screened for eye defects. Table 1 shows an overview of all tested deficiencies and their genetic interaction. 4,1% of all tested deficiencies showed a strong (up to 100% of the male offspring showed a phenotype) or medium (more than 1/3rd of the male offspring showed a phenotype) interaction. Deficiencies with a weak penetrance (less than 1/3rd of the male offspring showed a phenotype) were not further analysed. To reduce the 25 remaining deficiencies to the really interesting ones, additional parameters were investigated that are also affected in "dm^{P0}/Y; $pontin^{5.2}$/+" flies, such as the duration of development and adult weight. Based on these additional assays, we classified the deficiencies as shown in Table 2. Category 1 contains deficiencies that showed at least 2 defects besides the eye defect with *ey>*dm^{P0}. Category 2 encompasses deficiencies that affected one other feature and Category 3 reflects deficiencies that also affected the weight of control flies (dm^{P0rev}, a wildtype revertant of the allele dm^{P0}; Montero et al., 2008),

albeit more weakly). Deficiencies of Category 1 show the strongest interaction with *dmyc* and therefore we considered them most likely to also functionally interact with dMyc.

Table 3 shows a summary of candidate genes of the Category 1 deficiencies and an example for a Category 3 deficiency. To be able to narrow down the regions of candidate genes inside the 25 deficiencies, we tested all overlapping publicly available deficiencies by crossing them to the *ey>dm*^{P0} flies and scoring eye defects amongst the relevant progeny. Of the 25 deficiencies 23 were not investigated any further. Of these, 7 deficiencies were not further analysed, since additional smaller deficiencies collectively uncovering the same region were negative. These deficiencies might contain 2 genes that reveal the interaction with *ey>dm*^{P0} only when simultaneously deleted; alternatively, a background mutation unlinked to the deficiency might be responsible for the observed interaction. For 6 deficiencies we were not able to narrow down the region of interest to a handable number of genes. For 9 deficiencies (highlighted in yellow in Table 2) we were able to narrow down the region of interest to a few candidate genes, however, either the publicly available mutations in those genes gave no phenotype with *ey>dm*^{P0} or no such mutations were available. However, such mutations might become available in future times and should then be tested.

The remaining 2 deficiencies led to the identification of single candidate genes. In a first step, we were able to narrow down the region within Df(2L)Exel6005 that interacts with *ey>dm*^{P0} to two genes, *chinmo* and *CG31934,* and within Df(3R)ED5249 to 8 genes. Subsequently, we tested all available mutations of the candidate genes for interaction with the *ey>dm*^{P0} chromosome. Two genes, *chinmo* and *Delta*, showed a phenotype that reflected the phenotype observed with the deficiency. Therefore, we focused on those genes for further analysis.

Interaction strength	all Df	Exelixis Df	DrosDel Df
	605	476	129
strong	**14**	**12**	**2**
medium	**11**	**5**	**6**
weak	36	27	9

Table 1: Interacting deficiencies from the Exelixis and DrosDel collections. In total, 25 deficiencies were found to show a strong or intermediate interaction with *ey>dm*^{P0}, and further investigated. Df stands for deficiencies.

Deficiency	Weight	Vability	Development	dm^{P0}	$ey>dm^{P0}$	dm^{P0rev}	Category	Cytological location	
Df(2L)ED778	+			+	s		1	33E9	34A7
Df(2R)Exel7123					s		3	49D5	49E6
Df(2R)Exel6062					s		3	49E6	49F1
Df(2R)Exel7130	+		+	+	s	+	3	50D4	50E4
Df(2R)Exel6064					s		3	53C10	53D2
Df(2R)Exel6067					s		3	55F8	56A1
Df(2R)Exel6071					s		3	57B3	57B16
Df(3L)Exel6107	+			+	s		1	64E5	64F5
Df(3L)Exel6111	+				s		2	65E7	65F4
Df(3L)Exel6123	+		+		s	+	3	70D7	70E4
Df(3L)Exel6135	+		+		s		1	76B11	76C4
Df(3R)Exel6149			+		s		2	85A2	85A5
Df(3R)Exel6162					s		3	87A1	87B5
Df(3R)ED5942	+			+	s	+	3	91F12	92B3
Df(2L)Exel6005	+			+	m		1	22A3	22B1
Df(2R)ED1612					m		3	42A14	42E7
Df(3L)ED4079					m		3	61A5	61B1
Df(3L)ED4342	pupal lethal				m		1	64B1	64B13
Df(3L)ED4786				+	m		2	75F7	76A5
Df(3R)ED5558				+	m		2	86F9	87B10
Df(3R)Exel6171		+		+	m		1	87F14	88A4
Df(3R)Exel6273					m		3	94B2	94B11
Df(3R)ED6103	+			+	m		1	94D3	94E9
Df(3R)Exel6192					m		3	94B11	94D3
Df(3R)Exel6193	+			+	m		1	94D3	94E4

Table 2: The 25 strongly or moderately interacting deficiencies were analysed for weight reduction, developmental delay, reduced viability and defective eyes upon crossing to the dm^{P0}. According to the resulting phenotypes they were then subdivided into 3 categories: Category 1 for at least two clear defects, Category 2 for one clear defect, Category 3 for no defects, or various defects that were also seen (more weakly) in control crosses. Dark blue and "s" indicates strong, light blue and "m" medium, interactions with $ey>dm^{P0}$. A "+" stands for a significant effect on the analysed aspect. Specifically, a "+" was given when the weight of the flies was significantly changed (with $p<0.05$) as compared to control flies ("dm^{P0rev}; Df(x)/+"), when viability was reduced to less than 1/3rd of the expected number of flies, when the development was prolonged ≥ 2 days or if the eye morphology was affected with dm^{P0}. Deficiencies highlighted in yellow might ultimately allow the identification of the responsible "interacting gene". Deficiencies in bold led to the identification of Chinmo and Delta, respectively. A "+" in dm^{P0rev} indicates that the Df influenced not only the weight of dm^{P0} flies but also of dm^{P0rev} flies.

Deficiency	selected genes	cat.	coord. of 5`3` bp		cyt. loc.	
Df(2L)ED778	***bun***, *ref2, nub, Pick1, kek1, ACX,* ***Tor***	**1**	12534671	13154415	**33E9**	**34A7**
Df(3L)Exel6107	*Ubp64E, Myt1, mad2, Pole2, PGRP-LD, Pmi, Tektin-C, vn, Txl, Cralbp,* ***S6k***	**1**	5712191	5861823	**64E5**	**64F5**
Df(3L)Exel6135	*serp, Oat, LCP1, tey, Gß76C, Gyc76C*	**1**	19585782	19709572	**76B11**	**76C4**
Df(3R)ED5942	***Dl***, *Ino80, Dys, Vha13, ort, Nup58, bn1, GluClalpha, bnl*	**3**	15052033	15660826	**91F12**	**92B3**
Df(2L)Exel6005	*Eno, RFeSP,cbp, frtz,* ***chinmo****, mRpL48*	**1**	1556758	1739118	**22A3**	**22B1**
Df(3L)ED4342	*TFIIEß, Hexo1,dyl, Cip4, mRpS6, Syx17, Src64B, Tie*	**1**	4258613	4603313	**64B1**	**64B13**
Df(3R)Exel6171	*Mst87F, Nsf2, E5, ems, Art6+9, lpp, Orc2, rdx*	**1**	9638639	9809255	**87F14**	**88A4**
Df(3R)ED6103	*Tango12, klg, Or94a+b, Imd, Gr94a, sav, cenB1A, hh, unk, p53, fzo*	**1**	18714931	19074794	**94D3**	**94E9**
Df(3R)Exel6193	*α-Adaptin, Tango 12, cenB1A, klg, Or94a+b, Imd, Gr94a, sav, cenB1A, hh, unk, p53*	**1**	18715437	18991827	**94D3**	**94E4**

Table 3: Genes deleted by the indicated deficiencies are displayed (all Category 1 deficiencies and one Category 3 deficiency); for simplicity, only named genes are listed (i.e. no genes with only "CG" numbers). Highlighted in bold are genes of the Tor signalling pathway (*Tor, S6k*), *Dl*, *chinmo* and *TFIIEb* (RNA Polymerase II transcription initiation). Dark blue colour indicates strong, light blue medium, interactions with *ey>dm*^{P0}. "Coord. of 5`3`bp" stands for coordinates of 5'/3' breakpoint and "cyt. loc." stands for cytological location, cat. Stands for category.

2. Delta

2.1 Introduction to Delta

As will be shown below, the gene within Df(3R)ED5942 that was responsible for the genetic interaction with *dmyc*, could be identified as *Delta*.

Delta is a component of the Notch signalling pathway. The ligand Delta (Dl), like the ligand Serrate (Ser), binds to the big extracellular domain of the Notch-receptor (Rebay et al., 1991). The consequence of this binding is cleavage of the Notch intracellular domain by sequence specific proteases including presinilin and nicastrin. The Notch intracellular domain is translocated into the nucleus, where it binds to Suppressor of Hairless (Su(H)), together with the co-activator Mastermind (Mam). The complex can activate the Notch target genes, such as *enhancer of split-C*, by direct binding of Su(H) to the Su(H) binding sites inside the regulatory regions of those genes (Bailey and Posakony, 1995; Lecourtois and Schweisguth, 1995). In the absence of Delta and Serrate, the Notch receptor remains intact, and the repressor Hairless (H), together with the co-repressors Groucho (Gro) and C-terminal binding protein (CtBP) binds to Su(H) to repress the activation of Notch target genes (Furriols and Bray, 2000; Morel et al., 2001).

There are several reports that the Notch signalling pathway and Myc cooperate in vertebrates. For example, a combination of genetic and molecular data demonstrated that Myc is a direct transcriptional target of Notch1, participating as an indispensable downstream effector in N1(IC) (intracellular domain of Notch1)-induced tumourigenic action (Klinakis et al., 2006). Moreover, Notch signalling not only affects patterning, but also proliferation (Wu et al., 2007).

2.2 Genetic interaction between *Delta* and *dmyc*

The gene span of the deficiency in which *Delta* was found is shown in Figure 1. One other line, Df(3R)Exel6184, deleting a small region of 12 genes inside the cytological region that is deleted by Df(3R)ED5942, showed no eye phenotype when crossed to *ey>dm*^{P0}. In contrast, two other lines, Df(3R)Dl-M2 and Df(3R)Dl-BX12, showed an easily discernable eye phenotype in a *dmyc* hypomorphic background. Thus, we focused on the region that was deleted in all 3 interacting deficiencies which contains only 8 genes. All available mutants were ordered and tested for interaction with *ey>dm*^{P0}. *Dl*^{3}, which carries a loss-of-function mutation in *Delta*, displayed a strong eye phenotype in a hypomorphic *dmyc* background (Figure 2). The eyes were pear-shaped and rough, resembling the phenotype of "*ey>dm*^{P0}; Df ED5942/+" flies. All other tested mutants did not interact.

To confirm that *dmyc* and *Dl* interact with each other and to rule out that the effect we see is due to a background mutation, we ordered different *Delta* alleles and crossed them to various *dmyc* alleles. *Dl*^{3}, which is the strongest *Dl* allele, as well as Df(3R)ED5942 and Df(3R)Dl-BX12 showed a strong interaction with all the *dmyc* alleles tested. Those were *dm*^{P0}, *dm*^{P0} *tub*>dMyc>GAL4 *ey*-FLP (P-element insertion in the promoter region), *dm*^{PL35} *tub*>dMyc>GAL4 *ey*-FLP (P-element insertion at the end of the 2nd intron), *w dm*^{4} *tub*>dMyc>GAL4 *ey*-FLP (null allele) and *dm*^{1} (gypsy-element insertion in the 1st intron). The different alleles were generated on different genetic backgrounds. The lethal alleles *dm*^{PL35} and *dm*^{4}, as well as *dm*^{P0}, are partially rescued by the *tub*>dMyc>GAL4 transgene, except for the head capsule where the *dmyc* mutant phenotypes are revealed. In all cases, control flies (*dm*^{P0rev}) were not affected. *Dl*^{rev10}, an amorphic allele that lacks the promoter region, transcription start site and first exon of *Delta*, only showed an eye defect when simultaneously hemizygous for the *ey>dm*^{P0} chromosome, but not for any other *dmyc* allele that was tested. Thus, either *Dl*^{rev10} is not a null allele or *Dl*^{3} is antimorphic (e.g. it might act as a dominant-negative allele), since *Dl*^{3} showed a stronger genetic interaction with *dmyc*. *Dl*^{rev10} only showed an interaction when *Ser* was additionally mutated. *Dl*^{6B}, the weakest *Dl* allele, showed no interaction with any *dmyc* allele (see Table 4). In combination with strong overexpression of dMyc ("GM") a *Delta* mutation lead to rougher and bigger ommatidia. Thus, *Delta* is the gene, which is responsible for the genetic interaction with *dmyc*, since other *Dl* alleles gave comparable phenotypes and different alleles of *dmyc* showed this interaction.

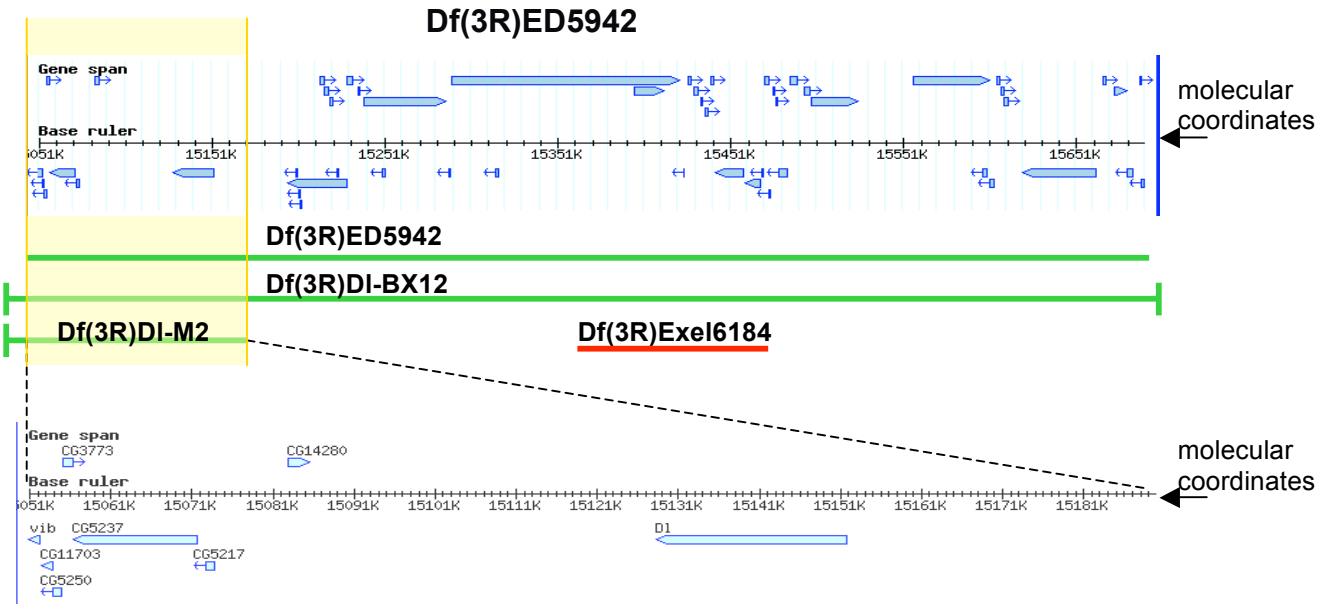

Figure 1: Genes deleted by the deficiency Df(3R)ED5942 (blue arrows). Shown are all interacting and non-interacting deficiencies. Interacting deficiencies are marked in green, non-interacting deficiencies in red. One deficiency in this region, Df(3R)Exel6184, showed no interaction with *ey>dm*^{P0}, two other deficiencies, Df(3R)Dl-BX12 and Df(3R)Dl-M2, showed a positive interaction with *ey>dm*^{P0} resulting in a rough and dented eye morphology. The region that is deleted by all 3 positive interacting deficiencies contains 8 genes, including *Delta*. Numbers indicate molecular coordinates on the 3rd chromosome, right arm.

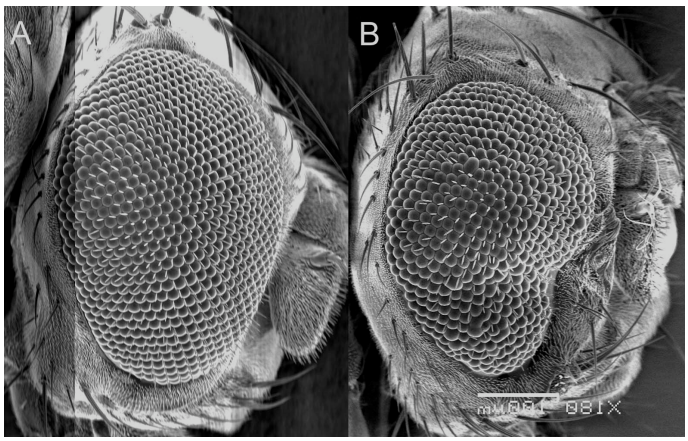

Figure 2: Genetic interaction between *Dl* and *dmyc*. Scanning electron microscope pictures of eyes that are hypomorphic for *dmyc* (panel A) or hypomorphic for *dmyc* and heterozygous for *Delta* (panel B). The rough and pear-shaped eye is comparable to the one of "*dm*^{P0}/Y; *pontin*$^{5.2}$/+" flies. Anterior is to the right. The depicted phenotype was observed for all flies with the corresponding phenotype (n=9).

Label:	Genotype:
A	*w dm*^{P0} *tub*>dMyc>GAL4 *ey*-FLP/Y
B	*w dm*^{P0} *tub*>dMyc>GAL4 *ey*-FLP/Y; *Dl*^{3}/+

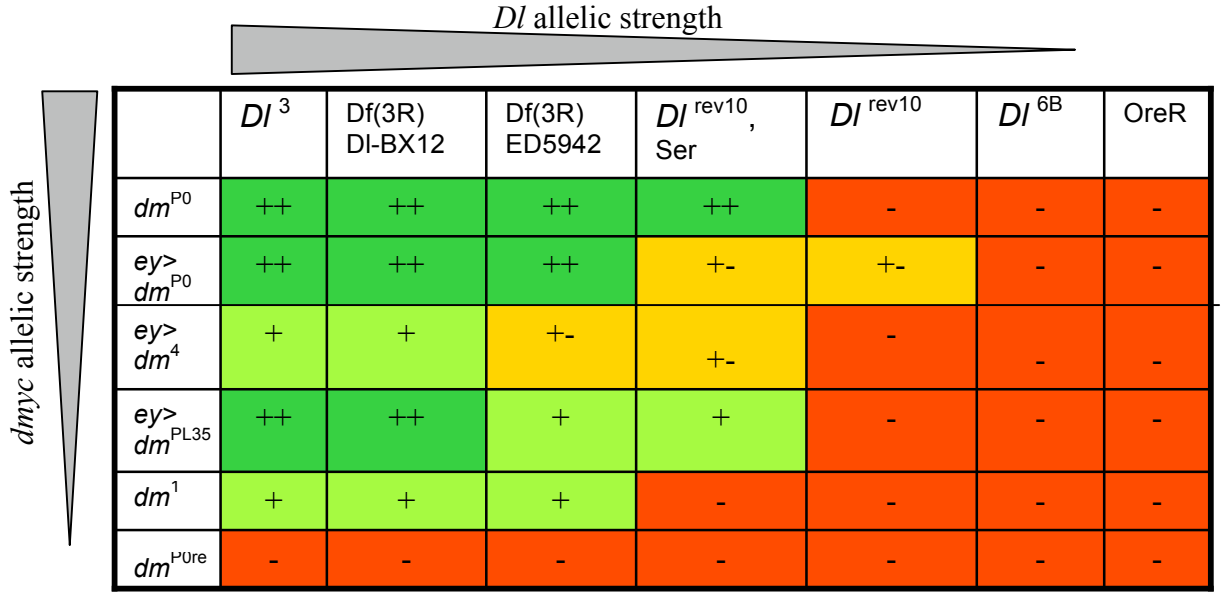

	Dl ^{3}	Df(3R) Dl-BX12	Df(3R) ED5942	*Dl* ^{rev10}, Ser	*Dl* ^{rev10}	*Dl* ^{6B}	OreR
dm^{P0}	++	++	++	++	-	-	-
ey>dm^{P0}	++	++	++	+-	+-	-	-
ey>dm^{4}	+	+	+-	+-	-	-	-
ey>dm^{PL35}	++	++	+	+	-	-	-
dm^{1}	+	+	+	-	-	-	-
dm^{Pure}	-	-	-	-	-	-	-

Table 4: Different *Delta* alleles were tested with a series of *dmyc* alleles for genetic interactions revealed by aberrant eye morphologies. *Dl*^{3} and Df(3R)Dl-BX12 are the strongest alleles, which showed an eye defect with all *dmyc* alleles, followed by the deficiency in which *Dl* was found. *Dl*^{6B}, a weak *Dl* allele showed no specific eye phenotype in flies that are mutant for *dmyc* and *Dl*. Green (and "++") indicates an eye phenotype in at least 80% of the F1, light green (and "+") stands for eye defects in 50-80% of the F1, orange (and "+-") indicates an eye defect in less than 50% of the scored flies, and red means no eye phenotype was observed. For each data point at least 16 flies were scored.

2.3 Interaction between Notch signalling components and *dmyc*

The best-described role for Dl is that of a ligand for Notch. This suggests that the Notch signalling pathway might interact with dMyc. To investigate if other components of the Notch signalling pathway interact with dMyc, various transgenes or mutants for Suppressor of Hairless (Su(H)), Hairless (H), Serrate (Ser), Notch (N), Lobe (L), *single-minded* (*sim*, a Notch signalling target gene) and *groucho* (*gro*) were tested for interaction with *ey>dm*^{P0} and control flies. Whenever an interaction was observed, the corresponding transgene was also tested with *dm*^{P0} itself. Although *Delta* and a dominant-negative version of *Ser* showed a genetic interaction with *ey>dm*^{P0}, all other components of the Notch signalling pathway (or its target genes) did not reveal an eye phenotype when hemizygous for the *ey>dm*^{P0} chromosome (see Table 5). Possibly, those transgenes were expressed too weakly to cause a genetic interaction with *ey>dm*^{P0}.

From the experiments above we can conclude that *Dl* and *dmyc* interact genetically, however other Notch signalling components do not seem to play a role for this interaction. As a next step, epistasis experiments with dMyc and homozygous mutations for Notch pathway components should be done to further investigate how (and if) the two pathways are connected. Since we focused on a different candidate dMyc interactor, we did not continue our investigations of Dl for the moment.

	ey>dm^{P0}/Y	*ey>dm*$^{+}$/Y	*dm*^{PO}/Y	*dm*^{POrev}/Y	comments
Su(H)	-	nt	nt	nt	
Su(H) GOF	++	++	-	-	
H	-	-	nt	nt	
H GOF	-	-	nt	nt	
L	-/+/++	nt	-/+/++	-/+/++	milder effects with *dm*^{P0rev} than with *dm*^{P0}
L GOF	++	++	-	-	
Dl	++	-	+	-	
Dl GOF	nt	nt	nt	nt	
Ser	-/+	nt	nt	nt	
Ser GOF	nt	nt	nt	nt	
N	-	-	nt	nt	
N GOF	+	+	nt	nt	
N LOF	+	+	nt	nt	
sim	-	nt	nt	nt	
gro	-	-	nt	nt	

Table 5: Different components of the Notch signalling pathway were tested for interaction with the hypomorphic allele *dm*^{P0}. Only *Dl* and a dominant-negative allele of *Serrate* showed an interaction with *dmyc* and not with control flies. A "++" is defined by an eye phenotype in at least 50% of the analysed flies, a "+" stands for eye defects in up to 50% of the analysed flies, and a "-" indicates that no eye phenotype was observed in these flies. If more than one sign is shown, different transgenes were tested with different outcomes; "nt" indicates that this interaction was not tested. GOF stands for UAS-transgenes expressing the corresponding cDNA, or a gain-of-function mutant allele in the case of H.

Transgene:	Genotype:
Su(H)	Su(H)^{1}
Su(H)GOF	UAS SU(H)^{VP16}
	UAS SU(H)
	UAS SU(H) (III)
H	*ey*-H$^{15-1}$
	sev-H$^{267.1}$
H GOF	H^{E31}(FRT-82B)
L	L$^{1-5}$
L GOF	UAS L (III)
Dl	Dl^{3}
Ser	SerlacZ
	Ser DN^{1}
N	N$^{I1N-ts1g2f1}$
N GOF	UAS ECN (II)
N LOF	UAS-N.dsRNA^{9G}
	UAS-N.dsRNA^{14E}
sim	*sim*^{2}
gro	*gro*^{1}
	gro^{C105}
	gro^{KG07117}

3. *CG31666/chinmo*

3.1 Identification of *CG31666/chinmo*

3.1.1 Deficiency screen

The Exelixis deficiency Df(2L)Exel6005 resulted in an intermediate eye phenotype in the initial screen with *ey>dm*^{P0} (see Table 2 and Figure 5, panel A). Further characterisation showed that "*dm*^{P0}/Y; Df(2L)Exel6005/+" flies had a strong eye phenotype and a clear reduction in weight, leading us to classify this deficiency as a strong *dmyc*-interactor (Category 1, Table 3).

Df(2L)Exel6005 is located on the left arm of the 2nd chromosome at cytological location 22A3-22B1 and deletes 17 genes. Two other deficiencies Df(2L)Exel8004 and Df(2L)Exel7007, that overlap Df(2L)Exel6005, did not show a genetic interaction with *ey>dm*^{P0}, but the deficiencies Df(2L)frtz14 and Df(2L)frtz24 positively interacted with *ey>dm*^{P0} (see Figure 3). Thus, only 2 genes remained as possible new *dmyc* interacting genes, *CG31666* and *CG31934* (see Figure 3).

In parallel, all available mutations uncovered by Df(2L)Exel6005 were tested for interaction with *ey>dm*^{P0}. However, all mutations outside of the region of overlap between Df(2L)Exel6005, Df(2L)frtz14 and Df(2L)frtz24 showed no interaction with *ey>dm*^{P0}. No alleles were reported for *CG31934* and no transgenes were available. Therefore, *CG31934* could not be tested for a genetic interaction with *dmyc*. Fortunately, it was not necessary anymore to analyse *CG13943* since we found out that another gene was responsible for the interaction with *dmyc*, *CG31666*. *CG31666* also called *Chinmo* showed a dominant interaction with *dmyc*. We tested 3 different *chinmo* alleles (*chinmo*^{108}, *chinmo*^{110}, *chinmo*^{134}; a gift from H.Stocker) for interaction with *ey>dm*^{P0} flies: flies with the genotype "*w dm*^{P0} *tub*>dMyc>GAL4 *ey*-FLP/Y; *chinmo*^{X}/+" were analysed for irregular ommatidia. All 3 alleles resulted in a rough and dented eye comparable to the phenotype that we observed in combination with the deficiency (see Figure 4). Thus, the gene that causes the phenotype in *ey>dm*^{P0}; Df(2L)Exel6005 is *chinmo*.

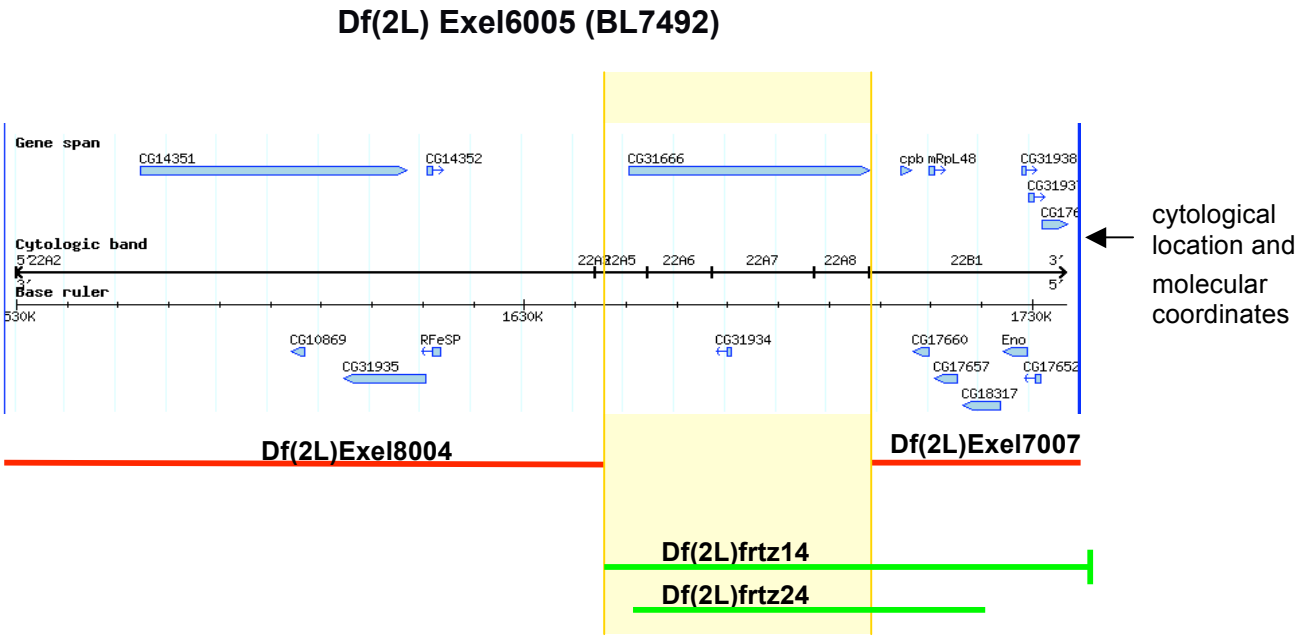

Figure 3: Gene span of interacting deficiency Df(2L)Exel6005. Shown is the cytological band that is deleted and all tested interacting and non-interacting deficiencies. Interacting deficiencies are marked in green, non-interacting deficiencies in red. Two other deficiencies in this region showed no interaction with *ey>dm*^{P0}, Df(2L)Exel8004 and Df(2L)Exel7007. In contrast, Df(2L)frtz14 and Df(2L)frtz24 showed an eye phenotype with *ey>dm*^{P0}. The region that overlaps between the interacting deficiencies and that is not affected by the non-interacting deficiencies contains only 2 genes, *CG31666 (Chinmo)* and *CG31934*. The same conventions apply as for Figure 1.

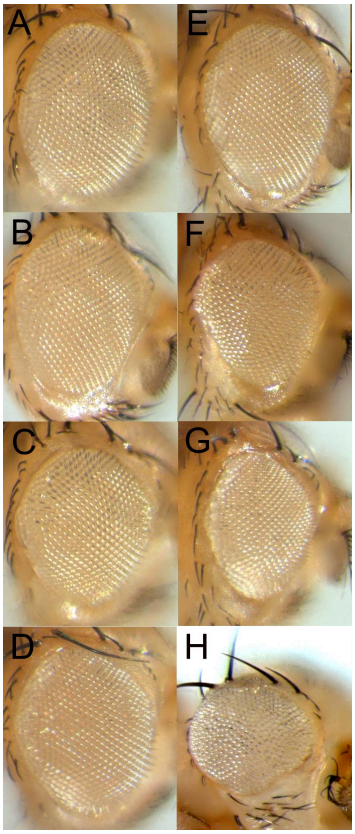

Figure 4: Interaction between the 3 *chinmo* alleles and *ey>dm*^{P0} (right column). The eyes are clearly distorted for all 3 *chinmo* alleles. Control *ey>dm*$^{+}$ flies (left column) are unaffected. The control chromosome is isogenic with the *chinmo* alleles and shows no interaction with *ey>dm*^{P0} (top row). The depicted phenotypes were observed for a majority of the flies with the corresponding phenotypes (n>50%). The experiment was performed in two independent biological replicates. Anterior is to the right.

Label:	Genotype:
A	*y w tub*>dMyc>GAL4 *ey*-FLP/Y; FRT-40/CyO, y^{+}
B	*y w tub*>dMyc>GAL4 *ey*-FLP/Y; FRT-40 *chinmo*^{108}/CyO, y^{+}
C	*y w tub*>dMyc>GAL4 *ey*-FLP/Y; FRT-40 *chinmo*^{110}/CyO, y^{+}
D	*y w tub*>dMyc>GAL4 *ey*-FLP/Y; FRT-40 *chinmo*^{134}/CyO, y^{+}
E	*w dm*^{P0} *tub*>dMyc>GAL4 *ey*-FLP/Y; FRT-40/CyO, y^{+}
F	*w dm*^{P0} *tub*>dMyc>GAL4 *ey*-FLP/Y; FRT-40 *chinmo*^{108}/CyO, y^{+}
G	*w dm*^{P0} *tub*>dMyc>GAL4 *ey*-FLP/Y; FRT-40 *chinmo*^{110}/CyO, y^{+}
H	*w dm*^{P0} *tub*>dMyc>GAL4 *ey*-FLP/Y; FRT-40 *chinmo*^{134}/CyO, y^{+}

3.1.2. Rescue of the eye phenotype caused by Df(2L)Exel6005 and *ey>dm*^{P0}

We received 2 UAS-transgenes of Chinmo (kind gift of H.Stocker). These transgenes are presumably weak, since they carry only 2 UAS-sites (enhancer sequences that are bound by the transcriptional activator GAL4 and thereby mediate transcriptional activation in transgenic flies expressing GAL4; the extent of transcriptional activation increases with the number of UAS-sites, and typical UAS-transgenes carry at least 5 such sites).

Even though these transgenes express a protein lacking one amino acid (Ser) as compared to the published *Drosophila* reference proteome, they were able to rescue the phenotype displayed by "*w dm*^{P0} *tub*>dMyc>GAL4 *ey*-FLP/Y; Df(2L)Exel6005/+" flies almost to wildtype appearance (see Figure 5).

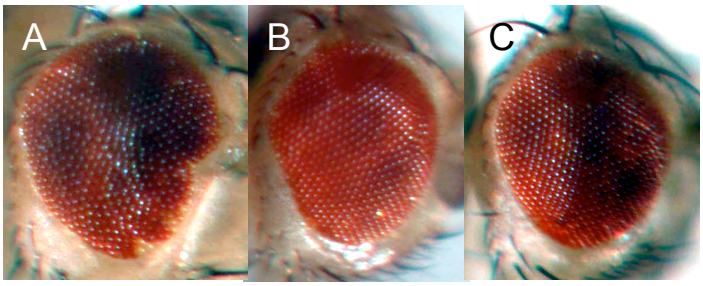

Figure 5: Rescue of the "*ey*>*dm*^{P0}/Y; Df(2L)Exel6005/+" eye phenotype by overexpression of a Chinmo transgene. Panels B and C show eyes from flies carrying two different Chinmo transgene insertions. The pear-shaped and dented eye phenotype is rescued completely in those flies. The depicted phenotypes were observed for a majority of the flies with the corresponding phenotypes (>80%). The experiment was performed in two independent biological replicates. Anterior is to the right.

Label:	Genotype:
A	*w dm*^{P0} *tub*>dMyc>GAL4 *ey*-FLP/Y; Exel6005/+
B	*w dm*^{P0} *tub*>dMyc>GAL4 *ey*-FLP/Y; Exel6005/UAS-Chinmo$^{T1.1}$
C	*w dm*^{P0} *tub*>dMyc>GAL4 *ey*-FLP/Y; Exel6005/+; UAS-Chinmo$^{T1.2}$/+

3.1.3 Chinmo gene and protein

Chinmo is a large gene comprising 9 exons and spanning a total length of 45`368 base pairs. The ORF starts at the end of the 5th exon and ends at the beginning of the 9th exon and codes for a protein of 604 amino acids. There are 3 transcripts (RA, RC, RD) that give rise to the same protein, and a fourth transcript (RB), which has a predicted second STOP codon and will give rise to a protein of 794 amino acids. This second STOP codon was never confirmed by ESTs (Figure 6).

The Chinmo protein has two recognisable domains, a BTB/POZ (**B**road complex, **T**ramtrack, **B**ric à Brac or **po**xvirus and **z**inc finger) domain at the N-terminus and two C_2H_2 zinc fingers at the C-terminus. BTB/POZ domains are found in proteins that are involved in diverse biological processes, like DNA damage response or cell cycle progression. BTB/POZ domains mediate homo-dimerisation and in some instances hetero-dimerisation and binding to DNA (Bardwell, Treisman, 1994).

Zinc fingers are involved in DNA binding. Classical C_2H_2-type zinc fingers (Znf) contain a short beta hairpin and an alpha helix (beta/beta/alpha structure), where a single zinc atom is held in place by Cys_2His_2 (C_2H_2) residues in a tetrahedral array. The C_2H_2 Znf motifs recognise DNA sequences by binding to the major groove of DNA via a short alpha-helix in the Znf, spanning 3-4 bases of the DNA (Wolfe et al., 2000). C_2H_2 Znfs can also bind to RNA and proteins.

Interestingly, the zinc-finger transcription factor Miz-1 that mediates repression by Myc also contains a BTB/POZ domain and Zn-fingers (Wanzel, 2003). So far, the fly homologue of Miz-1 has not been identified - many fly proteins contain BTB/POZ domains and Zn fingers, but none of them shows recognisable similarity to Miz-1 outside of these domains. Thus, taking into account the genetic interaction with *dmyc*, Chinmo might be a functional homolog of Miz-1 in flies.

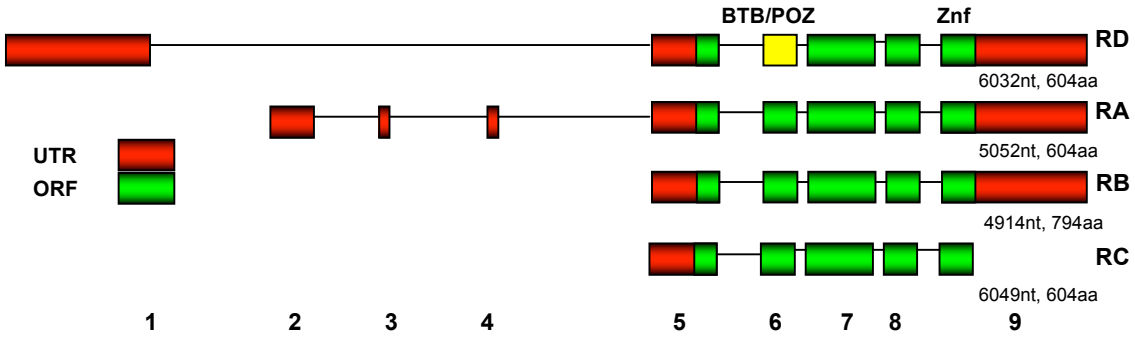

Figure 6: Schematic diagram of *chinmo* transcripts. The transcripts RA, RC and RD contain the same ORF, coding for a protein of 604 amino acids. Transcript RB is derived from an alternative splicing between exons 8 and 9, and contains an ORF with a predicted second stop-codon, coding for a protein of 794 amino acids length. Both protein isoforms contain a BTB/POZ domain and two C_2H_2 zinc fingers (Znf) that are shown in yellow in the RD isoform. Numbers indicate nucleotides (nt) and amino acids (aa) (right) and exons (bottom). Green shows the open reading frame (ORF) and red the untranslated region (UTR).

3.1.4. *ey*-FLP screen ("pinhead" screen)

Interestingly, Chinmo was also found earlier in an *ey*-FLP-screen for mutations in genes, which are involved in growth control (S. Oldham & E. Hafen, pers. communication). This so-called "pinhead screen" was based on the FLP/FRT-system (Newsome et al., 2000; Xu and Rubin, 1993). This system allows the generation of homozygous mutant clones by site-specific mitotic recombination. By expressing FLP recombinase under the control of *eyeless* regulatory sequences (*ey*-FLP) the recombination events are restricted to the developing head capsule. This promoter provides continuous high levels of FLP activity throughout the proliferative phase of eye and head development, resulting in a high frequency of mosaicism. Mitotic recombination occurs between two FRT sequences on homologous chromosome arms. One chromosome arm carries the FRT insertion as well as the mutation of interest and the other chromosome arm carries a w^+ marker and a *cell lethal* mutation (which prevents the survival of homozygous cells). The recombination results in 2 different daughter cells: an mutant cell bearing two copies of the mutant allele and a wildtype sister cell; the former is marked by the absence of the w^+, whereas the latter is w^+. To induce random mutations, males with the genotype "*y w ey*-FLP/Y; FRT-40/FRT-40" were mutagenised with EMS and crossed to females "*y w ey*-FLP; FRT-40 *cl* w^+/CyO, y^+." The offspring was screened for unbalanced flies with mosaic eyes. Flies with a smaller or bigger head were kept and established as stocks, complementation groups were established and some of the responsible genes causing a small head-phenotype were mapped.

One complementation group resulting in a small head was shown to affect the *chinmo*/*CG31666* gene. Eye section of *chinmo* alleles performed by A.Sulzer (Sulzer, 2003, diploma thesis) showed that the reduction in head size was based on a cell number reduction and not caused by a cell size reduction. Further interaction studies with different components of the Insulin signalling pathway, which affects growth and proliferation without affecting pattern formation, indicated that Chinmo does not function in the Insulin signalling pathway.

3.1.4.1 Characterization of the *chinmo* alleles

From the *ey*-FLP-screen, 3 different *chinmo* alleles were obtained (Figure 7). Allele $chinmo^{110}$ carries a C to T transition, which leads to an amino acid exchange from histidine (CAT) to tyrosine (TAT). Allele $chinmo^{108}$ has a deletion of 11 bp in the end of the 7th exon. This deletion leads to a frame shift and a premature STOP after 30 aa. Allele $chinmo^{134}$ is a base substitution from cytosine to thymine in the beginning of the 7th exon. This mutation leads to

a substitution of a codon for glutamine (CAG) with a STOP codon (TAG). In all three alleles the zinc finger domain is either mutated (*chinmo*^{110}) or completely deleted (*chinmo*^{108}, *chinmo*^{134}). A. Sulzer showed that *chinmo*^{110} was the weakest allele, followed by *chinmo*^{108} and *chinmo*^{134} (Sulzer, 2003, diploma thesis).

To characterise the strength of the different *chinmo* alleles in a different way we crossed them among one another and with the deficiency that deletes *chinmo* (Df(2L)Exel6005). The lines were balanced with a balancer (CyO, GFP), in order to distinguish the mutant from the heterozygous flies. Egg-lays were performed on apple agar plates and 100 eggs per cross were transferred onto fresh apple agar plates. The offspring was screened for heteroallelic mutant animals. All heteroallelic combinations cause embryonic lethality. Therefore, no conclusion can be drawn about the allelic strengths, however this experiment confirms that the Df(2L)Exel6005 indeed deletes *chinmo*, since not a single fly carrying both a *chinmo* allele and the deficiency was obtained.

Amongst other phenotypes, "*dm*^{P0}/Y; Df(2L)Exel6005/+" flies have a clear reduction in weight, compared to control flies. Control flies weigh 0,694g in average, whereas "*dm*^{P0}/Y; Df(2L)Exel6005/+" flies weigh 0.588g in average; for comparison, "*dm*^{P0}/Y; *pontin*$^{5.2}$/+" flies weigh 0,598g in average. To determine if the different *chinmo* alleles also cause a reduction in weight, flies carrying the different alleles were crossed to *dm*^{P0} or *dm*^{P0rev} flies and 20 appropriate sons were analysed for their weight and compared to control flies ("*dm*^{P0}/Y; iso/+", where "iso" stands for a chromosome that is isogenic with Df(2L)Exel6005). Only *chinmo*^{108} showed a significant reduction in weight. However, also wildtype flies were affected. Thus, the mutations of flies carrying the different *chinmo* alleles might not be strong enough to cause a weight reduction with *dm*^{P0}.

Flies carrying the genotype "*dm*^{P0}/Y; *chinmo*^{X}/+" were also tested for a developmental delay and a reduced viability. None of those flies had a prolonged development and only *chinmo*^{110} showed a slightly reduced viability in a *dm*^{P0} background.

These results show that the different *chinmo* alleles do not behave like the *pontin*$^{5.2}$ allele with respect to dMyc dependent processes like growth. Thus, Chinmo might not be involved in these processes or the alleles are to weak to cause such an effect. However, they strongly affect the proper regulation of eye size and shape when dMyc levels are reduced.

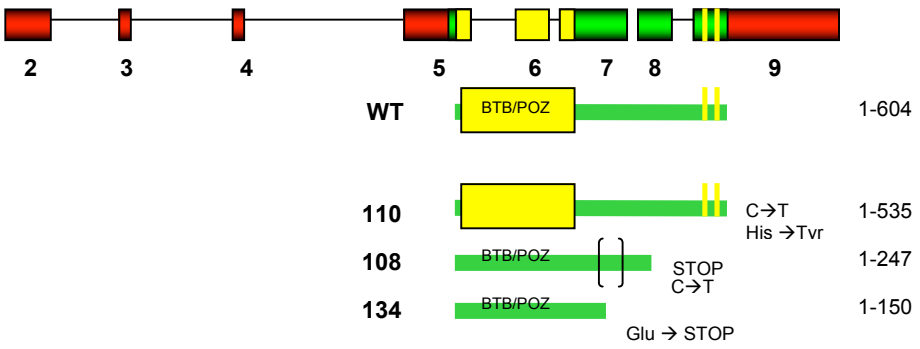

Figure 7: Schematic diagram of the different *chinmo* alleles. *chinmo*^{110} has most probably a non-functional Zn-finger due to a C-T transition that changes the first conserved histidine to a tyrosine. *chinmo*^{108} carries a deletion after the BTB/POZ domain, followed by a frame-shift and a premature stop codon, and allele *chinmo*^{134} contains a G-T transversion, which leads to a premature STOP. The BTB/POZ domain is located at amino acids 32-128 and the two zinc finger domains at amino acids 517-540 and 545-568. The numbers to the right indicate the amino acid coordinates of the mutant codons. The yellow boxes to the right indicate the 2 C_2H_2 zinc fingers of Chinmo.

3.1.4.2 Confirmation of "pinheads"

To validate the small heads that were observed in the *ey*-FLP-screen, we crossed the different *chinmo* alleles to FRT-40 *cl* w^+. All three crosses produced flies with small heads ("pinheads"). The phenotype for $chinmo^{134}$ was even stronger than the one that was observed in the *ey*-FLP-screen. The pictures to the right clearly show a reduction in ommatidial number and a rough eye phenotype for all alleles. The highest fraction of homozygous mutant ommatidia was obtained for $chinmo^{110}$ indicated by very rare w^+ ommatidia (see Figure 8). This observation confirms the small heads and the relative allelic strengths of the different *chinmo* alleles that were observed in the *ey*-FLP screen (Sulzer, 2003, diploma thesis).

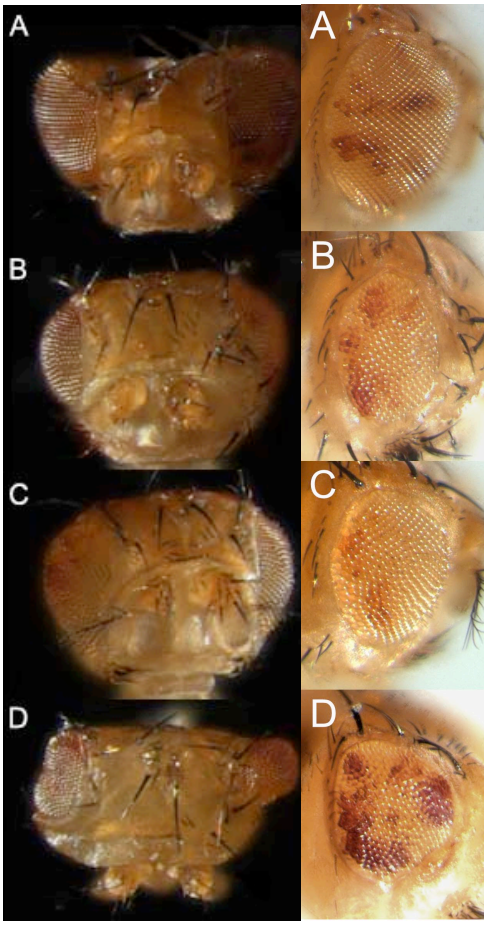

Figure 8: Phenotypes of the Chinmo mosaic eyes. The heads for *chinmo*^{108} (panels B) and *chinmo*^{110} (panels C) are clearly smaller than control heads (panels A). The head for *chinmo*^{134} (panels D) is clearly distorted. The overall eye size is reduced for all alleles and the eyes are rough (right panels). Anterior is to the right. Homozygous mutant tissue is represented by w^- ommatidia. The depicted phenotypes were observed for a majority of the flies with the corresponding phenotypes (100% of at least 2 analysed flies per genotype). The experiment was performed in two independent biological replicates

Label:	Genotype:
A	*y w tub*>dMyc>GAL4 *ey*-FLP; FRT-40/FRT-40 *cl* w^+
B	*y w tub*>dMyc>GAL4 *ey*-FLP; FRT-40 *chinmo*^{108}/FRT-40 *cl* w^+
C	*y w tub*>dMyc>GAL4 *ey*-FLP; FRT-40 *chinmo*^{110}/FRT-40 *cl* w^+
D	*y w tub*>dMyc>GAL4 *ey*-FLP; FRT-40 *chinmo*^{134}/FRT-40 *cl* w^+

3.1.5. *In vivo* mutagenesis screen

All lines from the *in vivo* mutagenesis screen (described earlier) that carried mutations on the second chromosome were crossed to the deficiency Df(2L)Exel6005 and tested for non-complementation in order to find a mutation in *chinmo*. Forty-four balanced screen lines were tested and one line, 380C1 resulted in offspring with a strongly reduced viability; the heteroallelic flies mostly died as pupae and only $1/5^{th}$ of the expected flies eclosed. These adults displayed a severe eye phenotype with rough, dented eyes and a reduced number of ommatidia and defective wings with blisters.

To prove that line 380C1 carries a mutation in *chinmo*, the 3 existing *chinmo* alleles were crossed to line 380C1. Indeed, the offspring that was obtained from the cross with $chinmo^{134}$ died as pupae. Some of these pupae were dissected and shown to have split heads, short mouthparts and small and rough ommatidia. The crosses with $chinmo^{108}$ and $chinmo^{110}$ also resulted in pupal lethality, however in these crosses $1/5^{th}$ of the expected flies reached adulthood. Those flies showed clear defects: Their wings were smaller and blistered, the thoraxes and the heads split, ommatidia small and rough, and the ocelli, a type of photoreceptor organs, were missing (Figure 9). This indicates that the allele 380C1 is indeed a new *chinmo* allele. From now on 380C1 will be referred to as $chinmo^{380C1}$. However, since heteroallelic combinations of the alleles $chinmo^{108}$, $chinmo^{110}$ and $chinmo^{134}$ result in embryonic lethality, but heteroallelic combinations with $chinmo^{380C1}$ reach pupal stage, $chinmo^{380C1}$ most probably is a hypomorphic allele.

In order to find the mutation in $chinmo^{380C1}$, we sequenced *chinmo*`s predicted exons 1, 2, 4, 5 and 9. So far, we have not found a mutation. Exon 3 and parts of exon 6, 7 and 8 still need to be analysed. However, if the mutation affects regulatory regions outside the coding sequences, we will not be able to find them by sequencing of the exons. It is also possible (although unlikely) that the non-complementation might be a result of a dominant intergenic non-complementation, i.e. affect a gene other than *chinmo*.

Figure 9: Transheteroallelic combinations of the screen line 380C1 with Df(2L)Exel6005 and different *chinmo* alleles resulted in completely distorted flies. The heads are split, the eyes are smaller with rough and dented ommatidia, the wings carry blisters and are smaller, and the thoraxes are split. The strongest phenotype was seen in trans with $chinmo^{134}$, since all $chinmo^{308C1/134}$ flies die as pupae. Panel D shows a dead pupa. The depicted phenotypes were observed for a majority of the flies with the corresponding genotypes. The experiment was performed in two independent biological replicates.

Label:	Genotype:
A	*y w*; $chinmo^{380C1}$/Df(2L)Exel6005
B	*y w*; $chinmo^{380C1}$/FRT-40 $chinmo^{108}$
C	*y w*; $chinmo^{380C1}$/FRT-40 $chinmo^{110}$
D	*y w*; $chinmo^{380C1}$/FRT-40 $chinmo^{134}$

3.1.6 Additional alleles

The Bloomington stock centre provides 2 different *chinmo* alleles: *chinmo*^{M33}, an EMS induced allele that carries a missense mutation in the BTB/POZ domain, which leads to an amino acid alteration from phenylalanine to isoleucine (F88I), and *chinmo*^{k13009}, which carries a P-element insertion in the first exon of *chinmo*. The Szeged *Drosophila* stock centre provides one allele: *chinmo*^{SH1971}, which carries a P-element insertion in the first exon of *chinmo*. All 3 alleles are recessive lethal. Flies with the genotype "*ey>dm*^{P0}/Y; *chinmo*^{M33}/+" showed a weak eye phenotype (in 11% of 18 analysed flies) and flies with the genotype "*ey>dm*^{P0}/Y; *chinmo* ^{k13009}/+" showed a strong eye phenotype (in 33% of 10 analysed flies). However, *chinmo*^{SH1971} did not interact at all with *ey>dm*^{P0}.

3.2 Effects of Chinmo on dMyc-dependent processes *in vivo*

3.2.1. A reduction in Chinmo levels strongly influences growth in *dmyc* null flies

Hemizygous *dmyc* null mutants (dm^4) appear to have a normal embryonic development and larvae hatch with normal frequencies. However, within 24 hours of hatching, these larvae are smaller than wildtype. After moulting into second instar, these larvae stop growing and most die soon afterwards (Pierce et al., 2004).

Flies that are null for *dmyc* but carry a ubiquitously expressed cDNA that rescues the null mutant phenotype in the whole fly (*w* dm^4 *tub*>dMyc>GAL4 *ey*-FLP), except in the eye, reach adulthood. However, their ommatidial size and number are clearly reduced. We were interested if a mutation in *chinmo* would enhance this phenotype since we could already show that *chinmo* affects eye development in a *dmyc* hypomorphic background, and a stronger *dmyc* allele might lead to an even more severe eye phenotype. Therefore, we analysed the eyes of flies with the genotype "*w* dm^4 *tub*>dMyc>GAL4 *ey*-FLP/Y; $chinmo^X$/+" (see Figure 10). In all 3 cases very few ommatidia, if any, were left. $chinmo^{134}$ showed the strongest effect. Those flies were dissected from their pupal cases, since they are not able to eclose anymore. These results confirm a strong genetic interaction between *chinmo* and *dmyc* with a second, independent *dmyc* allele.

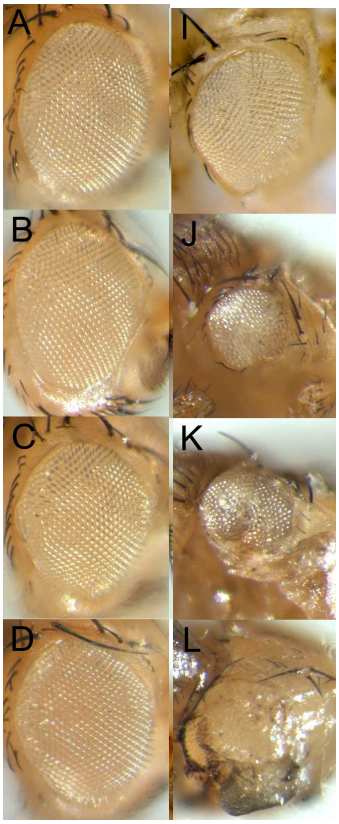

Figure 10: Interaction between the 3 c*hinmo* alleles and dm^4 (right). The eyes are clearly distorted for all 3 *chinmo* alleles. Control flies are unaffected (left columns). The control chromosome (top row) is isogenic with the *chinmo* alleles. Anterior is to the right. The depicted phenotypes were observed for a majority of the flies with the corresponding phenotypes. The experiment was performed in two independent biological replicates at two different temperatures (25°C, 18°C).

Label:	Genotype:
A	*y w tub*>dMyc>GAL4 *ey*-FLP; FRT-40/CyO, y^+
B	*y w tub*>dMyc>GAL4 *ey*-FLP; FRT-40 $chinmo^{108}$/CyO, y^+
C	*y w tub*>dMyc>GAL4 *ey*-FLP; FRT-40 $chinmo^{110}$/CyO, y^+
D	*y w tub*>dMyc>GAL4 *ey*-FLP; FRT-40 $chinmo^{134}$/CyO, y^+
I	*w* dm^4 *tub*>dMyc>GAL4 *ey*-FLP; FRT-40/CyO, y^+
J	*w* dm^4 *tub*>dMyc>GAL4 *ey*-FLP; FRT-40 $chinmo^{108}$/CyO, y^+
K	*w* dm^4 *tub*>dMyc>GAL4 *ey*-FLP; FRT-40 $chinmo^{110}$/CyO, y^+
L	*w* dm^4 *tub*>dMyc>GAL4 *ey*-FLP; FRT-40 $chinmo^{134}$/CyO, y^+

3.2.2 Chinmo and dMyc function in partially redundant pathways

To address the epistatic relationship between Chinmo and dMyc, we analysed doubly mutant flies. When dMyc levels are reduced (Figure 11E) the overall head size is reduced. When dMyc is completely absent (Figure 11I), the head is even smaller. In both cases, the overall structure of the head is well formed. Similarly, heads mutant for *chinmo* are small, but normally patterned (Figure 8). However, when Chinmo levels are reduced in a head-specific *dmyc* mutant background, the heads not only get smaller but also completely disrupted and they can be hardly recognized as fly heads. In a dm^{P0} background, $chinmo^{134}$ showed the strongest effects. The doubly mutant flies were not hatching anymore and had to be manually dissected from their pupal cases. Alleles $chinmo^{110}$ and $chinmo^{108}$ showed comparable effects: a reduction in head size and a decreased number of ommatidia. In a dm^{4} background, no Chinmo mutants were able to eclose, and $chinmo^{108}$ and $chinmo^{134}$ showed the strongest defects, followed by $chinmo^{110}$.

These data show that the phenotype caused by the complete absence of dMyc is exacerbated by a reduction of Chinmo. Thus, Chinmo retains at least some function in the absence of dMyc (as witnessed by the substantial development of "dm^{4} $chinmo^{+}$" heads as compared to "dm^{4} $chinmo^{-}$" heads). Conversely, assuming that the available *chinmo* alleles are null alleles, dMyc can direct substantial growth and development in the absence of Chinmo (compare "dm^{+} $chinmo^{-}$" and "dm^{4} $chinmo^{-}$"). Chinmo and dMyc therefore function in (partially) redundant pathways whose collective output is needed for head growth and development (these pathways are only partially redundant, since both "dm^{4} $chinmo^{+}$" and "dm^{+} $chinmo^{-}$" heads show clear growth defects). This interpretation may have to be changed if the tested *chinmo* alleles turn out to retain significant activity – in such a case it is possible that dMycs role in head development fully depends on Chinmo (but not *vice versa*). However, these results do not role out or confirm the possibility that, in part, dMyc and Chinmo also function in the same pathway, as was suggested by our earlier observations of a dominant interaction between *chinmo* and *dmyc*.

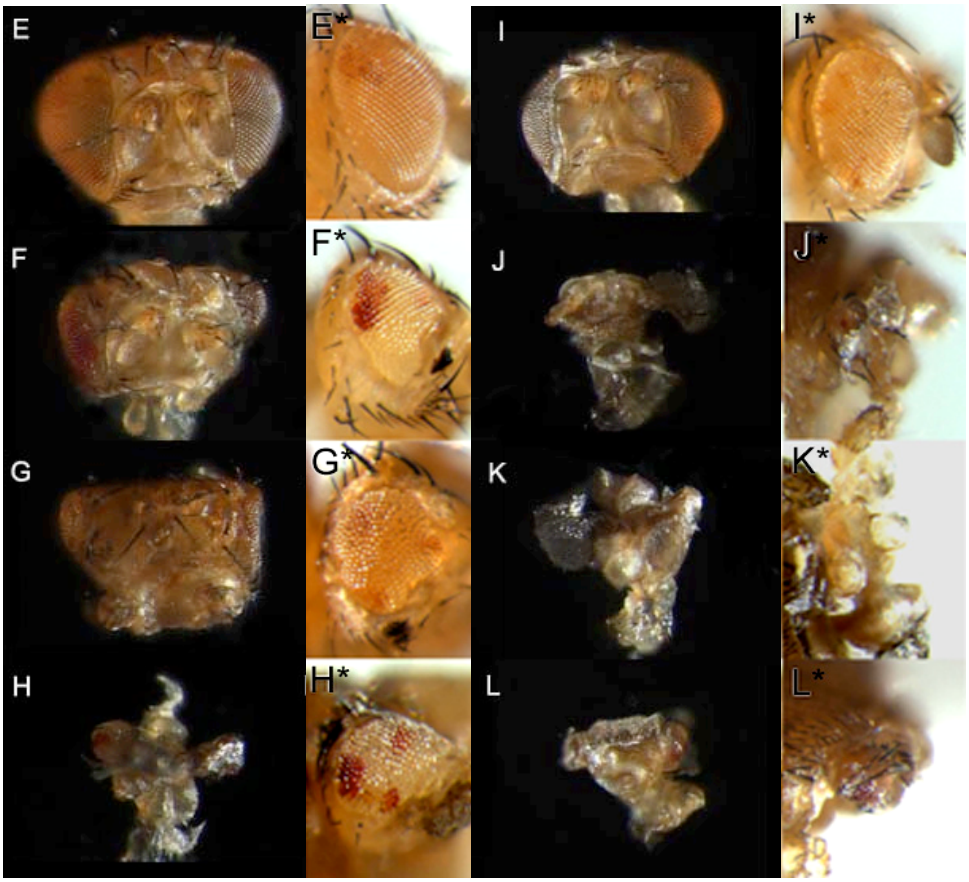

Figure 11: Phenotypes of the *chinmo* mosaic eyes in a dm^{P0} (E-H) or dm^{4} background (I-L). The heads for $chinmo^{108}$ (panel F), $chinmo^{110}$ (panel G) and $chinmo^{134}$ (panel H) are clearly smaller than control heads (panel E). All heads are clearly distorted. The overall eye size is reduced for all alleles (right panels, indicated with *). The phenotypes are even more severe in a dm^{4} mutant background (panels I-L). The depicted phenotypes were observed for a majority of the flies with the corresponding genotypes (80% of at least 2 analysed flies per genotype). Anterior is to the right. The experiment was performed in two independent biological replicates.

Label:	Genotype:
E	*w* dm^{P0} *tub*>dMyc>GAL4 *ey*-FLP; FRT-40/FRT-40 *cl* w^{+}
F	*w* dm^{P0} *tub*>dMyc>GAL4 *ey*-FLP; FRT-40 $chinmo^{108}$/FRT-40 *cl* w^{+}
G	*w* dm^{P0} *tub*>dMyc>GAL4 *ey*-FLP; FRT-40 $chinmo^{110}$/FRT-40 *cl* w^{+}
H	*w* dm^{P0} *tub*>dMyc>GAL4 *ey*-FLP; FRT-40 $chinmo^{134}$/FRT-40 *cl* w^{+}
I	*w* dm^{4} *tub*>dMyc>GAL4 *ey*-FLP; FRT-40/FRT40 *cl* w^{+}
J	*w* dm^{4} *tub*>dMyc>GAL4 *ey*-FLP; FRT-40 $chinmo^{108}$/FRT-40 *cl* w^{+}
K	*w* dm^{4} *tub*>dMyc>GAL4 *ey*-FLP; FRT-40 $chinmo^{110}$/FRT-40 *cl* w^{+}
L	*w* dm^{4} *tub*>dMyc>GAL4 *ey*-FLP; FRT-40 $chinmo^{134}$/FRT-40 *cl* w^{+}

3.2.3 Chinmo overexpression transgenes

So far, we only performed experiments in a Chinmo mutant background. We were also interested in how overexpression of Chinmo would affect dMyc-dependent processes *in vivo*. For this purpose, we obtained a *chinmo* cDNA from the Berkeley *Drosophila* Genome Project (BDGP Gold collection clone SD4616). This cDNA clone originates from RNA of *Drosophila* Schneider L2 cells and is cloned in the vector pOT2. We tagged the cDNA with an "AU1"-epitope tag and subcloned it first into pBluescript SK+ (Invitrogen) and subsequently into pUASTB (see Materials and Methods for detailed description), to produce the plasmid pUAS-Chinmo. This plasmid does not contain the 5` and 3`untranslated regions of *chinmo*.

Transgenic flies for Chinmo were established by using the ΦC31 integrase system. As a landing site for pUAS-Chinmo we chose 102D on the 4th chromosome to have the other chromosomes free for our investigations (pUAS-Chinmo^{IV}). Later on, pUAS-Chinmo was also integrated in the landing site ZH-86Fb by the Hafen laboratory, which kindly provided us with 2 different lines. Another UAS-transgene, which we will refer to as UAS-Chinmo$^{3`5`UTR}$, was kindly provided by the group of Tzumin Lee (Zhu et al., 2006). This UAS-Chinmo transgene contains the full-length cDNA including the 5' and 3' untranslated regions, which were shown to be important for proper gene expression (Zhu et al., 2006), but no epitope tag.

All UAS-transgenes were crossed to flies expressing GAL4 ubiquitously under the control of the *armadillo* or *tubulin* promoters, or in specific tissues under the control of *GMR* or *apterous* (eye and dorsal compartment of the wing disc, respectively). However, none of the crosses led to adult flies. Most of the flies overexpressing Chinmo died at early pupal stages (see Table 6). These results indicate that ectopic expression of Chinmo in at least some tissue(s) is not compatible with organismal survival. So far we don't know, which tissue this is. The experiment was performed by crossing flies carrying the transgenes pUAS-Chinmo^{IV} and UAS-dMyc to flies carrying the above-mentioned GAL4 drivers. As a control, flies carrying a pUAST transgene were used. When dMyc and Chinmo were overexpressed together the resulting offspring died earlier than flies overexpressing Chinmo alone. Control flies were not affected (data not shown). When the different Chinmo transgenes were crossed to flies with the genotype "*y w tub*>dMyc>GAL4 ey-Flp" the resulting offspring died during early pupal stages. For this reason, we were not able to perform the rescue experiment with our transgenes, which we had carried out to rescue the eye phenotype of a hypomorphic dMyc mutation over the deficiency, which deletes Chinmo with a weak (and wrong) UAS-transgene (see 3.1.2. and Figure 5).

Chinmo (III)	Chinmo (IV)	Chinmo (Zhu et al.)	GAL4-driver
nd	late pupal lethal	pupal lethal	***armadillo***
embryonic lethal	embryonic lethal	embryonic lethal	***tubulin***
embryonic lethal	embryonic lethal	embryonic lethal	***actin5C***
nd	early pupal lethal	nd	***apterous***
early pupal lethal	early pupal lethal	late pupal lethal	***GMR***
early pupal lethal	early pupal lethal	early pupal lethal	**GM**

Table 6: Overexpression of Chinmo leads to death with different GAL4 drivers. *Arm*-GAL4 and *tub*-GAL4 lead to ubiquitous expression, *GMR*-GAL4 and "GM" to expression in the eye and *ap*-GAL4 to expression in the dorsal compartment of the wing discs. Nd stands for not done. III and IV indicate the chromosomal location of the transgene. The different transgenes are similarly expressed. The shown phenotypes were observed for a majority of the flies with the corresponding genotypes.

3.2.4 Overexpression of Chinmo in clones

Overexpression of dMyc in clones in wing imaginal discs strongly enhances growth (Johnston et al., 1999). The results of the experiments we have performed up to now demonstrate that both, Chinmo and dMyc are necessary to support growth in the eye. This lead to the question, whether we can further enhance growth by overexpressing Chinmo and dMyc together in clones of wing imaginal discs.

To address this question, we used a line carrying an *act*>CD2>GAL4 cassette in combination with a UAS-GFP and a hs-FLP transgene. Upon heat-shock, recombination mediated by FLP recombinase takes place and leads to random clones within the whole disc, where GFP and the transgene of choice are overexpressed. Thus, we were able to directly determine the enhancement of clonal growth by dMyc and Chinmo either alone or in combination. After setting up the crosses at 25°C, the resulting offspring was heat-shocked at 37°C for 8 minutes at 48h or 72h AED. Wing imaginal discs were then isolated 5 days AED and pictures were taken on a compound microscope. Finally, the area of each clone was determined. Both clones induced at 48h and at 72h lead to the same outcome (Figures 12 and 15). dMyc overexpressing clones were at least twice the size of control clones, consistent with published observations (Johnston et al., 1999). Interestingly, clones that overexpress Chinmo were significantly smaller than control clones. This outcome was unexpected, given Chinmo's positive role in growth control. One possible explanation for this observation is that that overexpression of Chinmo induces apoptosis and thus reduces clonal size. This might also explain why overexpression of all UAS-Chinmo transgenes leads to lethality. An analogous observation was previously made for clones overexpressing dMycΔMB3 (see manuscript, Figure 4, 5). Thus, it could be speculated that dMyc induces apoptosis in cooperation with Chinmo.

However, dMyc-overexpression induces the same relative increase in clone size in the presence and in the absence of overexpressed Chinmo. Conversely, Chinmo overexpression induces the same relative decrease in clone size in the presence and in the absence of overexpressed dMyc. Thus, the effects of Chinmo and of dMyc on clone size are largely independent. It remains possible, though, that the ability of overexpressed dMyc to trigger apoptosis, which becomes apparent only at higher overexpression levels, is partly mediated by Chinmo.

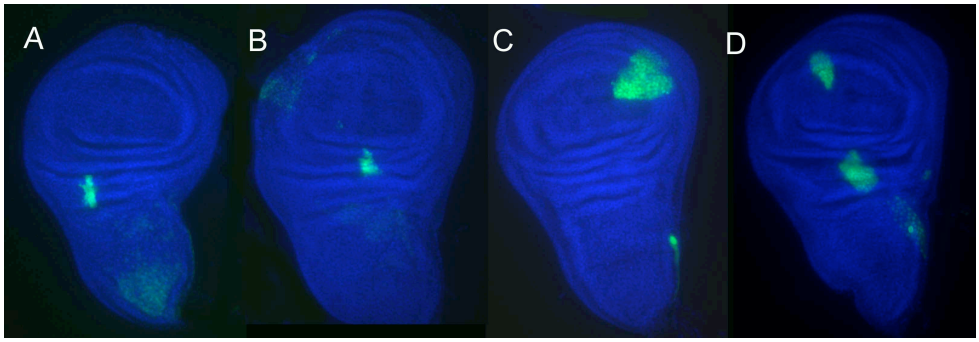

Figure 12: Overexpression of Chinmo and/or dMyc in clones in wing imaginal discs. The green spots are clones overexpressing GFP in combination with different transgenes: - (A), Chinmo (B), dMyc (C) or dMyc and Chinmo (D). The clones are 72 hours old. Chinmo clones are smaller than control clones (B vs. A), dMyc clones are bigger (C) and clones co-overexpressing dMyc and Chinmo reach a clone size between clones overexpressing dMyc and overexpressing Chinmo. The experiment was performed in two independent biological replicates.

Label:	Genotype:
A	*y w* hs-FLP; *act*>CD2>GAL4 UAS-GFP/ pUASTB
B	*y w* hs-FLP; *act*>CD2>GAL4 UAS-GFP/+; pUAS-Chinmo^{IV}/+
C	*y w* hs-FLP; *act*>CD2>GAL4 UAS-GFP/UAS-dMyc^{132}
D	*y w* hs-FLP; *act*>CD2>GAL4 UAS-GFP/UAS-dMyc^{132}; pUAS-Chinmo^{IV}/+

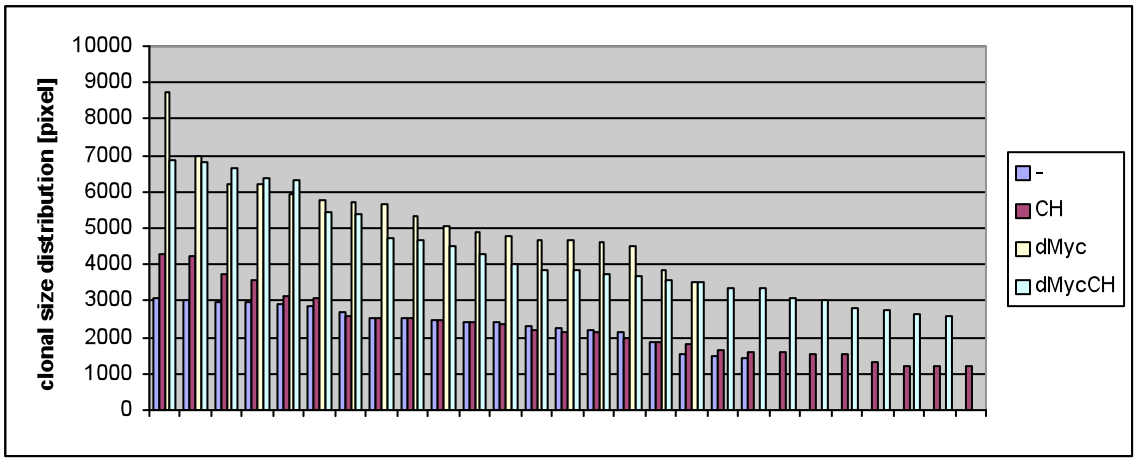

Figure 13: Clone size distribution (in pixel). Depicted are the sizes of clones overexpressing GFP alone (-), Chinmo (CH), dMyc (dMyc) or dMyc and Chinmo (dMycCH).

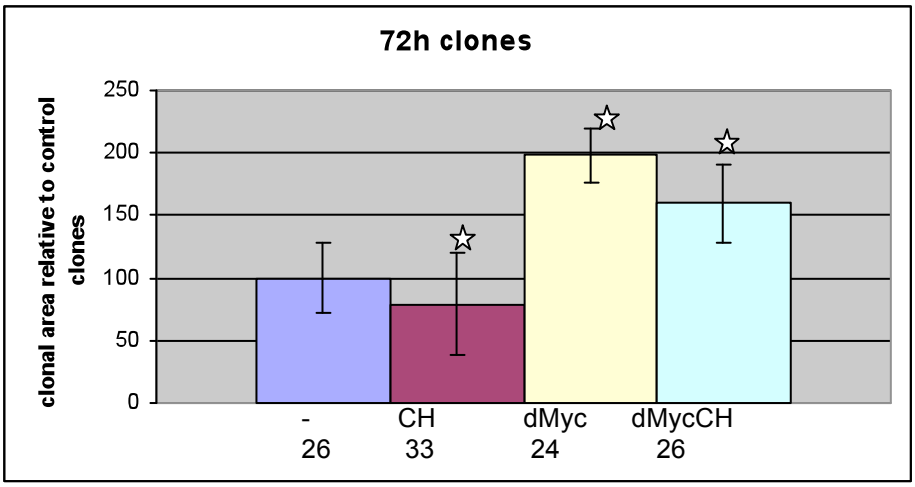

Figure 14: Size of clones overexpressing Chinmo. dMyc overexpressing clones are twice the size of control clones. Asterisks indicate p-values below 0.05 and thus a significant change compared to control clones (blue bar). Error bars indicate standard deviation of the mean. Measured were clones overexpressing GFP alone (-), overexpressing Chinmo (CH), overexpressing dMyc (Myc) or co-overexpressing dMyc and Chinmo (MycCH); the numbers of measured clones are indicated below.

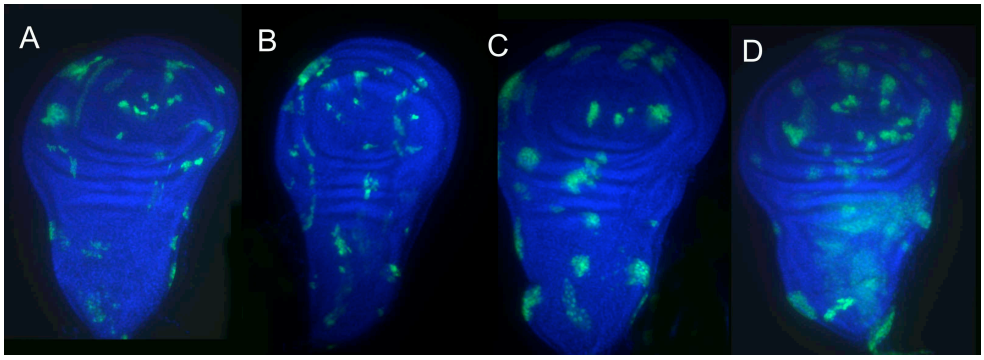

Figure 15: Overexpression of Chinmo in clones in wing imaginal discs. The green spots are clones overexpressing GFP in combination with different transgenes: - (A), Chinmo (B), dMyc (C) or dMyc and Chinmo (D). The clones are 48 hours old. Chinmo clones are smaller than control clones (B vs. A), dMyc clones are bigger (C) and clones co-overexpressing dMyc and Chinmo reach a clone size between clones overexpressing dMyc and overexpressing Chinmo.

Label:	Genotype:
A	*y w* hs-FLP; *act*>CD2>GAL4 UAS-GFP/ pUASTB
B	*y w* hs-FLP; *act*>CD2>GAL4 UAS-GFP/+; pUAS-Chinmo^{IV}/+
C	*y w* hs-FLP; *act*>CD2>GAL4 UAS-GFP/UAS-dMyc^{132}
D	*y w* hs-FLP; *act*>CD2>GAL4 UAS-GFP/UAS-dMyc^{132}; pUAS-Chinmo^{IV}/+

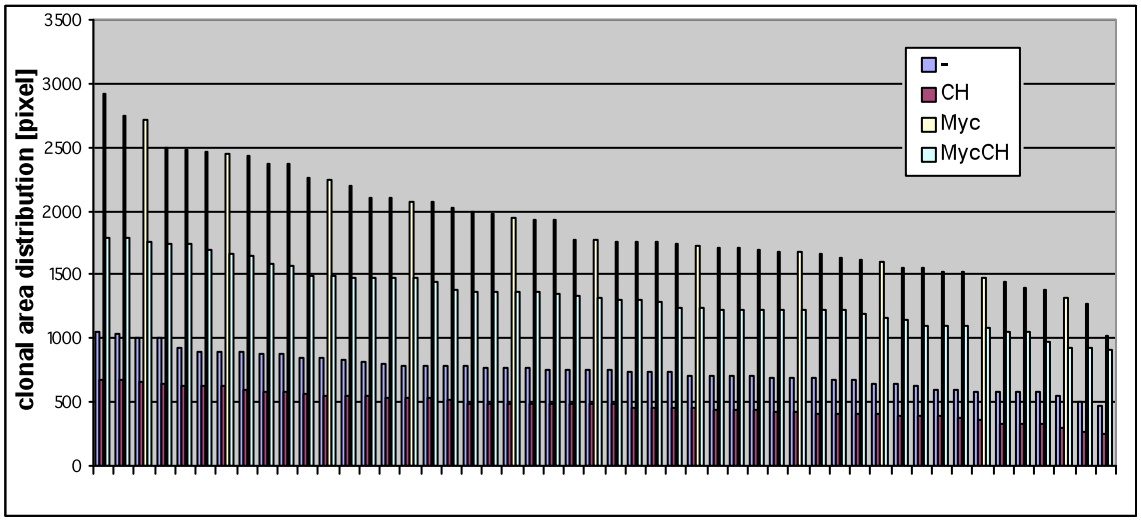

Figure 16: Clone area distribution (in pixel). Depicted are clones overexpressing GFP alone (-), Chinmo (CH), dMyc (Myc) or dMyc and Chinmo (MycCH).

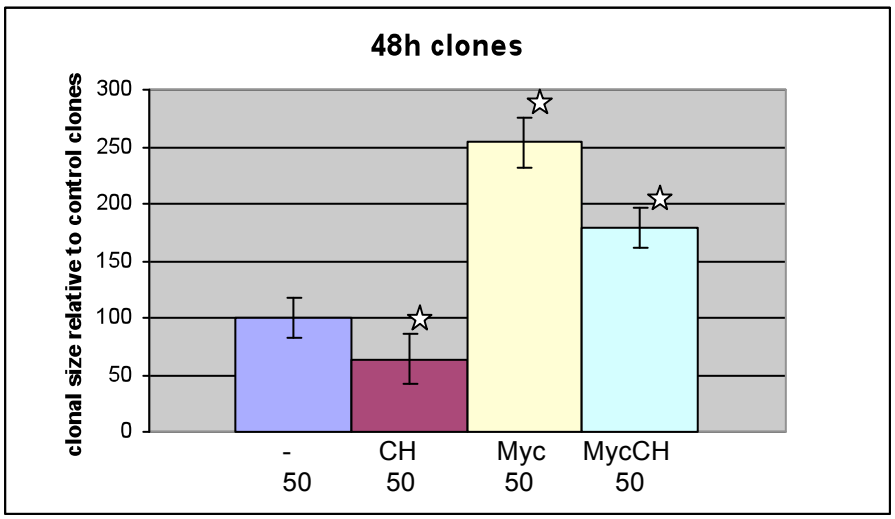

Figure 17: Size of clones overexpressing Chinmo and/or dMyc. dMyc overexpressing clones are twice the size of control clones. Asterisks indicate p-values below 0.05 and thus a significant change compared to control clones (blue bar). Error bars indicate standard deviation. Measured were clones overexpressing GFP alone (-), overexpressing Chinmo (CH), overexpressing dMyc (Myc) or co-overexpressing dMyc and Chinmo (MycCH); the numbers of measured clones are indicated below.

3.2.5 Overexpression of Chinmo leads to apoptosis

Clonal size upon overexpression of Chinmo is reduced compared to control clones. To confirm that this size reduction is due to induction of apoptosis, we overexpressed Chinmo in the dorsal compartment of the wing imaginal discs with *apterous*-GAL4.

Thus, we analysed wing imaginal discs that either overexpressed dMyc, Chinmo or both together. Since we could not dissect any discs after overexpression of Chinmo (they were too small or absent), we used the GAL80 temperature-sensitive system to overexpress the transgenes during a defined period. $GAL80^{ts}$ binds to and represses GAL4 under permissive conditions, and dissociates from GAL4 upon incubation at higher temperature (≥29°C). $GAL80^{ts}$ is expressed under control of the α–*tub84B* promoter and therefore inhibits GAL4 in the whole fly. Females with the genotype "*w*; *ap*-GAL4/CyO, y^{+}; $GAL80^{ts}$" were crossed to males either carrying a pUAS-Chinmo, a UAS-dMyc transgene, or both together. They were kept at 25°C for 4 days and on 29°C for another day. Five days AED, uncrowded wandering third instar larvae were dissected for their wing imaginal discs and stained for cleaved caspase-3. The pictures below clearly show that overexpression of Chinmo leads to apoptosis (Figure 18C). Apoptosis is also observed when dMyc is overexpressed, but to a lesser extent (Figure 18B), as described earlier (Montero et al., 2008). Co-overexpression of both Chinmo and dMyc leads to a massive induction of cell death (Figure 18D).

As a control for the $GAL80^{ts}$ system, a parallel cross was set up with the same flies but held at 29°C for the whole time. Those flies died at pupal stages (as do flies with the genotype "*ap*-GAL4; pUAS-Chinmo"). As a second control, the parents of the original cross were transferred to fresh tubes after 3 days and their offspring kept at 25°C. The resulting flies with the genotype "*y w*; *ap*-GAL4/+; UAS-dMyc/$GAL80^{ts}$; pUAS-$Chinmo^{IV}$/+" and " *y w*; *ap*-GAL4/+; $GAL80^{ts}$/+; pUAS-$Chinmo^{IV}$/+" had strong wing defects; the wings were smaller, bent down, and had blisters. This indicates that the GAL80 system could not repress all GAL4 activity at 25°C.

This observation could explain why overexpression of Chinmo transgenes with different GAL4 drivers leads to death prior to eclosion of the adult fly. However, they are in apparent contradiction with the results of the clonal experiment, where co-expression with dMyc increased the size of Chinmo-overexpressing clones; if dMyc and Chinmo co-operate in the induction of apoptosis, such clones would have been expected to be smaller than control clones or clones expressing either protein alone. It is conceivable, though, that the co-expression of dMyc has a net positive effect on clonal size (if dMyc-induced additional growth is bigger than the dMyc-induced extra apoptosis), or that the different expression

strength of the GAL4-drivers in the two experimental systems affects the degree to which dMyc induces apoptosis in either situation.

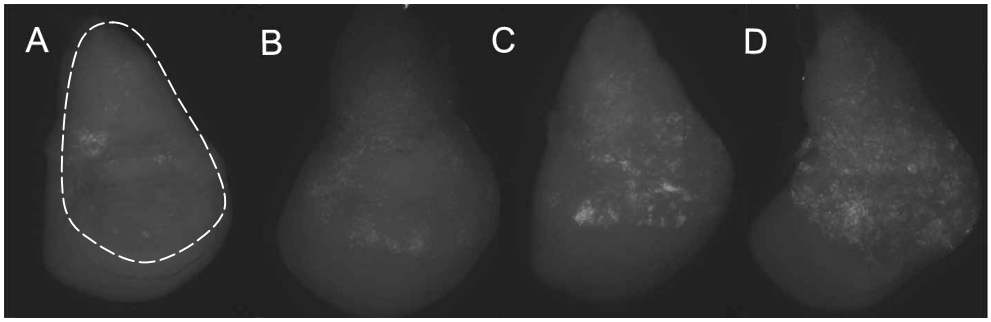

Figure 18: Anti-cleaved caspase 3 stainings of wing imaginal discs after overexpression of Chinmo and/or dMyc. Chinmo overexpression resulted in massive apoptosis as indicated by the white dots. The white line marks the area where the transgenes are expressed by *apterous*-GAL4. The depicted phenotypes were observed in a majority of the corresponding wings (n=10 for A-C, n=5 for D).

Label:	Genotype:
A	*w*; *ap*-GAL4/+; *tub*-GAL80^{ts}/pUASTB
B	*w*; *ap*-GAL4/+; *tub*-GAL80^{ts}/UAS-dMyc
C	*w*; *ap*-GAL4/+; *tub*-GAL80^{ts}/+; pUAS-Chinmo^{IV}/+
D	*w*; *ap*-GAL4/+; *tub*-GAL80^{ts}/UAS-dMyc; pUAS-Chinmo^{IV}/+

3.2.6 Overexpression of dMyc in a *chinmo* mutant background

So far, our data provide evidence that *chinmo* genetically interacts with *dmyc* to induce growth in the eye. Yet, there is no direct evidence for the dependence of dMyc on Chinmo to induce growth. To address this possibility, we used the MARCM (**M**osaic **A**nalysis with a **R**epressible **C**ell **M**arker) system (Lee and Luo, 1999) to overexpress dMyc in wing imaginal disc clones homozygous mutant for *chinmo*. Mosaic analysis using this technique relies on generation of homozygous mutant cells from heterozygous precursors via mitotic recombination. It combines the GAL80 repressor protein with the GAL4/UAS binary expression system and the FLP/FRT-system to genetically label clones. In the MARCM system, the activity of GAL4 is repressed by the GAL80 protein, resulting in unmarked cells that are heterozygous for both GAL80 and a mutation. After FLP/FRT-dependent site-specific mitotic recombination, homozygous mutant daughter cells emerge that lack GAL80 and hence possess an active GAL4 that can activate the reporter gene, UAS–GFP, and additional UAS-transgenes that may be present. Those clones are the only ones to show green fluorescence. The other daughter cells have two copies of GAL80, therefore GAL4 remains inactive and as a result no UAS-transgenes are expressed.

We established two different lines, one with the genotype "*y w;* (FRT-40 *chinmo*^{X}; UAS-dMyc)/ (SM5; TM6B,*Tb*)", and the other line without the dMyc transgene. C*hinmo*^{X} stands for the 3 different *chinmo* alleles from the *ey*-FLP-screen. Those flies were crossed to the MARCM line "*y w* hs-FLP UAS-GFP; (FRT-40 *tub*-GAL80; *tub*-GAL4)/(SM5; TM6B,*Tb*). Clones were induced in the offspring 48h AED by a brief heat-shock (20 minutes at 37°C) and at 120h AED uncrowded wandering non-*Tubby* larvae were collected and further analysed. The areas of at least 20 clones per genotype were determined. Overexpression of dMyc leads to an increase in clone size of 40%. This is not as strong as we observed earlier (see manuscript, Figure 5), but still significant, possibly because *tub*-GAL4 drives lower levels of dMyc overexpression than the *act*-GAL4 driver used in the earlier experiments. Clonal size is not reduced in *chinmo* mutant clones and the same results were obtained with different alleles. dMyc did not induce growth anymore in a *chinmo* mutant background (see Figure 20, 21). Thus, dMyc is dependent on Chinmo expression to induce cellular growth.

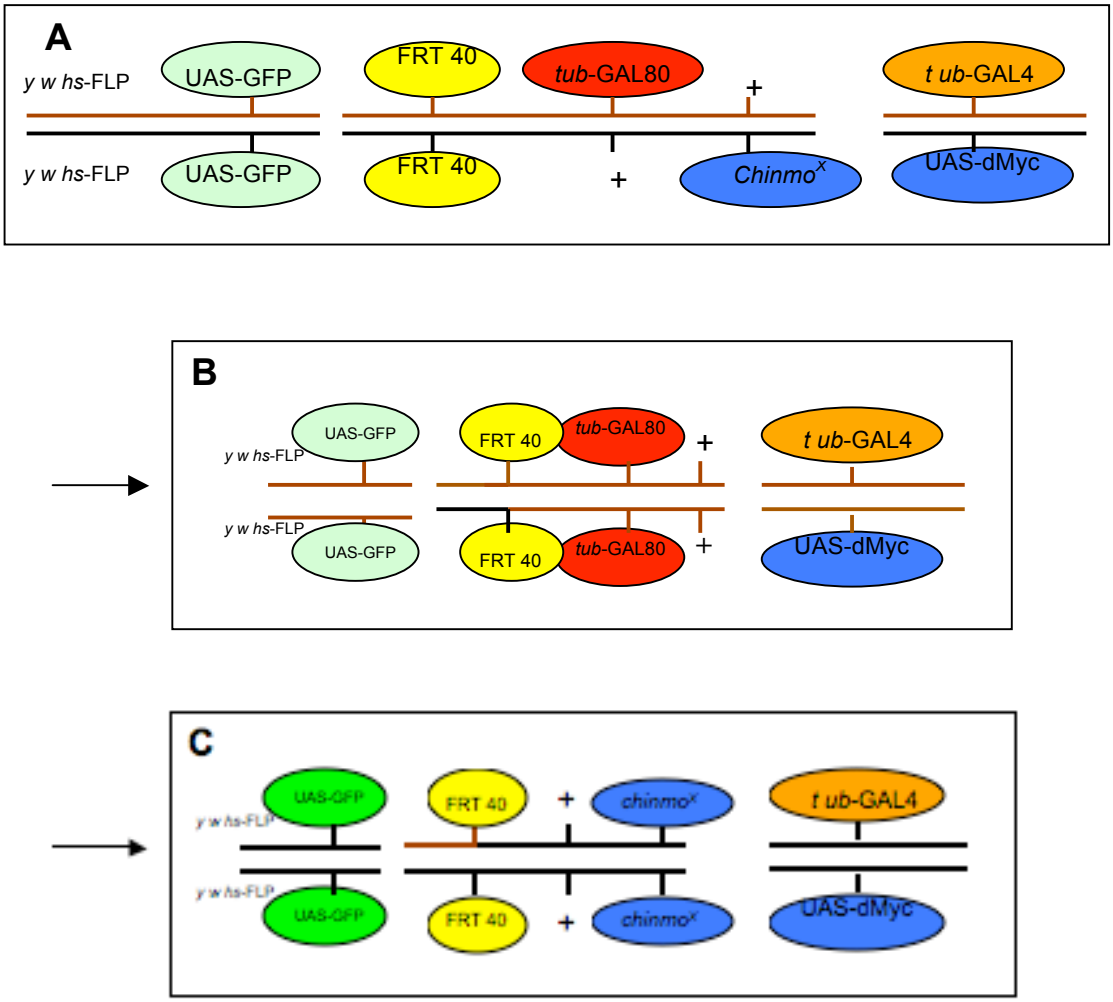

Figure 19: Illustration of the MARCM system. Panel A shows the mother cells: 5 different transgenes are located on different chromosome arms, the second chromosome carries a mutation in *chinmo*, distal of the FRT-site and in *trans* to *tub*-GAL80. After heat-shock, the FLP-recombinase induces mitotic recombination between the FRT-sites (yellow) which gives rise to two daughter cells, each of which is homozygous for the chromosome arm distal to the FRT-site (B,C). The cells in A and B neither express GFP nor any other transgene, since GAL80 inhibits the expression of *tub*-GAL4. The cell in C expresses GFP and other UAS-transgenes, and in addition, it is homozygous mutant for *chinmo*. Depending on the line we used, Myc is also expressed in those cells.

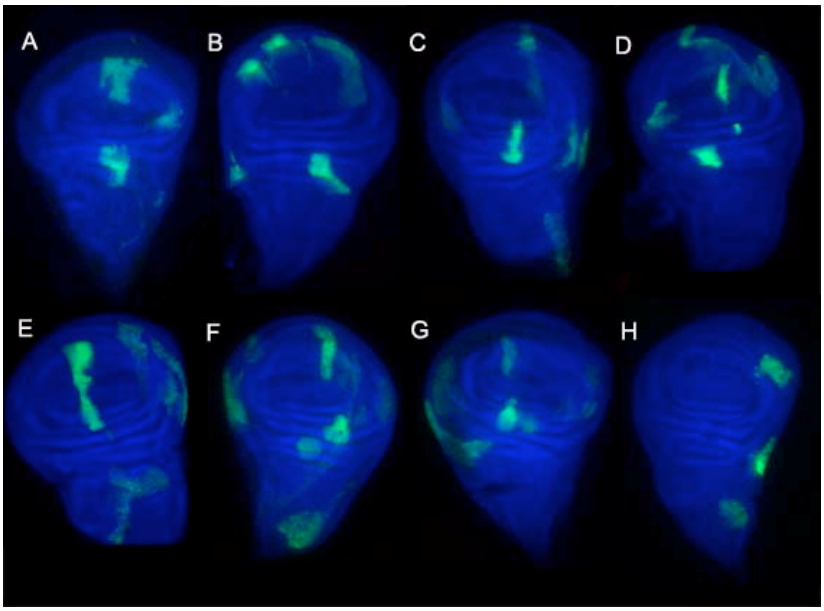

Figure 20: Clones homozygous mutant for the different Chinmo alleles (B, C, D), and overexpressing dMyc (F, G, H). Overexpression of dMyc in clones that are homozygous mutant for *chinmo* does not induce any overgrowth. Clones are green since they co-express UAS-GFP. The depicted phenotypes were observed in a majority of the corresponding wings (n=20).

Label:	Genotype of green fluorescent cells:
A	*y w* hs-FLP UAS-GFP; FRT-40/FRT-40; *tub*-GAL4/MKRS
B	*y w* hs-FLP UAS-GFP; FRT-40 *chinmo*^{108}/FRT-40 *chinmo*^{108}; *tub*-GAL4/+
C	*y w* hs-FLP UAS-GFP; FRT-40 *chinmo*^{110}/FRT-40 *chinmo*^{110}; *tub*-GAL4/+
D	*y w* hs-FLP UAS-GFP; FRT-40 *chinmo*^{134}/FRT-40 *chinmo*^{134}; *tub*-GAL4/+
E	*y w* hs-FLP UAS-GFP; FRT-40/FRT-40; *tub*-GAL4/UAS-dMyc
F	*y w* hs-FLP UAS-GFP; FRT-40 *chinmo*^{108}/FRT-40 *chinmo*^{108}; *tub*-GAL4/UAS-dMyc
G	*y w* hs-FLP UAS-GFP; FRT-40 *chinmo*^{110}/FRT-40 *chinmo*^{110}; *tub*-GAL4/UAS-dMyc
H	*y w* hs-FLP UAS-GFP; FRT-40 *chinmo*^{134}/FRT-40 *chinmo*^{134}; *tub*-GAL4/UAS-dMyc

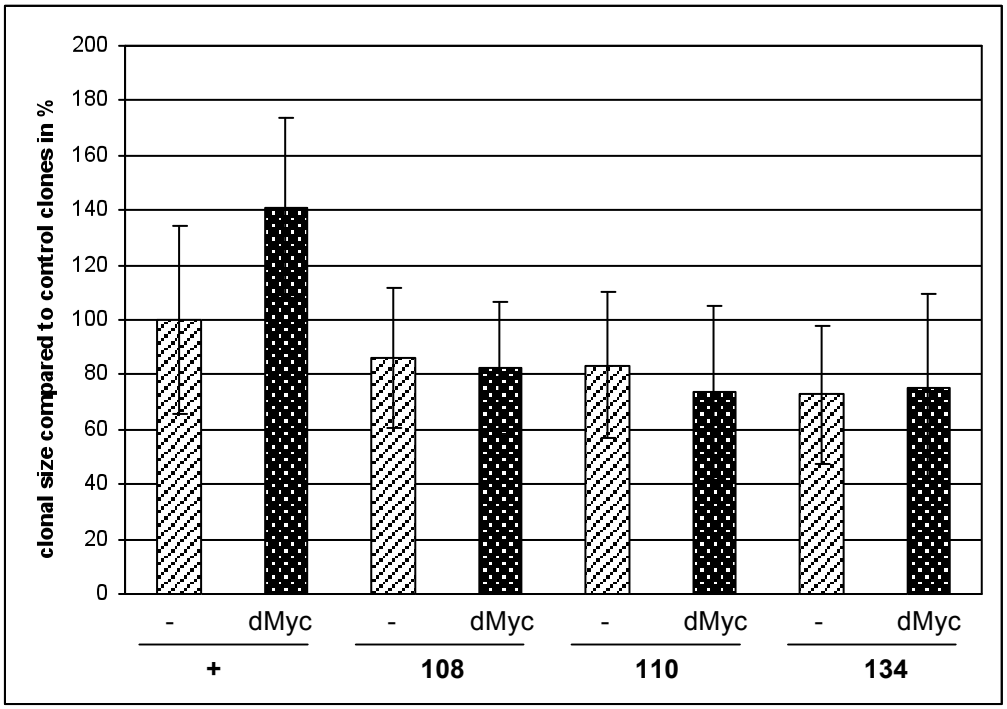

Figure 21: Size of clones overexpressing dMyc relative to control clones. Area of control clones (+) was set to 100%. Clonal size is increased upon overexpression of dMyc (2nd bar), however dMyc cannot induce growth anymore in a Chinmo mutant background (dark bars). Error bars indicate standard deviation. More than 20 clones per genotype were measured. The numbers under the x-axis indicate the *chinmo* alleles ("+" = wildtype).

Label:	Genotype of green fluorescent cells:
+	*y w* hs-FLP UAS-GFP; FRT-40/FRT-40; *tub*-GAL4/MKRS
+ dMyc	*y w* hs-FLP UAS-GFP; FRT-40/FRT-40; *tub*-GAL4/UAS-dMyc
108	*y w* hs-FLP UAS-GFP; FRT-40 *chinmo*^{108}/FRT-40 *chinmo*^{108}; *tub*-GAL4/+
108 dMyc	*y w* hs-FLP UAS-GFP; FRT-40 *chinmo*^{108}/FRT-40 *chinmo*^{108}; *tub*-GAL4/UAS-dMyc
110	*y w* hs-FLP UAS-GFP; FRT-40 *chinmo*^{110}/FRT-40 *chinmo*^{110}; *tub*-GAL4/+
110 dMyc	*y w* hs-FLP UAS-GFP; FRT-40 *chinmo*^{110}/FRT-40 *chinmo*^{110}; *tub*-GAL4/UAS-dMyc
134	*y w* hs-FLP UAS-GFP; FRT-40 *chinmo*^{134}/FRT-40 *chinmo*^{134}; *tub*-GAL4/+
134 dMyc	*y w* hs-FLP UAS-GFP; FRT-40 *chinmo*^{134}/FRT-40 *chinmo*^{134}; *tub*-GAL4/UAS-dMyc

3.2.7 Overexpression of Chinmo in a *dmyc* mutant background

As shown earlier, a mutation of both *dmyc* and *chinmo* in the eye led to the conclusion that both proteins cooperate to regulate growth in the eye. The MARCM clones (3.2.6) revealed that dMyc is dependent on Chinmo to induce growth in the wing imaginal discs. We were therefore interested, if the converse is also true, i.e. if Chinmo also (partially) depends on dMyc for the execution of its activities (be it growth or the induction of apoptosis). For this purpose, we used the "*tub*>dMyc>GAL4 *ey*-FLP" system to overexpress Chinmo only in the head, either in a wildtype (dm^{+}), a dm^{P0}, or a dm^{4} mutant background.

Flies with the genotype "*y w tub*>dMyc>GAL4 *ey*-FLP/Y; pUAS-Chinmo^{IV}/+" normally die at early pupal stages or even before. By reducing dMyc levels, not only the rate of metamorphosis was accelerated (the pupae were clearly differentiated and most of them died at late pupal stages), but also about $1/10^{th}$ of the expected number of flies eclosed (Figure 22). The overall survival was better in the dm^{P0} background as compared to the dm^{4} background (10% vs. 5%; $n \geq 4$). However, in either case the eclosed flies do not look very healthy, since they have only few ommatidia, a distorted head structure and dark spots on the eyes that are signs of cell death (Figure 22E). Note also that incubation of the flies at 18° instead of 25° did not increase the rate of survival, although GAL4 is known to be less active at the lower temperature, and hence less Chinmo is expected to be expressed at 18°.

These results are consistent with our previous observation that overexpression of Chinmo leads to apoptosis. In addition, they show that physiological levels of dMyc are required for whatever Chinmo does when it is overexpressed, since a reduction of dMyc levels is able to reduce Chinmo function.

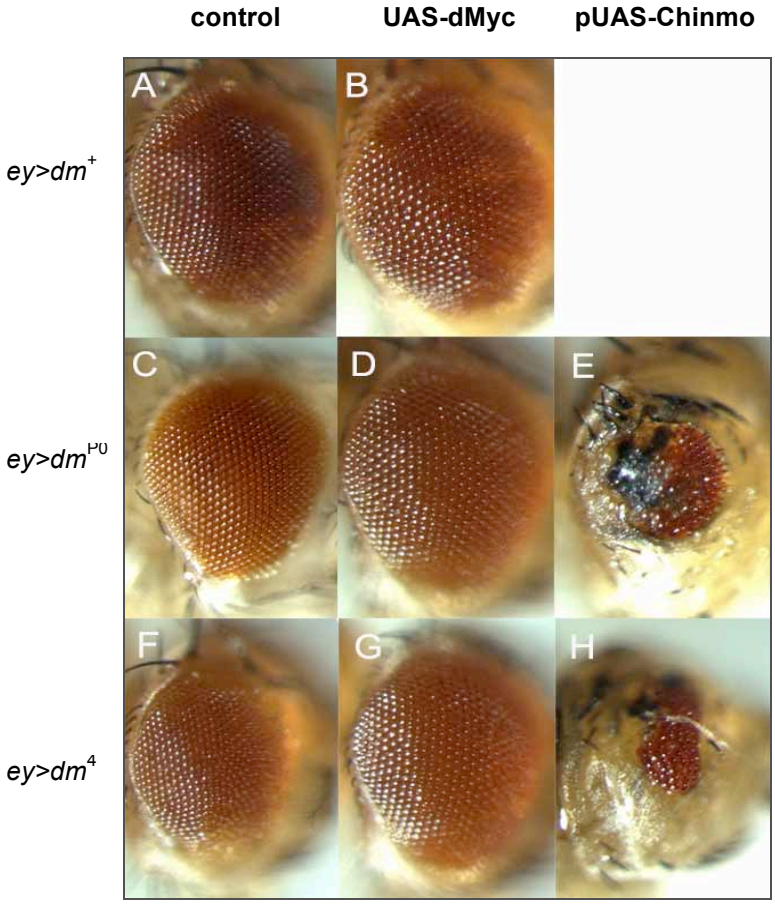

Figure 22: Reduction of dMyc levels allows Chinmo overexpressing flies to survive to adulthood. In a wildtype background no Chinmo overexpressing adult flies were obtained (top row, white rectangle). The middle column shows eye morphology upon overexpression of dMyc. Anterior is to the right. The experiment was performed in two independent biological replicates.

Label:	Genotype:
A	*y w tub*>dMyc>GAL4 *ey*-FLP; pUASTB/+
B	*y w tub*>dMyc>GAL4 *ey*-FLP; UAS-dMyc/+
C	*w* dm^{P0} *tub*>dMyc>GAL4 *ey*-FLP; pUASTB
D	*w* dm^{P0} *tub*>dMyc>GAL4 *ey*-FLP; UAS-dMyc/+
E	*w* dm^{P0} *tub*>dMyc>GAL4 *ey*-FLP; pUAS-$Chinmo^{IV}$/+
F	*w* dm^{4} *tub*>dMyc>GAL4 *ey*-FLP; pUASTB/+
G	*w* dm^{4} *tub*>dMyc>GAL4 *ey*-FLP; UAS-dMyc/+
H	*w* dm^{4} *tub*>dMyc>GAL4 *ey*-FLP; pUAS-$Chinmo^{IV}$/+

3.3 Molecular mechanism of Chinmo action - effect on dMyc levels

3.3.1 dMyc levels are not elevated upon Chinmo overexpression

In our previous experiments we showed that Chinmo and dMyc interact genetically. How this interaction takes place on a molecular basis concerned us in our next enquiries.

One possibility is that Chinmo overexpression elevates dMyc protein levels (e.g. by increasing dMyc stability) and all genetic interactions (*act* > clones, MARCM clones, pinheads) would be consistent with this. To test this possibility, we transfected S2 cells with UAS-dMyc alone or together with UAS-Chinmo and investigated if ectopic dMyc levels were increased upon co-expression with Chinmo. Cells were harvested after 48h and proteins were separated by SDS- PAGE and analysed on a Western blot (Figure 23). dMyc levels seemed to be enhanced upon overexpression of Chinmo, however also Tubulin levels (which served as a loading control) were elevated. To quantitate the dMyc and Chinmo protein amounts contained in the different samples, we repeated the assay but this time with fluorescent antibodies and the LI-COR Odyssey system. In contrast to chemiluminescence, fluorescent detection is static, since the fluorescence signal intensity is proportional to the amount of fluorophor, and this does not change with time (as long as the fluorophor is excited). Thus, proteins can be accurately quantified. The two proteins were detected with secondary antibodies that were conjugated with two different fluorescent dyes in order to discriminate between them (Figures 24 and 25). Two different measurements of the band intensity of two independent experiments- one exposed with the Licor system and one exposed with the chemiluminescence kit- revealed that dMyc levels in S2 lysates are equal if dMyc is overexpressed alone or in combination with Chinmo. Thus, Chinmo overexpression does not alter overexpressed dMyc levels in cell culture, suggesting that the genetic interactions described above are not due to a stabilisation of dMyc protein by Chinmo.

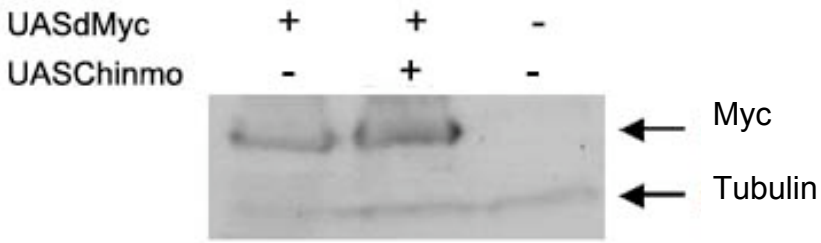

Figure 23: Western blot of S2 cells after overexpression of dMyc or dMyc and Chinmo together. dMyc levels are not elevated upon Chinmo overexpression. Tubulin is used as a control for protein levels. HRP-conjugated antibodies were used for visualization. Cell lysates were taken 48h after transfection. The experiment was performed in two independent biological replicates with the same outcome.

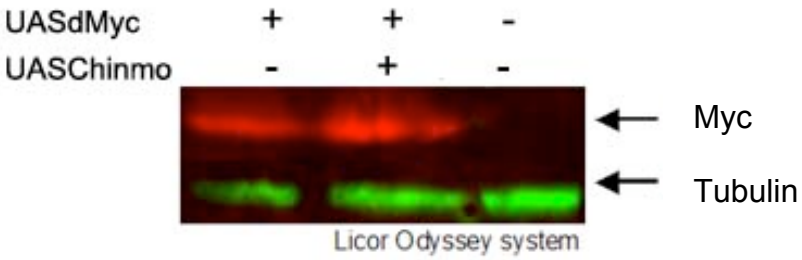

Figure 24: Western blot of S2 cells after overexpression of dMyc or dMyc and Chinmo together and analysis with the Licor Odyssey system. dMyc levels are not elevated upon Chinmo overexpression. Tubulin is used as a control for protein levels. Fluorescent antibodies were used for visualisation. Cell lysates were prepared 48h after transfection.

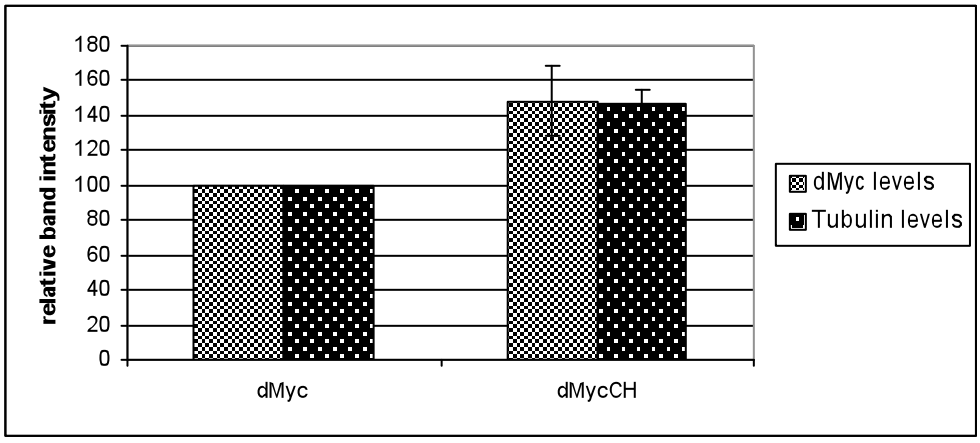

Figure 25: Protein levels in cells that overexpress dMyc either alone or in combination with Chinmo (CH). dMyc levels are increased upon Chinmo overexpression, however Tubulin levels are also increased. Therefore, the increase is not dMyc specific. Shown are averages of two independent measurements. Standard deviations indicate the error of the mean. 100% corresponds to the intensity observed in S2 cells overexpressing dMyc alone.

3.3.2 Endogenous dMyc levels are not elevated upon Chinmo overexpression

As a further experiment to address a possible effect of Chinmo on dMyc levels, we overexpressed Chinmo in S2 cells. Two parallel samples were treated with dsRNA against GFP or against *dmyc* (see Figure 26). dsRNA treatment against *dmyc* efficiently reduced endogenous dMyc levels as compared to the control sample treated with dsRNA against GFP. The blot shows that dMyc levels are unchanged in S2 cells overexpressing Chinmo, suggesting that Chinmo also does not affect endogenous dMyc amounts. We realise, however, that in such transient transfection experiments Chinmo is expressed only in a fraction of all cells (typically 20-50%), and that minor changes in dMyc protein levels that are limited to these transfected cells might go unnoticed in this experiment, where lysates of all cells (transfected and untransfected) are probed for the amount of dMyc. A definitive answer to the question whether Chinmo affects dMyc levels will require the use of cells stably expressing Chinmo. Such cells have been generated in the meantime (section 3.4.4), and the corresponding experiment will be carried out.

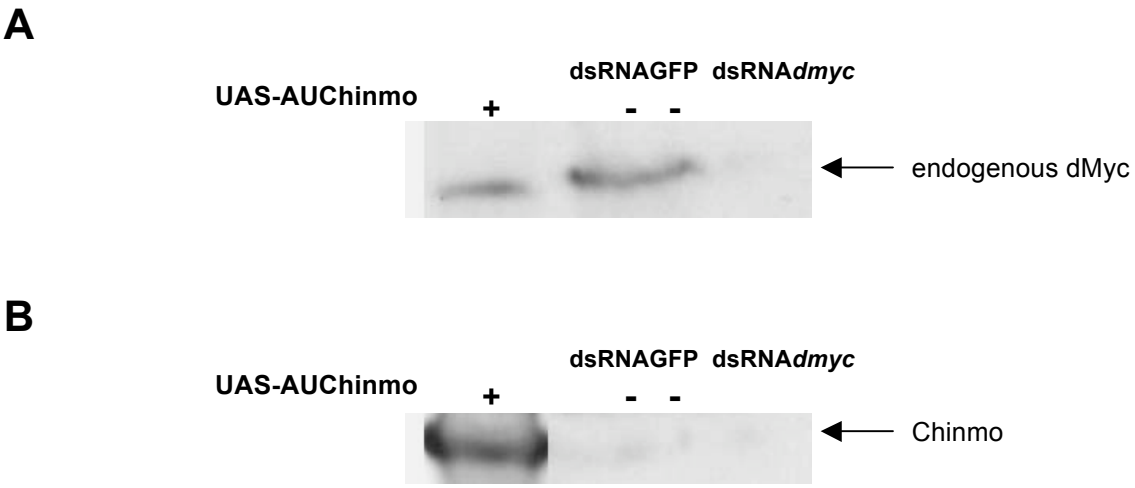

Figure 26: Western blot of S2 cell lysates. Endogenous dMyc levels are not increased upon overexpression of Chinmo. dMyc levels are greatly reduced after incubation with *dmyc* dsRNA for 48h (panel A). The *dmyc* dsRNA was directed against the 5`UTR of *dmyc*. The blot was stripped and re-probed with antibodies against the AU1-tag of Chinmo (panel B). The same experiment was performed twice with the same outcome.

3.4 Molecular mechanism of Chinmo action - effect on dMyc targets

3.4.1 Chinmo transactivates dMyc targets

Our previous experiments show that dMyc and Chinmo genetically interact, and they suggest that Chinmo does not affect dMyc levels. Nevertheless, Chinmo affects dMyc-dependent biological processes. Since these processes are thought to be caused by dMyc`s regulation of its target genes, Chinmo might be necessary for full transactivation of dMyc target genes. To address this possibility, we investigated the ability of Chinmo to transactivate dMyc dependent reporters. In a first experiment we analysed pure overexpression of Chinmo. We transfected *tubulin*-GAL4 and pUAS-Chinmo, either alone or in combination with UAS-dMyc, together with a dMyc-dependent luciferase reporter pair (see manuscript). Forty-eight hours after induction, the cells were lysed and relative reporter expression was analysed in a Wallac luminometer. Consistent with previous observations, dMyc overexpression increases the relative reporter ratio by about 2 fold as compared to control (UAS-dMyc without *tubulin*-GAL4; see Figure 27). Interestingly, Chinmo was able to transactivate the dMyc-dependent reporter on its own to the same extent as dMyc. When both transgenes were expressed at the same time, relative reporter activity was 45% higher as compared to cells expressing either Chinmo or dMyc alone.

This result raises the possibility that Chinmo acts as a co-activator of dMyc and it argues against the hypothesis that Chinmo might be the homologue of Miz-1, a dMyc co-repressor. However, Chinmo could still behave like Miz-1 in a different context (e.g. a different type of dMyc targets could behave differently than the targets represented by the luciferase reporter with respect to Chinmo activity, and furthermore Chinmo might have different properties upon high level overexpression than at endogenous levels).

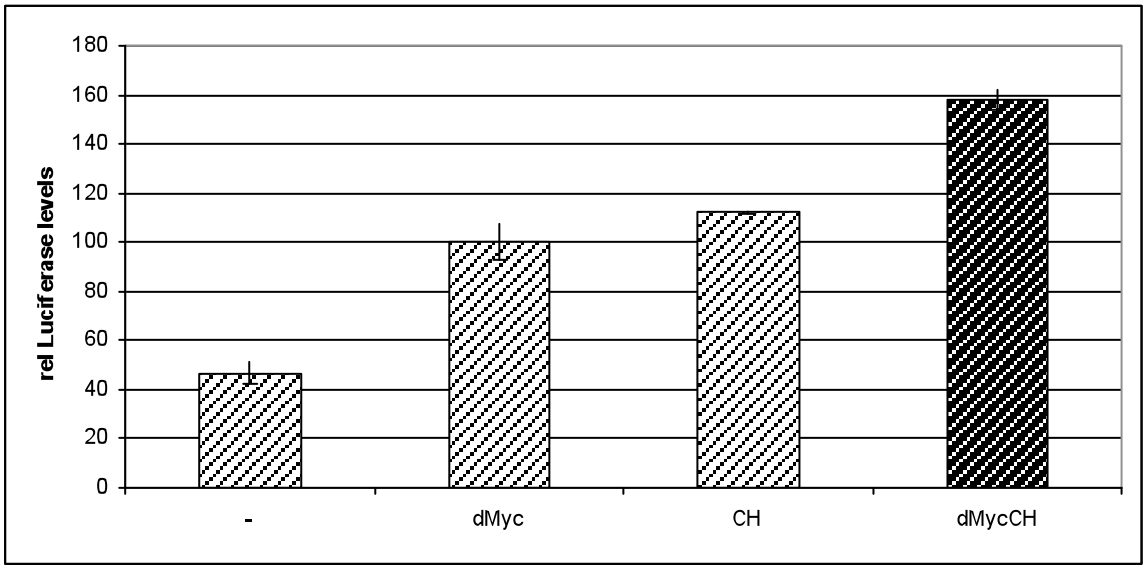

Figure 27: Activity of a *CG5033*-luciferase reporter upon overexpression of dMyc and/or Chinmo (CH). Chinmo is able to activate this dMyc reporter to the same extent as dMyc alone. Co-overexpression of dMyc elevates relative Luciferase levels even further. Cell lysates were taken 48h after transfection. Relative reporter activity after dMyc transfection was set to 100%. Error bars indicate standard deviation of two independent experiments.

3.4.2 Chinmo depends on dMyc to transactivate dMyc target genes

Chinmo activates a dMyc-dependent luciferase reporter to the same extent as dMyc. When dMyc and Chinmo are co-overexpressed, the transactivation potential is even elevated. In the following experiment we investigated whether the activation of a dMyc-reporter by Chinmo is dependent on the presence of dMyc. Chinmo, dMyc, *tub*-GAL4 and both reporter constructs, *Renilla* and firefly luciferase, were transfected in S2 cells in the presence or absence of dsRNA against *dmyc*. The dsRNA only degrades endogenous *dmyc* mRNA since it targets the 5`UTR of *dmyc*. Forty-eight hours after transfection of the S2 cells, Luciferase levels were measured in the cell lysates. Again, dMyc and Chinmo were able to transactivate the dMyc reporter and co-overexpression of both resulted in an enhanced transactivation potential (see Figure 28). Downregulation of endogenous *dmyc* levels reduced relative reporter activity in the sample overexpressing dMyc by 26%. When endogenous *dmyc* levels were downregulated in cells overexpressing Chinmo, the transactivation potential of Chinmo was clearly reduced. This was also the case when endogenous *dmyc* was depleted in cells overexpressing dMyc and Chinmo together. However, in both cases overexpressed Chinmo elevated relative reporter activity as compared to control samples even upon depletion of *dmyc* (Figure 28, compare sample "dsRNA*dmyc*" with "CH + dsRNA*dmyc*", and "dMycCH" with "dMycCH + dsRNA*dmyc*"). Thus, Chinmo is dependent on endogenous *dmyc* for efficient activation of a dMyc-dependent reporter, but partially activates this reporter even in the absence of *dmyc*. It still needs to be determined, though, whether this hypothetical dMyc-independent activation of the reporter is mediated by low levels of dMyc that might persist upon dsRNA against *dmyc*.

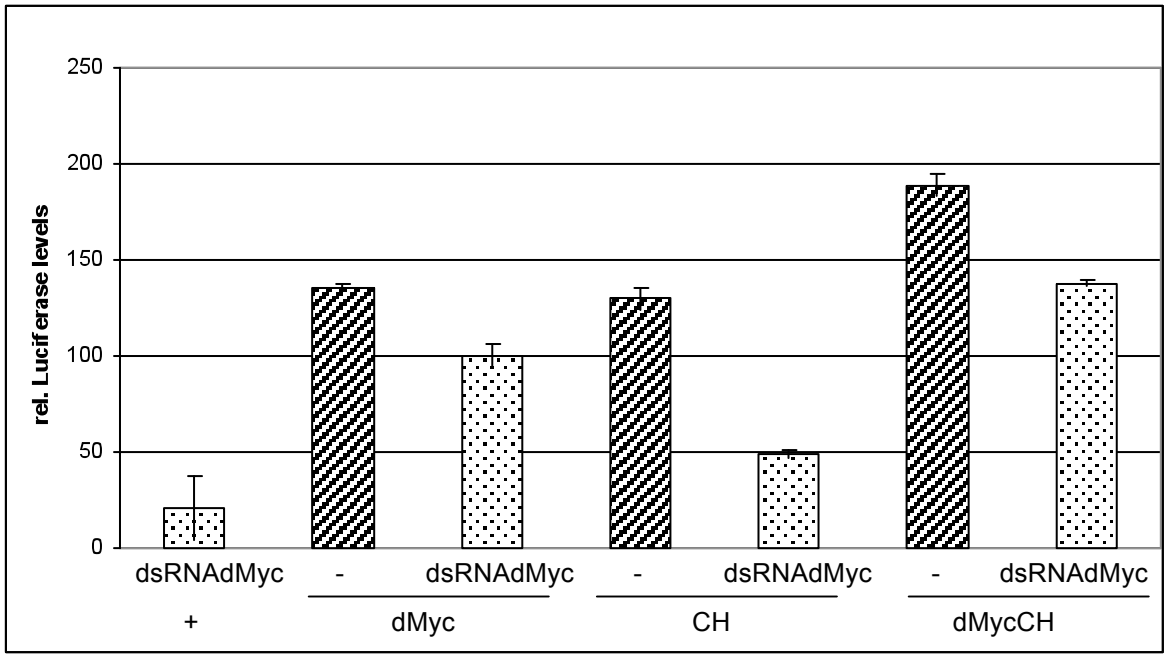

Figure 28: Transactivation of the *CG5033*-based dMyc-dependent reporter in the presence or absence of *dmyc* dsRNA. Chinmo only weakly transactivates the reporter when dMyc levels are reduced. Error bars indicate standard deviation of two independent experiments. Reporter activity was set to 100% for the sample expressing ectopic dMyc together with dsRNA against endogenous *dmyc*. Cell lysates were taken 48h after transfection. CH stands for pUAS-Chinmo, dMyc for UAS-dMycWT. dsRNA targets the 5`UTR of *dmyc* and only depletes endogenous *dmyc* mRNA, ectopically expressed dMyc is unaffected.

3.4.3 dMyc is not dependent on Chinmo for full transcriptional activation

Chinmo is dependent on the cooperation with dMyc to fully activate dMyc target genes in cell culture. We were interested if dMyc requires Chinmo for full transcriptional activation of dMyc target genes in S2 cells, as it was the case for induction of cell growth in clones in wing imaginal discs (MARCM clones). For this purpose, we synthesised dsRNA against *chinmo*. To test whether the dsRNA is functional, S2 cells were transfected with UAS-Chinmo, *tub*-GAL4 and dsRNA against *chinmo* and analysed at different time points thereafter (see Figure 29). Ninety-six hours after transfection, Chinmo levels were strongly reduced and undetectable on a Western blot, suggesting that all ectopically expressed Chinmo protein has decayed by that time. However, it might be argued that this observation could also be explained if overexpression of Chinmo causes apoptosis (as suggested by our earlier experiments with Chinmo overexpression in the fly) such that all cells expressing Chinmo have died by 96 hours after the transfection, and the only cells remaining in those wells are those that haven`t taken up any DNA. However, such a scenario is unlikely, since Chinmo overexpression can stimulate relative luciferase activity after 48h (when Chinmo protein is clearly present, Figure 28) and to comparable levels at 96h after transfection (see below, Figure 31, 42), arguing that undiminished quantities of Chinmo protein persist in cell populations even after 4 days – and hence that within 96h *chinmo* dsRNA eliminates all ectopically expressed Chinmo (and, by inference, endogenous Chinmo as well).

Thus, we repeated the Luciferase assays in the presence of *chinmo* dsRNA and analysed luciferase activity at 96h after transfection. In a first experiment we transfected cells with a control plasmid, pUASTB, alone or in combination with dsRNA against *chinmo* or dMyc. Figure 30 shows the resulting luciferase ratios. The expression of the reporter was decreased by 2.5 fold in the presence of dsRNA against *dmyc*, but dsRNA against *chinmo* had no effect.

In a second experiment, we overexpressed Chinmo and dMyc alone or together, in the presence or absence of dsRNA against *chinmo*. This experiment was performed in order to make sure that the knockdown of Chinmo reduces the effects of Chinmo overexpression on dMyc target genes. The dsRNA was at least partially functional, since it reduced the reporter activity of the samples expressing Chinmo (compare samples “dMycCH” with “dMycCH + dsRNA*ch*”, and “CH” with “CH + dsRNA*ch*”), although in both cases some residual Chinmo-dependent activity remained (compare samples “dMycCH + dsRNA*ch*” with “dMyc”, and “dsRNA*ch*” [which has only background reporter activity – see Figure 30] with “CH + dsRNA*ch*”). However, no effect of *chinmo* dsRNA on dMyc transactivation potential could be observed (compare samples “dMyc” and “dMyc + dsRNA*ch*”).

This suggests that Chinmo is not necessary for dMyc to transactivate its target genes in S2 cells. It further raises the possibility that Chinmo is not expressed in S2 cells. Indeed, according to the FLIGHT database (which contains microarray expression profiles of different cell lines) Chinmo was not detected in such experiments in Schneider S2, KC, S2R+ or S2C cells.

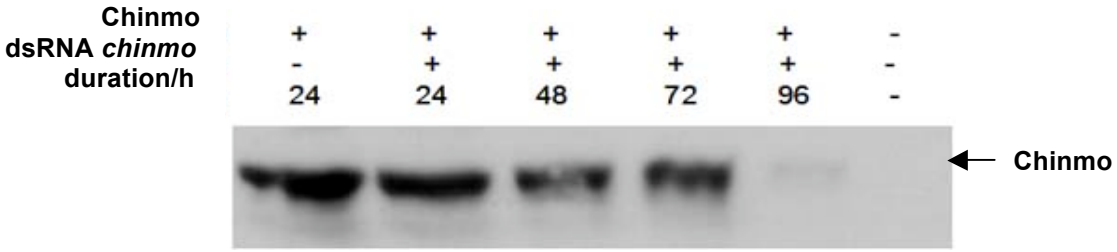

Figure 29: Reduction of transiently expressed Chinmo with co-transfected dsRNA in S2 cells. Cell lysates were taken at the indicated timepoints and directly used for Western blotting. Chinmo levels are strongly reduced after 96h. To detect Chinmo a primary antibody against the AU-tag of UAS-AU-Chinmo was used.

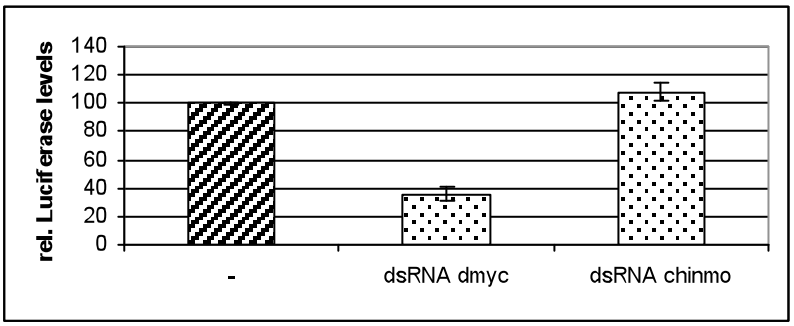

Figure 30: Transactivation of a dMyc-dependent reporter in the presence or absence of *chinmo* or *dmyc* dsRNA. Reduction of Chinmo levels does not reduce transcriptional activation of a dMyc-dependent reporter. Error bars indicate standard deviation for two independent experiments. Luciferase levels were analysed 96h after transfection. Control cells "-" were set to 100%. dsRNA targets the 5`UTR of *dmyc* and only depletes endogenous dMyc, ectopically expressed dMyc is unaffected.

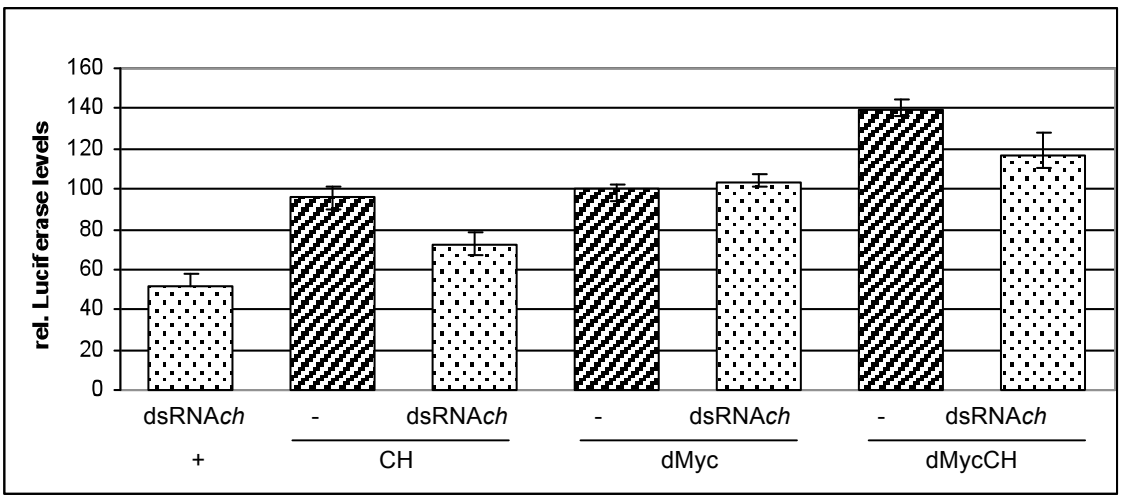

Figure 31: Transactivation of dMyc target genes in the presence or absence of *chinmo* dsRNA (dsRNA*ch*) upon overexpression of Chinmo and/or dMyc. Reduction of Chinmo levels does not influence transcriptional activation of target genes by dMyc. Lysates were taken 96h after transfection. Error bars indicate standard deviation from two independent experiments. Relative reporter activity was set to 100% for the sample containing overexpressed dMyc.

3.4.4 A cell line that stably expresses Chinmo

Our earlier experiments with transient transfection of Chinmo in S2 cells suffered from the drawback that only a limited (and unknown) fraction of all cells expressed the transfected Chinmo. To allow inducible expression of Chinmo in all cells of a pool, a *chinmo* cDNA was cloned under the control of a metallothioneine promoter, and transfected together with another plasmid containing a blasticidin resistance gene (pCoBlast) in S2 cells, that were then grown in selection medium containing blasticidin and thus, only cells that had taken up the plasmid survived.

After establishment of the cell line, the cells were tested with different copper sulphate concentrations and at different time points for induction of Chinmo expression. As depicted in Figure 32, the highest expression of Chinmo was obtained at 24 hours after the addition of $CuSO_4$ to 1 mM. For all further experiments these conditions were used.

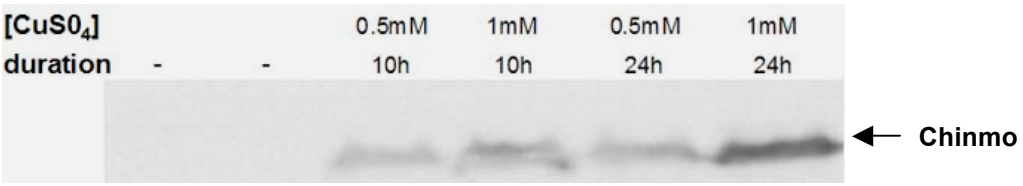

Figure 32: Western blot of S2-MT-Chinmo cell lysates after induction with copper sulphate. Highest induction was obtained at 24 hours with a concentration of 1mM $CuSO_4$ per ml medium. The "-" sample corresponds to non-transfected cells that were collected at time 0. Each lane corresponds to half a well of a six well plate (2.5 Mio. cells). To detect AU1-Chinmo rabbit anti-AU1 antibodies were used.

3.4.5. Chinmo can activate endogenous dMyc targets

Luciferase assays demonstrated that Chinmo can transactivate a dMyc-dependent reporter upon overexpression in S2 cells. Thus, we were interested if Chinmo is able to activate selected endogenous targets of dMyc upon overexpression. Five million S2 or S2-MT-Chinmo cells were treated with 1 mM $CuSO_4$ or remained untreated. Twenty-four hours after induction cells were lysed in TRIZOL and total RNA was extracted. After verification of the quality of the RNA on a bioanalyzer, cDNA was generated and the expression of selected genes was analysed by qRT-PCR.

A set of direct dMyc target genes had been identified earlier by microarray analysis in our lab (Hulf et al., 2005). A specific subset of those genes contained a dMyc binding site, the so-called E-box, downstream of their transcription start sites. Three of these genes *CG5033*, *nnp1*, and *fibrillarin* (all three transcribed by RNA polymerase II) were included in our selection. Another RNA Pol II-transcribed gene, *CG12295*, containing an upstream E-box, was also tested. *CG12295* is involved in synaptic vesicle fusion to presynaptic membranes and in cation transport (Ly and Verstreken, 2006). Also tested was *snoRNA*^{46}, a small RNA-coding gene situated within an intron of a Pol II-transcribed protein-coding gene. Small nucleolar RNAs (snoRNAs) are a class of small RNA molecules that guide chemical modifications (methylation or pseudouridylation) of ribosomal RNAs (rRNAs) and other RNA genes (tRNAs and other small nuclear RNAs (snRNAs)).

In addition, *snoRNA U3* and *tRNA*^{Leu}, genes transcribed by RNA Polymerase III, were included in our investigations, since it had been shown, that dMyc also controls the transcription of RNA Polymerase III dependent small RNA genes (Gomez-Roman et al., 2003; Steiger et al., 2008). Two biologically independent replicates were analysed per cell type and induction. Their levels were normalized to the reference genes *actin5C, Rab6* and *Sec24* and plotted against those from uninduced S2 cells (Figure 33).

The induction of Chinmo was quite efficient, since mRNA levels were 17-fold higher in induced than in uninduced S2-MT-Chinmo cells (blue bar, second row), whereas the baseline levels are equally low in uninduced S2 and S2-MT-Chinmo cells.

However, *dmyc* expression was not increased upon Chinmo overexpression, which is consistent with our previous observation that Chinmo overexpression does not affect dMyc protein levels (3.3.1). In contrast, 3 out of 4 E-box containing genes were strongly upregulated upon overexpression of Chinmo, namely *nnp1* (1.5 fold), *CG12295* (>2fold) and *fibrillarin* (2 fold).

The small RNA gene *snoRNA*^{46} was not significantly affected by overexpression of Chinmo ($p>0.05$). Thus, Chinmo is indeed able to positively regulate endogenous dMyc target genes. Four out of 5 genes, which were upregulated upon Chinmo overexpression, are involved in the processing of rRNA. Whether this activation requires dMyc remains to be tested.

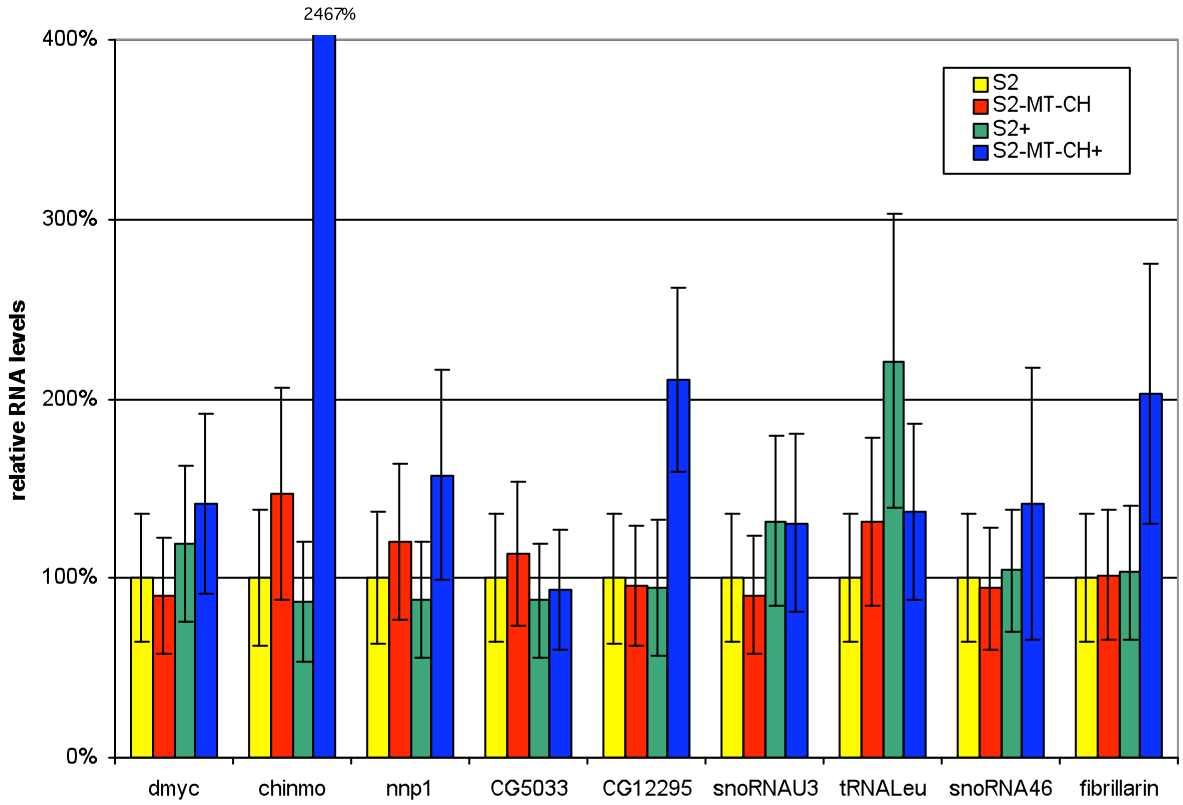

Figure 33: mRNA levels upon induction of *chinmo* relative to uninduced S2 cells. Transcript levels of different dMyc target genes as determined by qRT-PCR (normalised to the reference genes *actin5C, Sec24* and *Rab6*) are shown for S2-MT-Chinmo cells with Chinmo induction (S2-MT-CH+), without induction (S2-MT-CH), and S2 cells with (S2+) or without induction (S2). Transcript levels in uninduced S2 cells were set to 100%. Elevated Chinmo levels do not influence *dmyc* RNA levels, but affect 3 E-box containing target genes of dMyc, *nnp1*, *CG12295* and *fibrillarin. CG5033,* another E-box containing gene, the small RNA gene $snoRNA^{46}$, and two other RNA genes, $tRNA^{Leu}$ and *snoRNA U3* are not affected. Error bars indicate standard deviation from two independent biological replicates.

3.5. Molecular mechanism of Chinmo action - interaction of dMyc & Chinmo

3.5.1 Chinmo and dMyc interact physically

The data presented so far argue for a possible role for Chinmo as a co-activator of dMyc. These findings prompted us to explore if dMyc and Chinmo interact physically. A physical interaction with dMyc has for example been shown before for Pontin, the dMyc co-factor that prompted us to set up the screen in which Chinmo was found (Bellosta et al., 2005).

To assay a direct interaction, S2 cells were transfected with HA-dMyc alone or in combination with AU1-Chinmo. Forty-eight hours after transfection, cell lysates were prepared for co-immunoprecipitation. The resulting IP in the upper panel of Figure 34 shows that Chinmo interacts physically with dMyc. dMyc is only immunoprecipitated when Chinmo was present in the sample. The lysates in the lower panel show that dMyc was expressed in both samples. This observation presents evidence that Chinmo can form a complex with dMyc and is consistent with the notion that Chinmo functions as co-activator of dMyc.

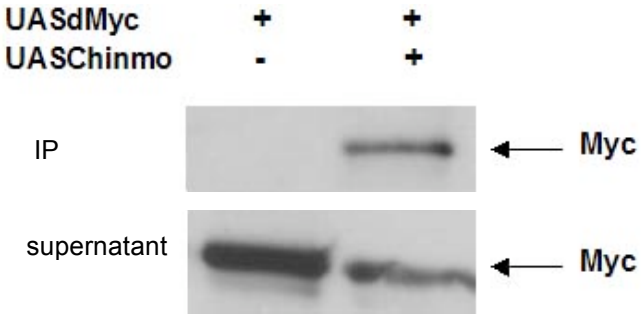

Figure 34: Western blot of co-immunoprecipitated cell lysates. dMyc was transfected into S2 cells alone or in combination with Chinmo, 48h after transfection the Chinmo-associated proteins were isolated by anti-AU1 IP and analysed by Western blot with anti-HA antibodies. The upper panel shows the IP, the lower panel the "supernatant" of cell lysates after incubation with antibodies and beads. Similar results were obtained in different independent experiments.

3.5.2 Mapping of the binding site for Chinmo in dMyc

Co-immunoprecipitations between Chinmo and dMyc showed that both proteins interact physically. To locate the precise binding site for Chinmo in the dMyc protein, we performed co-IP experiments between Chinmo and different dMyc mutants (details on the different constructs are described in the manuscript in Materials & Methods). In a first round we tested interactions between Chinmo and the dMyc mutants consisting of the N-terminus or containing deletions of the N-terminus, Myc Box 2, Myc Box 1+2 (ΔN-terminus) or of the N- and C-termini. The upper panel in Figure 35 depicts the resulting co-immunoprecipitations. That indeed all dMyc mutants are expressed is shown in the lower panel of Figure 35, where the supernatants of the co-IPs were loaded. All mutants were still able to bind Chinmo. For the N-terminus alone no conclusion can be drawn since it migrates at the same position as the light chain of the IgGs.

Since all of the mutants still bound Chinmo, we repeated the co-IP with additional dMyc mutants (see Materials + Methods for details), who contain bigger deletions, in order to narrow down the region for the binding site. The results of the co-IPs between Chinmo and the tested dMyc mutants are graphically illustrated in Figure 36. Interaction with Chinmo was reduced when the first 403 aa of the dMyc protein were missing and completely abolished with dMyc fragments lacking the first 523 aa or 626 aa. These observations indicate that the binding site for Chinmo in dMyc lies between amino acid 1-403.

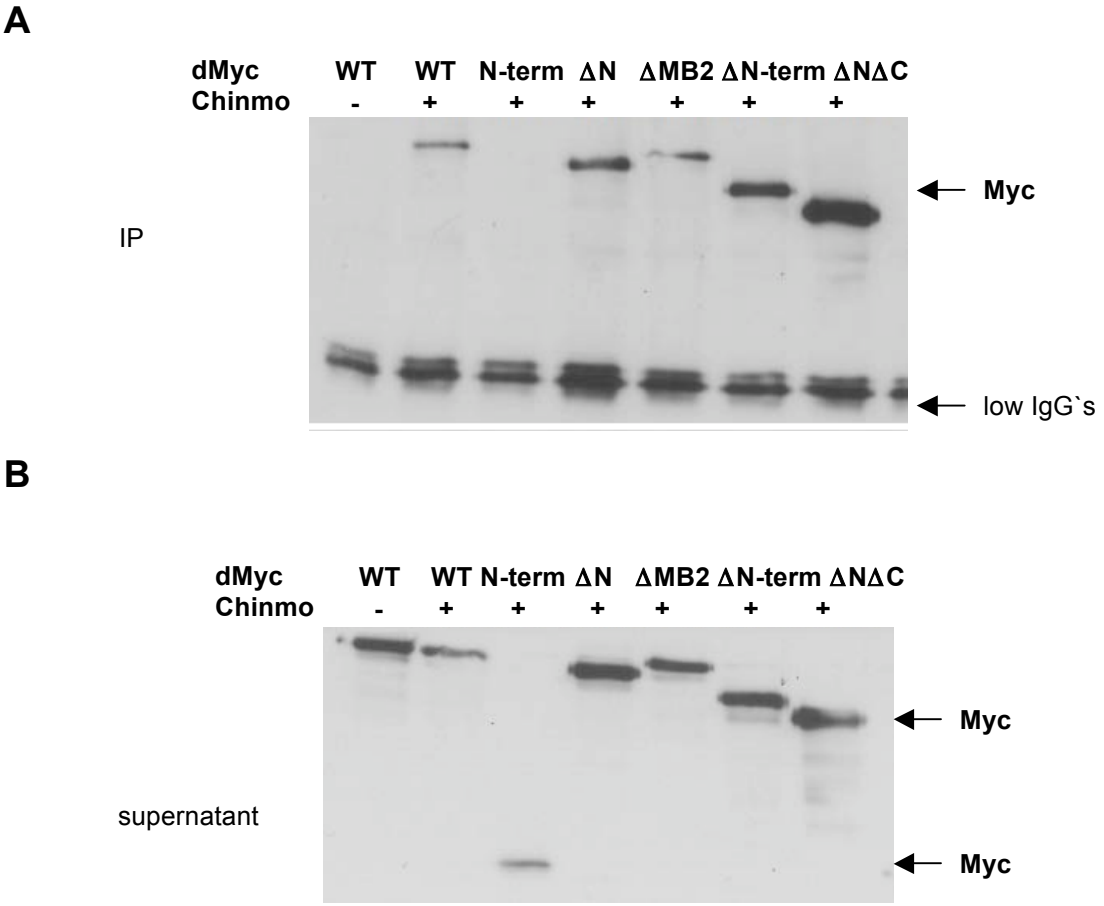

Figure 35: Western blot of anti-HA co-immunoprecipitates. Chinmo was transfected into S2 cells in combination with the indicated dMyc mutants, 48h after transfection the Chinmo-associated proteins were isolated by anti-AU1 IP and analysed by Western blot with anti-HA antibodies. The upper panel shows the IP, the lower panel the supernatant (after binding of the lysates to antibodies and beads). All tested dMyc mutants still bind Chinmo.

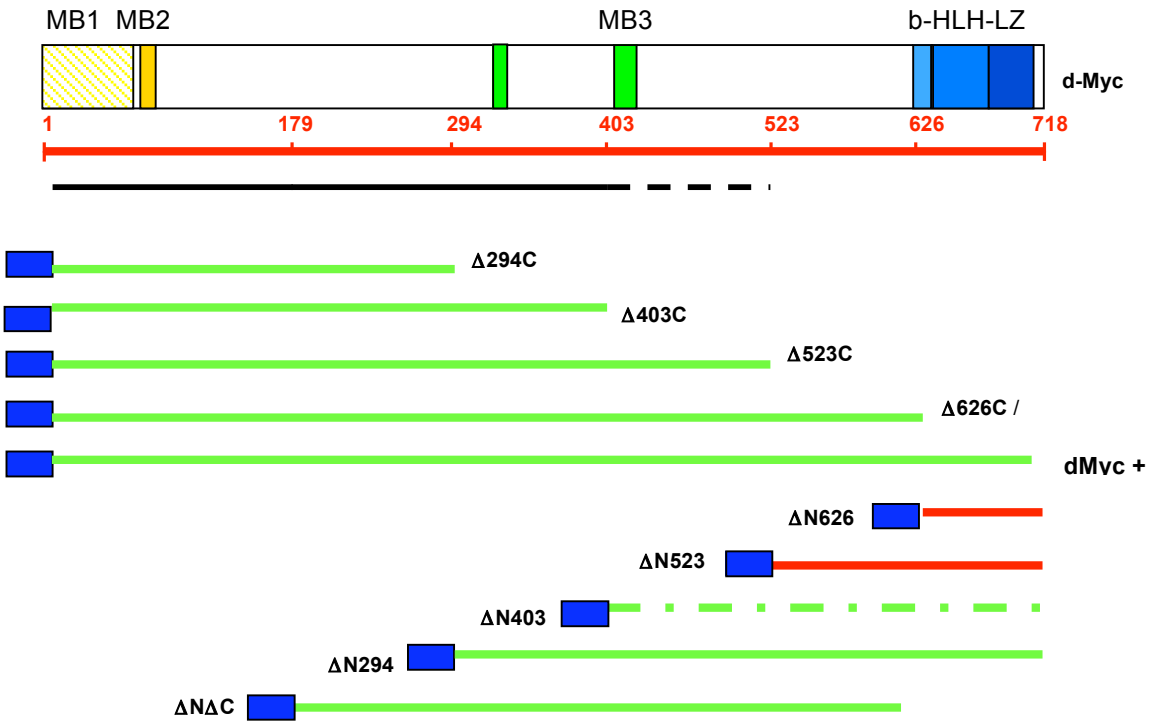

Figure 36: Schematic diagram of small dMyc mutants tested in co-immunoprecipitations for interaction with Chinmo. The binding site for Chinmo was located to aa 1-403 of the dMyc protein. The green lines indicate dMyc mutants that interacted with Chinmo, red lines stand for dMyc mutations that did not interact with Chinmo. Dashed lines indicated a weak interaction between Chinmo and the respective dMyc mutant. Numbers correspond to the first (Nxxx) or last (xxxC) amino acid present in the indicated mutant. The black line reflects the putative binding site for Chinmo in dMyc. The blue box reflects the N-terminal HA epitope tag.

3.5.3 Chinmo mutants

Chinmo binds to a centrally located region of the dMyc protein. Our next goal was to determine the interaction site for dMyc in Chinmo. There are two recognizable domains within the Chinmo protein: A BTB/POZ domain in the N-terminal part and 2 C_2H_2 zinc fingers located at the very C-terminus (for a precise description of the domains see 3.1.3). The BTB/POZ domain is located at aa 32-128 (according to Prosite), other predictions prospect aa 22-128 (Pfam), the two zinc fingers are located at aa 517-540 and 545-573. We established 2 different Chinmo mutants by deletion mutagenesis. ChinmoΔBTB lacks amino acids 32-128 and carries an amino acid substitution of two amino acids (Thr^{32} + Arg^{33}) instead, and ChinmoΔZnf lacks amino acid 517-604 (shown in Figure 37). Both constructs were cloned into pUASTB, as was the wildtype Chinmo plasmid.

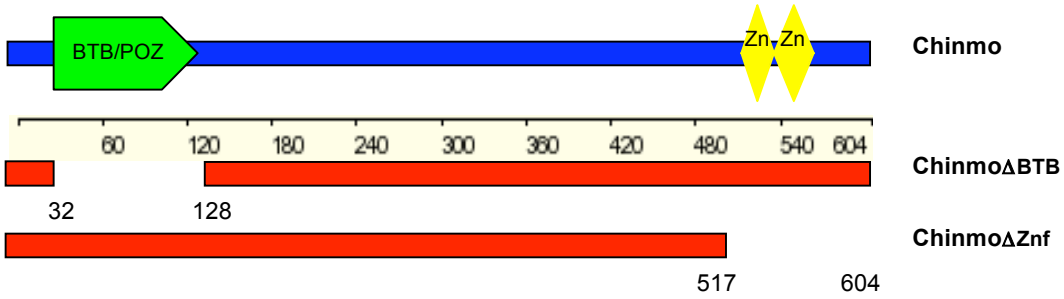

Figure 37: Schematic diagram of the established Chinmo mutants. ChinmoΔBTB lacks the BTB/POZ domain and ChinmoΔZnf lacks the complete C-terminus including the two C_2H_2 zinc fingers. Numbers indicate coordinates of the corresponding deletions. Coordinates indicate the first and last deleted amino acid.

3.5.4 A ChinmoΔBTB mutant is not able to transactivate dMyc target genes

Overexpression of Chinmo transactivates target genes to the same extent as dMyc and this effect can be further increased when dMyc is co-overexpressed. However, Chinmo`s ability to transactivate dMyc target genes is largely dependent on *dmyc*. For this reason and because of the finding that Chinmo interacts physically with dMyc, we propose that Chinmo acts a dMyc co-activator. To investigate if the two Chinmo mutants described above were still able to transactivate dMyc target genes, we performed a Luciferase assay. S2 cells were transfected with two luciferase reporter constructs and plasmids coding for wildtype or mutant Chinmo, alone or in combination with dMyc. Cell lysates were prepared 48h after transfection and relative Luciferase levels were measured.

As described before, Chinmo was able to transactivate dMyc target genes and this activation was enhanced by the presence of dMyc (see Figure 38, first 4 bars). A deletion of the BTB/POZ domain completely abolished Chinmo`s transactivation ability, suggesting that this domain is necessary for transcriptional activation by Chinmo. In contrast, a deletion of the zinc fingers even enhanced Chinmo`s transactivation ability, however co-overexpression with dMyc did not enhance this activation further.

To investigate if the transactivation potential of ChinmoΔZnf is dependent on dMyc, we repeated the Luciferase assay, but this time used dsRNA against endogenous *dmyc* to deplete *dmyc*. The second experiment confirmed the results of the first experiment that the deletion of the BTB domain abolishes and the deletion of the Zn fingers enhances Chinmo`s transactivation potential (see Figure 39). Not surprisingly, a reduction of endogenous *dmyc* levels strongly reduced this activity. Thus, also the massive boost caused by overexpression of a ChinmoΔZnf mutant is largely dependent on dMyc.

Altogether these data demonstrate that the BTB/POZ domain is necessary for Chinmo to transactivate dMyc target genes. Moreover, these data show that a deletion of the zinc fingers in Chinmo enhances Chinmo`s transactivation potential.

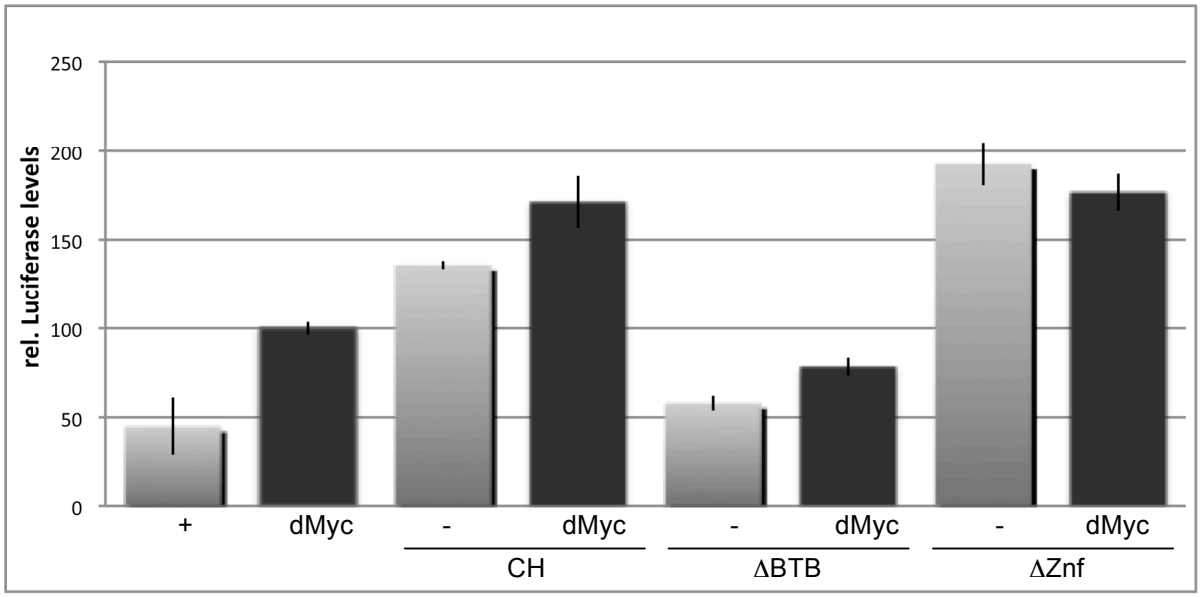

Figure 38: Relative Luciferase levels after overexpression of Chinmo (wildtype or mutants), either alone or together with dMyc. A deletion of the BTB/POZ domain completely abolished transactivation, whereas a deletion of the zinc fingers increases the signal even more. Lysates were taken 48h after transfection. Error bars indicate standard deviation from two independent experiments. Relative reporter level of the sample containing overexpressed dMyc was set to 100%.

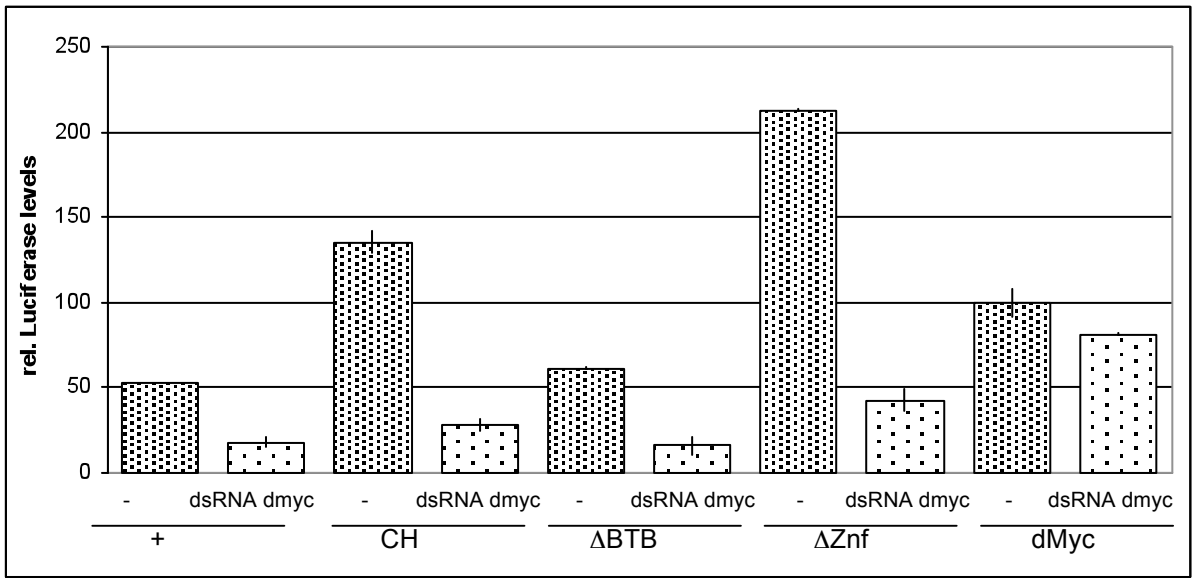

Figure 39: Relative Luciferase levels after overexpression of Chinmo variants or overexpression of Chinmo variants upon downregulation of *dmyc*. The ability of Chinmo variants to transactivate dMyc target genes is largely dependent on the presence of dMyc, since reduction of endogenous *dmyc* levels strongly reduces Chinmo`s transactivation ability. Lysates were taken 48h after transfection. Error bars indicate standard deviation from two independent experiments. Relative reporter activity for the sample overexpressing dMyc was set to 100%.

3.5.5. dMyc binds Chinmo most probably via the BTB/POZ domain

Encouraged by the previous results, we performed co-immunoprecipitations in order to test if binding to dMyc is affected in the Chinmo mutants. S2 cells were transfected with wildtype Chinmo or Chinmo mutants. Eight-eight hours after transfection cell lysates were prepared, immunoprecipitated and Western blotted (Figure 40). As shown earlier, wildtype Chinmo and dMyc physically interact with each other. Moreover, a deletion of the zinc fingers did not affect this binding (Figure 40A). However, no conclusion can be drawn yet for the interaction between dMyc and ChinmoΔBTB, since ChinmoΔBTB was only weakly expressed. dMyc was expressed in all samples, as shown in the central panel where the supernatants were analysed. Additionally, we investigated the expression levels of Chinmo (Figure 40B, where the blot was stripped and re-probed with anti-AU1 antibodies). This blot also suggests that a deletion in the BTB/POZ domain decreases Chinmo stability.

This experiment raises the possibility that binding to dMyc is required for transactivation by Chinmo, and that a deletion of the BTB domain might abolish both. However, it is equally possible that the lower abundance of ChinmoΔBTB accounts for its reduced transactivation potential, and that binding to dMyc is not required for this transactivation. To distinguish between these possibilities, conditions need to be found under which comparable levels of wildtype Chinmo, ChinmoΔBTB and ChinmoΔZnf can be expressed in S2 cells and assayed for their interaction with dMyc and their effect on a dMyc-dependent reporter.

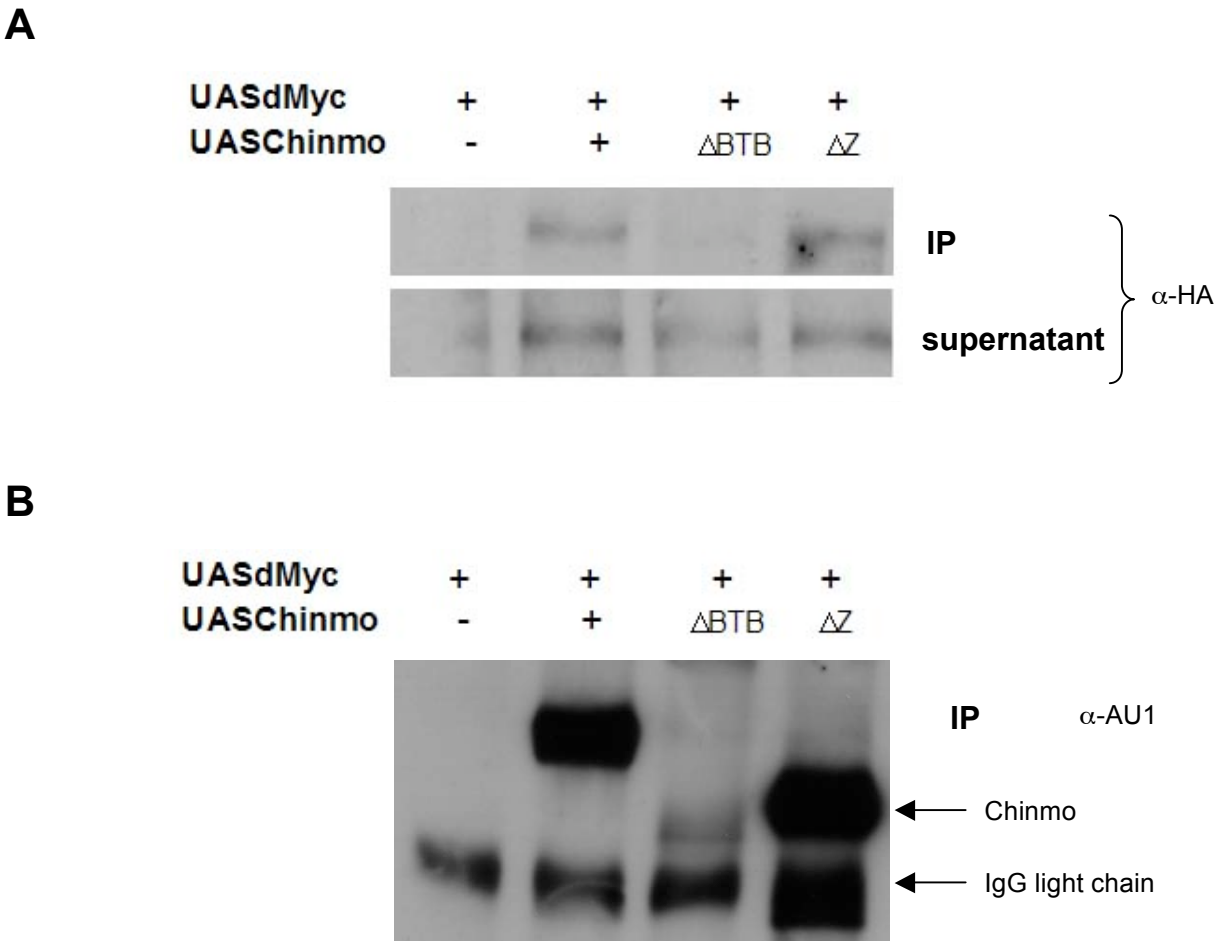

Figure 40: Western blot of co-IPs between dMyc and Chinmo variants. A deletion of the BTB/POZ domain abolishes co-IP with dMyc whereas a deletion of the zinc fingers has no effect on the interaction between Chinmo and dMyc. Moreover, Chinmo stability seems to be affected by these mutations. S2 cells were transfected with UAS-Myc in combination with a control plasmid (pUASTB), pUAS-Chinmo, pUAS-ChinmoΔBTB or pUAS-ChinmoΔZnf. Cell lysates were prepared 48h after transfection; Chinmo-complexes were immunoprecipitated with anti-AU1 antibodies and Western blotted with anti-HA antibodies (A). After exposition the blot was stripped and re-probed with anti-AU1 antibodies to detect Chinmo (B). The lower band in panel B shows the IgG light chain. ΔBTB indicates pUAS-ChinmoΔBTB and ΔZ indicates pUAS-ChinmoΔZnf.

3.6 Mechanism: The next layer

3.6.1 Interaction with *guftagu*

Most cellular processes require a tightly controlled coordination between synthesis and degradation of proteins. Ubiquitin ligases (E3) are multiprotein complexes that specifically recognize their substrates and mediate their ubiquitin-dependent degradation. Two classes of E3 ligases have been characterized: HECT-type and RING-H2-type E3s (reviewed in Glickman and Ciechanover, 2002). There are two major types of RING-H2 E3 ligases: the APC/C (anaphase-promoting complex/cyclosome) and the SCF complex (Skp1, Cullin, F-box) (reviewed in Deshaies, 1999). Recent work has revealed that the SCF complex is the prototype of an emerging family of Cullin-based ligases including the well-defined ECS complex (ElonginC–Cul2–SOCS) and the Cul3-based ligases (Geyer et al., 2003; Xu et al., 2003).

Cullin-based E3 ligases target substrates for ubiquitin-dependent degradation by the 26S proteasome. The structural homology between BTB proteins and Skp1 or ElonginC led to the hypothesis that BTB proteins might also directly interact with Cullins (Schulman et al., 2000). The functional relevance of a Cul3–BTB protein complex was demonstrated in *C. elegans*. In this system, a complex containing CUL-3 and the BTB protein MEL-26 is required for the ubiquitin-dependent degradation of the microtubule-severing protein MEI-1 in early embryos. Degradation of MEI-1 by the CUL-3/MEL-26 complex after meiosis is essential for the assembly of the mitotic spindle (Kurz et al., 2002; Pintard et al., 2003). There are two regions in MEL-26 required for interaction with CUL-3 ([M243, I245, D247]; [D281, Y283, L285]). Direct alignment with Chinmo did not show any homologies to this region, however, when the ortholog of MEL-26 was used (CG12537/Rdx/CG9924, according to Wormbase) 3 conserved regions were found, all located in between the BTB/POZ domain of Chinmo. Moreover, the transcription factor PLZF (promyelocytic leukaemia zinc-finger protein) interacts with CUL-3 in a two-hybrid assay, suggesting that a CUL3-based complex may indeed regulate transcription by controlling the stability of PLZF (Furukawa et al., 2003).

Because of these precedents, we were interested to determine if Chinmo might act as a component of a CUL3 complex to influence transcriptional regulation by dMyc.

In *Drosophila*, there is only one homolog of CUL3, called Guftagu. The *guftagu (gft)* gene consists of 5984 base pairs and codes for a protein of 773 amino acids. There are 3 different transcripts which all give rise to the same protein. Guftagu not only affects ubiquitin-dependent protein catabolic processes but also the induction of apoptosis and the regulation of cell cycle. For our experiments, different *gft* mutants and a *gft* RNAi line were tested for interaction with dMyc, in order to investigate if *dmyc* interacts in a similar way with *gft*/Cul3 as observed for Chinmo. We tested interaction of the hypomorphic allele *ey>dm*^{P0} and of "GM" (*y w*; *GMR*-GAL4 UAS-dMyc^{132}/+; UAS-dMyc^{13} UAS-dMyc^{42}/+) (both of which show an eye-specific phenotype) with different *gft* mutants. As controls, we crossed *ey>dm*$^{+}$ and *GMR*-GAL4 to the *gft* mutants. The *gft* mutants were the following: *gft*^{06430} (a P-element insertion in the first intron of *gft*, 228 bp from exon 2), *gft*^{2} (a 5bp deletion, resulting in a frame shift at amino acid 747 and a premature stop codon at amino acid 748), *gft*^{EY11031} (a P-element insertion outside the coding region in the C-terminus), and a UAS-*gft*-dsRNA transgene.

gft^{2} and *gft*^{06430} showed no effect in any of the crosses. However, *gft*^{EY11031} and the RNAi line affected "GM" eyes (see Figure 41D, H). Overexpression of *gft* RNAi in the eye by *GMR*-GAL4 did not change eye morphology (data not shown). The RNAi line additionally affected the eye phenotype of *ey>dm*^{P0} flies, but control flies were also affected (Figure 41A, B). Thus, reduction of Gft levels does not behave in the same way as a reduction in Chinmo levels, since *chinmo* alleles showed a clear defect with *ey>dm*^{P0} and not in control flies, moreover they did not affect "GM".

In a second assay, overexpression of Gft/CUL3 was tested with different ubiquitously expressed GAL4 drivers. Overexpression with the strong drivers *act5C*- and *tub*-GAL4 lead to lethality early in development (during embryogenesis); overexpression with *arm*-GAL4 allowed flies to complete development, but 50% of the female offspring had strong wing defects with blisters and disrupted wings. These phenotypes are comparable to the Chinmo overexpression phenotypes: blisters and disrupted wings were also observed upon overexpression of Chinmo with *ap*-GAL4 (GAL80^{ts} system; 3.2.5).

Taken together, no strong conclusions can be drawn from these experiments. As Gft is the only CUL3 in *Drosophila*, it would be expected to complex with several BTB/POZ proteins in addition to Chinmo, and hence the downregulation of *gft* should lead to broader defects than the loss of *chinmo*. On the other hand, the relative abundance (as well as the strength of the different mutant alleles) might be different for Gft and Chinmo, and therefore the mutant phenotypes could very well differ in different experimental situations. Finally, the

overexpression of either Gft or Chinmo lead to quite “non-specific” defects that were difficult to attribute to specific defects. Thus, our observations do not rule out or in the involvement of Gft in dMyc-dependent biological processes *in vivo*.

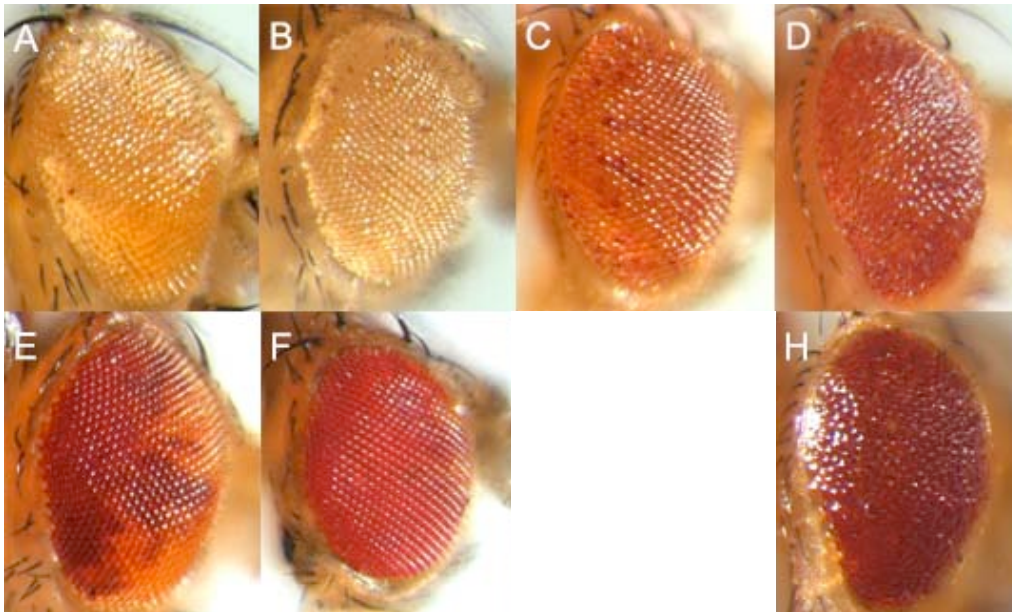

Figure 41: Reduction of *gft* levels in the eye does not affect *ey>dm*^{P0} eyes. However, strong overexpression of dMyc in a *gft* mutant background leads to a clear eye defect with big and rough ommatidia. Anterior is to the right.

Label:	Genotype:
A	*y w tub*>dMyc>GAL4 *ey*-FLP/Y; *gft*RNAi/+
B	*w dm*^{P0} *tub*>dMyc>GAL4 *ey*-FLP/Y; *gft*RNAi/+
C	*y w*/Y; (*GMR*-GAL4 UAS-dMyc^{132}; UAS-dMyc^{13} UAS-dMyc^{42})/(SM5^TM6B)
D	*y w*/Y; *GMR*-GAL4 UAS-dMyc^{132}/ *gft*RNAi; UAS-dMyc^{13} UAS-dMyc^{42}/+
E	*y w tub*>dMyc>GAL4 *ey*-FLP/Y; gft^{EY11031}/+
F	*w dm*^{P0} *tub*>dMyc>GAL4 *ey*-FLP/Y; gft^{EY11031}/+
H	*y w*/Y; *GMR*-GAL4 UAS-dMyc^{132}/gft^{EY11031}; UAS-dMyc^{13} UAS-dMyc^{42}/+

3.6.2 A dMyc dependent luciferase is not affected by *gft* RNAi

An RNAi screen to find new dMyc co-factors was previously performed in our lab. A selection of about 800 transcription-associated genes was analysed in this screen, including *guftagu* (M.Furrer, pers. communication). However, *gft* RNAi did not affect a dMyc-dependent reporter. If Chinmo and Gft work in the same complex, RNAi against *guftagu* might negatively affect the ability of overexpressed Chinmo to transactivate dMyc target genes. To address this possibility, S2 cells were transfected with UAS-dMyc or UAS-Chinmo in the presence or absence of *gft* RNAi. Cells were incubated for 96h, to give gft maximal time to decay; however, at present we have not confirmed that this RNAi against *gft* is effective and that the protein has been eliminated under these conditions. Ninety-six hours after transfection cell lysates were taken and analysed for their relative Luciferase levels (Figure 42). *Gft* dsRNA did not meaningfully reduce relative Luciferase levels in the absence of co-expressed proteins, (compare "–" to *gft* RNAi). Relative Luciferase levels upon overexpression of dMyc were not affected by a reduction of Gft levels, however *gft* RNAi reduced relative Luciferase levels after overexpression of Chinmo by 24%. This is comparable to the effect of *chinmo* dsRNA on relative Luciferase levels after overexpression of Chinmo. Thus, *gft* RNAi reduces Chinmo's ability to transcriptionally activate the reporter construct, but no effect was observed for overexpression of dMyc. Thus, Chinmo and Guftagu might act in the same complex to transactivate dMyc target genes.

However, we have recently obtained a UAS-CUL3 construct and thus we will be able to test the efficiency of *gft* RNAi. Moreover, we need to detect the ectopically expressed Gft by antibodies against *Drosophila* Gft. Furthermore, we can test the effect of overexpression of Gft/CUL3 in a Luciferase assay in the presence or absence of *dmyc* mRNA.

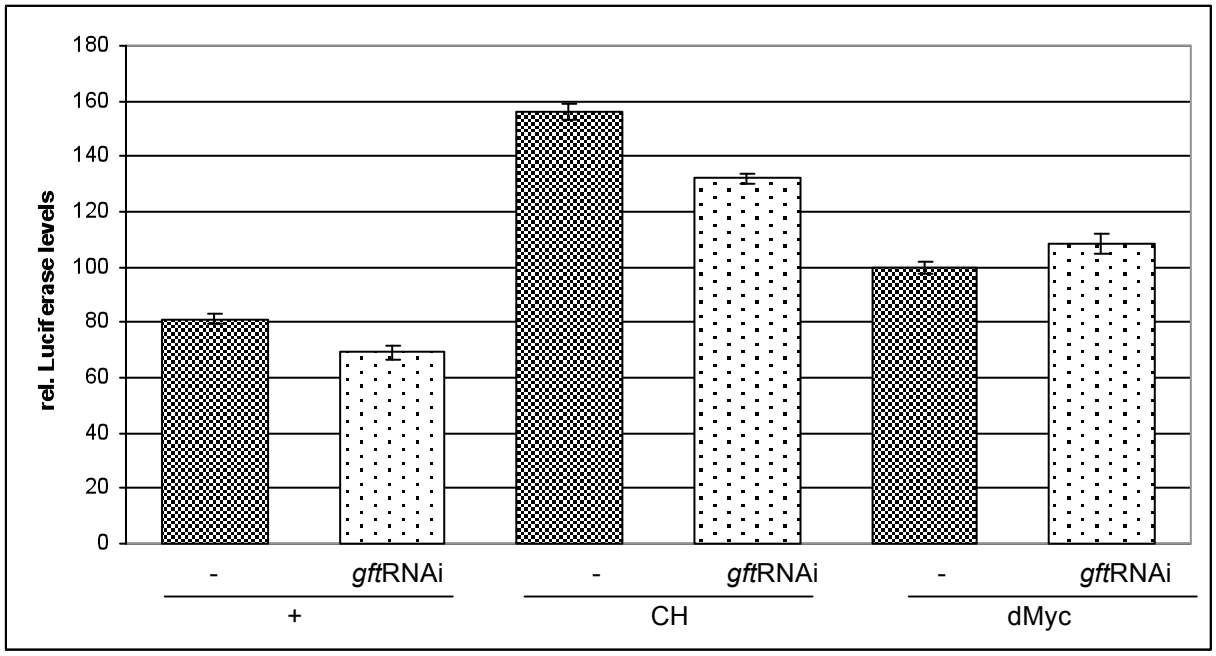

Figure 42: Relative Luciferase levels after overexpression of dMyc and Chinmo in the presence or absence of *gft*RNAi. Reduction of Gft levels does not affect transactivation by dMyc but slightly reduces transactivation by Chinmo. Lysates were taken 96h after transfection. Error bars indicate standard deviation from two independent experiments. The relative reporter activity in the sample overexpressing dMyc was set to 100%.

Discussion

In the first part of our investigations we examined the role of the different conserved domains of dMyc *in vivo* and could show that there is a strong requirement for all biological activities for the dMyc N-terminus, whereas the evolutionarily conserved MB2 domain is not absolutely essential *in vivo*. However, not only the *cis*-acting determinants of dMyc that we have described in the first chapter were of interest to this study. Also the *trans*-acting determinants influencing dMyc`s action were investigated to get a better understanding of Myc`s oncogenic properties. Thus, our further investigations were directed towards the proteins (protein complexes) that control dMyc`s biological activities. A screen to find new dMyc co-factors was performed and lead to the identification of *chinmo* and *Delta*, two novel genes that interacted genetically with *dmyc* and that were further investigated. In the first part of the discussion the genetic interaction between *Delta* and *dmyc* will be discussed. In the second part we present evidence that dMyc is dependent on Chinmo to fulfil at least some functions *in vivo* and that dMyc is an important partner of Chinmo. Genetic interaction studies followed by molecular analysis suggest a role for Chinmo as a direct dMyc co-activator.

Identification and characterization of Delta

Delta was found in the deficiency screen as a gene deleted among others in Df(3R)ED5942, a deficiency that showed a strong interaction with *ey>dm*^{P0}. In addition, this deficiency led to a weight reduction in a *dm*^{P0} background. The region of interest was narrowed down to 8 genes and one of them was *Delta* (*Dl*). A mutation in *Delta* led to comparable phenotypes as the Df(3R)ED5942, indicating that *Dl* was the gene responsible for the phenotype seen in "*ey>dm*^{P0}/Y; Df(3R)ED5942/+" animals. We show clear evidence that several *dmyc* mutants are affected by a reduction of *Dl* levels. Delta is a ligand of the Notch receptor. The Notch signalling pathway is mainly involved in cell-cell communications that control multiple cell differentiation processes during embryonic and larval life.

We set out to study the interaction between other components of the Notch signalling pathway and Myc to get a better understanding of the interaction between Delta and dMyc, but none of the tested factors affected dMyc function (Su(H), H, N, *sim*, *gro*, L). These results suggest either that Delta is the most limiting factor for the genetic interaction with *dmyc*, and that more severe mutant situations need to be tested for the other Notch-pathway components in order to reveal their interaction with *dmyc*, or that Dl functions outside of the Notch-

pathway; however, so far such functions have not been described. That Delta is involved in the regulation of growth and proliferation independently of Notch is supported by the findings that flies heterozygous for *Delta* and *Minutes* are very sick, whereas flies heterozygous for *Notch* and *Minutes* are not affected (A.C.Nagel, pers. communication).

Recent publications demonstrated that there is a connection between human c-Myc and Notch1. It was shown that Notch1 regulates similar biological processes as c-Myc, for example angiogenesis, and both of them are disregulated in cancers (reviewed in Bolos et al., 2007; Zhao et al., 2003). Moreover, *c-myc* was identified as a direct transcriptional target gene of the Notch1 pathway in T cell acute lymphoblastic leukaemia (T-ALL) (Sharma et al., 2007). Inhibition of Notch1 resulted in cell cycle arrest and apoptosis and decreased *c-myc* levels. Studies in human T-ALL cell lines also demonstrated that a direct Notch1-mediated activation of *c-myc* is required to maintain leukemic growth (Weng et al., 2006). However, the molecular mechanism behind this action still needs to be investigated.

Given this connection in vertebrates, we can speculate that Notch might also control the expression of *dmyc* in flies. Alternatively, dMyc might act upstream of the Notch signalling pathway by affecting Delta, thus activating Notch signalling. Third, both dMyc and Dl might act in parallel and redundant pathways to activate Notch, thus affecting eye growth, or they might converge on some target genes.

Based on the vertebrate data, the most appealing hypothesis is the first that suggests that Notch signalling controls dMyc activity. Thus, Notch might control *dmyc* mRNA levels (e.g. by controlling the transcription of the *dmyc* gene) or dMyc protein levels (e.g. by controlling dMyc protein stability). To address if Notch affects *dmyc* mRNA levels, RNA in situ hybridisations (or qRT-PCRs) in a Notch mutant background could be performed.

Hence, further investigations are necessary to determine the interaction between Delta (Notch) and dMyc. To understand this interaction might be a small step to get a better understanding of normal development or the molecular basis of tumours like acute lymphoblastic leukaemia or breast cancer (Efstratiadis et al., 2007).

Genetic identification and characterization of Chinmo

Genetic and molecular interaction between *chinmo* and *dmyc*

Chinmo, a BTB/POZ domain protein was found in four different genetic loss of function screens (for details on the screen see the results section).

Most of the genetic studies between Chinmo and dMyc were based on the three alleles we obtained from the *ey*-FLP ("pinhead") screen that was performed in the laboratory of E.Hafen. In a hypomorphic *dmyc* background heterozygosity for those *chinmo* alleles resulted in rough and dented eye phenotypes, which clearly indicates that dMyc and Chinmo interact genetically.

Our data also show that the overall eye size is further diminished when dMyc levels are reduced in heads that are predominantly homozygous mutant for *chinmo* ("pinheads"). Conversely, the *chinmo* mutants reduced the size of *dmyc* null mutant eyes leading to strongly distorted heads and the flies were not able to hatch anymore. This suggests that dMyc and Chinmo work in two parallel pathways to control growth and proliferation. Hence, Chinmo and dMyc control cell proliferation and cell growth independently. However, we cannot exclude that the two proteins function together to control some downstream effects in addition to the "Chinmo" and "Myc" pathway.

Eye size is determined by the combination of ommatidial number and ommatidial size. The *chinmo* alleles caused a small head due to a reduction in ommatidial number and did not affect rhabdomere size (Sulzer, 2003, diploma thesis). Therefore, two mechanisms of Chinmo action were considered. Chinmo could act as an inhibitor of apoptosis, thus leading to a cell number reduction in a *chinmo* mutant background. The second hypothesis suggests that Chinmo might promote cell cycle progression, allowing the cells to reach normal size, with a reduced cell number.

Our observations seem to argue against the hypothesis that Chinmo inhibits apoptosis. First, overexpression of Chinmo in the dorsal compartment of the wing disc induced apoptosis, and cell death was even more enhanced by co-overexpression of dMyc. If Chinmo inhibited apoptosis, we would not expect any apoptotic cells after overexpression of Chinmo. Second, overexpression of Chinmo, using different Chinmo transgenes with ubiquitously expressed GAL4-drivers, killed the flies mostly early in development. This death might also be linked to apoptosis, but we cannot rule out that those animals die for some other reason. Finally, overexpression of Chinmo kills wildtype flies (expressing endogenous *dmyc*) whereas the same Chinmo overexpression in a *dmyc*-mutant background allows some flies to survive. The

surviving flies had distinct black spots of apoptotic cells, which are indicative of cell death. Taken together, these observations show that elevated Chinmo levels lead to cell death. While it is possible that a reduction in Chinmo levels (as obtained in *chinmo* mutant tissues) has the same effect, and that *chinmo* mutant tissues contain fewer cells as a consequence of increased apoptosis, we favour the alternative explanation, that such *chinmo* mutant tissues suffer from impaired cell proliferation. Thus, Chinmo might promote cell cycle progression together with dMyc and induce apoptosis independently of dMyc. This combination was also seen by some positive regulators of proliferation, which do promote S-phase entry but also induce apoptosis when overexpressed (e.g. dMyc, E2F) (Asano et al., 1996).

One could think of different possibilities how Chinmo behaves when overexpressed. First, overexpression of Chinmo might enhance its normal function (e.g. regulation of growth, control of asymmetric cell division). Second, Chinmo might have a dominant-negative effect. Third, Chinmo overexpression might lead to neomorph effects, thus overexpression of Chinmo might overcome its normal function leading to a completely novel function (like apoptosis), e.g. if the additional amount of Chinmo protein might reach places where it is normally not found. The second hypothesis does most probably not apply since there is no dominant-negative effect of Chinmo overexpression, as it does not interfere with endogenous Chinmo (by comparison of *chinmo* mutant heads and heads that overexpress Chinmo). The first hypothesis might apply partially since overexpression of Chinmo does not seem to enhance eye size (by comparison of the very few animals that survived upon overexpression of Chinmo in a *dmyc* mutant background compared to *dmyc* mutant flies alone) or clonal size (since clonal size is reduced when Chinmo is overexpressed). In contrast, overexpression of Chinmo transactivates dMyc target genes to the same extent as dMyc alone and even enhances transactivation when co-overexpressed with dMyc. Moreover, Chinmo activates endogenous target genes involved in ribosomal biogenesis. Indeed, 3 out of 4 genes involved in ribosomal biogenesis were upregulated upon Chinmo overexpression indicating that Chinmo overexpression might enhance ribosomal biosynthesis and thus cell growth. However, the most likely hypothesis is the third one, since overexpression of Chinmo leads to organismal death. Interestingly, the defects of Chinmo overexpression are partially suppressed in a *dmyc* mutant background, which suggests that dMyc is limiting for Chinmo function. A reduction in dMyc levels might attenuate the strong effects caused by overexpression of Chinmo since some flies who normally die during early pupal stages reached adulthood when dMyc levels were reduced. In summary, Chinmo overexpression does not enhance its normal biological functions but its molecular functions and Chinmo

adopts novel functions when overexpressed, leading to neomorph phenotypes. This hypothesis does not allow us to draw any conclusion about Chinmo`s normal biological activities, however our data would present some ideas on the novel molecular activities that Chinmo adopts when overexpressed, namely the induction of apoptosis.

As mentioned above, overexpression of Chinmo activated transcription of dMyc target genes and a dMyc-dependent reporter, and the latter effect requires endogenous *dmyc* mRNA. On the other hand, depletion of *chinmo* in S2 cells had no effect on transactivation by dMyc. Further investigations suggested that Chinmo is not expressed in S2 cells. Hence, dMyc is not dependent on Chinmo to transactivate its target genes in S2 cells, although Chinmo might be required in other tissues, and ectopically expressed Chinmo might help to transactivate dMyc target genes also in S2 cells. Whether the activation of endogenous target genes by dMyc also requires Chinmo was not analysed but will be done in the future. This will be investigated in a tissue, where both Chinmo and dMyc are expressed. Since we have not succeeded to visualize Chinmo expression in the fly and thus we don`t know where Chinmo is active, we will take eye imaginal discs for that purpose. This tissue is appropriate for our experiments because we could show that Chinmo and dMyc are required for growth and development in the eye and their genetic interaction further suggests that the putative "Chinmo-dMyc" complex is active there. Thus, cDNAs derived from *chinmo* mutant heads with or without overexpression of dMyc will be analysed by qRT-PCR to have a look if dMyc is still able to activate certain target genes (e.g. genes involved in ribosomal biogenesis that were shown to be activated by Chinmo) in the absence of *chinmo*. One could imagine that Chinmo might be required only for certain target genes of dMyc (or in distinct tissues), but overexpression of Chinmo might nevertheless have a positive effect also on other targets. However, so far there is no evidence that overexpression of Chinmo stimulates growth since clones overexpressing Chinmo were not bigger than control clones.

Since Chinmo activates the transcription of dMyc target genes, we wanted to know by which molecular mechanism this occurs. One possibility was that Chinmo stabilizes dMyc and thus increases dMyc protein levels, however this was not the case. Our data support a different model of interaction- that Chinmo interacts physically with dMyc. To determine the binding site of Chinmo in dMyc, co-IP experiments with different dMyc mutants were carried out, which together indicate that the binding site lies in the central region of dMyc. The binding site for dMyc in Chinmo is most probably the BTB/POZ domain since a deletion of this region abolished dMyc binding, but ChinmoΔBTB was also weakly expressed. However, the

observation that BTB/POZ domains function as protein-protein binding domains supports our observations (Perez-Torrado et al., 2006).

There are two possibilities, how BTB-proteins might function: as transcription factors or as E3-ligases. One could think that a BTB-transcription factor recruits an E3-ligase to DNA thus influencing the transcription of target genes. BTB/POZ domains were for example shown to play a role in ubiquitin-dependent degradation by binding to Cullin-based E3 ligases (CUL-3) (Schulman et al., 2000). Therefore we were interested to find out if Chinmo mediates E3 ligase dependent ubiquitination and thus destabilizes and degrades proteins like histones or RNA Pol II in a complex with dMyc or dMyc itself. The only CUL-3 homologue known in *Drosophila* is *guftagu* and this gene was therefore tested for genetic interaction with *dmyc*. Different Gft mutants and a *gft* RNAi line did not show a significant effect on eye morphology in a *dmyc* mutant background or upon overexpression of dMyc. Moreover, depletion of *gft* did not affect the activation of a dMyc-dependent reporter by dMyc but it reduced the activation of Chinmo comparable to dsRNA against Chinmo. This would suggest, that Chinmo and Gft might act in the same complex to transactivate dMyc target genes. However, we need to demonstrate first if the RNAi against *gft* was indeed functional by detecting Gft levels before and after reduction by RNAi on a Western blot. Whether overexpression of CUL-3 affects transactivation of dMyc target genes will be investigated in future experiments.

The observation that a deletion of the BTB/POZ domain inhibited transactivation suggests that the BTB/POZ domain is necessary for transactivation of dMyc targets. We could also show that the enhanced activation of transcription by ChinmoΔZnf is fully dependent on the presence of dMyc because depletion of *dmyc* abolished this activation. The zinc finger might be necessary to induce growth and proliferation since all *ey*-FLP-screen alleles lack this domain or have a mutation in it, and these alleles impair the ability of overexpressed Myc to induce growth and proliferation. A model for the interaction between Chinmo and dMyc is depicted in Figure I.

The role of Chinmo and dMyc in neuronal development

In the LOF screen, from which Chinmo received its name, Chinmo was found to control temporal identity in neuronal progenitors (Zhu et al., 2006). It was shown that overexpression of Chinmo throughout the neuroblast lineage of the mushroom body in the *Drosophila* brain transformed late born neurons into early born neurons. This raised the question, whether dMyc plays a specific role in neuronal development and if this role is dependent on Chinmo.
Drosophila neuroblasts divide into a bigger apical daughter cell that retains neuroblast characteristics and a smaller basal ganglion mother cell (GMC) that divides once more into neurons and glial cells. In 2006, dMyc was demonstrated to influence this neuronal development. It was shown that dMyc is expressed in larval neuroblasts but not in the differentiating daughter cell. The growth inhibitor Brat posttranscriptionally inhibits dMyc in this cell. However, in clones mutant for *brat* dMyc is overexpressed in all cells, thus both daughter cells start to grow and behave like neuroblasts, which leads to neuronal proliferation and the formation of larval brain tumours (Betschinger et al., 2006). Moreover, dMyc was shown to promote neurogenesis in the embryonic PNS and the CNS (and possibly the larval PNS) (Orian et al., 2007). Thus, Myc is expressed in the nervous system in flies, where it is required for precursor cell proliferation and possibly cell fate determination of neuroblasts. This raises the possibility that dMyc and Chinmo might work together to regulate neuronal differentiation e.g. by defining specific neuron types. It will be interesting to determine whether this is the case. Corresponding experiments will be carried out, e.g. we will test *dmyc* mutants in the same set-up that was used for the characterization of Chinmo, to see whether dMyc is required in the same process as Chinmo. Moreover, we will investigate if overexpression of dMyc can transform late born neurons into early born neurons as it was shown for Chinmo overexpression.

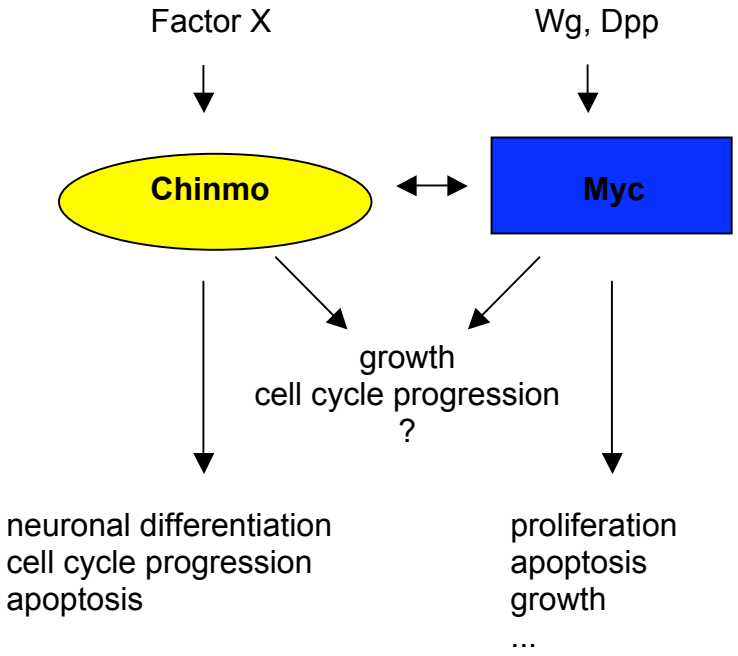

Figure I: Model of the interaction between Chinmo and dMyc. Chinmo and dMyc act both in separate pathways to specify either a temporal gradient in the mushroom body neuroblast lineage (Chinmo) or to control biological activities like proliferation or apoptosis (dMyc). However, both Chinmo and dMyc also act together e.g. in the regulation of cell growth most probably by activation of certain target genes. The observation that both proteins interact physically supports this model.

Conclusion

Our data reveal two novel dMyc interacting genes: *Delta*, which is involved in the Notch signalling pathway and *chinmo*.

It is necessary to understand how these trans-acting determinants influence Myc function to get a better understanding of Myc`s oncogenic properties.

We present evidence that dMyc depends on Chinmo to accurately fulfil its biological activities in wing imaginal discs. Interestingly, dMyc is limiting for Chinmo since the deleterious effects of Chinmo overexpression are suppressed by reduction of dMyc levels. Additionally, our data suggest that Chinmo binds dMyc physically via its BTB/POZ domain. Moreover, Chinmo activates not only endogenous target genes of dMyc associated with ribosomal biosynthesis and it activated the transcription but also a dMyc dependent luciferase reporter, and the latter effect requires endogenous *dmyc*. Thus, Chinmo might be a co-activator of dMyc, necessary for its biological functions *in vivo*.

Chinmo might also be expressed in humans and human c-Myc might interact with this human homologue of Chinmo. Therefore, this interaction might be relevant for cancer in some tissues.

Materials and Methods

1. Cloning and expression of dMyc proteins

A cDNA for wildtype dMyc with a triple HA-epitope at its N-terminus was subcloned into pBluescript SK+ (as an Asp718/EcoRI fragment) and later cloned into a pBS-vector (as an Asp718/XbaI fragment) carrying a single ΦC31 *att*B site, 5 UAS repeats, a *hsp70* basal promoter, the SV40 polyA signal, a *mini-white* gene as a marker and an ampicillin resistance protein for selection (Bischof et al., 2007). By site-directed mutagenesis the following mutant derivatives were created (numbering relative to untagged dMyc): dMycΔN: lacking amino acids 1–65 (cloned as Asp718/ApaI/ApaI/XbaI fragment); dMycMB2A: containing "AAAA" instead of "DCMW" (cloned as Asp718/SpeI/SpeI/XbaI fragment); dMycΔMB2: "GP" substituted for residues 68-84 (cloned as Asp718/ApaI/ApaI/XbaI fragment); dMycΔMB3: "F" substituted for residues 405-422 (cloned as Asp718/EcoRI/EcoRI/XbaI fragment). In addition, the same cDNAs were cloned under the control of the *β-tubulin* promoter (see Bellosta et al., 2005) into an analogous pBS-vector lacking UAS and *hsp70* sequences.

To determine the precise binding site of different proteins, which were shown to interact with dMyc, like Pont (Bellosta et al., 2005), Chinmo (D. Schwinkendorf, unpublished), dHCF (M. Balbi, personal communication), dLeo1 (M.Furrer, personal communication), different smaller dMyc mutations were generated. All mutations contain an N-terminal HA-tag in order to allow their visualization on an SDS-PAGE. All C-terminal deletions (N-terminus, Δ294C, Δ403C, Δ523C, ΔC) carry an MluI site, followed by a STOP codon and an XbaI site at their C-terminus, all N-terminal deletions (Δ626N, Δ523N, Δ403N, Δ294N, ΔNΔC) carry an MluI site at their N-terminus. For further Myc mutations of the central part of the protein, the different Myc fragments can therefore be combined. As a template for PCR reactions pUAST-HA-dMyc was used. C-terminal deletions were subcloned into the same vector after elimination of dMyc by Asp718/XbaI. N-terminal deletions were subcloned as MluI/XbaI fragment into pUAST-HA (A.Egli, unpublished). For internal deletions the MluI/XbaI fragment of any N-terminal deletion can be cloned into any C-terminal deletion construct via the same restriction sites.

The created constructs were (numbering relative to untagged dMyc):

N-terminus: lacking amino acids 179-719
Δ294C: lacking amio acids 294-719
Δ403C: lacking amino acids 403-719
Δ523C: lacking amino acids 523-719
ΔC-terminus: lacking amino acids 626-719
ΔN626: lacking amino acids 1-626
ΔN523: lacking amino acids 1-523
ΔN403: lacking amino acids 1-403
ΔN294: lacking amino acids 1-294
ΔN-terminus: lacking amino acids 1-179
ΔNΔC-terminus: lacking amino acids 1-179 and 626-719

Primer sequences for dMyc mutants/ fragments

construct	primer name	primer sequence (5'→3')
dMycWT	5UPn	GGGCGAATTGGGTACCCGCGAAATTGCTCG
	3LPn	GTGGCGCGACGCTTAGTGGGCGAGCTC
dMycΔN	MBIUPn	GCGGTAAAGGGCCCTTCTAGCGTAATCTGGAACGTC
	MBILP	GATGGGCCCCCAGAGATCCGCAACATCGAC
dMycMB2A	MB2UP	CCGTCGACTAGTATGTCCAGCTGTTTGACCAGC
	MB2LP	CCGTCGACTAGTTGCTGCTGCTGCGATGTTGCGGATCTCTGG
dMycΔMB2	MBIIdelUP	CACAGGGCCCCTCTGGCTTCATATCCTCCTC
	MBIIdelLP	CACAGGGCCCGGTAACGGTAATGGAATAGAG
dMycΔMB3	acidicUP3	GGGGAATTCCAAATTGGGACCATCGTCCAC
	acidicLP3	GACGAATTCCTACCCACAAATCCCTCGTGC

Primer pairs
dMycΔN: 5UPn + MBIUPn; MBILP + 3LPn
dMycMB2A: 5UPn + MB2LP; MB2UP + 3LPn
dMycΔMB2: 5UPn + MBIIdelLP; MBIIdelUP + 3LPn
dMycΔMB3: 5UPn + acidicUP3; acidicLP3 + 3LPn

construct	primer name	primer sequence (5'→3')
dMyc294C	dMyc_d294C	TTACTCTAGATTAACGCGTCGAATTGGAATGCTGGT TGAGCACATCG
dMyc403C	dMyc_d403C	GTACTCTAGATTAACGCGTCAAATTGGGACCATCGT CCACCATATCG
dMyc523C	dMyc_d523C	GTACTCTAGATTAACGCGTCGAACTGGAGGTGGTGA AGCTTGACTGC
dMycN294	dMyc_dN294	ATTCACGCGTACACGGGTGGCCAACAGCAGTTG
dMycN403	dMyc_dN403	ATTCACGCGTACGAGACCCCCTCAGATTCCGATG
dMycN523	dMyc_dN523	AAGCACGCGTACAACAAGGGACGCAAACGATCCAG
dMycN626	dMyc_dN626	CCACCACGCGTACAAGCGCAATCAGCACAATGA
Myc fragments	hsp70(+60)f	CGCAGCTGAACAAGCTAAACAATC
Myc fragments	SV40polyArev1	GTCACACCACAGAAGTAAGG

Primer pairs
all C-terminal fragments: primer as described above + hsp70(+60)f
all N-terminal fragments: primer as described above + SV40PolyArev1

2. Cloning and expression of Chinmo proteins

A cDNA (Gold SD 04616) with a single AU1-epitope was subcloned into pBluescript SK+ (Stratagene) and finally into a pBS-vector carrying a single ΦC31 *att*B site, 5 UAS repeats, a *hsp70* basal promoter, the SV40 polyA signal, a *mini-white* gene as a marker and an ampicillin resistance protein for selection (Bischof et al., 2007).

By site-directed mutagenesis the following mutant derivatives were created (numbering relative to untagged Chinmo): ChinmoΔBTB: "TR" substituted for amino acids 32-128; ChinmoΔZnf: lacking amino acids 517-604.

Establishment of S2-MT-Chinmo: To have an inducible system to express Chinmo in all cells of a S2 cell population, *chinmo* was cloned into a metallothioneine vector (pMTV5His). *Drosophila* S2 cells were plated out to 1 million cells in 1,6ml full media in a six-well-plate for 1h. Cells were transfected with 0,4µg (0,2µg/ 0,1µg) pMT-Chinmo DNA plasmid and 20ng (10ng/ 5ng) Blasticidin resistance plasmid (pCoBlast) and 10µl Cellfectin (Invitrogen) in serum-free medium. 15-16h after transfection full media was given for 48h before addition of 25µg Blasticidin. Cells were kept in selection medium for 10 days; afterwards, surviving cells were plated out in fresh medium containing Blasticidin.

Primer sequences for Chinmo and Chinmo mutants

construct	primer name	primer sequence (5'→3')
Chinmo	CG31666UP	GGGCGAATTGGGTACCCAAAATGGACACCTACCGCT ACATCATGGATCCGCAGCAGC
Chinmo	CG31666LP	GGTGGCGGCCGCTCTAGATTACTATGGTGAATGATTGCTGGC
ChinmoΔBTB	cBTBf1	GTGGTACCCAAAATGGACAC
	cBTBr1	GTTCTAGACTATTAACGCGTCAGTAGATCCGATTTGAACAGA
	cBTBf2	CAACGCGTCAACAACACATGGGCGACCT
	cBTBr2	CCTTCACAAAGATCCTCTAGA
ChinmoΔZnf	cZNr1	CGTCTAGACTATTACTTCTTACCGTCGGCCGTG

3. Tissue culture: transfections and biochemistry

3.1 Common to all experiments

Drosophila S2 cells were cultured at 24°C in 1x Schneider‘s *Drosophila* medium (Gibco/BRL), supplemented with 10% fetal bovine serum, 1% Penicillin/Strepavidin. To assess dMyc stability, $5x10^6$ cells were seeded per well of a 6-well culture plate and transfected in 1ml of serum-free medium containing 10µl Cellfectin (Invitrogen) and 10µg plasmid DNA.

3.2 **Cycloheximide and steady state protein levels in S2 cells**

5µg *tub*-GAL4 and 5µg UAS-plasmids were used for transfection; 15-16h later, complete medium was added for 48h, before cycloheximide (Sigma, ready made) was added to 100 µg/ml. Cells were harvested at the indicated time points and washed with 1xPBS, lysed in Laemmli sample buffer and analysed by SDS-PAGE and immunoblotting.
Steady-state protein levels were determined analogously, without cycloheximide treatment.
Primary antibody for Western blotting in both experiments was mouse anti-HA epitope (BAbCO) and mouse anti-α-Tubulin (Sigma), as secondary antibodies goat-anti-mouse-HRP (Jackson Immuno Research) was used.
To quantify the intensity of the individual bands Image J software was used. Each band was quantified by a rectangle, the background was substracted and the value for time point zero was set to 100%. The half-time was quantified with following formula: LN(2)/(LN(100/X)*t; whereas X is the percentage of band intensity and t the individual time of cycloheximide incubation.

3.3 Co-immunoprecipitation

For co-immunoprecipitation, S2 cells (co-transfected as described above [GCN5, TraI] or with 4µg tub-GAL4, 3µg UAS-plasmid, 3µg UAS-plasmid of interest [Pont, Chinmo]) were lysed in lysis buffer (250mM NaCl, 50mM Tris [pH 8], 5mM EDTA, 0.5% NP-40) containing protease inhibitors (Complete Protease Inhibitor Cocktail, Roche). After incubation on ice for 1h, lysates were precleared with protein G-sepharose beads (Amersham Pharmacia), followed by incubation with primary antibodies for 3h at 4° C.

After another incubation for 1h with protein G-sepharose beads, beads were washed 3 x for 5‘ with lysis buffer, SDS sample buffer was added and the samples analysed by SDS-PAGE and immunoblotting. Primary antibodies used for co-immunoprecipitation were: mouse anti-c-Myc epitope (9E10; Developmental Studies Hybridoma Bank), rabbit anti-dGCN5 (kindly provided by J. Workman), rabbit anti-AU1 (Alexis Biochemicals); for Western blotting: mouse anti-HA epitope (BAbCO), rabbit anti-HA epitope (Dunn Labortechnik GmbH).
Secondary antibodies were HRP-coupled anti-rabbit or anti-mouse (GE Healthcare, Jackson Immuno Research) and for detection the enhanced chemiluminescence kit (Amersham) was used.

3.4 Luciferase reporter experiments

Reporter assays were carried out as previously described (Hulf et al., 2005). Briefly, $1.3x10^6$ cells/well of a 24-well cell culture plate were transfected with 0.65ml serum-free medium containing 4.2µl Cellfectin (Invitrogen) and 2.6µg reporter plasmid DNA (consisting of a 1:1 mix of "*CG5033*^{wt}*-Renilla* luciferase" and "*CG5033*$^{\Delta Ebox}$-firefly luciferase" reporters) as well as 2.6µg UAS-plasmids (consisting of a 1:1 mix of *tub*-GAL4 and UAS-plasmids of interest). RNAi experiments included an amount of 0.08µg per dsRNA. After 15-16h, 0.65ml complete media was added; 24h later, cells were washed in 1xPBS, lysed in 1x Passive Lysis Buffer (Dual-Luciferase kit, Promega), and relative reporter expression determined on a Wallac luminometer.

Primer sequences for dsRNA

construct	primer name	primer sequence (5‘→3‘)
dsRNA*dmyc*	5’UTRfwd	CAGAGAATCGCTTTGTGGATTG
	5’UTRrev	GCTGAACATAGTTTCCG
dsRNA*chinmo*	CG31666RNAif	CGCTAATACGACTCACTATAGGGAGACGGATCTACTGGC CGATGTC
	CG31666RNAir	CGCTAATACGACTCACTATAGGGAGACAAGATGCCAGTG GATCCGC
*gft*RNAi	MF_EG_rev	CGTAATACGACTCACTATAGGGAGATGGCGCCCCTAGATG
	MF_EG_fw5	CGTAATACGACTCACTATAGGGAGATAGGTCTAGCCCCGC

4. *Drosophila* lines

Transgenic flies were established by integrating the different *att*B plasmids into the *att*P landing site ZH-86Fb (Bischof et al., 2007; http://www.frontiers-in-genetics.org/), and confirmed by PCR.

PCR conditions
Volume (total): 25µl. Primer pairs (10µM): 1µl each of iPCRSV40F1 or ZHattP14R respectively; genomic DNA: 0.2µg; Taq Polymerase buffer: 2.5µl; dNTP's: 0.5µl; Taq Polymerase: 0.2µl. Cycling parameters: 5 min 94° C, 35 x [30s 94° C, 30s 62°C, 1min 72° C], 5min 72°C, HOLD 4°C.

Primer sequences

construct	primer name	primer sequence (5'→3')
insertion	iPCRSV40F1	CTTGTTTATTGCAGCTTATAATGG
insertion	ZHattP14R	TGGTGCTAGAAACACCTTTCGAGCCG

4.1 Source of additional flies

GAL4 drivers, *gft* mutants (*Drosophila* stock centre at Bloomington)
BL12175: cn^1 P(PZ)gft^{06430}/CyO; ry^{506}
BL23866: gft^2 P(neoFRT)40A/CyO
BL20656: y^1 w^{67c23}; P(EPgy2)$gft^{EY11031}$
act-FRT-CD2-FRT-GAL4 (Neufeld et al., 1998)
GMR-FRT-w^+-FRT-GAL4 (Brogiolo et al., 2001)
tub-FRT-dMyc-FRT-GAL4 (De La Cova et al., 2004)
ago^1 & ago^3 (Moberg et al., 2001)
dm^{P0} (Johnston et al., 1999)
dm^2 (Maines et al., 2004)
dm^4 (Pierce et al., 2004)
$dmnt^1$ dm^4 (Pierce et al., 2008)
dm^{PL35} & dm^{PG45} (Benassayag et al., 2005)
UAS-Chinmo on III, *chinmo* alleles FRT-40 108, 110, 134 (kindly provided by H. Stocker)
UAS Chinmo FL (Zhu et al., 2006)
RNAi line *gft* (Barry Dickson, Vienna, Austria)
hs-FLP UAS GFP; *tub*-GAL80 FRT-40; *tub*-GAL4 (kindly provided by J. E. Treisman).

5. Analysis of adult flies

Flies were kept on standard *Drosophila* medium and testcrosses performed in a climate-controlled chamber at 25°.

Scanning electron microscope pictures were taken with a JEOL JSM-6360 LV microscope and a magnification of 180x. Flies were frozen at –20°C for at least one day, slowly defrosted at 0°C and directly used for electron microscopy. For determination of ommatidial size, the area of 20 centrally located ommatidia was determined from 5 fly eyes of the same genotype using Adobe Photoshop. The same photomicrographs were also used to determine the total number of ommatidia per eye. Obvious fusions of two ommatidia were counted as two individual ommatidia.

To determine adult weights, 1-2 day old adult flies were frozen at –20°C for at least one day, defrosted at room temperature and weighed on a Mettler Toledo MX5 microbalance.

6. Immunocytochemistry

6.1 TUNEL staining

For TUNEL staining of wing imaginal discs, wandering third instar larvae were fixed in 4% paraformaldehyde for 20', washed with 1x PBT (0.13M NaCL, 7mM Na2HP04, 3mM NaH_2P0_4, 0.1% Tween-20) for 20', post-fixed in ethanol/PBS (2:1) for 5' at –20°C, washed with 3 changes of 0.1% Tween-20/PBS over 15', pre-treated with 10mM sodium citrate (pH 6) for 30' at 70°C, equilibrated in Equilibration Buffer (ApopTag Red In Situ Apoptosis Detection Kit, Chemicon) for 10', then incubated with TdT enzyme (Chemicon kit) for 1h at 37°C, Stop/Wash Solution (Chemicon kit) for 10', Rhodamine-coupled anti-DIG antibodies (Chemicon kit) for 30', and 3 changes of 0.1% Tween-20/PBS (containing 0.5µg/ml Hoechst 33342 for the first step).

6.2 Anti-cleaved caspase 3 staining

For anti-cleaved caspase 3 stainings, wing imaginal discs of wandering third instar larvae were fixed in 4% paraformaldehyde/PBS for 20' at room temperature and washed 3 times with 1x PBX (0.13M NaCl, 7mM Na_2HP0_4, 3mM NaH_2P0_4, 0.1% Triton-X100) for 20'. Rabbit anti-cleaved caspase 3 (Cell Signalling Technology) was added at 1:300 over night at 4°C. Samples were washed with PBX, incubated with Texas Red-coupled anti-rabbit antibodies (Jackson Immuno Research Lab) and 0.5µg/ml Hoechst 33342 for 2 hours at room temperature, and washed again 3 times for 20' with PBX.

6.3 Overexpressing clones

For clonal area measurements, larvae carrying the *act*-FRT-CD2-FRT-GAL4 construct, UAS-GFP and the appropriate UAS-dMyc transgene, were heat-shocked for 10' at 37°C in a water bath, dissected 48h or 72h later, fixed in 4% paraformaldehyde for 20', and washed with 3 changes of PBT (containing 0.5µg/ml Hoechst 33342 for the first step) over 60'.
Wing discs were dissected and mounted in Vectashield Mounting Medium (Vectashield), and analysed on a Leica DMRA compound microscope at a 10x ocular magnification. Clonal area was determined from at least 40 clones per construct for 48h clones and at least 20 clones for 72h clones using Adobe Photoshop.

6.4 MARCM clones

Uncrowded wandering L3 larvae either mutant for *chinmo*, or overexpressing dMyc, or mutant for *chinmo* and overexpressing dMyc or wildtype were dissected for wing imaginal discs 120 hours after egg deposition. Heat-shocks were given at 37°C for 20' after 48h to obtain 72h clones. Wing discs were fixed in 4% paraformaldehyde for 20' and washed with 3 changes of PBT (containing 0.5µg/ml Hoechst 33342 for the first step) over 60'. Wing discs were dissected and mounted in Vectashield Mounting Medium (Vectashield), and analysed on a Leica DMRA compound microscope at a 10x ocular magnification. Clonal area was determined from at least 20 clones per construct for 48h clones and at least 20 clones for 72h clones using Adobe Photoshop.

6.5 Steady state protein levels *in vivo*

Steady state protein levels *in vivo* were determined from flies expressing HAdMyc transgenes under the control of a *tubulin* promoter (details described above). Uncrowded wandering larvae or adult males were directly mashed in Laemmli sample buffer or lysed in lysis buffer (250mM NaCl, 50mM Tris [pH 8], 5mM EDTA, 0,5% NP-40) containing protease inhibitors (Complete Protease Inhibitor Cocktail, Roche) for 1h. Laemmli sample buffer was added to lysates (1:1). Both extracts were loaded on a SDS-PAGE following immunoblotting. Primary antibody for Western blotting was rabbit anti-HA (1:1000; Dunn Labortechnik), secondary antibody was HRP-conjugated donkey anti-rabbit (1:3000; GE Healthcare).

6.6 QRT-PCR

6.6.1 qRT-PCR dMyc mutants

Male larvae with the genotype "*w dm*^{4} *tub*-FRT-dMyc-FRT-GAL4 hs-FLP; UAS-dMyc", grown under uncrowded conditions, were heat-shocked at wandering stage for 2h at 37°C in a water bath, collected 8h later into liquid nitrogen, and stored at -80°. To extract RNA, 10 whole larvae were homogenized in 1ml TRIZOL (Invitrogen) with a Polytron tissue homogenizer, following the manufacturers instructions. Upon precipitation, RNA was redissolved in 20µl RNAse-free water and analysed for its integrity on a Bioanalyzer (Agilent). Genomic DNA was eliminated using the Turbo DNAse free kit (Ambion) and cDNAs were synthesized from 1µg of template RNA using the Omniscript kit (Qiagen). Parallel control reactions containing only RNA provided templates for "-RT" samples. Quantitative real-time PCR (qRT-PCR) reactions were performed in triplicates on an ABI7900 Real Time PCR Instrument (Applied Biosystems), using the SYBR Green PCR Master Mix (Applied Biosystems). Data were analysed with SDS 2.0 software (Applied Biosystems) and Microsoft Excel, using the ΔΔCt method and the average of the expression levels of *actin5C*, *Rab6* and *Sec24* as internal reference for each biological sample.

Primer sequences

gene	primer name	primer sequence (5'→3')
Rab6	Rab6forw	TGCACGTGGCCAAGTCCTA
	Rab6rev	CAGCGAACGCGACTGCTA
Sec24	Sec24forw	CCACTCCCCTGCCATCCT
	Sec24rev	ACCCCAAACCCAGCAACA
CG5033	CG5033F1	TAACCGCTCGGCTTTAATTCA
	CG5033R1	CCCTTGCTCTTGGAGAATGG
dmyc(exon2)	qRTPCR2_ex2_dMycf	CCCGGCGGAAGTTTGC
	qRTPCR2_ex2_dMycr	CCCGATTTGCGGATAATGTC
dmyc(exon3)	qRTPCR2_ex3_dMycf	ACACGCGCTGCAACGAT
	qRTPCR2_ex3_dMycr	GTGGCACGAGGGATTTGTG
GAL4	GAL4forw	TTGAAATCGCGTCGAAGGA
	GAL4rev	CTCCAATGGCTAATATGCAGTTAAAA
CG18610	CG18610forw	TCGTCTGCGACCTGTCCTTT
	CG18610rev	ACCCAAAACCGATGGAGATTC
HA-tag	HAforw	GATAAACCCGATCAGCAAAAATG
	HArev	GCCCGCATAGTCAGGAACA

The remaining primers and the PCR conditions have been described (Steiger et al., 2008).

6.6.2 qRT-PCR for Chinmo

Drosophila S2 cells or S2 cells which stably express Chinmo after addition of copper sulphate (pMT Chinmo) were plated out to a concentration of $5x10^6$ cells per well of a 6-well culture plate. Copper sulphate was added to a concentration of 1000 µM for 24h, control cell lines were untreated. Cells were harvested and lysed in 1ml TRIZOL (Invitrogen). Total RNA, cDNA and qRT-PCR were performed as described above. Data were analysed with SDS 2.0 software (Applied Biosystems) and Microsoft Excel, using the ΔΔCt method and the average of the expression levels of *actin5C*, *Rab6* and *Sec24* as internal reference for each biological sample.

PCR conditions

Volume (total): 10µl. Primer pairs (10µM): 0.3µl; cDNA: 0.4µl; 2x SYBR GREEN: 5µl. Cycling parameters: 2 min 50° C, 10 min 95° C, 40 x [15 s 95° C, 1 min 60° C]. Dissociation curve measurements were included in the PCR run to document the specificity of the amplification reaction, and the "-RT" samples demonstrated the absence of contaminating genomic DNA.

Primer sequences

gene	primer name	primer sequence (5'3')
chinmo	CHqRTfwd	GGCCGCGTCGATTGC
	ChqRTrev	TCATCTTGGTGGCGTTCCAT
fibrillarin	fib_Right	ATGCGGTACTTGTGTGGATG
	fib_Left	ACGACAGTCTCGCATGTGTC

7. Additional Primers

Primer sequences and conditions for analysis of integration site/ sequencing

use	construct	primer name	primer sequence (5'→3')
sequencing	*chinmo*	rm3	GGCTGCAAATGCGGCGGC
sequencing	*chinmo*	rm4	CCATGCACTCCGAACGCGC
sequencing	*chinmo*	rm5	CCTGAGAGCTAAGGACACCG
sequencing	*chinmo*	rm6	GCATGCACTTCTCCAGTGCC
analysis	dMycMB2A	MIIanalMUT	CCCGCTGGACATACTAGTTGCTGCTGCTGC
analysis	dMycΔN	MIIanalWT	CAGCTGGACATCGCCGGCCACATGCAGTC
analysis	dMycΔMB3	ACanalUP	GGACGATGGTCCCAATTTGG
analysis	dMycWT	BASanalUP	GCCATGGATCGTAATTGGCAGC
		PBSBLP	GGTTCCTTCACAAAGATCC
		ACanalLP	GTTCTGATACGGTGTGCTCG
analysis	dMycΔMB2	MB2delanal	TCTATTCCATTACCGTTACCG

PCR conditions
Volume (total): 20µl. Primer pairs (10µM): 1µl each; genomic DNA: 0.4µl; Taq Polymerase buffer: 2µl; dNTPs: 1µl; Taq Polymerase: 0.2µl. Cycling parameters: 5 min 95°C, 35 x [30 s 92° C, 30 s 58°C, 30 s 72° C], 10 min 72°C, HOLD 4°C.

Primer for analysis of 380C1/BL7492 exons

construct	primer name	primer sequence (5'→3')
genomicDNA	Chex1f	CCACTGCACGCTTGTTCG
	Chex1r	CACTTCATCCGCTGCAGTT
	Chex2f	TCTGGGCACAAATGAAATGA
	Chex2r	TGACAAGTTGTGAATTTTTCATAAAT
	Chex3f	CCTTGAATACACTGAATACGCG
	Chex3r	ATGGAAAATTTCAAGTAAAAACACAAC
	Chex4f	AATCTTATGAATGTTCTCCTTTGCTT
	Chex4r	AGGGAGCTGCAGTGTTGG
	Chex5f	GAAAGCAAAACTAATCGCTCAA
	Chex5r	GAAAATGAAAGGAAGCGAGTC
	Chex6-9f	TAATATTCATATTCTAACGCATGTGAC
	Chex6-9r	TGCCATCTTGAGTGTTTTACGT
	Chex6-9b	GAGCAATAGGATGAGG
	Chex9f	AGTCATGAACGCCAACAAGG
	Chex9r	AGAGCCGAAAAAAGGAATTTTG
	Chex9b	GCCTGAGCACCCTAGC

PCR conditions
Volume (total): 20µl. Primer pairs (10µM): 1.5µl each; template DNA: 1µg; Buffer HF (GC): 2µl; DMSO: 0.6µl; $MgCl_2$: 0.5µl; dNTPs: 0.5µl; Phusion Polymerase: 0.2µl. Cycling parameters: 5 min 95° C, 35 x [30s 94° C, 30s 62°C, 30s 72° C], 10 min 72°C, HOLD 4°C.

References

Adhikary, S., Marinoni, F., Hock, A., Hulleman, E., Popov, N., Beier, R., Bernard, S., Quarto, M., Capra, M., Goettig, S.*, et al.* (2005). The Ubiquitin Ligase HectH9 Regulates Transcriptional Activation by Myc and Is Essential for Tumor Cell Proliferation. Cell *123*, 409-421.

Arvanitis, C., and Felsher, D.W. (2006). Conditional transgenic models define how MYC initiates and maintains tumorigenesis. Seminars in cancer biology *16*, 313.

Asano, M., Nevins, J.R., and Wharton, R.P. (1996). Ectopic E2F expression induces S phase and apoptosis in Drosophila imaginal discs. Genes & development *10*, 1422-1432.

Askew, D.S., Ashmun, R.A., Simmons, B.C., and Cleveland, J.L. (1991). Constitutive c-myc expression in an IL-3-dependent myeloid cell line suppresses cell cycle arrest and accelerates apoptosis. Oncogene *6*, 1915-1922.

Ayer, D.E., Kretzner, L., and Eisenman, R.N. (1993). Mad: a heterodimeric partner for Max that antagonizes Myc transcriptional activity. Cell *72*, 211-222.

Bailey, A.M., and Posakony, J.W. (1995). Suppressor of hairless directly activates transcription of enhancer of split complex genes in response to Notch receptor activity. Genes & development *9*, 2609-2622.

Battey, J., Moulding, C., Taub, R., Murphy, W., Stewart, T., Potter, H., Lenoir, G., and Leder, P. (1983). The human c-myc oncogene: structural consequences of translocation into the IgH locus in Burkitt lymphoma. Cell *34*, 779-787.

Bauer, A., Chauvet, S., Huber, O., Usseglio, F., Rothbacher, U., Aragnol, D., Kemler, R., and Pradel, J. (2000). Pontin52 and reptin52 function as antagonistic regulators of beta-catenin signalling activity. The EMBO journal *19*, 6121-6130.

Bellosta, P., Hulf, T., Diop, S.B., Usseglio, F., Pradel, J., Aragnol, D., and Gallant, P. (2005). Myc interacts genetically with Tip48/Reptin and Tip49/Pontin to control growth and proliferation during Drosophila development. Proceedings of the National Academy of Sciences of the United States of America *102*, 11799-11804.

Benassayag, C., Montero, L., Colombie, N., Gallant, P., Cribbs, D., and Morello, D. (2005). Human c-Myc isoforms differentially regulate cell growth and apoptosis in Drosophila melanogaster. Molecular and cellular biology *25*, 9897-9909.

Berberich, S.J., and Cole, M.D. (1992). Casein kinase II inhibits the DNA-binding activity of Max homodimers but not Myc/Max heterodimers. Genes & development *6*, 166-176.

Berg, T., Cohen, S.B., Desharnais, J., Sonderegger, C., Maslyar, D.J., Goldberg, J., Boger, D.L., and Vogt, P.K. (2002). Small-molecule antagonists of Myc/Max dimerization inhibit Myc-induced transformation of chicken embryo fibroblasts. Proceedings of the National Academy of Sciences of the United States of America *99*, 3830-3835.

Betschinger, J., Mechtler, K., and Knoblich, J.A. (2006). Asymmetric Segregation of the Tumor Suppressor Brat Regulates Self-Renewal in Drosophila Neural Stem Cells. Cell *124*, 1241.

Biegalke, B.J., Heaney, M.L., Bouton, A., Parsons, J.T., and Linial, M. (1987). MC29 deletion mutants which fail to transform chicken macrophages are competent for transformation of quail macrophages. J Virol *61*, 2138-2142.

Bischof, J., Maeda, R.K., Hediger, M., Karch, F., and Basler, K. (2007). An optimized transgenesis system for Drosophila using germ-line-specific phiC31 integrases. Proceedings of the National Academy of Sciences of the United States of America *104*, 3312-3317.

Bishop, J.M. (1982). Retroviruses and cancer genes. Advances in cancer research *37*, 1-32.

Bissonnette, R.P., Echeverri, F., Mahboubi, A., and Green, D.R. (1992). Apoptotic cell death induced by c-myc is inhibited by bcl-2. Nature *359*, 552-554.

Blackwood, E.M., and Eisenman, R.N. (1991). Max: a helix-loop-helix zipper protein that forms a sequence-specific DNA-binding complex with Myc. Science (New York, NY *251*, 1211-1217.

Bolos, V., Grego-Bessa, J., and de la Pompa, J.L. (2007). Notch signaling in development and cancer. Endocr Rev *28*, 339-363.

Bouchard, C., Dittrich, O., Kiermaier, A., Dohmann, K., Menkel, A., Eilers, M., and Luscher, B. (2001). Regulation of cyclin D2 gene expression by the Myc/Max/Mad network: Myc-dependent TRRAP recruitment and histone acetylation at the cyclin D2 promoter. Genes & development *15*, 2042-2047.

Bridges, C.B. (1935). Drosophila melanogaster: Legend for symbols, mutants, valuations. Drosophila Information Service *3*, 5-19.

Brogiolo, W., Stocker, H., Ikeya, T., Rintelen, F., Fernandez, R., and Hafen, E. (2001). An evolutionarily conserved function of the Drosophila insulin receptor and insulin-like peptides in growth control. Current Biology *11*, 213-221.

Conaway, R.C., Brower, C.S., and Conaway, J.W. (2002). Emerging roles of ubiquitin in transcription regulation. Science (New York, NY *296*, 1254-1258.

Conzen, S.D., Gottlob, K., Kandel, E.S., Khanduri, P., Wagner, A.J., O'Leary, M., and Hay, N. (2000). Induction of cell cycle progression and acceleration of apoptosis are two separable functions of c-Myc: transrepression correlates with acceleration of apoptosis. Molecular and cellular biology *20*, 6008-6018.

Cowling, V.H., Chandriani, S., Whitfield, M.L., and Cole, M.D. (2006). A conserved Myc protein domain, MBIV, regulates DNA binding, apoptosis, transformation, and G2 arrest. Molecular and cellular biology *26*, 4226-4239.

Cowling, V.H., and Cole, M.D. (2006). Mechanism of transcriptional activation by the Myc oncoproteins. Seminars in cancer biology *16*, 242.

Cowling, V.H., and Cole, M.D. (2007). The Myc Transactivation Domain Promotes Global Phosphorylation of the RNA Polymerase II Carboxy-Terminal Domain Independently of Direct DNA Binding. Mol Cell Biol *27*, 2059-2073.

Cowling, V.H., and Cole, M.D. (2008). An N-Myc truncation analogous to c-Myc-S induces cell proliferation independently of transactivation but dependent on Myc homology box II. Oncogene *27*, 1327-1332.

Crittenden, J.R., Skoulakis, E.M., Han, K.A., Kalderon, D., and Davis, R.L. (1998). Tripartite mushroom body architecture revealed by antigenic markers. Learning & memory (Cold Spring Harbor, NY *5*, 38-51.

Dang, C.V., O'Donnell, K.A., Zeller, K.I., Nguyen, T., Osthus, R.C., and Li, F. (2006). The c-Myc target gene network. Seminars in cancer biology *16*, 253.

De La Cova, C., Abril, M., Bellosta, P., Gallant, P., and Johnston, L.A. (2004). Drosophila myc regulates organ size by inducing cell competition. Cell *117*, 107-116.

de la Cova, C., and Johnston, L.A. (2006). Myc in model organisms: A view from the flyroom. Seminars in cancer biology *16*, 303.

Deshaies, R.J. (1999). SCF and Cullin/Ring H2-based ubiquitin ligases. Annual review of cell and developmental biology *15*, 435-467.

Dugan, K.A., Wood, M.A., and Cole, M.D. (2002). TIP49, but not TRRAP, modulates c-Myc and E2F1 dependent apoptosis. Oncogene *21*, 5835-5843.

Eberhardy, S.R., and Farnham, P.J. (2002). Myc recruits P-TEFb to mediate the final step in the transcriptional activation of the cad promoter. The Journal of biological chemistry *277*, 40156-40162.

Efstratiadis, A., Szabolcs, M., and Klinakis, A. (2007). Notch, Myc and breast cancer. Cell cycle (Georgetown, Tex *6*, 418-429.

Eichler, D.C., and Craig, N. (1994). Processing of eukaryotic ribosomal RNA. Progress in nucleic acid research and molecular biology *49*, 197-239.

Evan, G.I., Wyllie, A.H., Gilbert, C.S., Littlewood, T.D., Land, H., Brooks, M., Waters, C.M., Penn, L.Z., and Hancock, D.C. (1992). Induction of apoptosis in fibroblasts by c-myc protein. Cell *69*, 119-128.

Fanidi, A., Harrington, E.A., and Evan, G.I. (1992). Cooperative interaction between c-myc and bcl-2 proto-oncogenes. Nature *359*, 554-556.

Frank, S.R., Schroeder, M., Fernandez, P., Taubert, S., and Amati, B. (2001). Binding of c-Myc to chromatin mediates mitogen-induced acetylation of histone H4 and gene activation. Genes & development *15*, 2069-2082.

Freytag, S.O. (1988). Enforced expression of the c-myc oncogene inhibits cell differentiation by precluding entry into a distinct predifferentiation state in G0/G1. Molecular & Cellular Biology *8*, 1614-1624.

Freytag, S.O., Dang, C.V., and Lee, W.M. (1990). Definition of the activities and properties of c-myc required to inhibit cell differentiation. Cell Growth Differ *1*, 339-343.

Furriols, M., and Bray, S. (2000). Dissecting the mechanisms of suppressor of hairless function. Developmental biology *227*, 520-532.

Furukawa, M., He, Y.J., Borchers, C., and Xiong, Y. (2003). Targeting of protein ubiquitination by BTB-Cullin 3-Roc1 ubiquitin ligases. Nature cell biology *5*, 1001-1007.

Galaktionov, K., Chen, X., and Beach, D. (1996). Cdc25 cell-cycle phosphatase as a target of c-myc. Nature *382*, 511-517.

Gallant, P. (2006). Myc / Max / Mad in invertebrates - the evolution of the Max network CTMI *302*, 237-254.

Gallant, P. (2007). Control of transcription by Pontin and Reptin. Trends in Cell Biology *17*, 187.

Gallant, P., Shiio, Y., Cheng, P.F., Parkhurst, S.M., and Eisenman, R.N. (1996). Myc and Max homologs in Drosophila. Science (New York, NY *274*, 1523-1527.

Geyer, R., Wee, S., Anderson, S., Yates, J., and Wolf, D.A. (2003). BTB/POZ domain proteins are putative substrate adaptors for cullin 3 ubiquitin ligases. Molecular cell *12*, 783-790.

Glickman, M.H., and Ciechanover, A. (2002). The ubiquitin-proteasome proteolytic pathway: destruction for the sake of construction. Physiological reviews *82*, 373-428.

Gomez-Roman, N., Felton-Edkins, Z.A., Kenneth, N.S., Goodfellow, S.J., Athineos, D., Zhang, J., Ramsbottom, B.A., Innes, F., Kantidakis, T., Kerr, E.R.*, et al.* (2006). Activation by c-Myc of transcription by RNA polymerases I, II and III. Biochemical Society symposium, 141-154.

Gomez-Roman, N., Grandori, C., Eisenman, R.N., and White, R.J. (2003). Direct activation of RNA polymerase III transcription by c-Myc. Nature *421*, 290-294.

Grandori, C., Mac, J., Siebelt, F., Ayer, D.E., and Eisenman, R.N. (1996). Myc-Max heterodimers activate a DEAD box gene and interact with multiple E box-related sites in vivo. The EMBO journal *15*, 4344-4357.

Grant, P.A., Duggan, L., Cote, J., Roberts, S.M., Brownell, J.E., Candau, R., Ohba, R., Owen-Hughes, T., Allis, C.D., Winston, F., *et al.* (1997). Yeast Gcn5 functions in two multisubunit complexes to acetylate nucleosomal histones: characterization of an Ada complex and the SAGA (Spt/Ada) complex. Genes & development *11*, 1640-1650.

Grant, P.A., Schieltz, D., Pray-Grant, M.G., Yates, J.R., 3rd, and Workman, J.L. (1998). The ATM-related cofactor Tra1 is a component of the purified SAGA complex. Molecular cell *2*, 863-867.

Grewal, S.S., Li, L., Orian, A., Eisenman, R.N., and Edgar, B.A. (2005). Myc-dependent regulation of ribosomal RNA synthesis during Drosophila development. Nature cell biology *7*, 295-302.

Hann, S.R. (2006). Role of post-translational modifications in regulating c-Myc proteolysis, transcriptional activity and biological function. Seminars in cancer biology *16*, 288.

Hann, S.R., King, M.W., Bentley, D.L., Anderson, C.W., and Eisenman, R.N. (1988). A non-AUG translational initiation in c-myc exon 1 generates an N-terminally distinct protein whose synthesis is disrupted in Burkitt's lymphomas. Cell *52*, 185-195.

Harel-Bellan, A., Ferris, D.K., Vinocour, M., Holt, J.T., and Farrar, W.L. (1988). Specific inhibition of c-myc protein biosynthesis using an antisense synthetic deoxy-oligonucleotide in human T lymphocytes. J Immunol *140*, 2431-2435.

Heaney, M.L., Pierce, J., and Parsons, J.T. (1986). Site-directed mutagenesis of the gag-myc gene of avian myelocytomatosis virus 29: biological activity and intracellular localization of structurally altered proteins. Journal of Virology *60*, 167-176.

Heisenberg, M. (1998). What do the mushroom bodies do for the insect brain? an introduction. Learning & memory (Cold Spring Harbor, NY *5*, 1-10.

Herbst, A., Hemann, M.T., Tworkowski, K.A., Salghetti, S.E., Lowe, S.W., and Tansey, W.P. (2005). A conserved element in Myc that negatively regulates its proapoptotic activity. EMBO Rep *6*, 177-183.

Hermeking, H., Rago, C., Schuhmacher, M., Li, Q., Barrett, J.F., Obaya, A.J., O'Connell, B.C., Mateyak, M.K., Tam, W., Kohlhuber, F., *et al.* (2000). Identification of CDK4 as a target of c-MYC. Proceedings of the National Academy of Sciences of the United States of America *97*, 2229-2234.

Hershey, J.W. (1991). Translational control in mammalian cells. Annual review of biochemistry *60*, 717-755.

Hirst, S.K., and Grandori, C. (2000). Differential activity of conditional MYC and its variant MYC-S in human mortal fibroblasts. Oncogene *19*, 5189-5197.

Ho, J.S., Ma, W., Mao, D.Y., and Benchimol, S. (2005). p53-Dependent transcriptional repression of c-myc is required for G1 cell cycle arrest. Molecular and cellular biology *25*, 7423-7431.

Hopewell, R., and Ziff, E.B. (1995). The nerve growth factor-responsive PC12 cell line does not express the Myc dimerization partner Max. Molecular and cellular biology *15*, 3470-3478.

Hulf, T., Bellosta, P., Furrer, M., Steiger, D., Svensson, D., Barbour, A., and Gallant, P. (2005). Whole-genome analysis reveals a strong positional bias of conserved dMyc-dependent E-boxes. Molecular and cellular biology *25*, 3401-3410.

Hurlin, P.J., Queva, C., and Eisenman, R.N. (1997). Mnt: a novel Max-interacting protein and Myc antagonist. Current Topics in Microbiology & Immunology *224*, 115-121.

Hurlin, P.J., Queva, C., Koskinen, P.J., Steingrimsson, E., Ayer, D.E., Copeland, N.G., Jenkins, N.A., and Eisenman, R.N. (1995). Mad3 and Mad4: novel Max-interacting transcriptional repressors that suppress c-myc dependent transformation and are expressed during neural and epidermal differentiation. EMBO Journal *14*, 5646-5659.

Hurlin, P.J., Steingrimsson, E., Copeland, N.G., Jenkins, N.A., and Eisenman, R.N. (1999). Mga, a dual-specificity transcription factor that interacts with Max and contains a T-domain DNA-binding motif. The EMBO journal *18*, 7019-7028.

Hurlin, P.J., Zhou, Z.Q., Toyo-oka, K., Ota, S., Walker, W.L., Hirotsune, S., and Wynshaw-Boris, A. (2003). Deletion of Mnt leads to disrupted cell cycle control and tumorigenesis. The EMBO journal *22*, 4584-4596.

Ikura, T., Ogryzko, V.V., Grigoriev, M., Groisman, R., Wang, J., Horikoshi, M., Scully, R., Qin, J., and Nakatani, Y. (2000). Involvement of the TIP60 histone acetylase complex in DNA repair and apoptosis. Cell *102*, 463-473.

Iritani, B.M., and Eisenman, R.N. (1999). c-Myc enhances protein synthesis and cell size during B lymphocyte development. Proceedings of the National Academy of Sciences of the United States of America *96*, 13180-13185.

Jacob, S.T. (1995). Regulation of ribosomal gene transcription. The Biochemical journal *306 (Pt 3)*, 617-626.

Jansen, D.P., Meichle, A., Steiner, P., Pagano, M., Finke, K., Botz, J., Wessbecher, J., Draetta, G., and Eilers, M. (1993). Differential modulation of cyclin gene expression by MYC. Proceedings of the National Academy of Sciences of the United States of America *90*, 3685-3689.

Jeffers, J.R., Parganas, E., Lee, Y., Yang, C., Wang, J., Brennan, J., MacLean, K.H., Han, J., Chittenden, T., Ihle, J.N.*, et al.* (2003). Puma is an essential mediator of p53-dependent and -independent apoptotic pathways. Cancer cell *4*, 321-328.

Johnston, L.A., Prober, D.A., Edgar, B.A., Eisenman, R.N., and Gallant, P. (1999). Drosophila myc regulates cellular growth during development. Cell *98*, 779-790.

Jonsson, Z.O., Jha, S., Wohlschlegel, J.A., and Dutta, A. (2004). Rvb1p/Rvb2p recruit Arp5p and assemble a functional Ino80 chromatin remodeling complex. Molecular cell *16*, 465-477.

Karn, J., Watson, J.V., Lowe, A.D., Green, S.M., and Vedeckis, W. (1989). Regulation of cell cycle duration by c-myc levels. Oncogene *4*, 773-787.

Kato, G.J., Lee, W.M., Chen, L.L., and Dang, C.V. (1992). Max: functional domains and interaction with c-Myc. Genes & development *6*, 81-92.

Kenneth, N.S., Ramsbottom, B.A., Gomez-Roman, N., Marshall, L., Cole, P.A., and White, R.J. (2007). TRRAP and GCN5 are used by c-Myc to activate RNA polymerase III transcription. Proceedings of the National Academy of Sciences %R 101073/pnas0702909104 *104*, 14917-14922.

Kim, S., Li, Q., Dang, C.V., and Lee, L.A. (2000). Induction of ribosomal genes and hypertrophy by adenovirus-mediated expression of c-Myc in vivo. Proceedings of the National Academy of Sciences of the United States of America *97*, 11203-11208.

Kim, S.S., Shago, M., Kaustov, L., Boutros, P.C., Clendening, J.W., Sheng, Y., Trentin, G.A., Barsyte-Lovejoy, D., Mao, D.Y., Kay, R.*, et al.* (2007). CUL7 is a novel antiapoptotic oncogene. Cancer research *67*, 9616-9622.

Kim, S.Y., Herbst, A., Tworkowski, K.A., Salghetti, S.E., and Tansey, W.P. (2003). Skp2 regulates Myc protein stability and activity. Molecular cell *11*, 1177-1188.

Klinakis, A., Szabolcs, M., Politi, K., Kiaris, H., Artavanis-Tsakonas, S., and Efstratiadis, A. (2006). Myc is a Notch1 transcriptional target and a requisite for Notch1-induced mammary tumorigenesis in mice. Proceedings of the National Academy of Sciences of the United States of America *103*, 9262-9267.

Koskinen, P.J., Ayer, D.E., and Eisenman, R.N. (1995). Repression of Myc-Ras cotransformation by Mad is mediated by multiple protein-protein interactions. Cell Growth & Differentiation *6*, 623-629.

Kretzner, L., Blackwood, E.M., and Eisenman, R.N. (1992). Myc and Max proteins possess distinct transcriptional activities. Nature *359*, 426-429.

Kurusu, M., Nagao, T., Walldorf, U., Flister, S., Gehring, W.J., and Furukubo-Tokunaga, K. (2000). Genetic control of development of the mushroom bodies, the associative learning centers in the Drosophila brain, by the eyeless, twin of eyeless, and Dachshund genes. Proceedings of the National Academy of Sciences of the United States of America *97*, 2140-2144.

Kurz, T., Pintard, L., Willis, J.H., Hamill, D.R., Gonczy, P., Peter, M., and Bowerman, B. (2002). Cytoskeletal regulation by the Nedd8 ubiquitin-like protein modification pathway. Science (New York, NY *295*, 1294-1298.

Landschulz, W.H., Johnson, P.F., and McKnight, S.L. (1988). The leucine zipper: a hypothetical structure common to a new class of DNA binding proteins. Science (New York, NY *240*, 1759-1764.

Lecourtois, M., and Schweisguth, F. (1995). The neurogenic suppressor of hairless DNA-binding protein mediates the transcriptional activation of the enhancer of split complex genes triggered by Notch signaling. Genes & development *9*, 2598-2608.

Lee, T., Lee, A., and Luo, L. (1999). Development of the Drosophila mushroom bodies: sequential generation of three distinct types of neurons from a neuroblast. Development (Cambridge, England) *126*, 4065-4076.

Lee, T., and Luo, L. (1999). Mosaic analysis with a repressible cell marker for studies of gene function in neuronal morphogenesis. Neuron *22*, 451-461.

Lee, T.C., Li, L.H., Philipson, L., and Ziff, E.B. (1997). Myc represses transcription of the growth arrest gene gas1. Proceedings of the National Academy of Sciences of the United States of America *94*, 12886-12891.

Leone, G., Degregori, J., Sears, R., Jakoi, L., and Nevins, J.R. (1997). Myc and ras collaborate in inducing accumulation of active cyclin e/cdk2 and e2f. Nature *387*, 422-426.

Li, L.H., Nerlov, C., Prendergast, G., MacGregor, D., and Ziff, E.B. (1994). c-Myc represses transcription in vivo by a novel mechanism dependent on the initiator element and Myc box II. Embo Journal *13*, 4070-4079.

Lindsley, D.L., and Zimm, G.G. (1992). The Genome of Drosophila melanogaster (San Diego, New York, Boston, London, Sydney, Tokyo, Toronto, Academic Press).

Loo, L.W., Secombe, J., Little, J.T., Carlos, L.S., Yost, C., Cheng, P.F., Flynn, E.M., Edgar, B.A., and Eisenman, R.N. (2005). The transcriptional repressor dMnt is a regulator of growth in Drosophila melanogaster. Molecular and cellular biology *25*, 7078-7091.

Lutterbach, B., and Hann, S.R. (1994). Hierarchical phosphorylation at N-terminal transformation-sensitive sites in c-Myc protein is regulated by mitogens and in mitosis. Molecular and cellular biology *14*, 5510-5522.

Ly, C.V., and Verstreken, P. (2006). Mitochondria at the synapse. Neuroscientist *12*, 291-299.

Maines, J.Z., Stevens, L.M., Tong, X., and Stein, D. (2004). Drosophila dMyc is required for ovary cell growth and endoreplication. Development (Cambridge, England) *131*, 775-786.

Marcu, K.B., Bossone, S.A., and Patel, A.J. (1992). myc function and regulation. [Review]. Annual review of biochemistry *61*, 809-860.

Marhin, W.W., Chen, S.J., Facchini, L.M., Fornace, A.J., and Penn, L.Z. (1997). Myc represses the growth arrest gene gadd45. Oncogene *14*, 2825-2834.

Mateyak, M.K., Obaya, A.J., Adachi, S., and Sedivy, J.M. (1997). Phenotypes of c-Myc-deficient rat fibroblasts isolated by targeted homologous recombination. Cell Growth & Differentiation *8*, 1039-1048.

McMahon, S.B., Van, B.H., Dugan, K.A., Copeland, T.D., and Cole, M.D. (1998). The novel ATM-related protein TRRAP is an essential cofactor for the c-Myc and E2F oncoproteins. Cell *94*, 363-374.

McMahon, S.B., Wood, M.A., and Cole, M.D. (2000). The essential cofactor TRRAP recruits the histone acetyltransferase hGCN5 to c-Myc. Molecular & Cellular Biology *20*, 556-562.

Menssen, A., and Hermeking, H. (2002). Characterization of the c-MYC-regulated transcriptome by SAGE: identification and analysis of c-MYC target genes. Proceedings of the National Academy of Sciences of the United States of America *99*, 6274-6279.

Meyer, N., Kim, S.S., and Penn, L.Z. (2006). The Oscar-worthy role of Myc in apoptosis. Seminars in cancer biology *16*, 275.

Moberg, K.H., Bell, D.W., Wahrer, D.C., Haber, D.A., and Hariharan, I.K. (2001). Archipelago regulates Cyclin E levels in Drosophila and is mutated in human cancer cell lines. Nature *413*, 311-316.

Moberg, K.H., Mukherjee, A., Veraksa, A., Artavanis-Tsakonas, S., and Hariharan, I.K. (2004). The Drosophila F box protein archipelago regulates dMyc protein levels in vivo. Curr Biol *14*, 965-974.

Montero, L., Muller, N., and Gallant, P. (2008). Induction of apoptosis by Drosophila Myc. Genesis *46*, 104-111.

Morel, V., Lecourtois, M., Massiani, O., Maier, D., Preiss, A., and Schweisguth, F. (2001). Transcriptional repression by suppressor of hairless involves the binding of a hairless-dCtBP complex in Drosophila. Curr Biol *11*, 789-792.

Moreno, E., and Basler, K. (2004). dMyc transforms cells into super-competitors. Cell *117*, 117-129.

Muratani, M., and Tansey, W.P. (2003). How the ubiquitin-proteasome system controls transcription. Nature reviews *4*, 192-201.

Neufeld, T.P., de la Cruz, A.F., Johnston, L.A., and Edgar, B.A. (1998). Coordination of growth and cell division in the Drosophila wing. Cell *93*, 1183-1193.

Newsome, T.P., Asling, B., and Dickson, B.J. (2000). Analysis of Drosophila photoreceptor axon guidance in eye-specific mosaics. Development (Cambridge, England) *127*, 851-860.

Nilsson, J.A., Maclean, K.H., Keller, U.B., Pendeville, H., Baudino, T.A., and Cleveland, J.L. (2004). Mnt loss triggers Myc transcription targets, proliferation, apoptosis, and transformation. Molecular and cellular biology *24*, 1560-1569.

Orian, A., Delrow, J.J., Rosales Nieves, A.E., Abed, M., Metzger, D., Paroush, Z.e., Eisenman, R.N., and Parkhurst, S.M. (2007). A Myc Groucho complex integrates EGF and Notch signaling to regulate neural development. Proceedings of the National Academy of Sciences *104*, 15771-15776.

Orian, A., Van Steensel, B., Delrow, J., Bussemaker, H.J., Li, L., Sawado, T., Williams, E., Loo, L.W., Cowley, S.M., Yost, C.*, et al.* (2003). Genomic binding by the Drosophila Myc, Max, Mad/Mnt transcription factor network. Genes & development *17*, 1101-1114.

Oster, S.K., Mao, D.Y., Kennedy, J., and Penn, L.Z. (2003). Functional analysis of the N-terminal domain of the Myc oncoprotein. Oncogene *22*, 1998-2010.

Park, J., Kunjibettu, S., McMahon, S.B., and Cole, M.D. (2001). The ATM-related domain of TRRAP is required for histone acetyltransferase recruitment and Myc-dependent oncogenesis. Genes & development *15*, 1619-1624.

Parks, A.L., Cook, K.R., Belvin, M., Dompe, N.A., Fawcett, R., Huppert, K., Tan, L.R., Winter, C.G., Bogart, K.P., Deal, J.E.*, et al.* (2004). Systematic generation of high-resolution deletion coverage of the Drosophila melanogaster genome. Nat Genet *36*, 288-292.

Patel, J.H., Du, Y., Ard, P.G., Phillips, C., Carella, B., Chen, C.J., Rakowski, C., Chatterjee, C., Lieberman, P.M., Lane, W.S.*, et al.* (2004). The c-MYC oncoprotein is a substrate of the acetyltransferases hGCN5/PCAF and TIP60. Molecular and cellular biology *24*, 10826-10834.

Perez-Torrado, R., Yamada, D., and Defossez, P.A. (2006). Born to bind: the BTB protein-protein interaction domain. Bioessays *28*, 1194-1202.

Pierce, S.B., Yost, C., Anderson, S.A., Flynn, E.M., Delrow, J., and Eisenman, R.N. (2008). Drosophila growth and development in the absence of dMyc and dMnt. Developmental biology *315*, 303-316.

Pierce, S.B., Yost, C., Britton, J.S., Loo, L.W., Flynn, E.M., Edgar, B.A., and Eisenman, R.N. (2004). dMyc is required for larval growth and endoreplication in Drosophila. Development (Cambridge, England) *131*, 2317-2327.

Pintard, L., Willis, J.H., Willems, A., Johnson, J.L., Srayko, M., Kurz, T., Glaser, S., Mains, P.E., Tyers, M., Bowerman, B.*, et al.* (2003). The BTB protein MEL-26 is a substrate-specific adaptor of the CUL-3 ubiquitin-ligase. Nature *425*, 311-316.

Popov, N., Wahlstrom, T., Hurlin, P.J., and Henriksson, M. (2005). Mnt transcriptional repressor is functionally regulated during cell cycle progression. Oncogene *24*, 8326-8337.

Rebay, I., Fleming, R.J., Fehon, R.G., Cherbas, L., Cherbas, P., and Artavanis-Tsakonas, S. (1991). Specific EGF repeats of Notch mediate interactions with Delta and Serrate: implications for Notch as a multifunctional receptor. Cell *67*, 687-699.

Rogers, S., Wells, R., and Rechsteiner, M. (1986). Amino acid sequences common to rapidly degraded proteins: the PEST hypothesis. Science (New York, NY *234*, 364-368.

Roussel, M.F., Cleveland, J.L., Shurtleff, S.A., and Sherr, C.J. (1991). Myc rescue of a mutant CSF-1 receptor impaired in mitogenic signalling. Nature *353*, 361-363.

Ryder, E., Ashburner, M., Bautista-Llacer, R., Drummond, J., Webster, J., Johnson, G., Morley, T., Chan, Y.S., Blows, F., Coulson, D.*, et al.* (2007). The DrosDel Deletion Collection: A Drosophila Genomewide Chromosomal Deficiency Resource. Genetics %R 101534/genetics107076216 *177*, 615-629.

Salghetti, S.E., Kim, S.Y., and Tansey, W.P. (1999). Destruction of Myc by ubiquitin-mediated proteolysis: cancer-associated and transforming mutations stabilize Myc. The EMBO journal *18*, 717-726.

Schreiber-Agus, N., Stein, D., Chen, K., Goltz, J.S., Stevens, L., and DePinho, R.A. (1997). Drosophila Myc is oncogenic in mammalian cells and plays a role in the diminutive phenotype. Proceedings of the National Academy of Sciences of the United States of America *94*, 1235-1240.

Schuhmacher, M., Staege, M.S., Pajic, A., Polack, A., Weidle, U.H., Bornkamm, G.W., Eick, D., and Kohlhuber, F. (1999). Control of cell growth by c-Myc in the absence of cell division. Current Biology *9*, 1255-1258.

Schulman, B.A., Carrano, A.C., Jeffrey, P.D., Bowen, Z., Kinnucan, E.R., Finnin, M.S., Elledge, S.J., Harper, J.W., Pagano, M., and Pavletich, N.P. (2000). Insights into SCF ubiquitin ligases from the structure of the Skp1-Skp2 complex. Nature *408*, 381-386.

Scioscia Hsiko Ait, S. (2004). Mutagenese-Screen nach Genen, die mit *dmyc* interagieren. (Zürich, Universität Zürich, diploma thesis), pp. 48.

Sears, R., Nuckolls, F., Haura, E., Taya, Y., Tamai, K., and Nevins, J.R. (2000). Multiple Ras-dependent phosphorylation pathways regulate Myc protein stability. Genes & development *14*, 2501-2514.

Secombe, J., Li, L., Carlos, L., and Eisenman, R.N. (2007). The Trithorax group protein Lid is a trimethyl histone H3K4 demethylase required for dMyc-induced cell growth. Genes & development *21*, 537-551.

Seoane, J., Le, H.V., and Massague, J. (2002). Myc suppression of the p21(Cip1) Cdk inhibitor influences the outcome of the p53 response to DNA damage. Nature *419*, 729-734.

Sharma, V.M., Draheim, K.M., and Kelliher, M.A. (2007). The Notch1/c-Myc pathway in T cell leukemia. Cell cycle (Georgetown, Tex *6*, 927-930.

Shen, X., Mizuguchi, G., Hamiche, A., and Wu, C. (2000). A chromatin remodelling complex involved in transcription and DNA processing. Nature *406*, 541-544.

Sommer, A., Bousset, K., Kremmer, E., Austen, M., and Luscher, B. (1998). Identification and characterization of specific dna-binding complexes containing members of the myc/max/mad network of transcriptional regulators. Journal of Biological Chemistry *273*, 6632-6642.

Spotts, G.D., Patel, S.V., Xiao, Q.R., and Hann, S.R. (1997). Identification of downstream-initiated c-myc proteins which are dominant-negative inhibitors of transactivation by full-length c-myc proteins. Molecular & Cellular Biology *17*, 1459-1468.

Staller, P., Peukert, K., Kiermaier, A., Seoane, J., Lukas, J., Karsunky, H., Moroy, T., Bartek, J., Massague, J., Hanel, F.*, et al.* (2001). Repression of p15INK4b expression by Myc through association with Miz-1. Nature cell biology *3*, 392-399.

Steiger, D. (2007). Analysis of the Max Network in *Drosophila*. (Zürich, Universität Zürich, Ph.D. thesis), pp. 173.

Steiger, D., Furrer, M., Schwinkendorf, D., and Gallant, P. (2008). Max-independent functions of Myc in *Drosophila melanogaster*. Nat. Genetics *40*, 1084 – 1091.

Steiner, P., Rudolph, B., Muller, D., and Eilers, M. (1996). The functions of Myc in cell cycle progression and apoptosis. Prog Cell Cycle Res *2*, 73-82.

Sulzer, A. (2003). A Screen for Mutations in Genes Involved in Growth Control in *Drosophila melanogaster*. (Zürich, Universität Zürich, diploma thesis), pp. 71.

Sundberg, T.B., Ney, G.M., Subramanian, C., Opipari, A.W., Jr., and Glick, G.D. (2006). The immunomodulatory benzodiazepine Bz-423 inhibits B-cell proliferation by targeting c-myc protein for rapid and specific degradation. Cancer research *66*, 1775-1782.

Toyo-oka, K., Bowen, T.J., Hirotsune, S., Li, Z., Jain, S., Ota, S., Escoubet-Lozach, L., Garcia-Bassets, I., Lozach, J., Rosenfeld, M.G.*, et al.* (2006). Mnt-deficient mammary glands exhibit impaired involution and tumors with characteristics of myc overexpression. Cancer research *66*, 5565-5573.

Trumpp, A., Refaeli, Y., Oskarsson, T., Gasser, S., Murphy, M., Martin, G.R., and Bishop, J.M. (2001). c-Myc regulates mammalian body size by controlling cell number but not cell size. Nature *414*, 768-773.

van Steensel, B., and Henikoff, S. (2000). Identification of in vivo DNA targets of chromatin proteins using tethered dam methyltransferase. Nat Biotechnol *18*, 424-428.

Vastrik, I., Kaipainen, A., Penttila, T.L., Lymboussakis, A., Alitalo, R., Parvinen, M., and Alitalo, K. (1995). Expression of the mad gene during cell differentiation in vivo and its inhibition of cell growth in vitro. Journal of Cell Biology *128*, 1197-1208.

Vita, M., and Henriksson, M. (2006). The Myc oncoprotein as a therapeutic target for human cancer. Seminars in cancer biology *16*, 318.

von der Lehr, N., Johansson, S., Wu, S., Bahram, F., Castell, A., Cetinkaya, C., Hydbring, P., Weidung, I., Nakayama, K., Nakayama, K.I.*, et al.* (2003). The F-box protein Skp2 participates in c-Myc proteosomal degradation and acts as a cofactor for c-Myc-regulated transcription. Molecular cell *11*, 1189-1200.

Walker, W., Zhou, Z.Q., Ota, S., Wynshaw-Boris, A., and Hurlin, P.J. (2005). Mnt-Max to Myc-Max complex switching regulates cell cycle entry. J Cell Biol *169*, 405-413.

Wang, Y.H., Liu, S., Zhang, G., Zhou, C.Q., Zhu, H.X., Zhou, X.B., Quan, L.P., Bai, J.F., and Xu, N.Z. (2005). Knockdown of c-Myc expression by RNAi inhibits MCF-7 breast tumor cells growth in vitro and in vivo. Breast Cancer Res *7*, R220-228.

Wanzel, M., Herold, S., and Eilers, M. (2003). Transcriptional repression by Myc. Trends Cell Biol *13*, 146-150.

Welcker, M., Orian, A., Jin, J., Grim, J.A., Harper, J.W., Eisenman, R.N., and Clurman, B.E. (2004). The Fbw7 tumor suppressor regulates glycogen synthase kinase 3 phosphorylation-dependent c-Myc protein degradation. Proceedings of the National Academy of Sciences of the United States of America *101*, 9085-9090.

Weng, A.P., Millholland, J.M., Yashiro-Ohtani, Y., Arcangeli, M.L., Lau, A., Wai, C., Del Bianco, C., Rodriguez, C.G., Sai, H., Tobias, J.*, et al.* (2006). c-Myc is an important direct target of Notch1 in T-cell acute lymphoblastic leukemia/lymphoma. Genes & development *20*, 2096-2109.

Wert, M., Kennedy, S., Palfrey, H.C., and Hay, N. (2001). Myc drives apoptosis in PC12 cells in the absence of Max. Oncogene *20*, 3746-3750.

Wierstra, I., and Alves, J. (2008). The c-myc promoter: still MysterY and challenge. Advances in cancer research *99*, 113-333.

Wolfe, S.A., Nekludova, L., and Pabo, C.O. (2000). DNA recognition by Cys2His2 zinc finger proteins. Annual review of biophysics and biomolecular structure *29*, 183-212.

Wood, M.A., McMahon, S.B., and Cole, M.D. (2000). An ATPase/helicase complex is an essential cofactor for oncogenic transformation by c-Myc. Molecular cell *5*, 321-330.

Wu, C.-H., van Riggelen, J., Yetil, A., Fan, A.C., Bachireddy, P., and Felsher, D.W. (2007). Cellular senescence is an important mechanism of tumor regression upon c-Myc inactivation. Proceedings of the National Academy of Sciences *104*, 13028-13033.

Wu, S., Cetinkaya, C., Munoz-Alonso, M.J., von der Lehr, N., Bahram, F., Beuger, V., Eilers, M., Leon, J., and Larsson, L.G. (2003). Myc represses differentiation-induced p21CIP1 expression via Miz-1-dependent interaction with the p21 core promoter. Oncogene *22*, 351-360.

Xiao, Q., Claassen, G., Shi, J., Adachi, S., Sedivy, J., and Hann, S.R. (1998). Transactivation-defective c-MycS retains the ability to regulate proliferation and apoptosis. Genes & development *12*, 3803-3808.

Xu, L., Wei, Y., Reboul, J., Vaglio, P., Shin, T.H., Vidal, M., Elledge, S.J., and Harper, J.W. (2003). BTB proteins are substrate-specific adaptors in an SCF-like modular ubiquitin ligase containing CUL-3. Nature *425*, 316-321.

Xu, T., and Rubin, G.M. (1993). Analysis of genetic mosaics in developing and adult Drosophila tissues. Development (Cambridge, England) *117*, 1223-1237.

Yeh, E., Cunningham, M., Arnold, H., Chasse, D., Monteith, T., Ivaldi, G., Hahn, W.C., Stukenberg, P.T., Shenolikar, S., Uchida, T.*, et al.* (2004). A signalling pathway controlling c-Myc degradation that impacts oncogenic transformation of human cells. Nature cell biology *6*, 308-318.

Zars, T. (2000). Behavioral functions of the insect mushroom bodies. Current opinion in neurobiology *10*, 790-795.

Zervos, A.S., Gyuris, J., and Brent, R. (1993). Mxi1, a protein that specifically interacts with Max to bind Myc-Max recognition sites [published erratum appears in Cell 1994 Oct 21;79(2):following 388]. Cell *72*, 223-232.

Zhao, J.J., Gjoerup, O.V., Subramanian, R.R., Cheng, Y., Chen, W., Roberts, T.M., and Hahn, W.C. (2003). Human mammary epithelial cell transformation through the activation of phosphatidylinositol 3-kinase. Cancer cell *3*, 483-495.

Zhu, S., Lin, S., Kao, C.-F., Awasaki, T., Chiang, A.-S., and Lee, T. (2006). Gradients of the Drosophila Chinmo BTB-Zinc Finger Protein Govern Neuronal Temporal Identity. Cell *127*, 409.

Acknowledgements

First and foremost, I would like to thank my supervisor Peter Gallant for his constant support. Especially for the fruitful discussions and for his open ear whenever I had any problems to solve.

Exceptionally, I would like to thank my former and current lab members and friends: Dominik Steiger, Michael Furrer, Regina Perez, Miriam Balbi, Rene Oetterli, Anja Egli, Nadine Müller and Sonali Mohanti for a great time in the lab, for a pleasant working atmosphere, for the nice lunchtimes and coffee breaks, for a wonderful time outside the lab but also for the great input to my project and for making me familiar me with the Swiss (and Indian) culture.

I would like to thank especially the laboratories of E.Hafen and K.Basler, but also the laboratories of Ch.Lehner, S.Luschnig, D.Bopp, Ch.Frei and W.Krek for their input to my project during our seminars.

I`d like to thank J.Bischof for providing me with flies and plasmids for using the ϕC31 integrase system, H.Stocker for the *chinmo* alleles and the Chinmo transgenes, P.Geuking for his support on the deficiencies and all the other labs who provided us with fly stocks, plasmids and antibodies.

I would also like to thank the people in the background for cleaning our laboratories (Frau Lopez), for sterilization, fresh plates and pre-fly food preparation (Maria+Guiseppe), for flyfood (“the cook”+Herr Egger), for sequencing (R.Grunder, A.Strässle), for qRT-PCR (M.Moser), for electron microscopy (Ch.Hugentobler) and for IT-support (M.Nakano, T.Siegenthaler).

Finally I`d like to thank my family, my boyfriend Roman Suter and my friends Erica Bogan and Itay Nakdimon for motivating and supporting me.

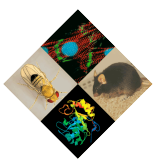

uzh | eth | zürich
Zurich Ph.D. Program
in Molecular Life Sciences

Curriculum Vitae

Personal Information

- Nationality: German
- Date of Birth: 31st of March, 1980
- Place of Birth: Stuttgart, Bad Cannstatt

Education

06/ 2004 - 06/2008
University of Zurich, Zurich, Switzerland
Member of the MLS Ph.D. program
- *Ph.D. in Natural science*

10/1999- 04/2004
University of Hohenheim, Stuttgart-Hohenheim, Germany
- *Diploma in biology*

Hauptfach: Genetik
Nebenfach: Mikrobiologie
Nebenfach: Biochemie

09/1996- 06/1999
Ernährungswissenschaftliches Gymnasium, HN-Böckingen, Germany
- *Allgemeine Hochschulreife*

Publications

Nagel, A.C., Wech, I., Schwinkendorf, D. and Preis, A. (2007). Involvement of co-repressors Groucho and CtBP in the regulation of single-minded in *Drosophila*. Hereditas *144*, 195-205.

Steiger, D., Furrer, M., Schwinkendorf, D. and Gallant, P. (2008). Max-independent functions of Myc in *Drosophila. melanogaster* Nat. Genetics *40*, 1084 – 1091.

Schwinkendorf, D. and Gallant, P. (submitted). The conserved Myc box 2 and Myc box 3 regions are important, but not essential, for Myc function *in vivo*.

Additional experiences

03/04 Intro course I: structural biology, dev. biology I
09/04 Intro course II: dev. Biology II, cell biology, scientific exposition, ethics
11/04 MLS retreat, Einsiedeln, poster
06/05-05/06 students representative
10/05 MLS retreat, Lenk, poster
10/06 MLS retreat, Chandolin, poster
02/08 course "start of a successful career", ETH
04/08 *Drosophila* conference, San Diego, poster

Glattalstr. 118i, 8052 Zürich, PHONE: +41-76-206 33 22, email: daniela@schwinkendorf.info